Pump Two-Phase Performance Program
Volume 3: Transient Tests

NP-1556, Volume 3
Research Project 301

Final Report, September 1980

Work Performed by

COMBUSTION ENGINEERING, INC.
C-E Power Systems
1000 Prospect Hill Road
Windsor, Connecticut 06095

Authors
W. G. Kennedy
M. C. Jacob
J. C. Whitehouse
J. D. Fishburn
G. J. Kanupka

Project Manager
D. F. Streinz

Prepared for

Electric Power Research Institute
3412 Hillview Avenue
Palo Alto, California 94304

EPRI Project Manager
K. A. Nilsson

Water Reactor System Technology Program
Nuclear Power Division

ORDERING INFORMATION

Requests for copies of this report should be directed to Research Reports Center (RRC), Box 50490, Palo Alto, CA 94303, (415) 965-4081. There is no charge for reports requested by EPRI member utilities and affiliates, contributing nonmembers, U.S. utility associations, U.S. government agencies (federal, state, and local), media, and foreign organizations with which EPRI has an information exchange agreement. On request, RRC will send a catalog of EPRI reports.

NOTICE

Prepared by
Combustion Engineering, Inc.
Windsor, Connecticut

EPRI PERSPECTIVE

PROJECT DESCRIPTION

This final report under RP301 documents the findings of an experimental research effort to develop a data base on reactor coolant pump single- and two-phase performance behavior. Tests were performed on a geometrically scaled model of an actual reactor coolant pump. Both steady-state and transient blowdown tests were performed over sufficiently large ranges of thermal-hydraulic operating conditions and typical pump performance parameters to cover calculated hypothetical loss-of-coolant accident (LOCA) conditions.

PROJECT OBJECTIVES

Current analytic pump models used in LOCA analyses are based on a limited amount of experimental data. The goals of this project were (1) to establish a sufficiently large data base of steady-state and transient pump performance data to substantiate, and ultimately improve, analytic pump models currently used for reactor coolant pump LOCA analysis; and (2) to obtain data on pump characteristics under two-phase transient blowdown conditions to aid the evaluation of reactor coolant pump overspeed.

PROJECT RESULTS

The pump data base collected in this project is considered sufficiently large and diverse to cover a significant range of pump performance of primary importance to LOCA analysis. Initial evaluation of the test results indicates that pump rated head and torque degrade significantly under two-phase flow conditions. Pump free-wheeling speed (pump motor power off) is closely coupled to the volumetric flow rate through the pump during a blowdown transient. The maximum free-wheeling speed observed was near twice the rated speed for a discharge break equal to the flow area of the pump. For smaller size discharge breaks, the peak speed observed was less than twice the rated speed. With electric power to the pump drive motor on throughout the blowdown, however, the pump speed was maintained at an almost constant value.

Additional reduction and analysis of this data base is required before it can be used to support the development of an improved analytic model for pump two-phase performance.

This final report consists of eight volumes, as presented in the table of contents in the first volume. Volumes 1, 2, 3, 4, and 7 present the results and conclusions, as well as substantial discussion and description, of the entire project and the test data. Volumes 5 and 6 present the tabulated test data in computer printout and graphic format, which will be useful for further analyses. Volume 8 contains a description of the data processing methods. Volumes 2 through 8 are available from the Research Reports Center* upon request.

Kjell A. Nilsson, Project Manager
Nuclear Power Division

---

*Research Reports Center
P.O. Box 50490
Palo Alto, CA 94303
(415) 965-4081

ABSTRACT

The primary objective of the C-E/EPRI Pump Two-Phase Performance Program was to obtain sufficient steady-state and transient two-phase empirical data to substantiate and ultimately improve the reactor coolant pump analytical model currently used for LOCA analysis. A one-fifth scale pump, which geometrically models a reactor coolant pump, was tested in steady-state runs with single- and two-phase mixtures of water and steam over ranges of operating conditions representative of postulated loss-of-coolant accidents. Transient tests were also run to evaluate the applicability of the steady-state-based calculational models to transient conditions.

This project has produced test data which can appropriately be utilized for reactor coolant pump modeling in LOCA analyses. The steady-state test data show general coherence of the test results and overall pump performance trends for a model pump that should be representative of a reactor coolant pump to the extent that scaling laws apply. Both head and torque data correlate well in the form of homologous curves. Two-phase head degradation curves are approximately comparable to head degradation curves obtained in other test programs. Two-phase torque degradation curves have also been developed. The collected data should be useful for analytical model development.

Volume III: Transient Tests

CONTENTS

CONTENTS (Cont'd.)

ILLUSTRATIONS

ILLUSTRATIONS (Cont'd.)

ILLUSTRATIONS (Cont'd.)

ILLUSTRATIONS (Cont'd.)

ILLUSTRATIONS (Cont'd.)

TABLES

Section 1

INTRODUCTION

The model pump test facility was constructed at the Kreisinger Development Laboratories at Combustion Engineering, Inc., Windsor, Connecticut, during 1974 and 1975. A schematic view of the loop is given in Figure 1-1. The scale model pump and test system are described in detail in Volume VII - Test Facility Description.

The transient tests with the scale model test pump were performed to measure and display its performance characteristics. The tests were not scaled simulations of Nuclear Steam Supply System (NSSS) loss-of-coolant accidents (LOCAs), because the test system was not designed to simulate an NSSS. Rather, the scale model pump was tested for a number of different initial conditions, over ranges of various parameters, to learn how the scale model pump performance relates to these parametric changes. This knowledge will then be used to analytically model the pump behavior, which then, using the scaling criteria, can be used to predict full-size NSSS pump behavior.

Sixteen transient blowdown tests were conducted in this project with about 40 independent measurements recorded on magnetic tape during each transient.

The parametric variations investigated in the transient blowdown testing included suction and discharge line break locations, different break area sizes, different pump operating modes, and various initial test system steady-state thermodynamic conditions.

The various sections in this volume describe the test procedures, the test performed, and the results and associated analysis. The transient data are presented separately in Volume VI - Transient Data.

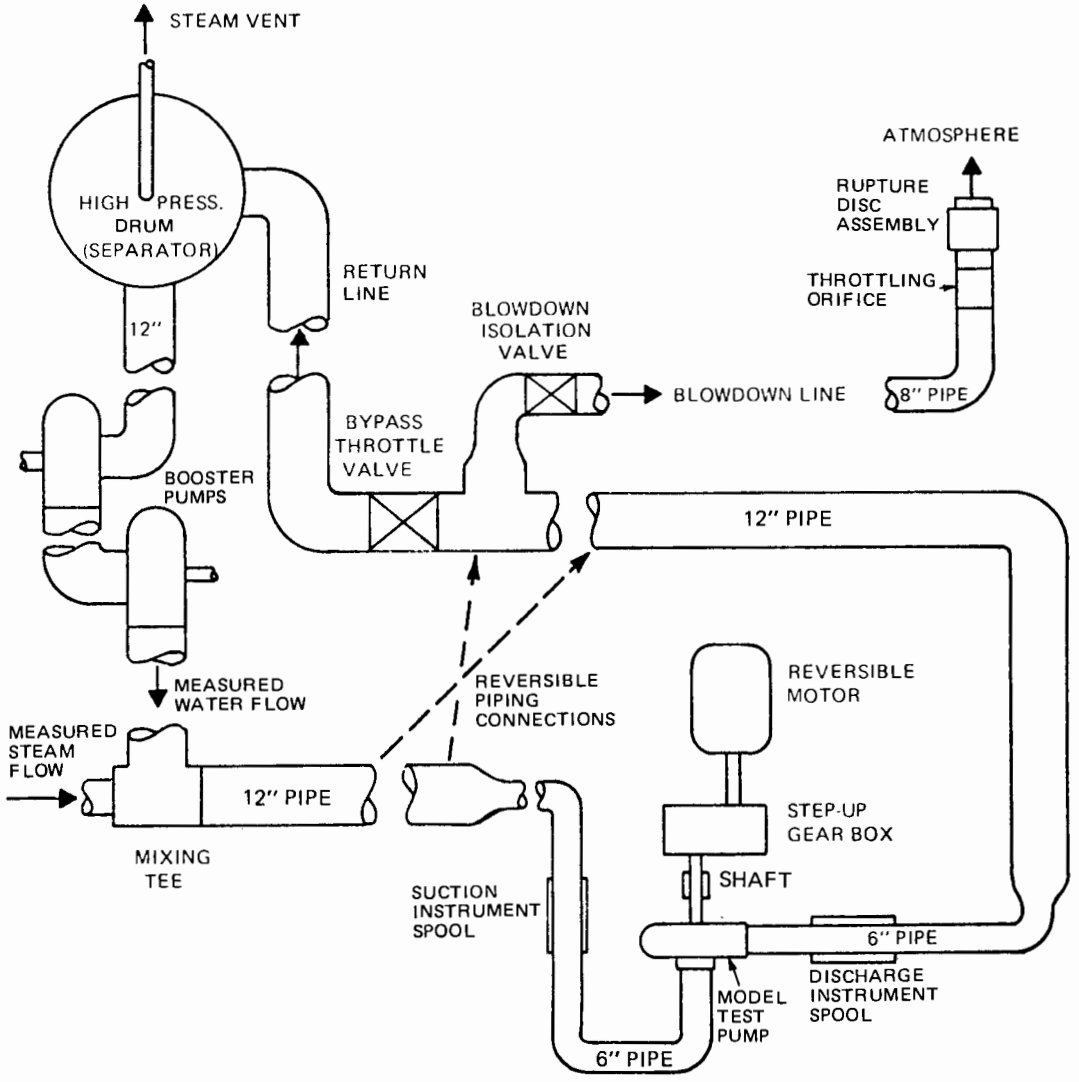

Figure 1-1. Basic Elements of Pump Test System (Schematic Plan View)

Section 2

TEST PROCEDURES

2.1 SYSTEM CONFIGURATIONS AND OPERATING MODES

The test loop used for the transient pump performance blowdown tests, which was the same loop used for the steady-state tests (See Volume II), was initially checked out by means of shakedown transient tests. For these tests, the system was operated with a pipe section in place of the model pump as a precaution not to damage the pump. The test pump was then installed in the loop, and another moderate preliminary blowdown test was run to gain additional operating experience on the loop, model pump, and instrumentation. Subsequently, performance testing of the model pump under transient conditions began.

Prior to startup of the test loop for a blowdown sequence, the loop had to be configured for the specific blowdown test conditions. Tests simulating discharge line breaks were piped such that the loop water was pumped from the high pressure drum through the booster pumps to the suction side of the test pump. The blowdown pipe, blowdown nozzle, rupture disc assembly, and blowdown stop valve were piped to the test pump discharge. Thus, for a simulated discharge pipe rupture, the test loop was configured in a forward flow mode (Figure 1-1). To obtain a simulated suction pipe rupture, it was necessary to modify the suction and discharge piping to the test pump such that the loop water from the booster pumps entered the discharge side of the test pump. The suction of the test pump was then piped to the blowdown piping as well as the return piping to the high pressure drum. With the loop in the reverse flow configuration, loop water would flow backwards through the test pump during the preparatory stages of the blowdown sequence. For each test, the break location was either at the discharge side or the suction side of the test pump. No tests were performed where both sides of the pump were connected to the break location.

With the loop configured for either forward or reverse flow mode, the specified blowdown break area size was selected. An orifice plate made to these specifications was inserted in the rupture disc assembly. The rupture discs, selected for the specified pressure requirements for the transient, were also inserted in the rupture disc assembly.

Pump trip logic circuits were then modified to provide for the pump motor operating condition specified for the test. The pump could either be locked, tripped, or remain powered after rupture, depending on test specifications. Locked rotor tests were accomplished by installing a special locking device on the motor shaft, in which case the pump impeller remained stationary during the entire blowdown sequence. With the proper blowdown configuration established, startup for the transient test could begin.

A standard blowdown procedure was developed during the test program and was utilized for all but the first few blowdown sequences. A description of this procedure is provided in Section 5 of Volume VII, Test Facility Description.

Special test loop procedures, which were integral with the initial system setup prior to the start of a blowdown test, and special post blowdown procedures, were not part of the standard transient test procedure. The standard procedure will be covered briefly but will not be repeated in detail here.

For transient pump performance tests, steady-state operation at desired combinations of fluid pressure level, void fraction, volumetric flow rate, and impeller speed, as in the case of steady-state pump performance tests, were established. When satisfactory steady-state operation was achieved, data measurements were initiated and shortly thereafter the blowdown transient was started through activation of the rupture disc assembly.

Various types of transient tests were conducted on the model pump based on break size, break location relative to the pump, and mode of test pump motor operation during the blowdown. The various modes of motor operation during the transient were:

- motor power turned off at the start of the blowdown, and the rotor allowed to free-wheel.

- motor power off with the rotor locked.
- motor power remaining on and the rotor speed maintained at the initial steady-state value.

These basic test pump blowdown modes are indicated in Figure 2-1.

Details of the initial operating conditions, test procedures, and transient measurements for all transient tests are provided in the following sections and in Volume VII, Test Facility Description.

2.2 INSTRUMENTATION AND DATA RECORDING

Two categories of instrumentation were utilized during testing. These were defined as loop instrumentation and test instrumentation. Loop instruments were those which enabled the operator to attain the specified loop conditions, and test instruments were those which measured the parameters utilized for analysis of the test pump performance during the transient blowdown tests. The test instrumentation was checked out a number of times during the preparatory stages of a blowdown test. Gamma densitometers, pressure and differential pressure cells, thermocouples, drag discs, turbine meters and the torque meter were all checked and calibrated prior to the actual blowdown. With some exceptions among the drag discs and turbine meters, all instrumentation used for transient testing was the same as that used for steady-state testing. Figure 4-1 of Volume VII, Test Facility Description, delineates all instrumentation used. A comprehensive list and detailed description of all instrumentation can be found in Volume VII, Section 4.

In preparation for a blowdown, the test loop was started in a single-phase water mode. Data scans were taken at various points in the pre-blowdown sequence for calibration purposes. These scans were taken with the relatively low speed data scanner and with the analog FM recording system. The data scanner allowed the operator to retrieve the data quickly for pre-blowdown checks and provided information used in deriving the final calibration constants. The analog data recorded on the FM system served only as a permanent record for the data obtained during steady-state, pre-blowdown data acquisition.

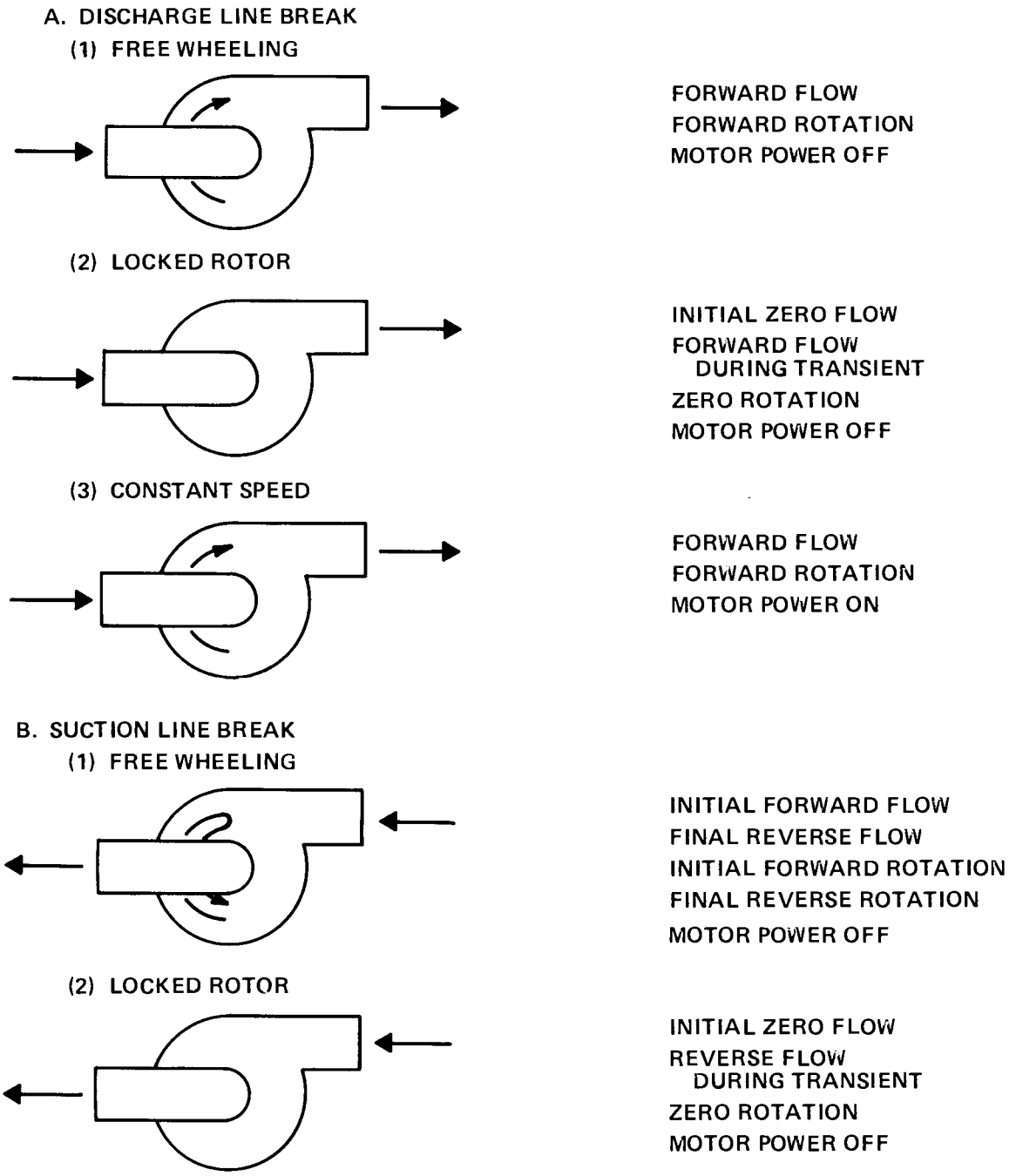

Figure 2-1. Blowdown Transient Pump Test Modes

During the actual blowdown the FM multiplex data acquisition system became the primary system due to its high-frequency recording capability. The scanner was also utilized as a backup and allowed preliminary analysis of the blowdown to be made while the FM tape was processed. Final analysis of most parameters was based on FM system data due to the better resolution of parameter values obtainable from this source. The scanner data was also useful since it contained readings of instruments that were not recorded on the FM tape. Scanner data included up to 69 channels of test instrument readings, while only 39 of the more relevant channels were recorded on FM tape.

Once all specified pre-blowdown conditions had been met and all pre-blowdown calibrations had been performed, the blowdown sequence was initiated. The data scanner was turned on manually prior to initiating the blowdown sequence timer. The FM recording system was automatically started prior to the rupture of the rupture discs.

A detailed description of the transient test data acquisition systems is given in Section 4 of Volume VII, Test Facility Description.

2.3 TEST PROCEDURE DESCRIPTION

2.3.1 Pre-Startup Procedures

Once the blowdown test conditions were established, the blowdown test procedure could begin. Prior to startup certain mechanical modifications and instrument calibrations were accomplished. Loop configuration, that is piping for forward or reverse flow, was according to requirements of the test. The rupture discs and proper blowdown orifice were installed in the rupture disc assembly. The pump torque meter was calibrated and the gamma densitometer air point calibration was accomplished with the loop dry. Calibration of each channel of the FM data acquisition system was done to verify functional capability. The blowdown sequence timer was set to either trip the test pump motor or to allow it to continue operating after the rupture, unless locked rotor was specified.

2.3.2 Startup Procedure

Startup commenced with the loop being filled with deaerated water at approximately 175°F. Pressure and differential pressure cells were bled to remove trapped air. Flow through the loop was started and brought to 30% rated pump flow at

which time a gamma densitometer low temperature water point was recorded as well as all pressure and differential pressure cell zero values. Drag disc and turbine meter calibration readings were also taken.

Calibration and zero data taken were checked and analyzed. If all instrumentation was operating within specifications the loop was heated to 300°F with steam supplied by the test boiler to the HP Drum. A drag disc temperature dependency calibration check was then made and thermocouples were calibrated against the RTD's.

A functional check of all mechanical and electrical instrumentation and components was made.

The loop temperature was then raised to 425°F, and all instruments checked at 300°F were again checked by recording data and analyzing it. If all systems and instrumentation performed satisfactorily, then the loop was brought to 850 psia. A drag disc temperature dependency check was made and a gamma densitometer hot-water point was taken. Pressure and differential pressure cells were again zeroed and data recorded. Drag disc and turbine meter hot calibrations were done.

Data reduction personnel reviewed the above startup data taken for adequacy in updating instrument constants to be used in data reduction.

The system was then brought to the pre-blowdown condition which was stipulated by the test matrix. Data from all instruments were then recorded on the scanner and FM systems. These data were reduced and reviewed as the final pre-blowdown check.

The operator then established the proper water inventory by adding or draining water from the drum, and action was taken to isolate certain auxiliary components from the effect of the blowdown.

2.3.3 Blowdown Procedure

After completion of the preparatory steps described above, the blowdown sequence timer was actuated to start the FM data acquisition and initiate the blowdown

transient by setting in motion a sequence of timed, predetermined events. First, the flow control valve was commanded to close to prevent a backflow of water from the HP drum during the blowdown. Next, bursting of the rupture discs was triggered. Shortly thereafter, the test pump was tripped, if called for in the test plan.

The transient was recorded on both the data scanner and the FM multiplex system. At the completion of the blowdown and after all post-blowdown special procedures had been carried out, the data acquisition systems were turned off. Instrumentation calibration data was taken to record post-blowdown gamma densitometer steam point, FM calibration voltages, clock reading and tape footage.

The system was then cooled and the torque meter uncoupled. Data were recorded for torque meter, drag disc and turbine meter post-blowdown zero values. At this point the transient test was completed.

Additional details on the blowdown procedure are provided in Section 5 of Volume VII, Test Facility Description.

Section 3

TRANSIENT TESTS CONDUCTED

3.1 TEST PHASES

The transient tests were conducted in two distinct phases, Phases I and II. The intermission that separated these phases provided time for data evaluation and interpretation, recalibration of instruments, modifications to instrumentation, servicing of equipment, and review and modification of plans and procedures for additional transient tests.

The Phase I transient tests in most part were exploratory in nature. These were performed in that manner to gain information on test loop and pump blowdown behavior at progressively increasing break sizes. Operational safety limits imposed on the model test pump required test results on pump peak speed and shaft torque to be taken on small breaks before additional blowdown tests with larger orifice sizes could be performed. Before each new blowdown test in Phase I was conducted, additional test instrumentation was installed and/or new calibration techniques for certain measuring instruments were employed.

More organized and complete testing was conducted during Phase II based on the experience gained on the test loop and pump blowdown behavior, loop blowdown procedures, and instrumentation during Phase I. Therefore, more consistent blowdown data were generated in Phase II. These tests cover a variety of break sizes and initial operating conditions. The purpose was to generate a pump test transient data bank spanning a wide range of performance conditions typical of the postulated NSSS LOCA conditions. Phase II test coverage included small, intermediate and large size breaks, and five different modes of pump operation.

Detailed descriptions of tests in Phases I and II and their objectives are provided below in the discussion of the transient test matrix.

3.2 TEST MATRIX

The transient test matrix is an array of operating modes and initial operating conditions from which test system blowdowns proceeded and contains information on break sizes and locations. All blowdown tests started from steady-state operation with either all liquid in the test loop at slightly subcooled conditions, or a two-phase mixture at a relatively low void fraction condition at the suction side of the test pump. The booster pump rotors were locked during the blowdown runs, and therefore initial steady-state loop circulation, if any, was generated by the test pump. Rupture of the diaphragms at the end of the blowdown line then initiated depressurization of the loop, and the fluid flashed to progressively higher void fractions until the flow through the pump was all steam.

As discussed in the Preliminary Test Plan (Reference 1, Section 9.3) the purposes of the test system blowdown runs do not require that any one test blowdown reproduce the time history of any one calculated NSSS LOCA blowdown. Rather, it is sufficient that somewhere in the assortment of test system blowdowns there are a number of times when the model pump operating conditions at least momentarily pass through the range of conditions typical of NSSS LOCA blowdowns, and that at these times the test transients be sufficiently representative of LOCA's to check the applicability of a calculation model based on data from steady-state tests. Thus, the objective of selecting the preliminary matrix combinations of initial operating conditions and kinds of blowdown was to generate a series of pump transients, portions of which would pass through various parts of typical NSSS LOCA pump operating ranges, and which can be compared with results of steady-state test measurements ranging over some of the same, or similar, operating conditions. The method of choosing initial operating conditions specified in the Preliminary Test Plan (Reference 1) is briefly summarized below.

During the planning stages of the program, the pump conditions to be expected during test system blowdowns were calculated using the CEFLASH-4A computer code (Reference 2). Figure 3-1 shows a node and flowpath diagram schematically indicating how the test system has been modeled in such calculations. It was desired that predictions of test system blowdown rates be realistic, and therefore, the discharge coefficient was set at 0.6, a value generally agreed to come closer to matching experimental data than the 1.0 required in LOCA calculations. It was further postulated that pump performance in the different

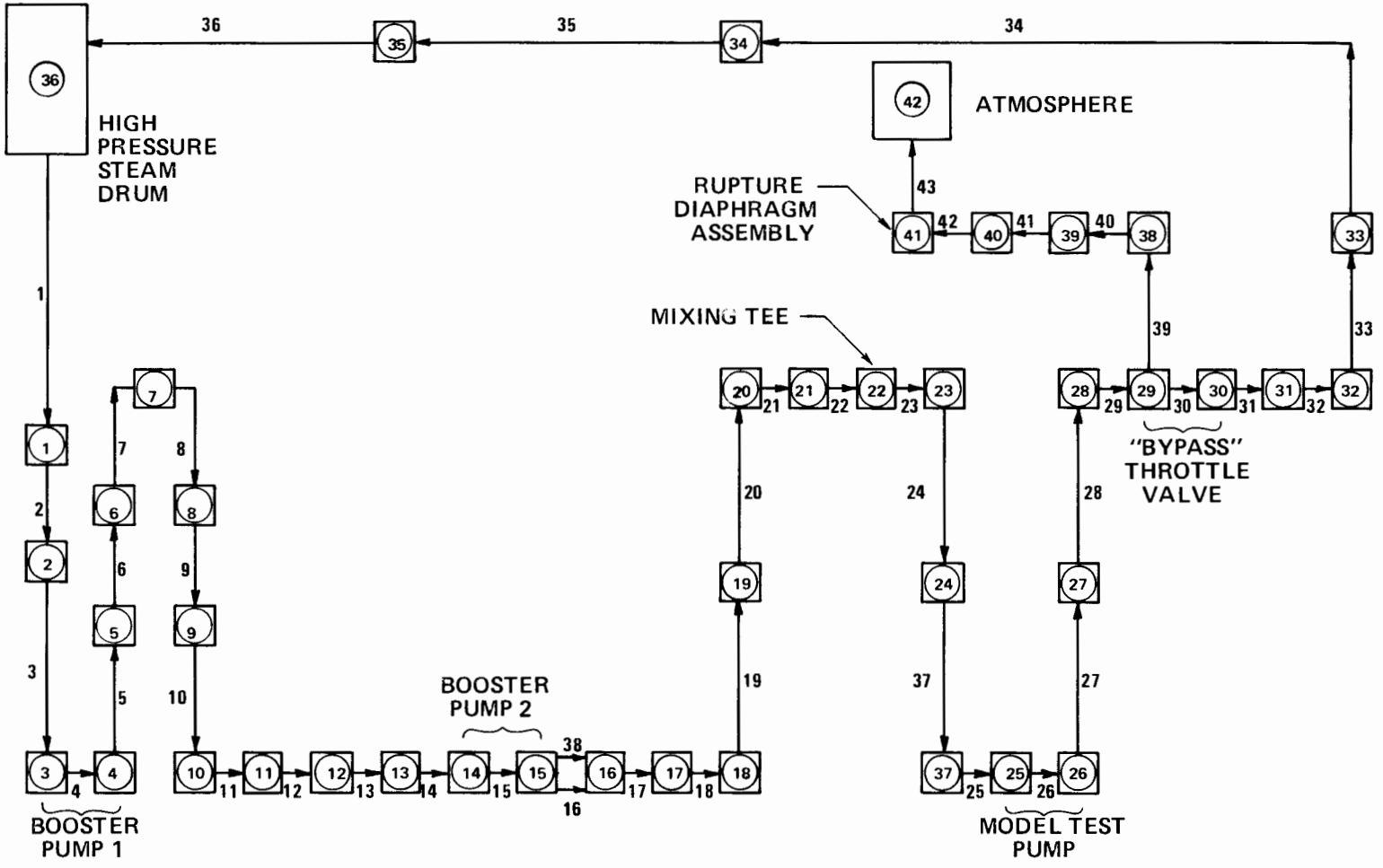

Figure 3-1. CEFLASH-4A Nodal Map of Pump Test Facility

situations (NSSS LOCA's, transient tests, and steady-state tests) can be compared by matching operating conditions, (i.e., P_{inlet}, α_F, and N and Q in percent of rated values) as far as possible or, when further scaling is required, using certain key parameters and homologous ratios (α_F, ν/α_N, and flow regime) as comparison criteria for both steady-state and transient cases, plus $d\alpha_F/dt$ for transients.

In the Preliminary Test Plan (Reference 1) the variations of pump average void fraction (α_F) versus time after start of vaporization are shown for a number of representative NSSS LOCA's. The envelope of these curves and some examples of intermediate curves are shown in Figure 3-2, along with predicted curves for representative test system forward flow blowdowns with a full-area break. It was expected from these curves that the test system could produce blowdowns with $d\alpha_F/dt$ up to one-half of large break LOCA rates. This rate of change of void fraction is considered adequate to check the use of steady-state performance data to derive a dynamic pump calculational model since, if large break LOCA rates cause significant differences between steady-state and transient performance, it is expected that the comparison between steady-state data and data for a test system blowdown, with $d\alpha_F/dt$ up to one-half of that for large break LOCAS would indicate some appreciable deviations, although not to the same degree. Typical calculated variations of α_F versus ν/α_N for NSSS and test system blowdowns are plotted in Figure 3-3, showing predicted test system behavior in the NSSS range.

Representative variations of α_N, the ratio of actual pump speed to rated speed, are shown in Figure 3-4 as compiled from NSSS LOCA calculations and test system blowdown calculations. The normalized speed, α_N, was not regarded as a primary transient parameter since (1) the main effects of speed are included in the normalized flow/speed parameter ν/α_N, and (2) the rotational inertia of the pump impeller and the drive system is large enough that velocity changes associated with impeller acceleration are considered to be small compared to fluid inertial response rates. Furthermore, it was not intended that a test system blowdown duplicate the time history of any LOCA blowdown, and thus speed variations during a test blowdown are not to be used directly to indicate LOCA overspeeds. Instead, LOCA overspeeds are predicted by the calculational model as the cumulative effect of angular accelerations dependent on net torque and moment of inertia. Therefore, hydraulic torque along with pump head

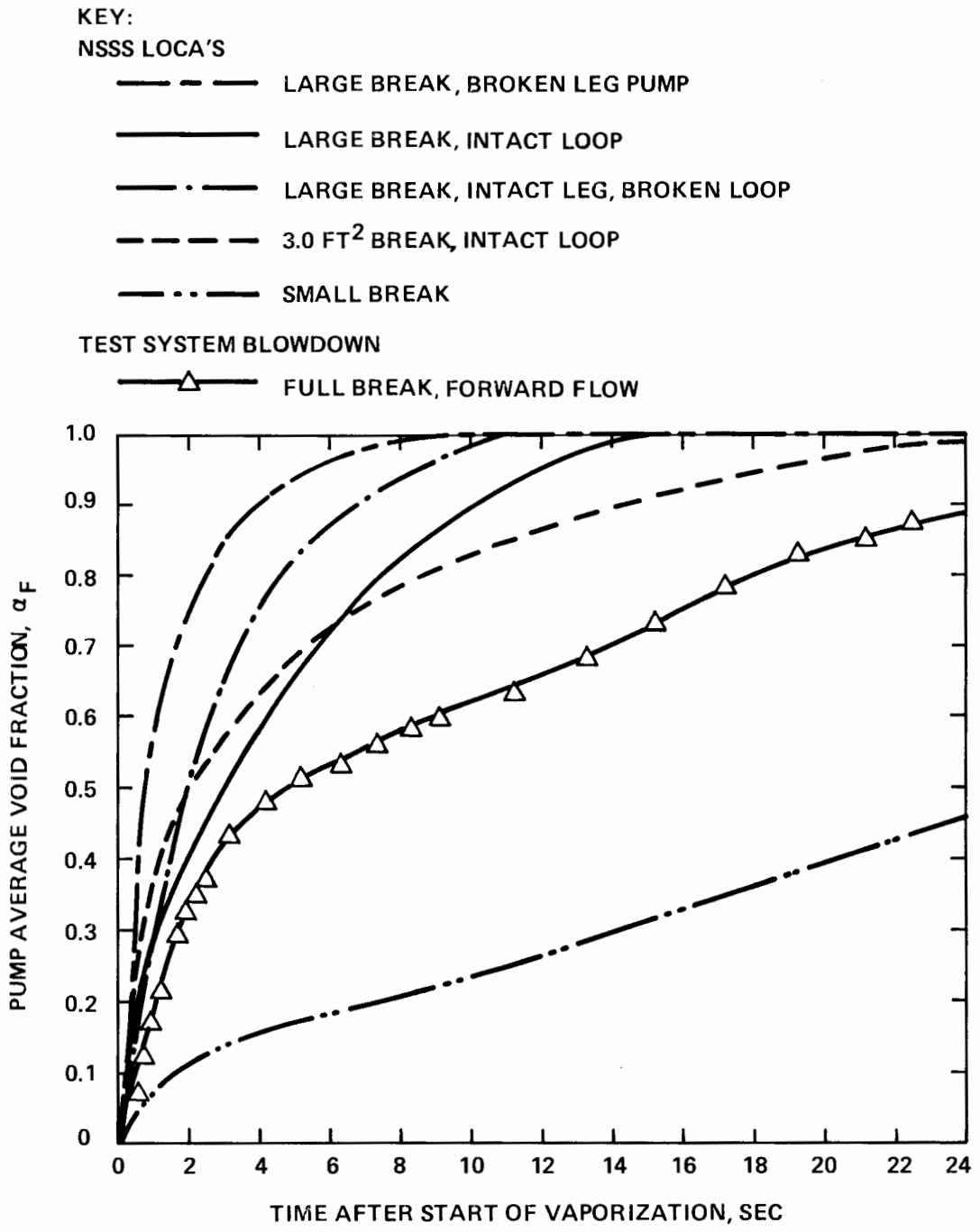

Figure 3-2. Typical Calculated NSSS and Test System Blowdowns, Pump Average Void Fraction Vs Time

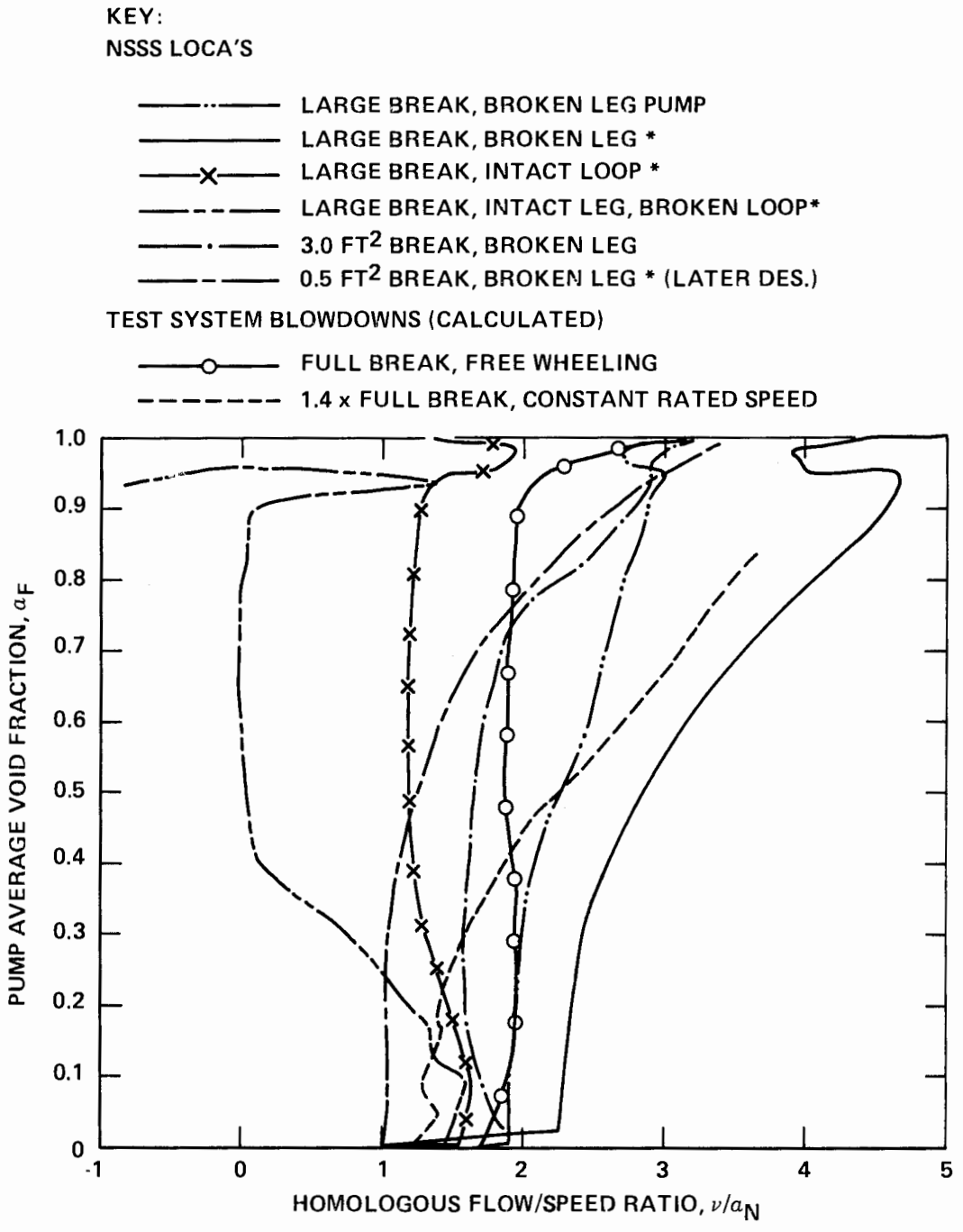

Figure 3-3. Typical Calculated NSSS and Test System Blowdowns For Discharge Leg Breaks ν/α_N vs α_F

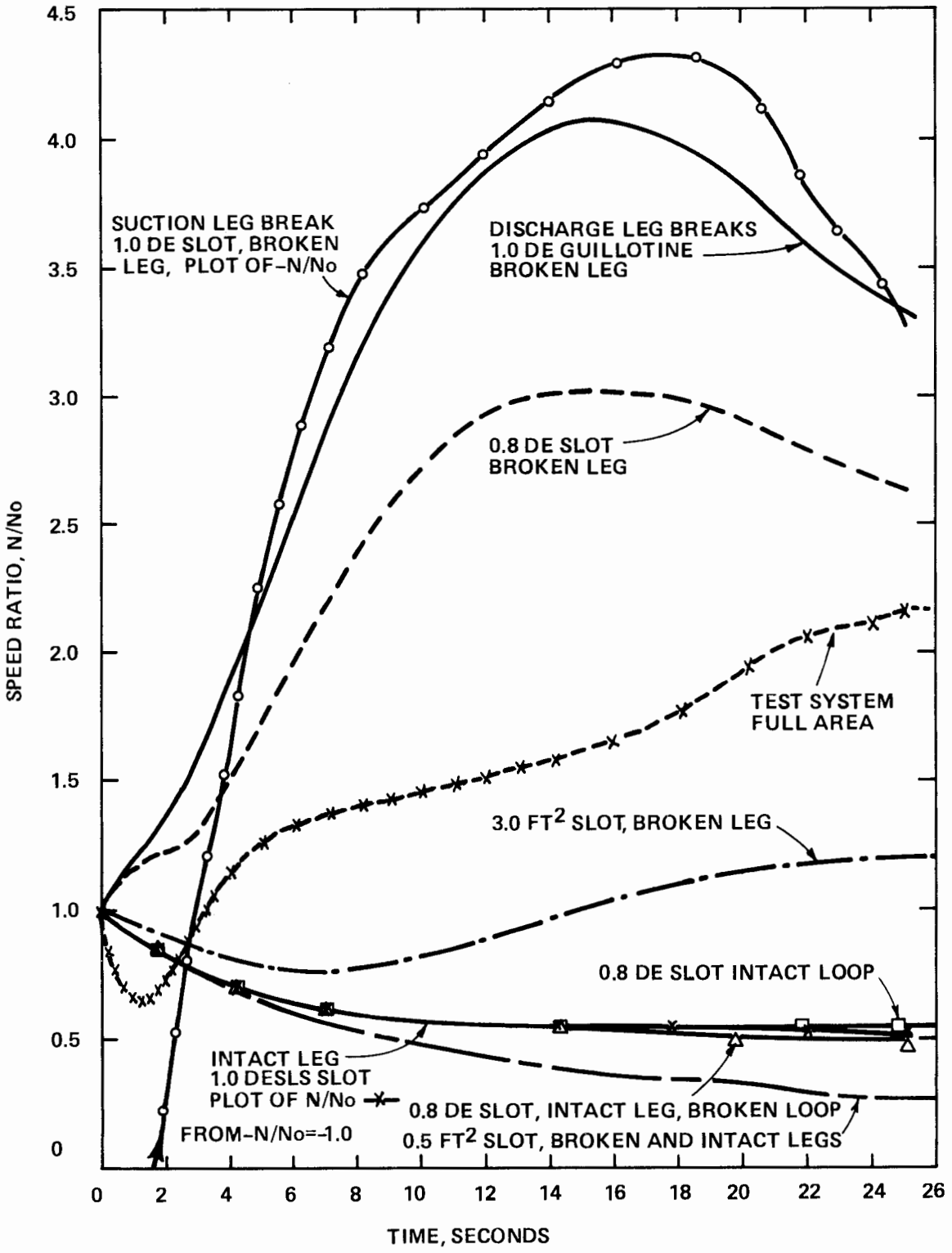

Figure 3-4. Pump Speed Ratios for Typical Calculated NSSS and Test System Blowdowns

at various operating conditions is the key empirical information needed to calculate overspeed, and was determined from the measured shaft torque and calculated friction and windage and acceleration torques in the transient tests to check the calculational model.

Pump speed versus time is an additional general indicator of the strength of the initial surge and subsequent sustained rates of volume flow. Figure 3-4 shows the contrast between speed changes in the intact loop and broken leg pumps. The calculated test system transients shown for full area forward flow blowdown indicate that the test system would achieve significant accelerations and reach speeds approximately twice the rated speed, about as high as allowable in the test facility.

The preliminary transient test matrix of Reference 1 was modified during transient testing as indicated by the initial operating conditions, break sizes, and break locations of Tables 3-1 and 3-2 for the transient tests. The test process included "feeling out" the test loop under transient test conditions to evaluate the actual initial operating conditions that were achieved, peak test pump speeds obtained, blowdown test sequence followed for each test, and the adequacy of actual test instrumentation. For instance, during Phase I testing one of the major concerns in the interpretation of the volumetric flow rates measured or calculated centered on the flow regime encountered at the pump suction instrument spool (SIS). Early blowdowns in this phase were conducted with a 6-inch long mixing plate to reduce separation of the two-phase mixture flowing out of the 90° elbow a few feet upstream of the suction instrument spool. Some of the later tests in Phase I were performed without the mixing plate to evaluate the effect of this plate on homogenizing the suction flow. Thus, the preliminary test matrix was thought of as a dynamic plan which mapped out an approach, but was adjusted in response to actual test results obtained.

As previously noted, Phase I transient tests were exploratory in nature, and more systematic and organized transient testing was performed during Phase II. Actual initial operating conditions and break sizes and locations for Phase I tests are presented in Table 3-1. Seven different transient tests were conducted during this phase. Five of these were forward flow (discharge break) blowdowns and the remaining two were reverse flow (suction break) transient tests. The

Table 3-1

SUMMARY OF PHASE I TRANSIENT TESTS

Test No.	Pre-Blowdown Conditions			Break Size* (%)	Break Location	Pump Mode	Mixing Plate
	Suction Pressure (PSIA)	Suction Norm. Flow Rate ν	Normalized Pump Speed α_N				
246	1050	0.00	0.00	36	Discharge	Locked Rotor	In
252	925	0.60	1.00	36	Discharge	Free-Wheeling	In
475	1160	0.00	0.00	57	Suction	Locked Rotor	Out
497	945	0.80	0.98	29	Suction	Free-Wheeling	Out
676	960	0.98	1.02	57	Discharge	Free-Wheeling	In
701	970	1.08	1.00	57	Discharge	Free-Wheeling	Out
846	965	0.94	1.00	57	Discharge	Constant Speed	Out

* Break size is a percentage of the 6" diameter inlet (or exit) area of the test pump.

Table 3-2

SUMMARY OF PHASE II TRANSIENT TESTS

Test No.	Pre-Blowdown Conditions			Break Size* (%)	Break Location	Pump Mode	Mixing Plate
	Suction Pressure (PSIA)	Suction Norm. Flow Rate ν	Normalized Pump Speed α_N				
1156	945	0.95	1.00	57	Discharge	Free-Wheeling	Out
1179	975	0.75	1.00	34	Discharge	Free-Wheeling	Out
1211	1010	0.95	1.00	5	Discharge	Constant Speed	Out
1267	1000	0.00	0.00	100	Discharge	Locked Rotor	Out
1319	950	1.00	1.00	100	Discharge	Free-Wheeling	Out
1351	1000	0.70	0.75	100	Discharge	Constant Speed	Out
1380	950	0.50	1.00	5	Discharge	Free-Wheeling	Out
1465	985	0.00	0.00	100	Suction	Locked Rotor	Out
1511	1030	0.40	0.20	15	Suction	Free-Wheeling	Out

* Break size is a percentage of the 6" diameter inlet (or exit) area of the test pump.

first Phase I test (Test 246) was a discharge break employing a break size of approximately 36 percent. Break size is defined as a percentage of the 6 inch diameter inlet or exit area of the test pump. Fluid in the test loop was initially stagnant, and was a few degrees subcooled, even at the suction side of the pump, for this test. The mixing plate was employed during the transient and the initial suction side pressure was approximately 1050 psia. The bypass throttle valve was closed approximately one second after rupture of the diaphragms, and the pump rotor was locked during the transient. The results of this test indicated the extent of the flow, hydraulic torque and pump head variations to be expected for a similar blowdown test with the pump rotor free wheeling. The second test (Test 252) in Phase I was such a test with the motor power tripped immediately after rupture of the diaphragms and the pump rotor allowed to free-wheel during the transient. The break size was the same as that employed for Test 246, and the initial flow was approximately 60 percent of the rated flow. Since just the test pump was running to develop this flow immediately before rupture, the suction side pressure could not be maintained at or above the saturation pressure, and consequently, the fluid at the suction side of the pump was a mixture of water and steam even prior to rupture. Both test 246 and 252 were completed without pre-blowdown instrument calibration procedures. It became evident, as part of the learning process associated with large scale testing, that instrument calibration updating was necessary up to a point just prior to rupture in order to obtain meaningful data. The blowdown standard test procedure was developed at that time to accommodate this need.

The next two tests (Tests 475 and 497) in Phase I were reverse flow (suction break) blowdowns, one with the rotor locked, and the other with the rotor allowed to free-wheel during the transient. The break size for Test 475 was approximately 57 percent and for Test 497 about 29 percent. The mixing plate was not utilized for these tests. The highest suction side pressure for any of the transient tests was realized for Test 475 which had an initial suction pressure of about 1160 psia. For Test 497, the initial suction pressure remained below 1000 psia as in other tests with initial loop circulation.

The final three tests (Tests 676, 701 and 846) during Phase I were forward flow tests with the initial suction pressure close to 1000 psia. However, the suction side pressure did reach higher values momentarily, due to a change in

1) 2 minutes after rupture (pressure must be $\leq$ 100 psi), close PAC 12 and PAC 16 booster pump injections (accomplished 1 minute, 40 seconds after rupture)

2) 45 seconds after Step #1 initiation, close test pump injection FW-7 (accomplished 2 minutes, 25 seconds after rupture).

3) 45 seconds after Step #2 initiation, close blowdown valve HPS-2 (Valve closed at 2 minutes, 55 seconds after rupture).

4) 20 seconds after Step #3 initiation, open blowdown valve with test pump and booster pump injections closed (Valve began to open at 3 minutes, 30 seconds and was fully open at 4 minutes 30 seconds after rupture).

5) 2 minutes after Step #4 initiation, terminate blowdown and cool down (terminated at 7 minutes after rupture).

Notes A) If the feedwater is overpressurized, do not open injection - open feedwater controller manually or DA-8 and control feedwater pressure to 400 or 500 psi.

B) If blowdown is terminated before 100 psi, blow down loop to 100 psi, then follow steps 1-5.

In order to complete the range of free rotor discharge breaks, Test 1380 employed a small break size of five percent. The motor power was turned off during the transient, for this test. This test was run in accordance with the standard blowdown procedure except that the triplex feed pump was inadvertently secured by the operator at 6 minutes 30 seconds after rupture. This action caused no adverse system effects but may have caused some change in data being taken at the same time. Additionally, the suction-side RTD(L-55) and its associated thermal well were replaced prior to the start of the blowdown sequence. One suction-side drag disc (L-1) behaved erratically.

The last two transient tests (Test 1465 and 1511) in Phase II were reverse flow (suction break) tests. Test 1465 was a locked rotor blowdown test which employed a 100 percent break size to assess the magnitude of the torque that would be experienced by an NSSS anti-rotation device. As was the case with all locked rotor blowdowns, the fluid in the loop was initially stagnant for this test. The last test (Test 1511) in Phase II was a free-wheeling reverse flow blowdown with initial loop circulation. The initial pump speed was 0.20 times rated, and the initial suction pressure was about 1000 psia. The break size was approximately 15%. The purpose here was to generate transient data for pump overspeed and flow rates for an intermediate size reverse flow blowdown test. Additionally, the special post-blowdown procedure used in Test 1351 was also implemented in Tests 1465 and 1511.

Section 4

TEST DATA

4.1 MEASURED AND DERIVED PARAMETERS USED IN DATA PRESENTATION

Pump performance is generally measured and described in terms of head and torque for a given speed, volumetric flow rate and fluid density, plus pressure and void fraction. For the transient tests, most of these parameters were directly measured and the others were derived from the measured parameters. The transient data presented in plot form in subsequent sections and volumes include both the measured and derived parameters. A summary of the data processing and presentation formats are given in the sections that follow.

During a transient test, the raw measured data was continuously recorded in analog form on the FM Multiplex Recording System for up to 39 measuring instruments. Subsequently, these analog FM data were digitized at prescribed sampling frequencies 200 samples/sec and 20 samples/sec. On the basis of instrument calibrations, selected discrete digitized data was converted into numbers quantifying the test system blowdown performance in engineering units. These resulting quantities are considered measured data and consist of thermocouple temperatures, pressures, differential pressures, gamma densitometer densities (or specific volumes), turbine meter velocities, drag disc momentum fluxes, pump rotational speed, shaft torque, and seal injection outflow. Values for these parameters are plotted as fuctions of time to graphically display the data. In addition, tabulation of these data are generated in hard copy printout form.

Derived parameters are considered to be those obtained by combining or manipulating the measured data. Certain derived parameters are obtained from published data, such as the ASME steam table property data. Some others are obtained from analytical equations containing the measured and/or derived parameters. Derived parameters for the transient tests include non-dimensional and dimensional volumetric flow rates, void fraction, pump head, friction and windage

torque, hydraulic torque, mass flow rates, integrated masses, momentum fluxes, test pump seal injection mass flow rate in and out, and net injection mass flow rate at the test pump. Also calculated are measurement uncertainties for various instrument measurements. A summary of how various parameter values are generated from the raw measured data or the reduced measured data is given in Section 4.2 below. A visual schematic display of how the measured and derived data are related is presented in Table 4-1.

4.2 DATA REDUCTION AND PROCESSING METHODS

The data reduction and processing methods were used to convert the acquired raw blowdown test data into useful operating and performance parameters in engineering units. The process employed in the reduction of transient data is shown in Figure 4-1 using graphic symbols to represent data storage devices, data processing codes and data display devices. To maintain the identity of the data as it is transferred into the various forms, the following indexing information is necessary:

a. Instrument Location Number (ILN), and

b. FM Channel Number (FCN).

The instrument location number identifies the physical location of a measuring device, as given in the Piping and Instrumentation Diagram (P&ID) for the test facility (See Figure 4-2). The FM channel number indicates the channel of the FM Multiplex Recording System to which a particular instrument was connected, and this can be found in the Instrumentation List (See Table 4-2). The correlation between the instrument location number and the FM channel number is also contained in the Instrumentation List.

Changes to the instrument location numbers occurred infrequently and were recorded by revising the P&ID. Changes to the FM channel numbers from test to test occurred when additional blowdown instrumentation was provided and/or when a particular instrument assigned to a FM channel was not operational. These changes are reflected in the Instrumentation List for each blowdown test. The FM channel numbers are used as the master indices to tie together the Instrumentation List, the Calibration Constant Data File, the FM-Multiplex Recording System, the Transient Data Reduction Program (TDR), and the Output.

Table 4-1

MEASURED AND DERIVED PARAMETERS

PARAMETER	REQUIRED QUANTITIES	REQUIRED MEASUREMENTS	MEASUREMENT LOCATIONS
Flow Regime	Density (ρ) distribution: γ-densitometer	3 beam densities	Pump SIS Pump suction flange Pump DIS
	or		
	V_{SL}, V_{SG} — Q as below	(See below)	
	V_{SL}, V_{SG} — α_F as below	(See below)	
	V_{SL}, V_{SG} — A pipe - Known		
Drum Inventory	Liquid head	ΔP	Drum, bottom-to-top
	Liquid density	°F	Drum lower region
Volumetric Flow Rate (Q, ν)	V_{avg} — V at a point (turbine meter)	V	Pump SIS Pump DIS
	V_{avg} — Assumed velocity profile		
	Q rated - Known		
	A pipe - Known		
	or		
	V_{avg} — ρ as below	3 beam densities	Pump SIS Pump DIS
	V_{avg} — ρV^2 — Drag disc at a point	ρV^2	
	V_{avg} — ρV^2 — Assumed profile		
	Q rated - Known		
	A pipe - Known		

Table 4-1 (Cont'd.)

MEASURED AND DERIVED PARAMETERS

PARAMETER	REQUIRED QUANTITIES	REQUIRED MEASUREMENTS	MEASUREMENT LOCATIONS
Fluid Mixture Density (ρ)	V_{avg} - as above (from turbine meter)	V (See above)	Pump SIS, Pump DIS
	ρV^2 — Drag disc at a point	ρV^2	Pump SIS, Pump DIS
	ρV^2 — Assumed profile	ρV^2	Pump SIS, Pump DIS
	or		
	γ-ray attenuation: γ-densitometer	3 beam strengths	Pump SIS, Pump suction flange, Pump DIS
	Density distribution	3 beam strengths	Pump SIS, Pump suction flange, Pump DIS
Time	Measured - data recorder	t	
Pump Shaft Acceleration	Pump Speed (N) - Measured	N	Pump shaft
	Time - Measured as above	t	
Mass Flow Rate ($\dot{M}$)	Q as above	(See above)	Pump SIS, Pump DIS
	ρ as above	(See above)	Pump SIS, Pump DIS
Integrated Mass	$\dot{M}$ as above	(See above)	Pump SIS, Pump DIS
	t as above	(See above)	Pump SIS, Pump DIS
Void Fraction (α_F)	Fluid mixture density - as above (from γ-densitometer)	(See above)	Pump SIS, Pump DIS
	ρ sat liquid	°F or P	Pump SIS, Pump DIS
	ρ sat vapor	°F or P	Pump SIS, Pump DIS

Table 4-1 (Cont'd.)

MEASURED AND DERIVED PARAMETERS

PARAMETER	REQUIRED QUANTITIES		REQUIRED MEASUREMENTS	MEASUREMENT LOCATIONS
Pressure (P)	Measured		P	Pump SIS Pump DIS
Pump Head (H, h)	ΔP pump		ΔP	Pump SIS-to-DIS
	ρ_{in}, ρ_{out}, or ρ_{avg} as above		(See above)	Pump inlet flange-to-outlet flange
Pump Speed (N, α_N)	N	Measured	N	Pump shaft
	N_{Rated}	Known		
Pump Torque (T_{hyd}, β_h)	T_{Shaft}	Measured	T	Pump shaft
	$T_{friction\ \&\ windage}$	N as above		
		P_{SIS} as above		
	T_{rated}	Known		
	$T_{acceleration}$	Shaft Acceleration as above	(See above)	
		Inertia of pump and coupling		

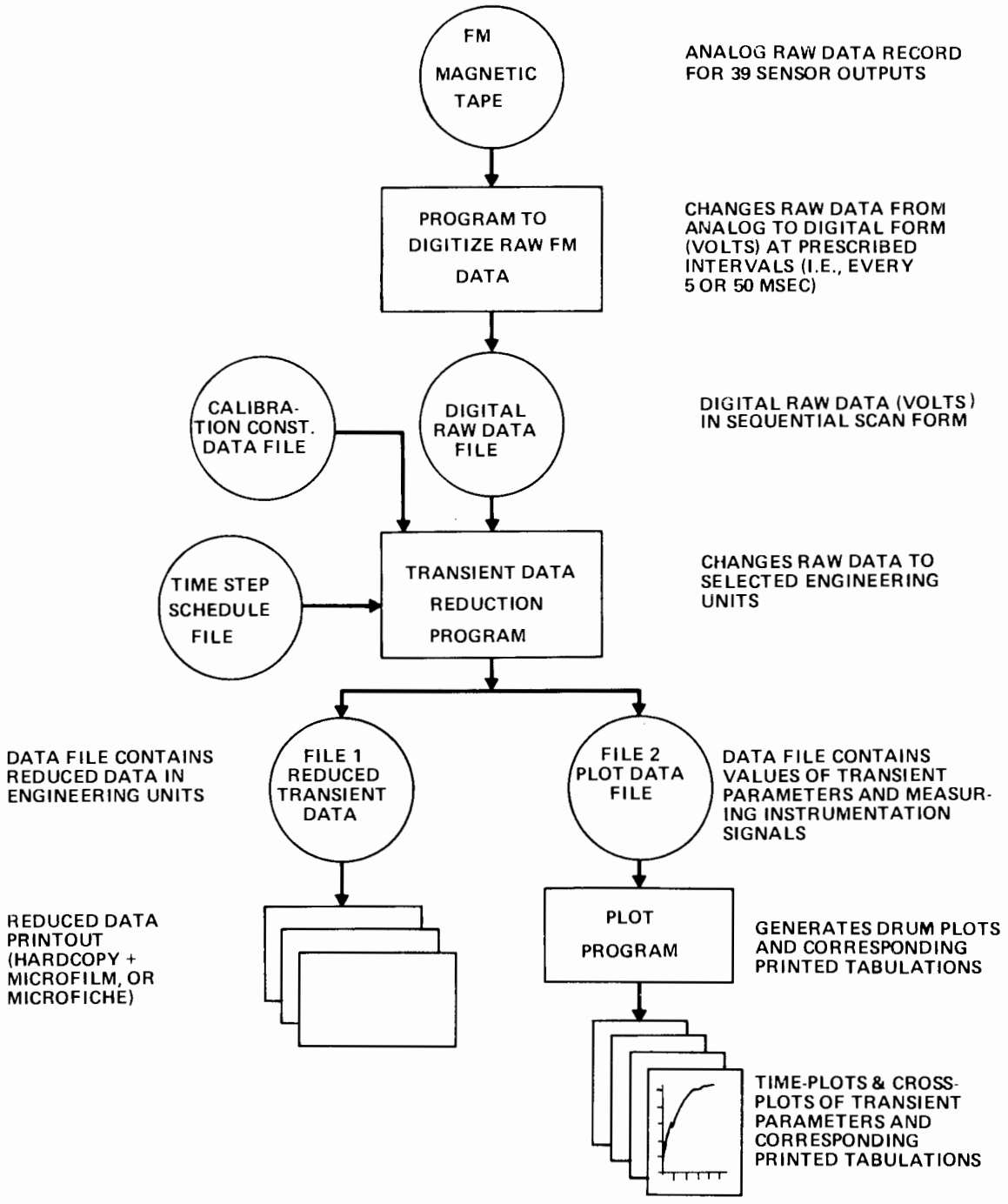

Figure 4-1. Data Reduction Sequence

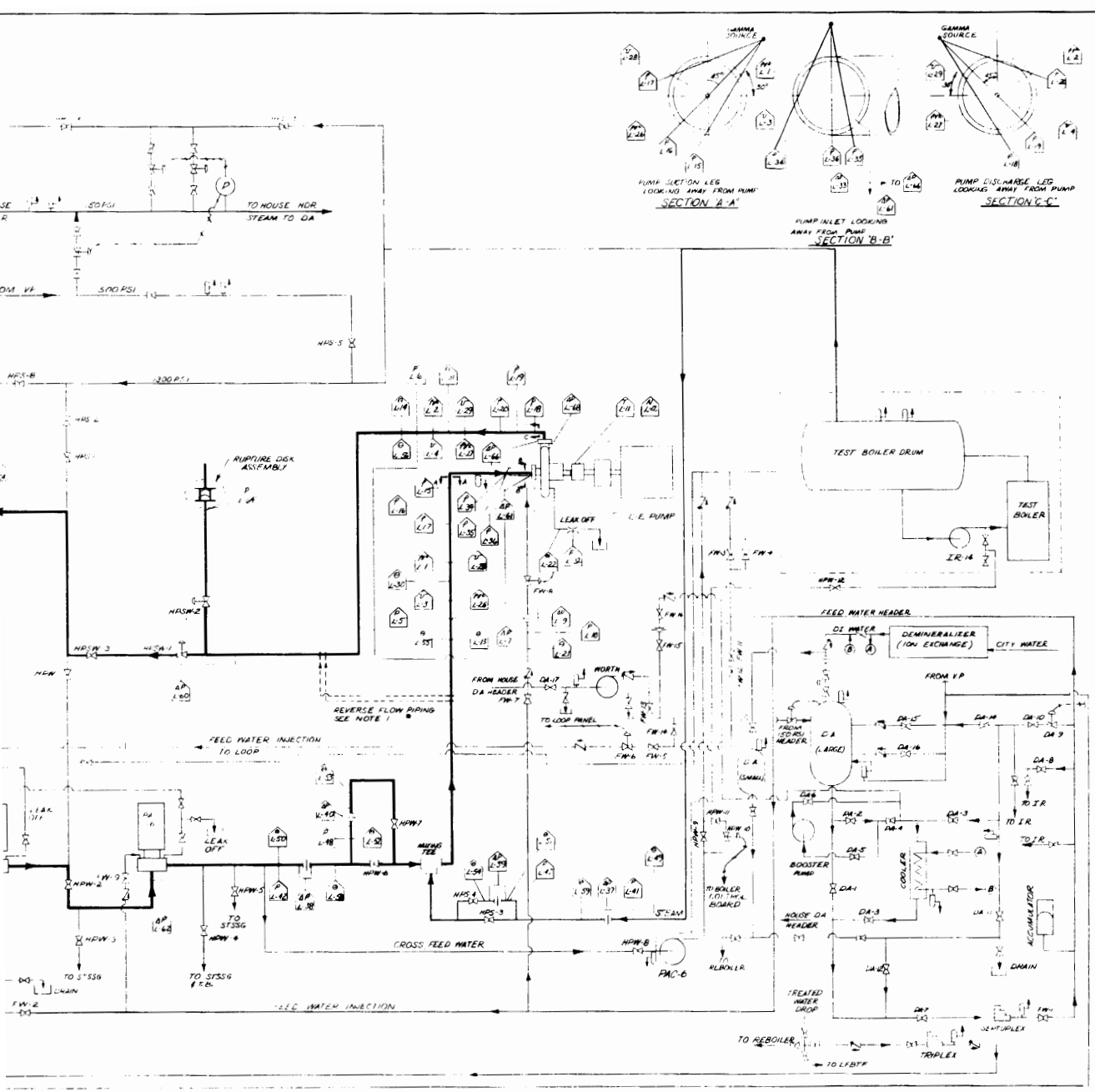

INSTRUMENTATION

P - PRESSURE CELL
ΔP - DIFFERENTIAL PRESSURE
θ - TEMPERATURE
TC - TURBINE METER
DD - DRAG DISK
ρ - DENSITOMETER
⟵ - PNEUMATIC SIGNAL

LO - LUBRICATION OIL
F - MAGNETIC FLOW METER
T - TORQUE METER
N - SPEED METER
TC - THRUST PADS
JG - THRUST PADS

LOCATION No.	DESCRIPTION	RANGE	SCANNER NUMBER	
L-1	SUCTION LEG DRAG DISK (HI)	VARIED	S-1	
L-2	DISCHARGE LEG DRAG DISK (HI)	VARIED	S-2	
L-3	SUCTION LEG TURBINE METER (LO)	VARIED	S-3	S-28 *
L-4	DISCHARGE LEG TURBINE METER (LO)	VARIED	S-4	S-29 **
L-5	SUCTION LEG PRESURE CELL	0-1500 PSI	S-5	
L-6	DISCHARGE LEG PRESURE CELL	0-1500 PSI	S-6	
L-7H	PUMP LEG-TO-LEG ΔP CELL (BLH)	± 500 PSID	S-7	
L-7H	PUMP LEG-TO-LEG ΔP CELL	VARIED	S-7A	
L-7L	PUMP LEG-TO-LEG ΔP CELL (BLH)	± 200 PSID	S-8	
L-7	PUMP LEG-TO-LEG ΔP CELL	VARIED	S-8A	
L-9	PUMP INJECTION INLET ΔP CELL	0-25 PSID	S-9	
L-10	PUMP INJECTION INLET PRESURE CELL	0-1500 PSID	S-10	
L-11	PUMP TORQUE METER	0-200/0-2000 ft-lb	S-11	
L-12	PUMP SPEED METER	0-10,000 RPM	S-12	
L-13	SUCTION LEG THERMOCOUPLE	0-600°F	S-13	
L-14	DISCHARGE LEG THERMOCOUPLE	0-600	S-14	
L-15	SUCTION LEG DENSITOMETER, BEAM 1	0-62.4 lb/ft³	S-15	
L-16	SUCTION LEG DENSITOMETER, BEAM 2	0-62.4 lb/ft³	S-16	
L-17	SUCTION LEG DENSITOMETER BEAM 3	0-62.4 lb/ft³	S-17	
L-18	DISCHARGE LEG DENSITOMETER, BEAM 1	0-62.4 lb/ft³	S-18	
L-19	DISCHARGE LEG DENSITOMETER, BEAM 2	0-62.4 lb/ft³	S-19	
L-20	DISCHARGE LEG DENSITOMETER, BEAM 3	0-62.4 lb/ft³	S-20	
L-21	PUMP INJECTION INLET THERMOCOUPLE	0-600°F	S-21	
L-22	PUMP INJECTION OUTLET THERMOCOUPLE	0-600°F	S-22	
L-23	HIGH PRESURE DRUM ID THERMOCOUPLE	0-800°F	S-23	
L-24	HIGH PRESURE DRUM OD THERMOCOUPLE	0-800°F	S-24	
L-25	HIGH PRESURE DRUM LEVEL ΔP CELL	0-25 PSID	S-25	
L-26	SUCTION LEG DRAG DISK (LOWER)	VARIED	S-26	
L-27	DISCHARGE LEG DRAG DISK(LOWER)	VARIED	S-27	
L-28	SUCTION LEG TURBINE METER	VARIED	S-28	S-3 *
L-29	DISCHARGE LEG TURBINE METER	VARIED	S-29	S-4 **
L-30	SUCTION LEG DRAG DISK THERMOCOUPLE	0-600° F	S-30	
L-31	DISCHARGE LEG DRAG DISK THERMOCOUPLE	0-600°F	S-31	
L-32	PUMP INJECTION OUTLET FLOW	VARIED	S-32	
L-33	INLET ACROSS PIPE ΔP	± 300 in.	S-33	
L-34	INLET DENSITOMETER, BEAM 3	0-62.4 lb/ft³	S-34	
L-35	INLET DENSITOMETER, BEAM 1	0-62.4 lb/ft³	S-35	
L-36	INLET DENSITOMETER, BEAM 2	0-62.4 lb/ft³	S-36	
L-37L	MAIN STEAM ORIFICE ΔP CELL	0-3.5 PSID	S-37	
L-37H	MAIN STEAM ORIFICE ΔP CELL	0-25 PSID	S-43	
L-38L	MAIN WATER ORIFICE ΔP CELL	0-3.5 PSID	S-38	
L-38M	MAIN WATER ORIFICE ΔP CELL	0-25 PSID	S-44	
L-38H	MAIN WATER ORIFICE ΔP CELL	VARIED	S-45	
L-39L	BYPASS STEAM ORIFICE ΔP CELL	0-3.5 PSID	S-39	
L-39H	BYPASS STEAM ORIFICE ΔP CELL	0-25 PSID	S-45	
L-40L	BYPASS WATER ORIFICE ΔP CELL	0-3.5 PSID	S-40	
L-40H	BYPASS WATER ORIFICE ΔP CELL	0-25 PSID	S-46	
L-41	MAIN STEAM ORIFICE PRESURE CELL	0-1500 PSI	S-41	
L-42	MAIN WATER ORIFICE PRESURE CELL	0-1500 PSI	S-42	
L-47	BYPASS STEAM ORIFICE PRESURE CELL	0-1500 PSI	S-47	
L-48	BYPASS STEAM ORIFICE PRESURE CELL	0-1500 PSI	S-48	
L-49	MAIN STEAM ORIFICE THERMOCOUPLE	0-600°F	S-49	
L-50	MAIN WATER ORIFICE THERMOCOUPLE	0-600°F	S-50	
L-51	BYPASS STEAM ORIFICE THERMOCOUPLE	0-600°F	S-51	
L-52	BYPASS WATER ORIFICE THERMOCOUPLE	0-600°F	S-52	
L-53	BYPASS WATER ORIFICE RTD	0-600°F	S-53	
L-54	BYPASS STEAM ORIFICE RTD	0-600°F	S-54	
L-55	SUCTION LEG RTD	0-600°F	S-55	
L-56	DISCHARGE LEG RTD	0-600°F	S-56	
L-57	AMBIENT TEMPERATURE THERMOCOUPLE	0-200°F	S-57	
L-58	MAIN WATER ORIFICE RTD	0-600°F	S-58	
L-59	MAIN STEAM ORIFICE RTD	0-600°F	S-59	
L-60	LOOP FLOW CONTROL VALVE ΔP CELL	0-200 PSID	S-60	
L-61	SUCTION LEG TO INLET FLANGE ΔP CELL	0-10 PSID	S-61	
L-62	PAC 16 ΔP CELL	0-200 PSID	S-62	
L-64	BLOWDOWN LEG PRESSURE CELL	0-1500 PSI	S-64	
L-65	H P DRUM PRESSURE CELL	0-1500 PSI	S-65	
L-66	TEST PUMP FLANGE TO FLANGE ΔP CELL	VARIED	S-66	
L-68	PUMP VOLUTE TO IMPELLER BACK ΔP CELL	0-25 PSID	S-68	

* FOR TESTS 209-243 and 290-453

** FOR TESTS 209 → 609

VALVE IDENTIFICATION

VALVE No.	DESCRIPTION
HPS-1	BOILER DRUM TO H.P. DRUM ISOLATION VALVE
HPS-2	BOILER DRUM TO H.P. DRUM ISOLATION VALVE
HPS-3	MAIN STEAM FLOW VALVE (6" ANGLE VALVE)
HPS-4	STEAM BYPASS VALVE
HPS-5	VP BOILER TO LOOP ISOLATION VALVE (CROSS TIE SYSTEM)
HPS-6	PNEUMATIC VENT FOR TEST BOILER AND LOOP
HPS-7	PNEUMATIC VENT FOR TEST BOILER AND LOOP
HPS-8	TEST BOILER TO VENT ISOLATION VALVE
HPS-9	H.P. DRUM TO VENT ISOLATION VALVE
HPS-10	H.P. DRUM TO VENT ISOLATION VALVE
HPS-11	2" VENT ON TOP OF H.P. DRUM
HPS-14	LOOP STEAM TO HOUSE HEADER
HPS-15	BOILER STEAM TO HOUSE HEADER
HPS-16	MAIN MANUAL VENT VALVES
HPS-17	BYPASS MANUAL VENT VALVES

VALVE No.	DESCRIPTION
HPW-1	DRUM INTERNAL ISOLATION VALVE
HPW-2	LOOP ISOLATION VALVE
HPW-3	ST'SSG ISOLATION VALVE
HPW-4	ST'SSG ISOLATION VALVE
HPW-5	ST'SSG ISOLATION VALVE
HPW-6	MAIN WATER FLOW CONTROL VALVE
HPW-7	BYPASS WATER FLOW CONTROL VALVE
HPW-8	PAC 6 SUCTION VALVE
HPW-9	PAC 6 MAIN FLOW CONTROL VALVE
HPW-10	PAC 6 PNEUMATIC BYPASS CONTROL VALVE
HPW-11	PAC 6 MANUAL BYPASS SHUT-OFF VALVE
HPW-12	PAC 6 BLOWDOWN CIRCULATION VALVE

VALVE No.	DESCRIPTION
FW-1	SEPTUPLEX OUTLET VALVE
FW-2	TRIPLEX OUTLET VALVE (LOCATED AT MEZZANINE LEVEL)
FW-3	LARGE BOILER FEED VALVE
FW-4	SMALL BOILER FEED VALVE
FW-5	MANUAL LOOP FEEDWATER VALVE
FW-6	PNEUMATIC LOOP FEEDWATER VALVE
FW-7	TEST PUMP INJECTION MANUAL SHUT OFF
FW-8	TEST PUMP INJECTION CONTROL VALVE
FW-9	PAC-16 SEAL INJECTION VALVE
FW-10	PAC-12 SEAL INJECTION VALVE
FW-11	SEPTUPLEX LOOP FEEDWATER VALVE
FW-12	SEPTUPLEX LOOP FEEDWATER VALVE
FW-13	WORTHINGTON CENTRIFUGAL OUTLET VALVE
FW-14	WORTHINGTON CENTRIFUGAL LOOP FEEDWATER VALVE
FW-15	WORTHINGTON CENTRIFUGAL OUTLET BYPASS
FW-16	WORTHINGTON CENTRIFUGAL OUTLET BYPASS

VALVE No.	DESCRIPTION
HPSW-1	TPPP LOOP FLOW CONTROL VALVE
HPSW-2	TPPP BLOWDOWN VALVE
HPSW-3	TPPP ISOLATION VALVE

NOTES:

1) FOR REVERSE FLOW TESTING, PIPING SWITCH IS MADE AS INDICATED

2) DIFFERENTIAL PRESSURE CELLS ARE INSTALLED SO THAT A PRESSURE RISE IN POSITIVE FLOW DIRECTION, AS INDICATED BY THE ARROWS IS DEFINED AS POSITIVE. FOR REVERSE FLOW TESTING, THE DIFFERENTIAL PRESSURE CELL AT LOCATION L-61 IS REVERSED

FIGURE 4-1

PIPING & INSTRUMENTATION DIAGRAM

CE / EPRI PUMP TEST FACILITY

DRAWN	N/A	9-AUG-78
CHECKED	[illegible]	9-AUG-78
APPROVED	M. C. Wittel	9-30-78

E-K-900145-54 | 0

TABLE 4-2

TYPICAL INSTRUMENTATION LIST

Scanner Channel Number	Instrument Location Number	Serial Number	FM Number	Date Calib.	Description	Range
0			F-1		Short for DVM	
1	L-1	3728	F-2		Pump Suction Drag Disc (Hi)	0-600,000 #/ft-sec^2
2	L-2	3729	F-3		Pump Discharge Drag Disc (Hi)	0-600,000 #/ft-sec^2
3	L-3	0950977	F-4		Pump Suction Turbine Meter (Lo)	0-300 ft/sec
4	L-4	0950978	F-5		Pump Discharge Turbine Meter (Lo)	0-300 ft/sec
5	L-5	969	F-6	6/1/77	Pump Suction Pressure Cell	0-1500 psi
6	L-6	455	F-7	6/1/77	Pump Discharge Pressure Cell	0-1500 psi
7	L-7	48557	F-8	6/2/77	Pump D/P Cell (Hi) (Leg-to-leg)	0-500 psid (BLH)
7A	L-7	68853		6/4/77	Pump D/P Cell (Hi) (Leg-to-leg)	-100/0/200 psid
8	L-7	44081	F-9	6/4/77	Pump D/P Cell (Lo) (Leg-to-leg)	0-200 psid (BLH)
8A	L-7	12795		6/2/77	Pump D/P Cell (Lo) (Leg-to-leg)	-8/0/+16 psid
9	L-9	12792	F-22	6/2/77	Pump Inlet Injection D/P Cell	0-25 psid
10	L-10	68872		6/8/77	Pump Inlet Injection Pressure Cell	0-1500 psid
11	L-11	83	F-12		Pump Torque Meter	0-1200 ft-lbs

TABLE 4-2 (Cont'd.)

TYPICAL INSTRUMENTATION LIST

Scanner Channel Number	Instrument Location Number	Serial Number	FM Number	Date Calib.	Description	Range
12	L-12		F-13		Pump Speed Meter	0-10,000 RPM
13	L-13		F-14		Pump Suction Thermocouple	0-600°F
14	L-14		F-15		Pump Discharge Thermocouple	0-600°F
15	L-15	A-566	F-16		Pump Suction Densitometer, Lower Beam A-1	0-62.4 lb/ft^3
16	L-16	A-102	F-17		Pump Suction Densitometer, Center Beam B-1	0-62.4 lb/ft^3
17	L-17	A-111	F-18		Pump Suction Densitometer, Upper Beam C-1	0-62.4 lb/ft^3
18	L-18	A-569	F-19		Pump Discharge Densitometer, Lower Beam A-2	0-62.4 lb/ft^3
19	L-19	A-101	F-20		Pump Discharge Densitometer, Center Beam B-2	0-62.4 lb/ft^3
20	L-20	A-567	F-21		Pump Discharge Densitometer, Upper Beam C-2	0-62.4 lb/ft^3
21	L-21				Pump Inlet Injection Flow Thermocouple	0-600°F
22	L-22				Pump Outlet Injection Flow Thermocouple	0-600°F

TABLE 4-2 (Cont'd.)

TYPICAL INSTRUMENTATION LIST

Scanner Channel Number	Instrument Location Number	Serial Number	FM Number	Date Calib.	Description	Range
23	L-23				High Pressure Drum ID Thermocouple	0-800°F
24	L-24				High Pressure Drum OD Thermocouple	0-800°F
25	L-25	29066		6/6/77	High Pressure Water Level D/P Cell	0-2.5 psid
26	L-26	4160	F-27		Pump Suction Drag Disc (Lo)	1,000,000 #/ft-sec^2
27	L-27	4159	F-28		Pump Discharge Drag Disc (Lo)	1,000,000 #/ft-sec^2
28	L-28	0950979	F-10		Pump Suction Turbine Meter (Hi)	0-300 ft/sec
29	L-29	0950980	F-23		Pump Discharge Turbine Meter (Hi)	0-300 ft/sec
30	L-30		F-31		Pump Suction DD Thermocouple	0-600°F
31	L-31		F-32		Pump Discharge DD Thermocouple	0-600°F
32	L-32		F-33		Pump Injection Outlet Flow (Magn. F.M.)	0-100 GPM
33	L-33	45077		6/8/77	Pump Suction D/P BLH (Inlet/ Across Pipe - 90°)	0 $\pm$ 500 inches H_2O
34	L-34	HJ457	F-35		AECL Densitometer, Outer Beam (X)	0-62.4 lb/ft^3
35	L-35	6Q125	F-36		AECL Densitometer, Inner Beam (Y)	0-62.4 lb/ft^3
36	L-36	HJ459	F-37		AECL Densitometer, Center Beam (Z)	0-62.4 lb/ft^3

TABLE 4-2 (Cont'd.)

TYPICAL INSTRUMENTATION LIST

Scanner Channel Number	Instrument Location Number	Serial Number	FM Number	Date Calib.	Description	Range
37	L-37	49282		6/4/77	Main Steam Orifice DP Cell (Lo)	0-3.5 psid
38	L-38	49280	F-11	6/6/77	Main Water Orifice DP Cell (Lo)	0-3.5 psid
39	L-39	49283		6/4/77	Bypass Steam Orifice DP Cell (Lo)	0-3.5 psid
40	L-40	49281		6/6/77	Bypass Water Orifice DP Cell (Lo)	0-3.5 psid
41	L-41	18285		6/1/77	Main Steam Orifice Pressure Cell	0-1500 psi
42	L-42	18386	F-25	6/1/77	Main Water Orifice Pressure Cell	0-1500 psi
43	L-43	12797		6/2/77	Main Steam Orifice DP Cell (Hi)	0-25 psid
44	L-44	12794		6/4/77	Main Water Orifice DP Cell (Hi)	0-25 psid
45	L-45	12793		6/3/77	Bypass Steam Orifice DP Cell (Hi)	0-25 psid
46	L-46	12796		6/3/77	Bypass Water Orifice DP Cell (Hi)	0-25 psid
47	L-47	968		6/1/77	Bypass Steam Orifice Pressure Cell	0-1500 psi
48	L-48	971		6/2/77	Bypass Water Orifice Pressure Cell	0-1500 psi
49	L-49				Main Steam Orifice Thermocouple	0-600°F
50	L-50		F-34		Main Water Orifice Thermocouple	0-600°F
51	L-51				Bypass Steam Orifice Thermocouple	0-600°F

TABLE 4-2 (Cont'd.)

TYPICAL INSTRUMENTATION LIST

Scanner Channel Number	Instrument Location Number	Serial Number	FM Number	Date Calib.	Description	Range
52	L-52				Bypass Water Orifice Thermocouple	0-600°F
53	L-53	88159		6/6/77	Bypass Water Orifice RTD	0-600°F
54	L-54	88160		6/10/77	Bypass Steam Orifice RTD	0-600°F
56	L-56	14374		6/7/77	Pump Discharge RTD	0-600°F
57	L-57				Ambient Temperature	0-200°F
58	L-58	88163		6/6/77	Main Water Orifice RTD	0-600°F
59	L-59	88158		6/8/77	Main Steam Orifice RTD	0-600°F
60	L-73	45516		6/6/77	Loop Flow Control Valve DP Cell	0-200 psid
61	L-74	47673		6/3/77	Pump Suction (Inlet Leg-to-Flange)	0-10 psid
62	L-62				Not Used	
63					Not Used	
64	L-79	18384	F-29	6/2/77	Blowdown Leg Pressure Cell	0-1500 psi
65	L-65	1035	F-30	6/2/77	H.P. Drum Pressure Cell	0-1500 psi
66	L-66	45517	F-39	6/6/77	Pump Flange to Flange DP Cell	-100/0/200 psid

TABLE 4-2 (Cont'd.)

TYPICAL INSTRUMENTATION LIST

Scanner Channel Number	Instrument Location Number	Serial Number	FM Number	Date Calib.	Description	Range
67			F-26		Blowdown Sequence Indicator	
68	L-68	47674		6/7/77	Pump Impeller (Front-to-Back) D/P	0-25 psid
69	L-80	45518	F-38	6/7/77	Main Water Orifice D/P	0-100 psid

The data reduction sequence as shown in Figure 4-1 involves the followings steps.

1. Digitization of the analog FM data at prescribed sampling frequencies, 200 samples/sec and 20 samples/sec, which results in the creation of the Digitized Raw Data File.

2. Creation of the Time Step Schedule File containing the desired schedule of calculation intervals. A maximum of 5000 time values can be employed to process transient data currently.

3. Creation of the Calibration Constant Data File which contains the conversion constants for the instruments employed in the blowdown test.

4. Using these files as input, the Transient Data Reduction Program (TDR) converts the raw data into selected parameters in engineering units.

5. The output of the data reduction program can be obtained as hard copy printout, microfilm or microfiche and/or stored as a data file for later use in plotting.

6. The plot data file can be employed in conjunction with the experimental data plot program described in Volume VIII to produce computer generated plots of desired parameters.

The above process, made up of the components as shown in Figure 4-1 enables the raw transient test data acquired by the FM-Multiplex System during the blowdown tests to be converted into useful operating and performance parameters in an orderly fashion.

4.2.1 Conversion of FM Channel Outputs to Engineering Units

4.2.1.1 Measured Parameters. The FM Multiplex Recording System operates on a higher range of voltages than does the data scanner digital voltmeter. Therefore, the signal from a given transducer receives additional amplification before being fed into the FM system. A voltage recorded by the FM system as read out by the analog-to-digital conversion system is next converted to the equivalent scanner millivolt reading by multiplying by the constant, scanner millivolt to FM volt ratio, appropriate for the particular transducer and FM channel. This ratio is furnished for each channel (See Table 4-3) and is incorporated directly into the code because changes are rare. Also, before this equivalent scanner millivoltage is inserted in the pertinent conversion equation, the "instrument zero" voltage for zero input to the sensor is subtracted out because the conversion equation was developed on the basis of the zero-adjusted scanner millivoltage.

$$RC = E\left[\frac{\text{Scanner Millivolt}}{\text{FM Volt}}\right] - Z \qquad (4\text{-}1)$$

where

RC is the zero-adjusted millivolt input from the transducer to the scanner,

E is the voltage indicated by the FM system, and

Z is the "instrument zero" and is the output in millivolts from the instrument for zero input to the sensor.

The detailed conversions for the various types of devices are given below. In the equations, K is the index number obtained by subtracting 1 from the FM channel number, C(1,K) thru C(6,K) are the calibration constants and C(7,K) is the uncertainty derived from calibration data.

1. Thermocouples

The temperature θ_C in °C is the solution of:

$$\sum_{J=1}^{9}\left[PAC(J)\ \theta_C^{(J-1)}\right] + 125\ e^{-0.5\left\{\frac{\theta_C - 127}{65}\right\}^2} = 1000\ [RC + 2.6621) \qquad (4\text{-}2)$$

where PAC(J) is a standard data pack (See Reference 3) contained within the program.

An equation similar to Equation (4-2) is developed in Reference 4 for the normal reference point temperature of 32.18°F (Ice Point). Equation (4-2) employs a reference point temperature of 150°F.

2. Pressure Cells

$$P = C(1,K)\rho + C(2,K) + C(3,K)RC + C(4,K)(RC)^2 + P_a \qquad (4\text{-}3)$$

Table 4-3

Scanner Millivolt to FM Volt Ratios

Instrument	Conversion Ratio Set 1*	Set 2**
1. Thermocouples	2	2
2. Pressure Cells	16	16
3. Differential Pressure Cells		
(i) DP Cells across pump	20	20
(ii) All other DP cells	16	16
4. Drag Discs		
(i) HI-Suction	20	38.29
(ii) HI-Discharge	20	38.41
(iii) LO-Suction	20	38.48
(iv) LO-Discharge	20	38.50
5. Turbine Meters	20	20
6. Gamma Densitometer	20	20
7. Speed Meter	20	20
8. Torque Meter	20	39.216
9. Magnetic Flow Meter	--	16

* Set 1 was employed for Tests 246, 252, 475 and 497 in Phase I.

** Set 2 was employed for all Phase II tests and all other Phase I tests.

where P is the absolute pressure in psia,
P_a is the atmospheric pressure in psia, and
ρ is the density of the fluid in lbm/in^3.

The first term on the right hand side of Eq. (4-3) accounts for the static pressure difference between the location of the pressure tap in the loop and the location of the pressure transducer.

3. Differential Pressure Cells

$$\Delta P = C(1,K)\rho+[C(2,K)+C(4,K)P+\{C(3,K)+C(5,K)P\}(RC)]C(6,K) \quad (4\text{-}4)$$

where ΔP is the differential pressure in psi,
P is a system pressure representative of pressure level at the differential pressure cell, psia.

4. Drag Discs

$$(\rho V^2)_{dd}=C(1,K)+C(2,K)\ [RC-C(3,K)(T-T_{ref})] \quad (4\text{-}5)$$

where (ρV^2) is the momentum flux in $lbm/ft\text{-}sec^2$,
T is a measured temperature in the drag disc structure in °F, and
T_{ref} is the reference temperature in the term which compensates for temperature effects in the drag disc structure and sensor. For final post-test data reduction T_{ref} is 525 °F.

5. Turbine Meters

$$V_{tm} = C(1,K) + C(3,K)\ RC \quad (4\text{-}6)$$

where V_{tm} is the fluid velocity in ft/sec.

6. Gamma Densitometer

$$\rho_{gd} = C(1,K) + C(2,K)\log_e[RC-C(3,K)] \quad (4\text{-}7)$$

where ρ_{gd} is the density in lbm/ft^3.

7. Speedmeter

$$N_S = C(1,K)+C(2,K)C(4,K)RC \tag{4-8}$$

where N_S is the speed in rpm.

8. Torque Meter

$$\tau_s = \frac{-C(2,K)\ [RC-C(3,K)]}{12} \tag{4-9}$$

where τ_s is the shaft torque in ft-lbf.

9. Magnetic Flowmeter

$$Q = C(1,K)RC \tag{4-10}$$

where Q is the volume flow rate in gpm.

This equation is not included in the TDR program versions, TDRFWD1UPD, TDRREV1UPD and TDRFWD2UPD.

4.2.1.2 Derived Parameters. The detailed conversions for the various derived parameters calculated are given below.

1. Friction Torque

From the friction and windage torque tests (see Volume II) the following expression was provided for the friction torque in ft-lbf.

$$\tau_f = [-0.018(P_{avg}-P_{atm})+0.0000305(P_{avg}-P_{atm})^2+0.08098|N_S| \\ -4.155x10^{-6}\ N_S^2]/12 \tag{4-11}$$

where P_{avg} is the arithmetic average of the pump inlet and exit pressures in psia. This formulation represents a slightly different fit to the friction and windage data than was used for steady-state data reduction (See Volume VIII, Data Processing Methods). The small

differences are comparable to the friction data uncertainties and are of little consequence except possibly near all steam conditions (See Volume II, Section 5.4.5).

2. Hydraulic Torque

From the equation which describes the change in pump impeller speed, the hydraulic torque in ft-lbf can be expressed as:

$$\tau_h = \tau_s - \tau_f - \frac{I_p}{g_c} \frac{d\omega}{dt} \qquad (4\text{-}12)$$

where I_p is the moment of inertia of the pump rotor and coupling in lbm-ft^2,
g_c is the gravitational constant, 32.174 lbm-ft/lbf-sec^2, and
ω is the angular velocity of the pump rotor in rad/sec.

3. Test Pump Injection Flow In

The test pump seal injection inlet flow is determined from the differential pressure measurement across the orifice in the inlet injection line. The ASME Power Test Codes, Flow Measurement Section (Ref. 5) give this mass flow rate in lbm/hr as:

$$W_i = 359\ C\ D_o^2\ F_a\ Y\ (27.673\ \Delta P/v)^{1/2} \qquad (4\text{-}13)$$

where ΔP is the differential pressure across the orifice in psi,
v is the fluid specific volume in ft^3/lbm,
C is the discharge coefficient of the orifice,
D_o is the orifice diameter in inches,
F_a is the orifice thermal expansion factor, and
Y is a fluid expansion factor for compressibility.

The test pump injection flow in is not calculated in the TDR program versions, TDRFWD1UPD, TDRREV1UPD, and TDRFWD2UPD.

4. Test Pump Injection Flow Out

The magnetic flow meter measures this flow rate as Q gallons per minute, and the mass flow rate in lbm/hr can be expressed as:

$$W_o = \frac{60\ \rho Q}{7.4805} \qquad (4\text{-}14)$$

The TDR program versions, TDRFWD1UPD, TDRREV1UPD, and TDRFWD2UPD do not include this equation for the calculation of injection flow out.

5. Net Injection Flow At the Test Pump

$$W_\ell = W_o - W_i \qquad (4\text{-}15)$$

This equation is not included in the TDR program versions, TDRFWD1UPD, TDRREV1UPD, and TDRFWD2UPD.

6. Fluid Void Fraction

The fluid void fractions at various locations are calculated from the fluid densities either directly measured at these locations (gamma densitometer) or determined from other instrument measurements (turbine meter and drag disc). In addition, the vapor and liquid saturation properties are also used.

Combining drag disc and turbine meter measurements, the corresponding density of the two phase mixture is written as:

$$\rho_{mix} = (\rho V^2)_{dd}/(V_{tm})^2$$

where $(\rho V^2)_{dd}$ is the momentum flux measured by the drag disc in lbm/ft-sec^2, and

V_{tm} is the velocity measured by the turbine meter.

The local void fraction of the mixture is expressed as:

$$\alpha_F = \frac{\rho_\ell - \rho_{mix}}{\rho_\ell - \rho_v}$$

where ρ_ℓ, ρ_v are the saturation densities of the liquid and vapor, respectively.

The saturation properties are obtained from the ASME steam tables using the local pressure.

7. Volumetric Flow Rate

- Drag Disc - Gamma Densitometer Combination

$$Q = \left[\frac{(\rho V^2)_{dd}}{\rho_{gd}}\right]^{1/2} A_c \times 60 \times 7.48 \qquad (4\text{-}17)$$

where Q is the volumetric flow rate in gpm, and
A_c is the cross-sectional area of the nominal six inch suction and discharge pipe legs, 0.181 ft^2 (6" Sch. 140).

- Turbine Meter

$$Q = V_{tm} A_c \times 60 \times 7.48 \qquad (4\text{-}18)$$

8. Momentum Flux

The momentum flux in $lbm/ft\text{-}sec^2$ is either directly measured (by the drag disc) or computed from two instrument measurements, namely from the gamma densitometer measurement and the turbine meter measurement as:

$$\rho V^2 = (\rho_{gd})(V_{tm})^2 \qquad (4\text{-}19)$$

9. Mass Flow Rate

The mass flow rate in lbm/sec using various instrument measurements is calculated as follows.

- Drag Disc - Gamma Densitometer Combination

$$\dot{M} = ((\rho V^2)_{dd}\, \rho_{gd})^{1/2}\, A_c \qquad (4\text{-}20)$$

- Turbine Meter - Gamma Densitometer Combination

$$\dot{M} = \rho_{gd} V_{tm} A_c \qquad (4\text{-}21)$$

10. Integrated Mass

The amount of mass that has flowed through the suction or discharge side of the pump over a given time is computed by using the trapezoidal rule to numerically integrate the mass flow rate function.

Thus, at any time t, the integrated mass in lbm can be expressed as:

$$MI(t) = MI(t-\Delta t)+1/2[|\dot{M}(t)|+|\dot{M}(t-\Delta t)|]\Delta t \qquad (4\text{-}22)$$

where Δt is the time step size employed for data processing.

Various normalized pump parameters are also derived from the primary and derived parameters indicated above. For the initial data presentation, these normalizations are based on the rated (normal peak efficiency) values of performance parameters from the manufacturer's cold water tests of the model test pump which are as follows:

Head	252 ft
Flow	3500 gpm
Speed	4500 rpm
Torque	308 ft-lbf(at 62.3 lbm/ft^3 density)

4.2.2 Output Description of Reduced Transient Data

The final output of the TDR program can be in the form of hard copy (paper) printout and/or microfiche of the information on the hard copy printout, and/or a disc file (plot data file) containing an assortment of extracted and further derived parameters of special interest (See Table 4-4). Details of the TDR program are provided in Volume VIII, Data Processing Methods.

Table 4-4

STANDARD PLOT FILE PARAMETERS FOR THE TRANSIENT DATA REDUCTION CODE

Plot No.*	Plot Type**	Parameter Designator	Description of Parameter
1	1	PSUCT	Pump Suction Pressure
2	1	PDISCH	Pump Discharge Pressure
3	1	PBDN	Blowdown Leg Pressure
4	11	TSUCT	Pump Suction Fluid Temperature
5	11	TDISCH	Pump Discharge Fluid Temperature
6	5	SGD1RHØ	Density Beam 1 GD Suction
7	5	SGD2RHØ	Density Beam 2 GD Suction
8	5	SGD3RHØ	Density Beam 3 GD Suction
9	5	DGD1RHØ	Density Beam 1 GD Discharge
10	5	DGD2RHØ	Density Beam 2 GD Discharge
11	5	DGD3RHØ	Density Beam 3 GD Discharge
12	5	AECL1RHØ	Density Beam 1 AECL GD
13	5	AECL2RHØ	Density Beam 2 AECL GD
14	5	AECL3RHØ	Density Beam 3 AECL GD
15	7	SGD1VF	Void Fraction Beam 1 GD Suction
16	7	SGD2VF	Void Fraction Beam 2 GD Suction
17	7	SGD3VF	Void Fraction Beam 3 GD Suction
18	7	DGD1VF	Void Fraction Beam 1 GD Discharge
19	7	DGD2VF	Void Fraction Beam 2 GD Discharge
20	7	DGD3VF	Void Fraction Beam 3 GD Discharge
21	7	AECL1VF	Void Fraction Beam 1 AECL GD
22	7	AECL2VF	Void Fraction Beam 2 AECL GD
23	7	AECL3VF	Void Fraction Beam 3 AECL GD
24	2	SGDDDLNU	Norm. Vol. Flow Rate LØ-DD/GD2 Suction
25	2	SGDDDHNU	Norm. Vol. Flow Rate HI-DD/GD2 Suction
26	2	STMLNU	Norm. Vol. Flow Rate LØ-TM Suction

* Employed as the designator index in the BUFFER 1 and BUFFER 2 subroutines

** Employed in the experimental data plot program

Table 4-4 (Cont'd.)

STANDARD PLOT FILE PARAMETERS FOR THE TRANSIENT DATA REDUCTION CODE

Plot No.*	Plot Type**	Parameter Designator	Description of Parameter
27	2	STMHNU	Norm. Vol. Flow Rate HI-TM Suction
28	2	DGDDDLNU	Norm. Vol. Flow Rate LØ-DD/GD2 Discharge
29	2	DGDDDHNU	Norm. Vol. Flow Rate HI-DD/GD2 Discharge
30	2	DTMLNU	Norm. Vol. Flow Rate LØ-TM Discharge
31	2	DTMHNU	Norm. Vol. Flow Rate HI-TM Discharge
32	12	SGDDDHMFR	Mass Flow Rate HI-DD/GD2 Suction
33	12	SGDDDLMFR	Mass Flow Rate LØ-DD/GD2 Suction
34	12	DGDDDHMFR	Mass Flow Rate HI-DD/GD2 Discharge
35	12	DGDDDLMFR	Mass Flow Rate LØ-DD/GD2 Discharge
36	6	SGDTMLMFX	Momentum Flux GD2/LØ-TM Suction
37	6	SGDTMHMFX	Momentum Flux GD2/HI-TM Suction
38	6	SDDLMFX	Momentum Flux LØ-DD Suction
39	6	SDDHMFX	Momentum Flux HI-DD Suction
40	6	DGDTMLMFX	Momentum Flux GD2/LØ-TM Discharge
41	6	DGDTMHMFX	Momentum Flux GD2/HI-TM Discharge
42	6	DDDLMFX	Momentum Flux LØ-DD Discharge
43	6	DDDHMFX	Momentum Flux HI-DD Discharge
44	3	HDPSI	Pump Head in psi
45	4	PHSN	Norm. Static Pump Head
46	4	PHTN	Norm. Total Pump Head
47	8	PMPSPDN	Norm. Pump Speed
48	9	SHFTTØRN	Norm. Pump Shaft Torque
49	9	HYDRTØRN	Norm. Pump Hydraulic Torque
50	13	SGDDDHIM	Integrated Mass HI-DD/GD2 Suction
51	13	SGDDDLIM	Integrated Mass LØ-DD/GD2 Suction

* Employed as the designator index in the BUFFER 1 and BUFFER 2 subroutines

** Employed in the experimental data plot program

Table 4-4 (Continued)

STANDARD PLOT FILE PARAMETERS FOR THE TRANSIENT DATA REDUCTION CODE

Plot No.*	Plot Type**	Parameter Designator	Description of Parameter
52	13	DGDDDHIM	Integrated Mass HI-DD/GD2 Discharge
53	13	DGDDDLIM	Integrated Mass LØ-DD/GD2 Discharge
54	12	SGDTMHMFR	Mass Flow Rate HI-TM/GD2 Suction
55	12	SGDTMLMFR	Mass Flow Rate LØ-TM/GD2 Suction
56	12	DGDTMHMFR	Mass Flow Rate HI-TM/GD2 Discharge
57	12	DGDTMLMFR	Mass Flow Rate LØ-TM/GD2 Discharge
58	10	PMPACCEL	Pump Acceleration in rad/sec^2
59	9	FRICTØRN	Norm. Pump Friction & Windage Torque
60	13	SGDTMHIM	Integrated Mass HI-TM/GD2 Suction
61	13	SGDTMLIM	Integrated Mass LØ-TM/GD2 Suction
62	13	DGDTMHIM	Integrated Mass HI-TM/GD2 Discharge
63	13	DGDTMLIM	Integrated Mass LØ-TM/GD2 Discharge
64	12	INJINMFR	Pump Injection Mass Flow Rate In
65	12	INJØUTMFR	Pump Injection Mass Flow Rate Out
66	12	INJLEAKMFR	Seal Injection Leakage Mass Flow Rate

* Employed as the designator index in the BUFFER 1 and BUFFER 2 subroutines

** Employed in the experimental data plot program

4.3 DATA FORMAT

4.3.1 Analog And Digital Data Files

The FM Data Acquisition System used for the transient tests consisted of an 8-track FM tape recorder together with a 40-channel FM multiplex system. Five data channels were multiplexed onto each track of the tape recorder. Therefore, the analog magnetic tape record consists of eight tracks of five channels each for every blowdown.

The analog tape acquired for each transient was converted to a digitized tape which could be directly used by a high speed digital computer. The actual digitization process was accomplished with a special purpose mini-computer system. Each of the 40 channels of FM data (39 channels of data and one channel for voltmeter short) was sampled at a predetermined rate and the analog signal converted into a voltage which was stored as a number on the digitized magnetic tape.

Sample rates of 200 and 20 samples per second were used. The resulting digitized data tape for each transient contained the 200 sample/sec records of all 40 channels for up to the first six minutes of the transient followed by the 20 sample/sec records for the entire length of the analog tape. This digitized magnetic tape record was entered into the C-E computer for access by the Transient Data Reduction Program. Further details of the FM system and digitization process may be found in Volume VIII, Data Processing Methods.

4.3.2 Time Plots and Cross Plots

Plotting of the reduced data is accomplished by means of the experimental data plot program described in Volume VIII. This program has the capability of plotting as many as 5000 points for any measured or derived parameter, and can generate both time-plots and cross-plots. The time plot refers to an X-Y plot of any pump or loop parameter versus time. The time value is represented on the X-axis while the parameter values are represented on the Y-axis. Occasionally, cross-plots of pump and/or loop blowdown parameters are of interest and the plot program is capable of generating such plots. It refers to an X-Y plot of any one pump or loop parameter versus any other pump or loop parameter. For almost all the blowdown tests, the time-plots of transient data were machine-generated (i.e., by employing the experimental data plot program described in

Volume VIII). However, the machine-generated cross-plots exhibited a large amount of oscillations, and were found to be cumbersome for analysis purposes. Consequently, cross-plots were manually generated (hand-drawn) after smoothing out the time-plot curves of the pump and/or loop parameters for which the cross-plots were to be generated. These cross-plots include void fraction (α_F) versus normalized pump volumetric flow rate to normalized pump speed ratio (ν/α_N), superficial liquid velocity (V_{SL}) versus superficial vapor velocity (V_{SG}), normalized pump speed (α_N) versus normalized pump volumetric flow rate (ν), and void fraction (α_F) versus pressure (P).

In addition to the time and cross plots generated from FM data, similar plots could also be generated from scanner data recorded during each transient test. While the data scanner was considerably slower than the FM system, it was capable of recording outputs from all 67 instruments, whereas the FM system was limited to recording data from only 39 instruments. Those instruments considered most important for data analysis were recorded on the FM system. Additional parameters considered desirable for both presentation and analysis purposes were plotted from the scanner data. Additionally, both scanner and FM plots were generated for certain parameters for comparison purposes to aid in assessing the overall quality of the transient data. A description of the scanner data acquisition system can be found in Volume VII. A description of the scanner data reduction and plot program is provided in Volume VIII. Scanner plots generated for each transient test are contained in Volume VI.

4.3.3 Extent of Data in Report Versus Data Available

Almost all the transient data presented in this report are in plot form, either as time-plots or as cross-plots. At times, selected transient parameter values are presented in tabular form as in the case of the comparison of transient data versus steady-state data (See Volume IV). A list of which types of data compilation are included in this report and which are otherwise available is given in Table 4-5. A more detailed list of data that are not presented in the report but available in EPRI files is as follows:

1. Raw FM analog signals for each transient test on magnetic tape. Approximate blowdown duration: 7 - 25 minutes

2. Digitized raw data for each transient at two different sampling frequencies, namely 20 samples/sec and 200 samples/sec on magnetic tape. The 200 samples/sec data covers a blowdown duration of approximately 300 seconds.

3. Raw scanner data in millivolts for the transient parameters at 5 second time intervals on magnetic tape.

Table 4-5

AVAILABILITY OF
TRANSIENT (BLOWDOWN) DATA COMPILATIONS

Included in Report (Volume/Section No.)	Available in EPRI Files
Matrix Table of tests (III/3.2)	Raw FM analog data
Time-plots of blowdown (III/5, VI/2) parameters	Raw data for each transient at digitizing frequencies of 20 samples/sec and 200 samples/sec.
Cross-plots of blowdown (III/5) parameters	Raw scanner data
Scanner time-plots of blowdown parameters (VI/3)	Calibration constants for each transient
Calibration data for each (VIII/2) blowdown test	
Comparisons with steady-state (IV/2) performance	
Special topic curves (III/5.7)	

4.4 SAMPLES OF TEST DATA

The reduced data for the transient tests are not readily amenable for presentation in a compact summary table form, since it encompasses a large number of parameter values for a large number of distinct time intervals. Instead, most of the reduced transient data is presented in plot form, either as time-plots or as cross-plots (See Volume VI). A summary of the actual initial operating conditions and other pertinent conditions for all the transient tests is provided in Section 3.2. In addition, values of pump operating and performance parameters for selected times during the blowdown are presented in tabular form in Volume IV, Section 2, for comparison with steady-state data. These parameters include pressures, volumetric flow rates, void fractions, densities, pump speed and head, and hydraulic torque.

Since the bulk of the transient data is presented in plot form, indexes to the data plots for each test were developed to aid in identifying individual plots. The transient tests were grouped according to the number of instruments employed for each test, which resulted in three groups of tests and corresponding indexes. These indexes are presented in Tables 4-6 through 4-8 and consist of plot numbers and descriptions of the corresponding plot parameters. Because of instrument malfunctions, which did occur at various times during testing, it was not possible to generate all the plots listed in these standard index tables for each test of a specific group. For this reason individual indexes were also developed to identify any deviations from the standard indexes. The individual indexes and associated plots for each transient test can be found in Volume VI, Transient Data.

As described in Section 4.2, the transient plot parameters consist of pressures, temperatures, densities, void fraction, normalized volumetric flow rates, mass flow rates, momentum fluxes, pump head, normalized pump speed, normalized shaft and hydraulic torques, and integrated masses. In addition, for selected tests, plots of seal injection flow in and out, and net injection flow into the mainstream at the test pump are also available.

The plot duration for the transient test parameters varied somewhat. Typically it is 280 seconds for intermediate (30-40%) and full (100%) size breaks and 560 seconds for small (5%) breaks. These time durations were

arrived at by considering such factors as amount of time required for the blowdown line pressure to reach a value of approximately 20 psia, and special purpose testing performed towards the end of the blowdown (blowdown valve closing and opening, test pump seal injection valve closing or opening, etc.). Samples of the blowdown plots for typical transient tests are presented in Figures 4-3 through 4-13.

The transient test data are presented in Volume VI.

Table 4-6

Standard Plot File Parameters for Phase I
Tests 246, 252, 475 & 497

Plot No.	Description of Parameter
1	Pump Suction Pressure
2	Pump Discharge Pressure
3	Blowdown Line Pressure
4	Pump Suction Temperature
5	Pump Discharge Temperature
6	Density Beam 1 GD Suction
7	Density Beam 2 GD Suction
8	Density Beam 3 GD Suction
9	Density Beam 1 GD Discharge
10	Density Beam 2 GD Discharge
11	Density Beam 3 GD Discharge
12	Density Beam 1 AECL GD
13	Density Beam 2 AECL GD
14	Density Beam 3 AECL GD
15	Void Fraction Beam 1 GD Suction
16	Void Fraction Beam 2 GD Suction
17	Void Fraction Beam 3 GD Suction
18	Void Fraction Beam 1 GD Discharge
19	Void Fraction Beam 2 GD Discharge
20	Void Fraction Beam 3 GD Discharge
21	Void Fraction Beam 1 AECL GD
22	Void Fraction Beam 2 AECL GD
23	Void Fraction Beam 3 AECL GD
24	Norm. Vol. Flow Rate LO-DD/GD2 SUC.
25	Norm. Vol. Flow Rate LO-DD/GD2 DISCH.
26	Norm. Vol. Flow Rate HI-DD/GD2 SUC.
27	Norm. Vol. Flow Rate HI-DD/GD2 DISCH.
28	Norm. Vol. Flow Rate LO-TM Suction
29	Norm. Vol. Flow Rate HI-TM Discharge
30	Mass Flow Rate HI-DD/GD2 Suction
31	Mass Flow Rate LO-DD/GD2 Suction

Table 4-6 (Cont'd.)

Standard Plot File Parameters for Phase I
Tests 246, 252, 475 & 497

Plot No.	Description of Parameter
32	Mass Flow Rate HI-DD/GD2 Discharge
33	Mass Flow Rate LO-DD/GD2 Discharge
34	Momentum Flux GD2/LO-TM Suction
35	Momentum Flux GD2/HI-TM Discharge
36	Momentum Flux HI-DD Suction
37	Momentum Flux HI-DD Discharge
38	Momentum Flux LO-DD Suction
39	Momentum Flux LO-DD Discharge
40	Pump Head in Psi
43	Norm. Pump Speed
44	Norm. Pump Shaft Torque
45	Norm. Pump Hydraulic Torque
46	Integrated Mass HI-DD/GD2 Suc.
47	Integrated Mass LO-DD/GD2 Suc.
48	Integrated Mass HI-DD/GD2 Disch.
49	Integrated Mass LO-DD/GD2 Disch.
51	Mass Flow Rate LO-TM/GD2 Suction
52	Mass Flow Rate HI-TM/GD2 Discharge
55	Integrated Mass LO-TM/GD2 Suction
56	Integrated Mass HI-TM/GD2 Disch.

Table 4-7

Standard Plot File Parameters for Phase I
Tests 676, 701 & 846

Plot No.	Description of Parameter
1	Pump Suction Pressure
2	Pump Discharge Pressure
3	Blowdown Line Pressure
4	Pump Suction Temperature
5	Pump Discharge Temperature
6	Density Beam 1 GD Suction
7	Density Beam 2 GD Suction
8	Density Beam 3 GD Suction
9	Density Beam 1 GD Discharge
10	Density Beam 2 GD Discharge
11	Density Beam 3 GD Discharge
12	Density Beam 1 AECL GD
13	Density Beam 2 AECL GD
14	Density Beam 3 AECL GD
15	Void Fraction Beam 1 GD Suction
16	Void Fraction Beam 2 GD Suction
17	Void Fraction Beam 3 GD Suction
18	Void Fraction Beam 1 GD Discharge
19	Void Fraction Beam 2 GD Discharge
20	Void Fraction Beam 3 GD Discharge
21	Void Fraction Beam 1 AECL GD
22	Void Fraction Beam 2 AECL GD
23	Void Fraction Beam 3 AECL GD
24	Norm. Vol. Flow Rate LO-DD/GD2 Suction
25	Norm. Vol. Flow Rate HI-DD/GD2 Suction
26	Norm. Vol. Flow Rate LO-TM Suction
27	Norm. Vol. Flow Rate HI-TM Suction
28	Norm. Vol. Flow Rate LO-DD/GD2 Discharge
29	Norm. Vol. Flow Rate HI-DD/GD2 Discharge
30	Norm. Vol. Flow Rate LO-TM Discharge
31	Norm. Vol. Flow Rate HI-TM Discharge

Table 4-7 (Cont'd.)

Standard Plot File Parameters for Phase I
Tests 676, 701 & 846

Plot No.	Description of Parameter
32	Mass Flow Rate HI-DD/GD2 Suction
33	Mass Flow Rate LO-DD/GD2 Suction
34	Mass Flow Rate HI-DD/GD2 Discharge
35	Mass Flow Rate LO-DD/GD2 Discharge
36	Momentum Flux GD2/L)-Tm Suction
37	Momentum Flux GD2/HI-TM Suction
38	Momentum Flux LO-DD Suction
39	Momentum Flux HI-DD Suction
40	Momentum Flux GD2/LO-TM Discharge
41	Momentum Flux GD2/HI-TM Discharge
42	Momentum Flux LO-DD Discharge
43	Momentum Flux HI-DD Discharge
44	Pump Head in psi
47	Norm. Pump Speed
48	Norm. Pump Shaft Torque
49	Norm. Pump Hydraulic Torque
50	Integrated Mass HI-DD/GD2 Suction
51	Integrated Mass LO-DD/GD2 Suction
52	Integrated Mass HI-DD/GD2 Discharge
53	Integrated Mass LO-DD/GD2 Discharge
54	Mass Flow Rate HI-TM/GD2 Suction
55	Mass Flow Rate LO-TM/GD2 Suction
56	Mass Flow Rate HI-TM/GD2 Discharge
57	Mass Flow Rate LO-TM/GD2 Discharge
60	Integrated Mass HI-TM/GD2 Suction
61	Integrated Mass LO-TM/GD2 Suction
62	Integrated Mass HI-TM/GD2 Discharge
63	Integrated Mass LO-TM/GD2 Discharge

Table 4-8

Standard Plot File Parameters for Phase II Blowdown Tests

Plot No.	Description of Parameter
1	Pump Suction Pressure
2	Pump Discharge Pressure
3	Blowdown Leg Pressure
4	Pump Suction Fluid Temperature
5	Pump Discharge Fluid Temperature
6	Density Beam 1 GD Suction
7	Density Beam 2 GD Suction
8	Density Beam 3 GD Suction
9	Density Beam 1 GD Discharge
10	Density Beam 2 GD Discharge
11	Density Beam 3 GD Discharge
12	Density Beam 1 AECL GD
13	Density Beam 2 AECL GD
14	Density Beam 3 AECL GD
15	Void Fraction Beam 1 GD Suction
16	Void Fraction Beam 2 GD Suction
17	Void Fraction Beam 3 GD Suction
18	Void Fraction Beam 1 GD Discharge
19	Void Fraction Beam 2 GD Discharge
20	Void Fraction Beam 3 GD Discharge
21	Void Fraction Beam 1 AECL GD
22	Void Fraction Beam 2 AECL GD
23	Void Fraction Beam 3 AECL GD
24	Norm. Vol. Flow Rate LØ-DD/GD2 Suction
25	Norm. Vol. Flow Rate HI-DD/GD2 Suction
26	Norm. Vol. Flow Rate LØ-TM Suction
27	Norm. Vol. Flow Rate HI-TM Suction
28	Norm. Vol. Flow Rate LØ-DD/GD2 Discharge
29	Norm. Vol. Flow Rate HI-DD/GD2 Discharge
30	Norm. Vol. Flow Rate LØ-TM Discharge
31	Norm. Vol. Flow Rate HI-TM Discharge

Table 4-8 (Cont'd.)

Standard Plot File Parameters for Phase II Blowdown Tests

Plot No.	Description of Parameter
32	Mass Flow Rate HI-DD/GD2 Suction
33	Mass Flow Rate LØ-DD/GD2 Suction
34	Mass Flow Rate HI-DD/GD2 Discharge
35	Mass Flow Rate LØ-DD/GD2 Discharge
36	Momentum Flux GD2/LØ-TM Suction
37	Momentum Flux GD2/HI-TM Suction
38	Momentum Flux LØ-DD Suction
39	Momentum Flux HI-DD Suction
40	Momentum Flux GD2/LØ-TM Discharge
41	Momentum Flux GD2/HI-TM Discharge
42	Momentum Flux LØ-DD Discharge
43	Momentum Flux HI-DD Discharge
44	Pump Head in psi
47	Norm. Pump Speed
48	Norm. Pump Shaft Torque
49	Norm. Pump Hydraulic Torque
50	Integrated Mass HI-DD/GD2 Suction
51	Integrated Mass LØ-DD/GD2 Suction
52	Integrated Mass HI-DD/GD2 Discharge
53	Integrated Mass LØ-DD/GD2 Discharge
54	Mass Flow Rate HI-TM/GD2 Suction
55	Mass Flow Rate LØ-TM GD2 Suction
56	Mass Flow Rate HI-TM/GD2 Discharge
57	Mass Flow Rate LØ-TM/GD2 Discharge
60	Integrated Mass HI-TM/GD2 Suction
61	Integrated Mass LØ-TM/GD2 Suction
62	Integrated Mass HI-TM/GD2 Discharge
63	Integrated Mass LØ-TM/GD2 Discharge
64	Pump Injection Mass Flow Rate In
65	Pump Injection Mass Flow Rate Out
66	Seal Injection Leakage Mass Flow Rate

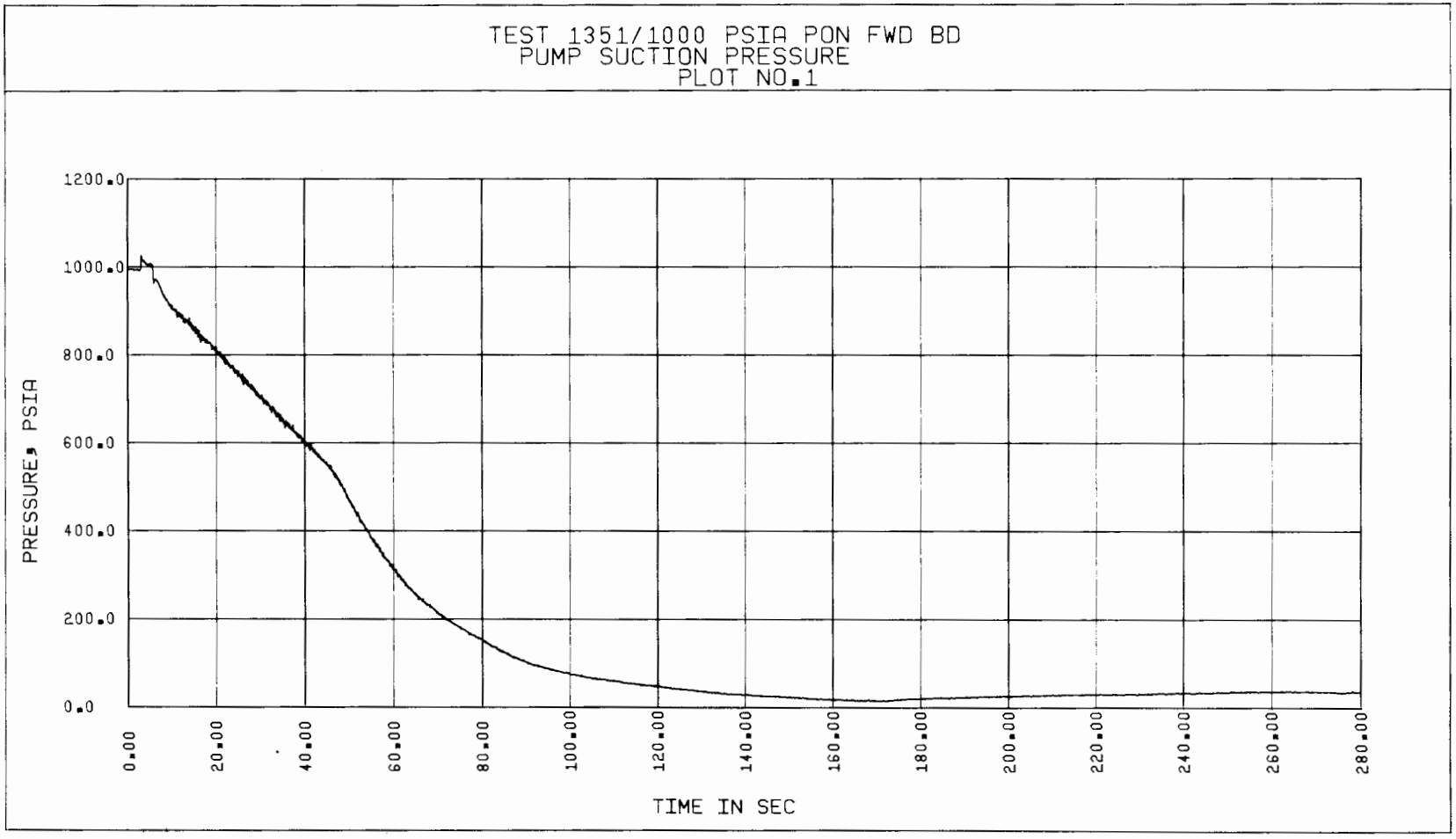

Figure 4-3. Test 1351, Pump Suction Pressure vs Time

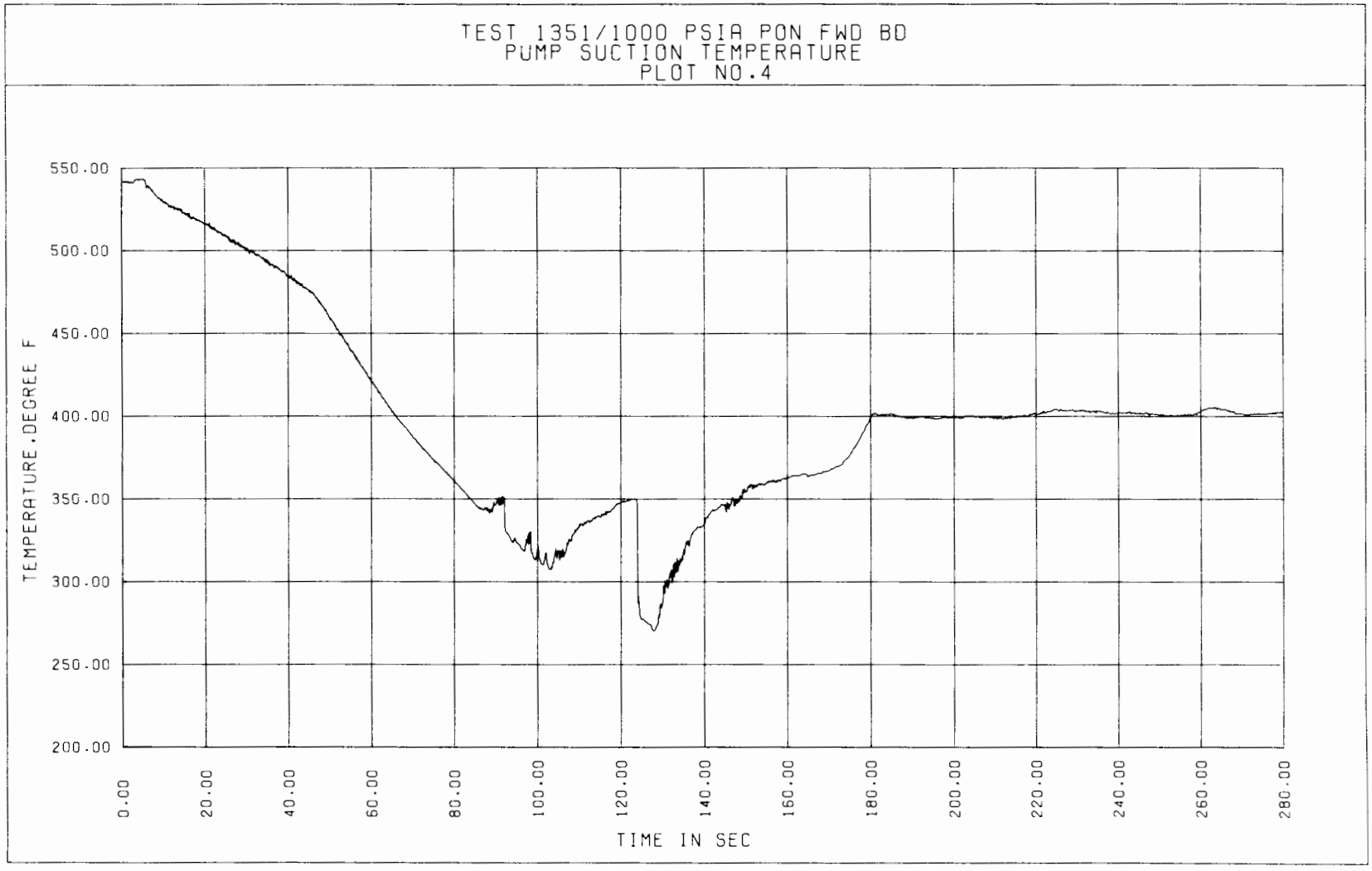

Figure 4-4. Test 1351, Pump Suction Fluid Temperature vs Time

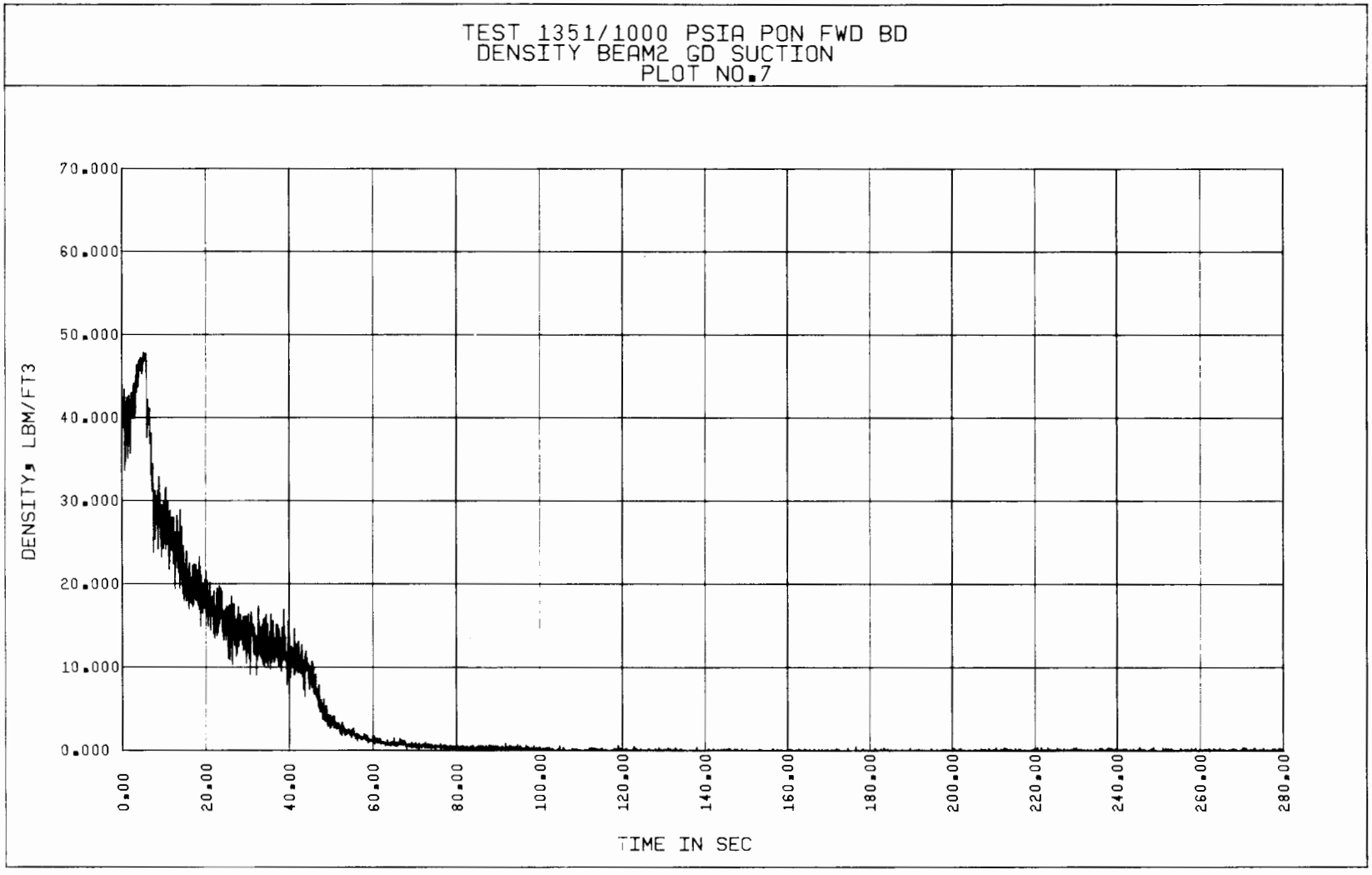

Figure 4-5. Test 1351, Suction Density vs Time

Figure 4-6. Test 1351, Suction Void Fraction vs Time

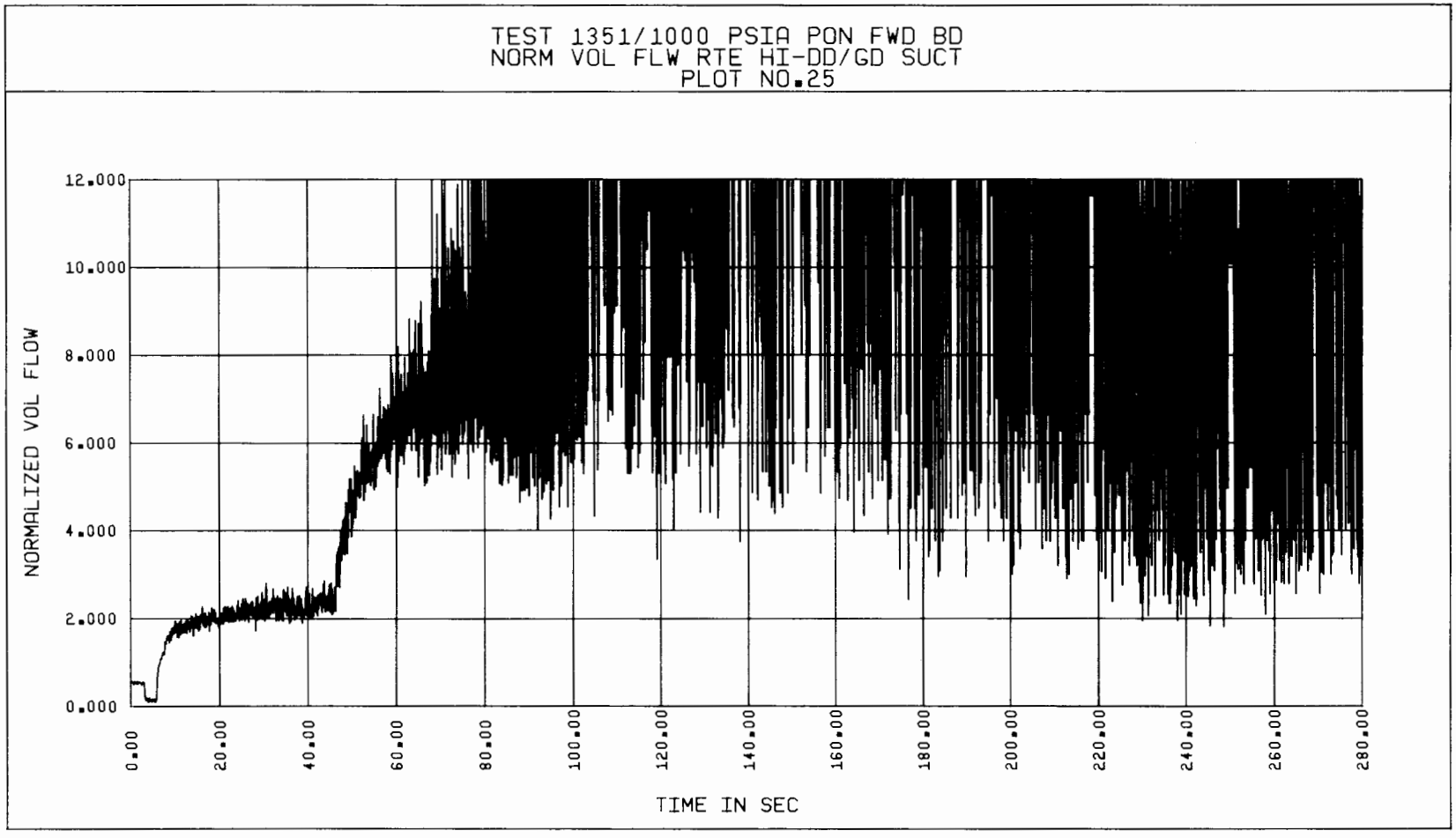

Figure 4-7. Test 1351, Normalized Suction Volumetric Flow Rate vs Time

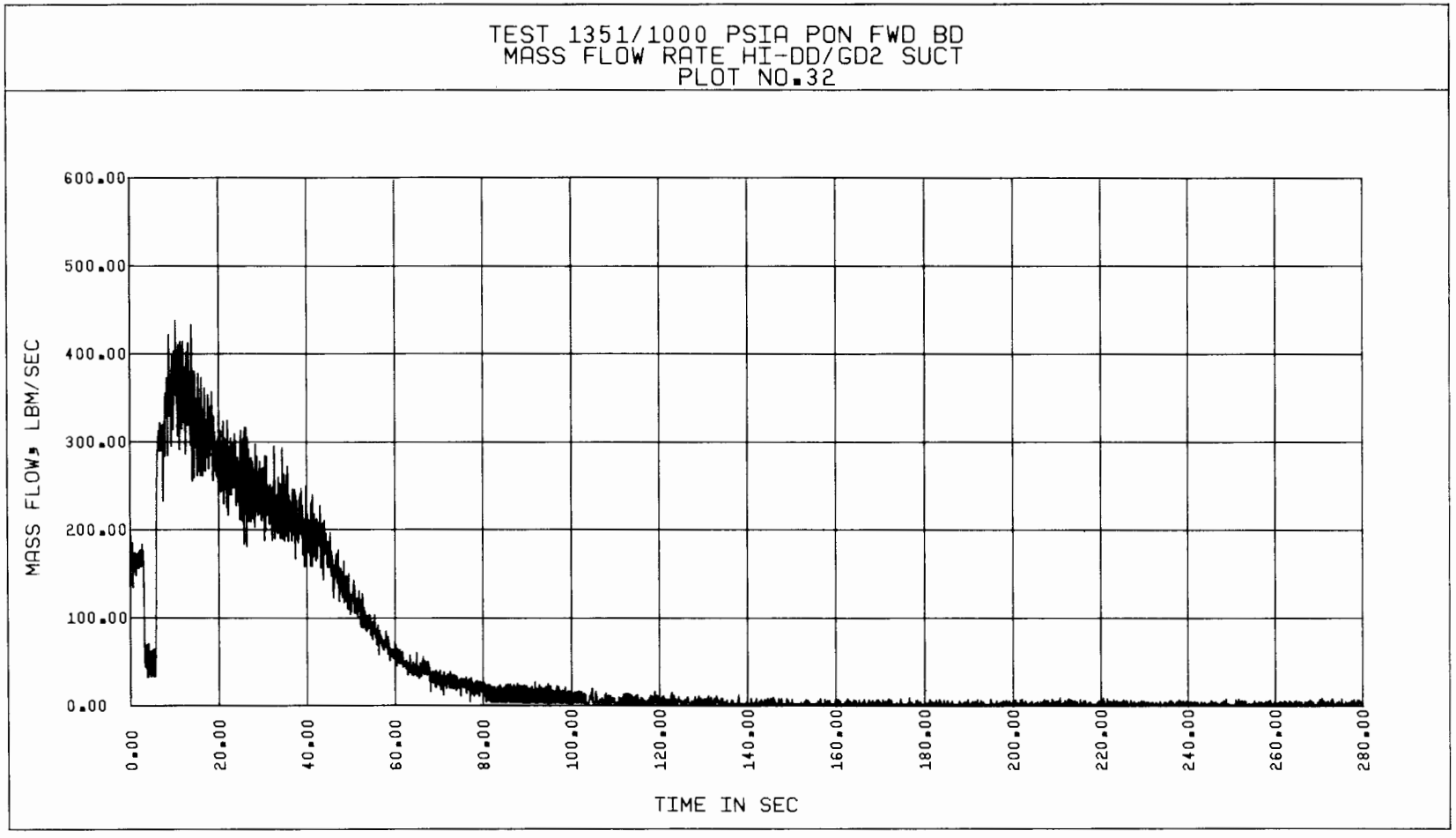

Figure 4-8. Test 1351, Suction Mass Flow Rate vs Time

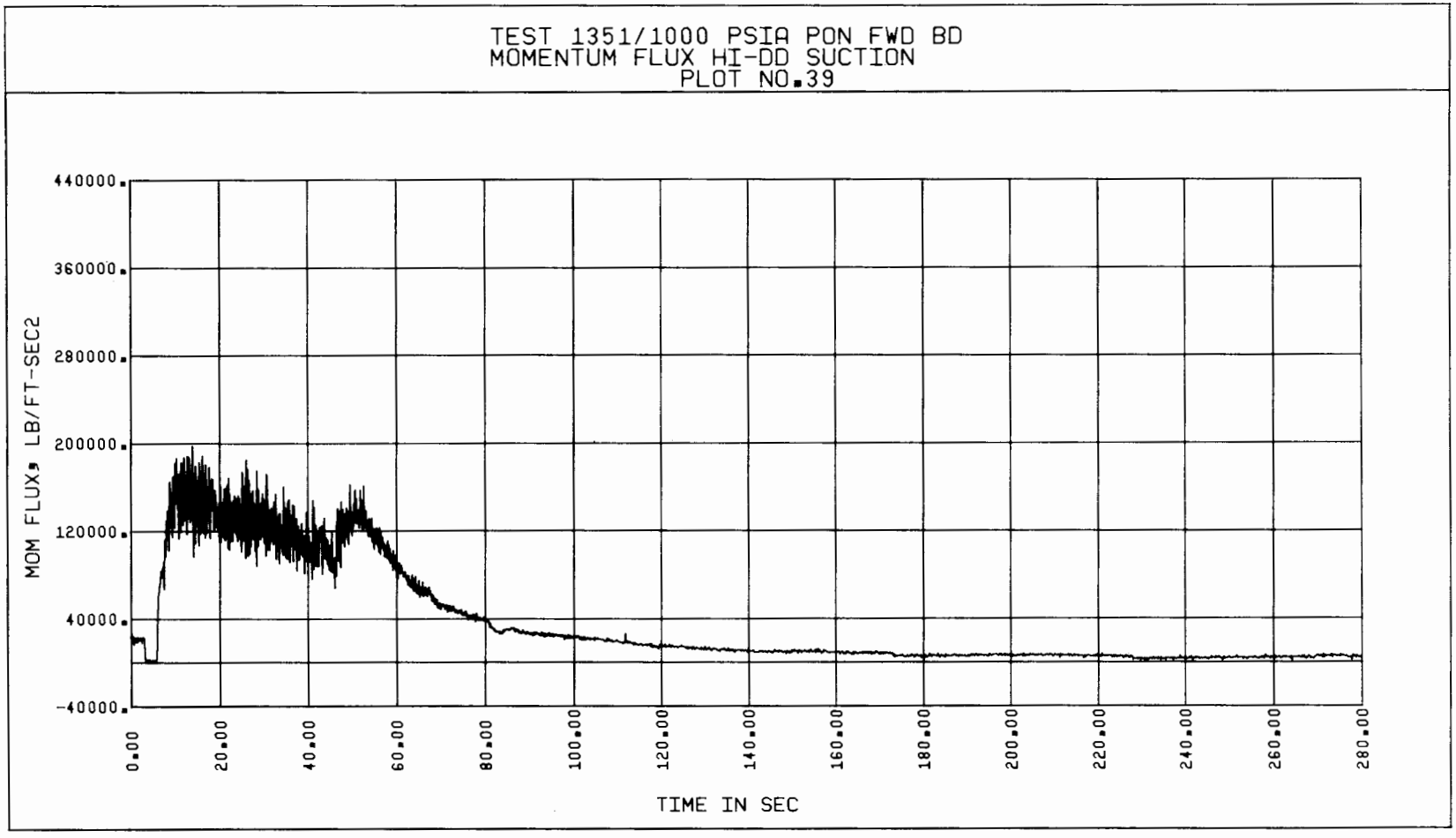

Figure 4-9. Test 1351, Suction Momentum Flux vs Time

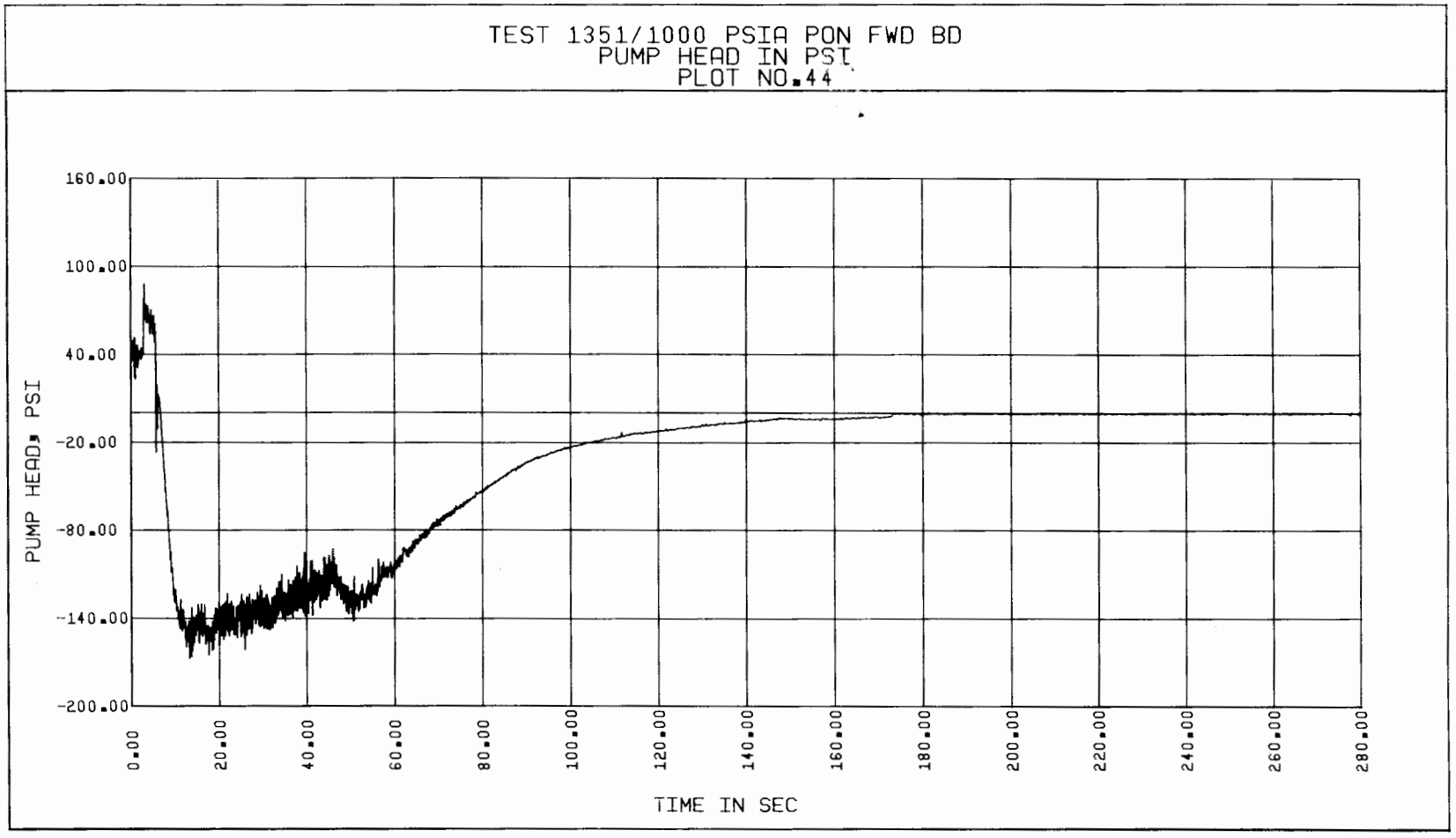

Figure 4-10. Test 1351, Pump Head vs Time

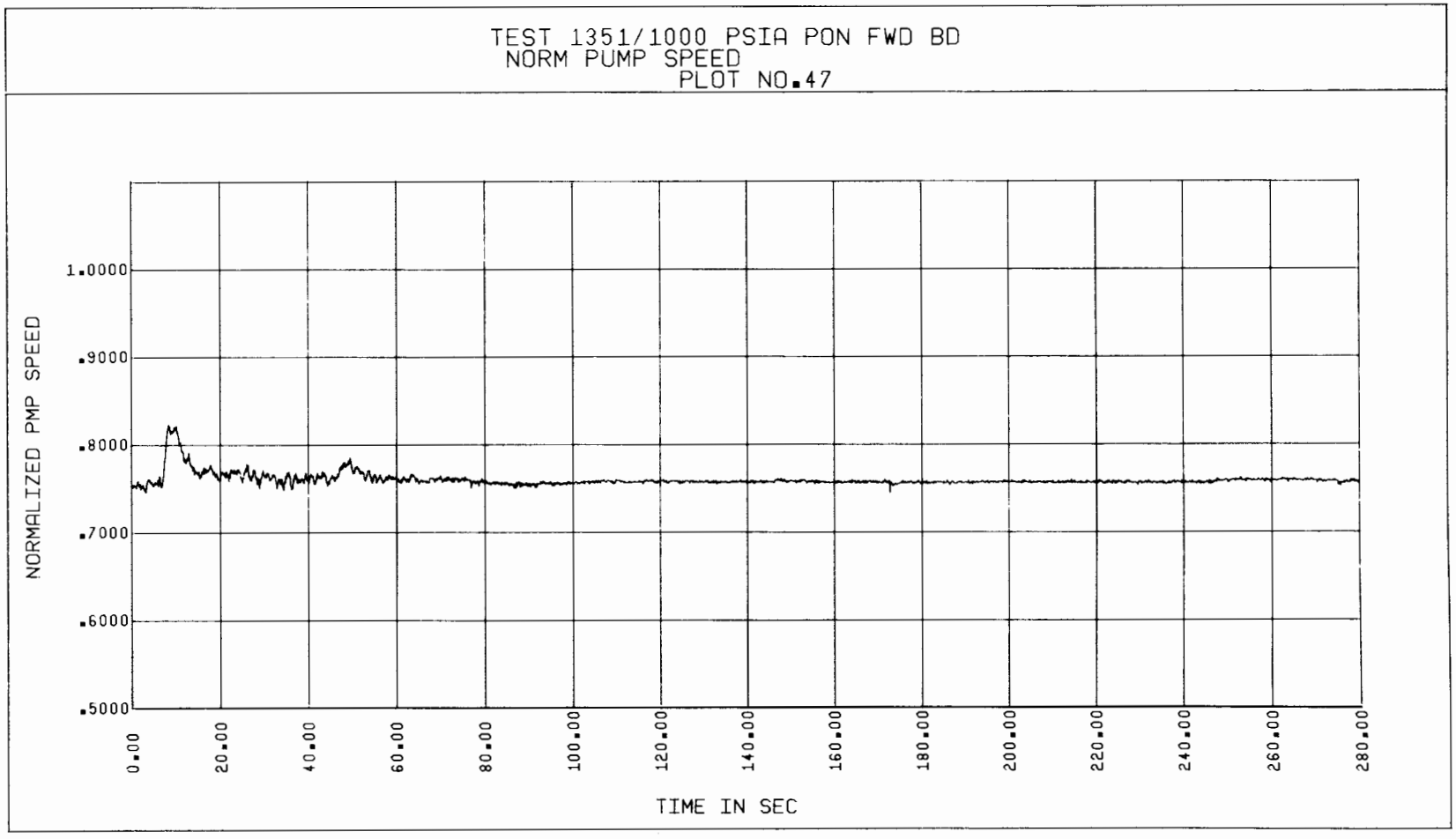

Figure 4-11. Test 1351, Normalized Pump Speed vs Time

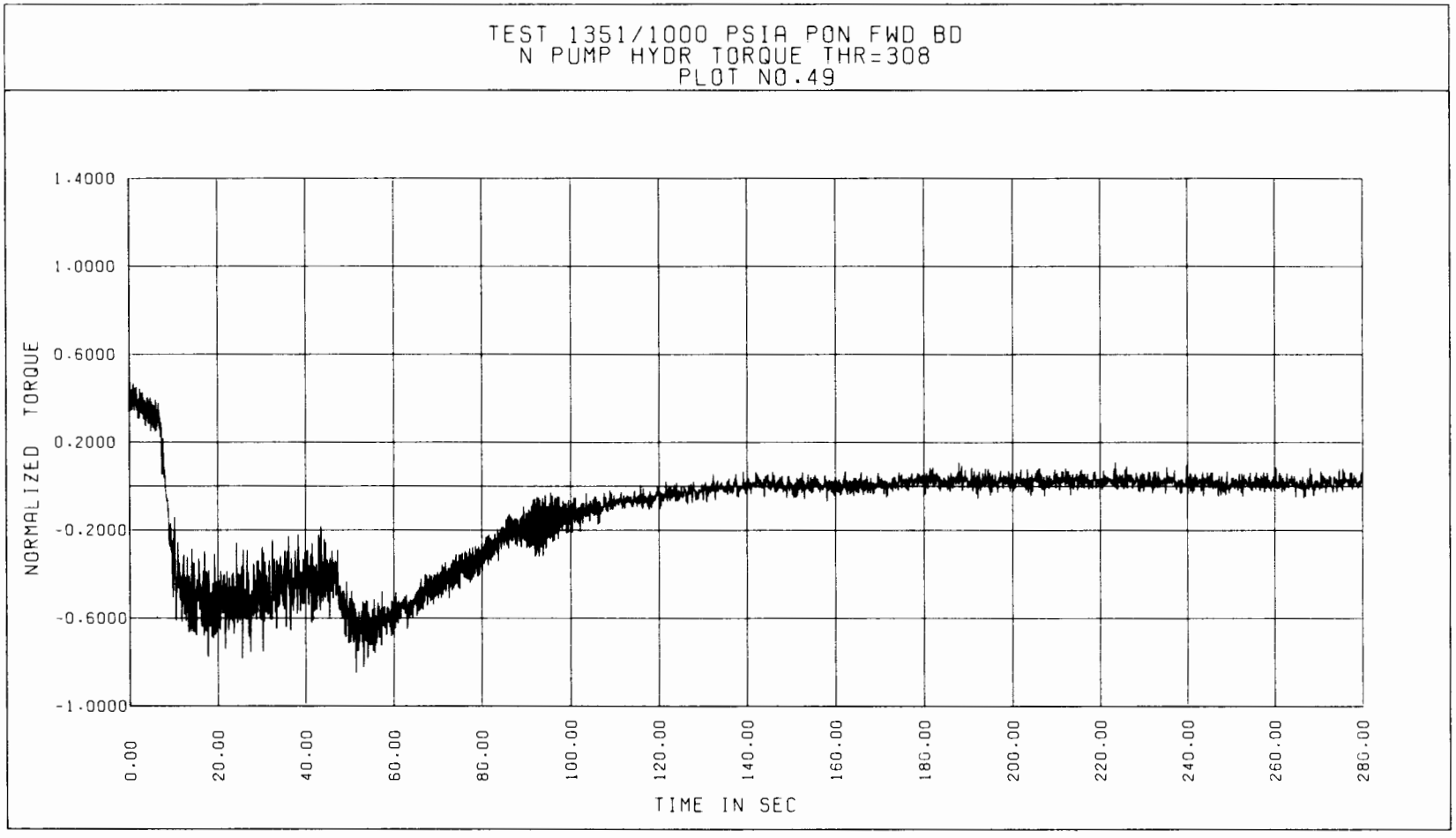

Figure 4-12. Test 1351, Normalized Hydraulic Torque vs Time

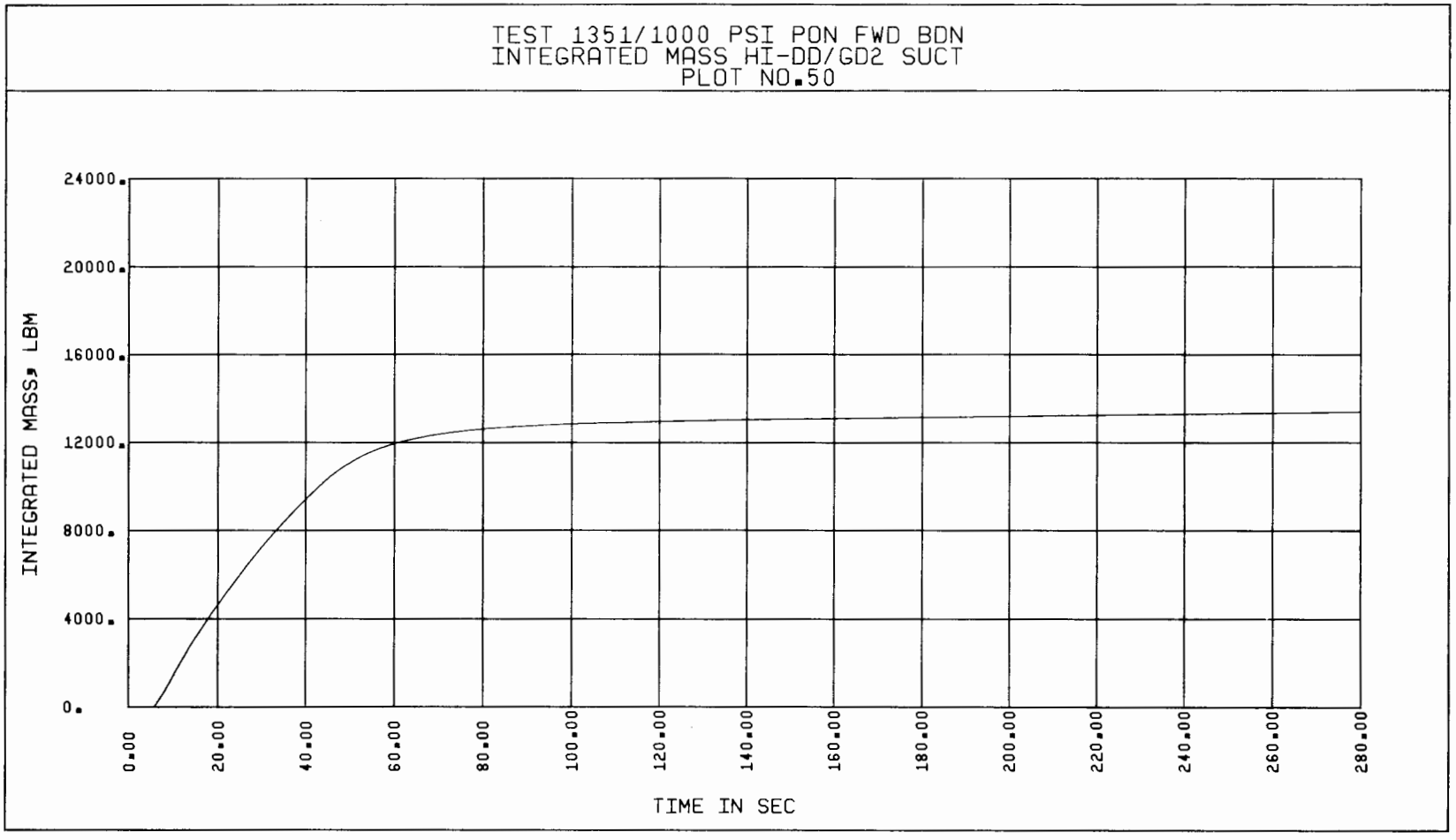

Figure 4-13. Test 1351, Integrated Suction Mass Flow vs Time

Section 5

DATA ANALYSIS

The transient data analysis in this report is aimed at

- presenting the reduced transient data in an orderly fashion,
- an assessment of data consistency,
- selecting key sample blowdown tests for comparison with steady-state test results,
- determining the average volumetric and mass flow rates at the suction and discharge sides of the pump, and then extracting performance "snapshots" from the results of the key blowdown tests, and
- observation on overall trends, and special topics such as similarity scaling and flow regime.

5.1 DATA QUALIFICATION AND CONSISTENCY ANALYSIS

As a subsequent step in the data reduction process described in Section 4.2, the data presented in this report were subjected to a review to verify that they were consistent and reasonable. Where possible, instrument channel outputs were compared to test predictions, previous test results, corresponding parameter channel outputs, and calculated quantities. In many instances, these consistency checks were performed as data plot overlays. Several techniques have been developed and employed to perform consistency checks on the presented data and these techniques are discussed here briefly.

Comparison of measured temperature with the saturation temperature based on the pressure measurement at the same location provided a method to verify temperature data consistency. However, this technique was valid only during the saturated blowdown transient until the time at which the measurement location voided of liquid. After voiding occurred, the measured temperature increased above the corresponding saturation temperature due to radiant heating

of the thermocouple element by the walls of the piping. A comparison of the saturation and measured temperature is presented in Figure 5-1. It is seen that the measured suction temperature agrees fairly well with the saturation temperature corresponding to the measured suction pressure up to about 90 seconds, after which the measured temperature remains higher than the saturation temperature due to radiant heating of the thermocouple.

Data consistency checks for the pressure measurements were provided by two distinct methods; one involving comparison of pressure instruments at various locations for each test, and the other involving the loop pressure levels towards the end of the blowdown. Figure 5-2 presents the suction, discharge and blowdown line pressures for Test 1351. During the initial 5.7 seconds of steady-state conditions prior to rupture, the suction pressure is the lowest pressure, the discharge pressure is the highest of all three pressures, and the blowdown line pressure remains in between the suction and discharge pressures. This is because the test pump develops a positive head corresponding to the single-phase flow through it. The spike in each of the pressure curves is a result of the closing off of the return line throttle valve before rupture. This action causes the pump to realize the shut-off head momentarily and the pump flow to stagnate. Rupture of the diaphragms is indicated by the sudden drop off of the blowdown line pressure curve. The fluid condition will also change from two-phase to single-phase with slight subcooling during this process. Depending upon the mode of pump motor operation, the suction side pressure could be higher or lower than the discharge side pressure after rupture. For the forward flow blowdown tests with the pump rotor free-wheeling, the suction pressure should be higher than the discharge pressure and vice versa for the reverse flow blowdown with the rotor free-wheeling, after rupture. For locked rotor blowdowns, the suction pressure is expected to be slightly higher than the discharge pressure during the initial steady-state time period due to the elevation difference (Note that the initial flow for the locked rotor blowdown is negligible). After rupture, the suction pressure should remain higher than the discharge pressure for forward flow tests, and vice versa for the reverse flow blowdown tests. For blowdown runs with pump motor power on, the suction pressure may or may not be higher than the discharge pressure depending upon the speed at which the rotor is allowed to rotate and the transient two-phase flow through the pump. Towards the end of the blowdown, loop pressures are expected to come to equilibrium with

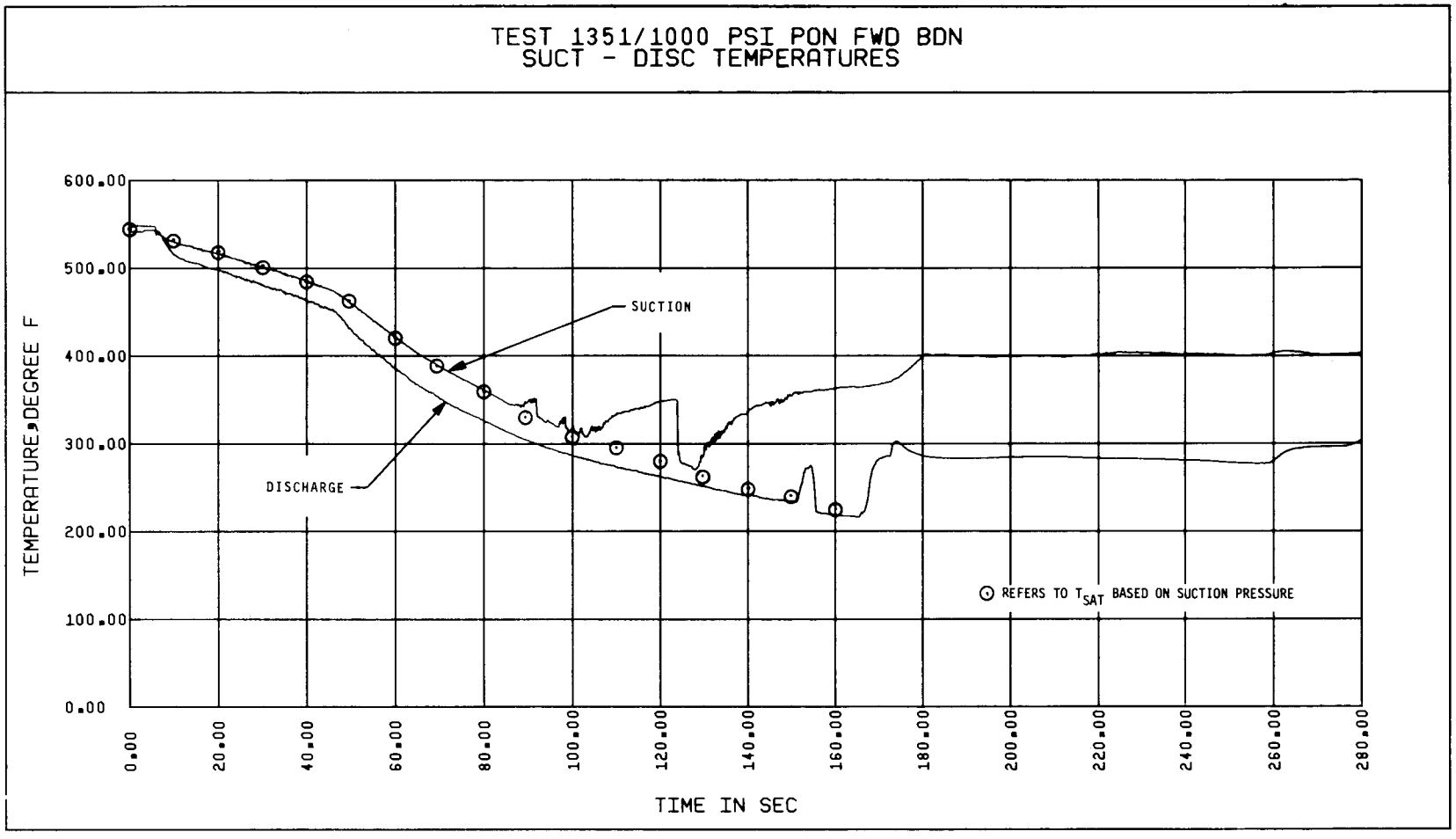

Figure 5-1. Test 1351, Suction and Discharge Fluid Temperatures vs Time

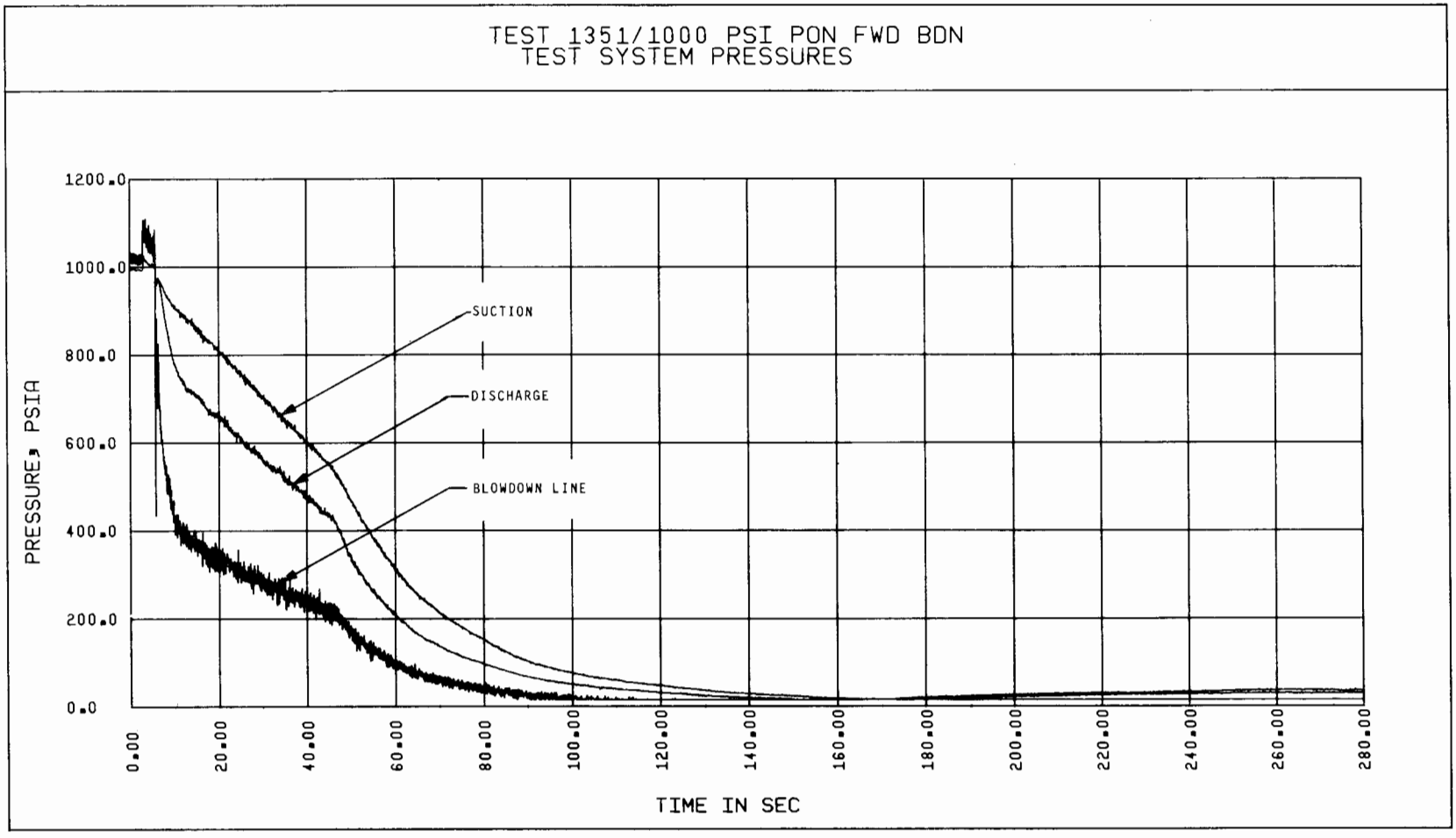

Figure 5-2. Test 1351, Test System Pressure vs Time

atmospheric pressure. For Test 1351, the blowdown isolation valve (HPSW-2) was closed at about 167 seconds (about 173 seconds plot time in Figure 5-2) after rupture. Therefore, the loop pressures just before 173 seconds in Figure 5-2 are compared against atmospheric pressure of approximately 14.7 psia. It is seen that the curves plotted in this figure indicate values that range between 15.0 and 16.5 psia at this time. Within instrument uncertainty limits, this value for the loop pressures towards the end of the blowdown is considered close enough to atmospheric pressure. Pressure measurement data for various blowdown tests were checked by means of the two methods discussed above, and were found to be consistent and reasonable.

Data consistency checks were also performed for the differential pressure measurements. These involved comparisons of the differential pressure measurements with the differential pressure computed by subtracting appropriate absolute pressure measurements at steady-state and transient conditions. Since absolute pressures were not measured at some differential pressure taps, not all differential pressure measurements could be checked in this manner. Also, for relatively small differential pressure values at high loop pressures the uncertainities in the absolute pressure measurements were comparable to the differential pressure measurement itself, reducing the significance of the comparison between the computed differential pressure value with the measured value. Another means of checking the consistency of the DP cell measurements is by considering the measured value of the differential pressures for zero flow conditions in the loop. For stagnant fluid conditions, the differential pressure between instrument spools should be approximately zero (except for a small elevation pressure differential). Thus, the DP cell should return to zero immediately after the blowdown isolation valve (HPSW-2) is closed. The pump head, which is measured by a differential pressure cell, is presented in Figure 5-3 for Test 1351. At approximately 173 seconds the blowdown isolation valve was shut for this test and, as indicated by this figure, the differential pressure across the pump (pump head) did become approximately zero.

The validity of the measured data from the drag discs was established by comparing momentum flux values directly measured by the drag discs with values computed from the orifice measured mass flow rates and the densities determined from an energy balance calculation under both steady-state single-phase (liquid) and two-phase fluid conditions. The turbine meter velocity measurements were

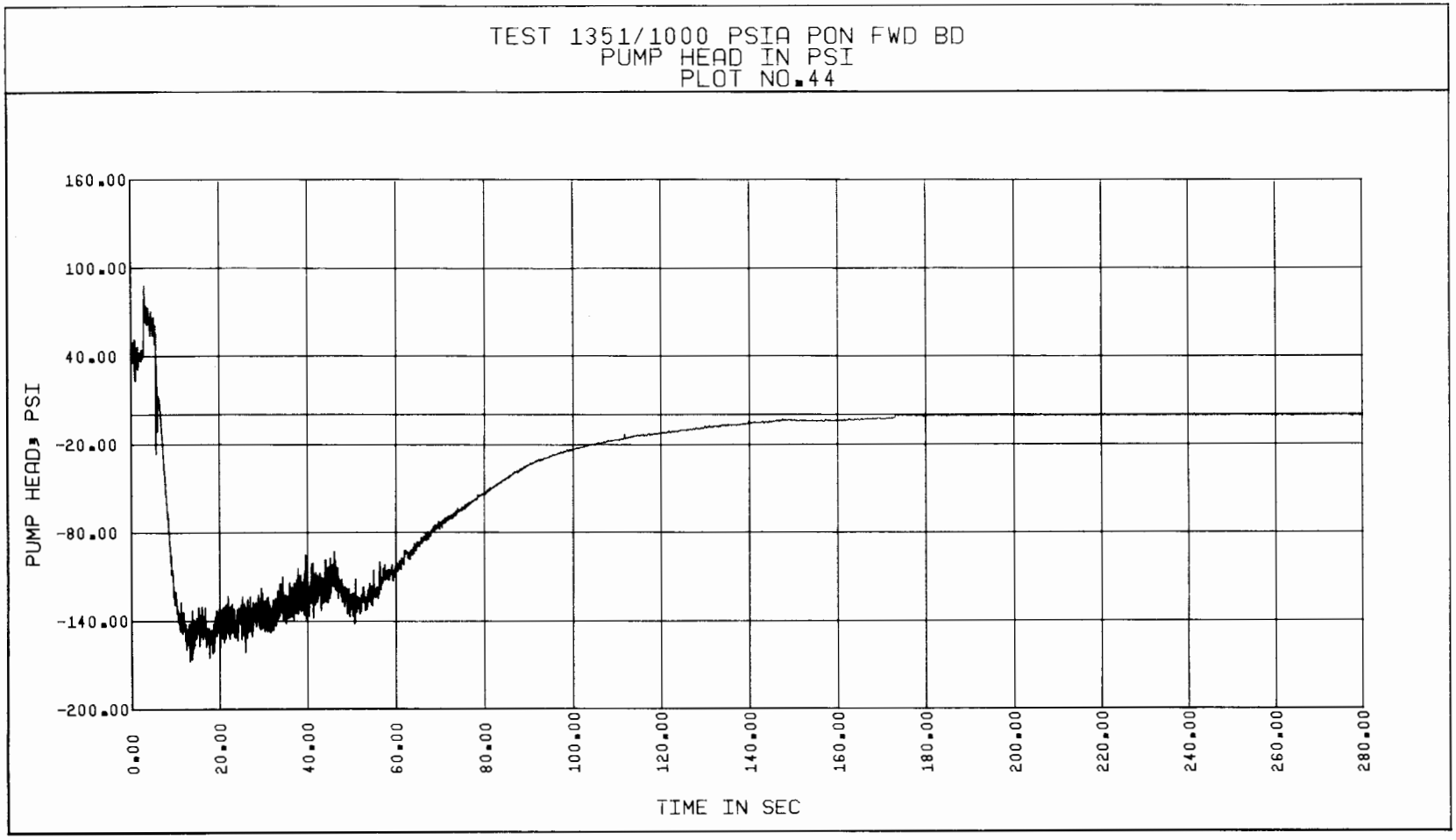

Figure 5-3. Test 1351, Pump Head vs Time

similarly checked against the orifice determined velocities, under steady-state single-phase and two-phase fluid conditions. Another method of checking the consistency of the data measured by the drag discs and turbine meters involves consideration of the measurements by these instruments at and beyond the time at which the blowdown isolation valve was shut. These instruments should read zero values for stagnant fluid conditions within the loop. Typical plots of drag disc and turbine meter readings are shown in Figure 5-4 and 5-5, respectively, for Test 1351. As indicated earlier, the blowdown isolation valve was closed at about 173 seconds, and the fluid is expected to be stagnant at this time. It is seen that the high turbine meter at the suction does read approximately zero, if the noise signals are disregarded. However, the high drag disc does not fully return to zero values at and beyond 173 seconds, as seen from Figure 5-4. This may be due to any of several reasons, one of which is the instrument uncertainty. For most of the drag discs, this uncertainty was in the range of 3000-5000 $lbm/ft\text{-}sec^2$. Another reason for these instruments not returning to zero values may be instrument malfunction during blowdown runs. It has been verified that some of the drag discs and turbine meters failed during transient testing. Discussion of malfunctioned instrument measurements is provided in subsequent sections of this volume, where key blowdown results are analyzed.

To evaluate the consistency of the loop average densities several means were employed. The gamma densitometer reads the fluid densities directly in the form of attenuations. At steady-state these densities were compared against the average density determined from orifice measurements and energy balance calculations. A further check on the validity of the gamma densitometer involved the determination of the end-point densities. For almost all the blowdowns, prior to rupture, the fluid attained single-phase conditions, and at that time the density of the fluid should be equal to the saturation liquid density for the corresponding temperature and pressure. Towards the end of the blowdown tests (typically 250 to 600 seconds), the fluid densities should be less than or equal to the saturation densities (steam) for the respective pressures and temperatures, except at locations where there is significant seal injection leakage flow into the mainstream. This is because the transfer of wall heat causes any residual blowdown liquid to vaporize. This observation was employed as a criterion for validating the density measurements towards the end of the blowdown tests.

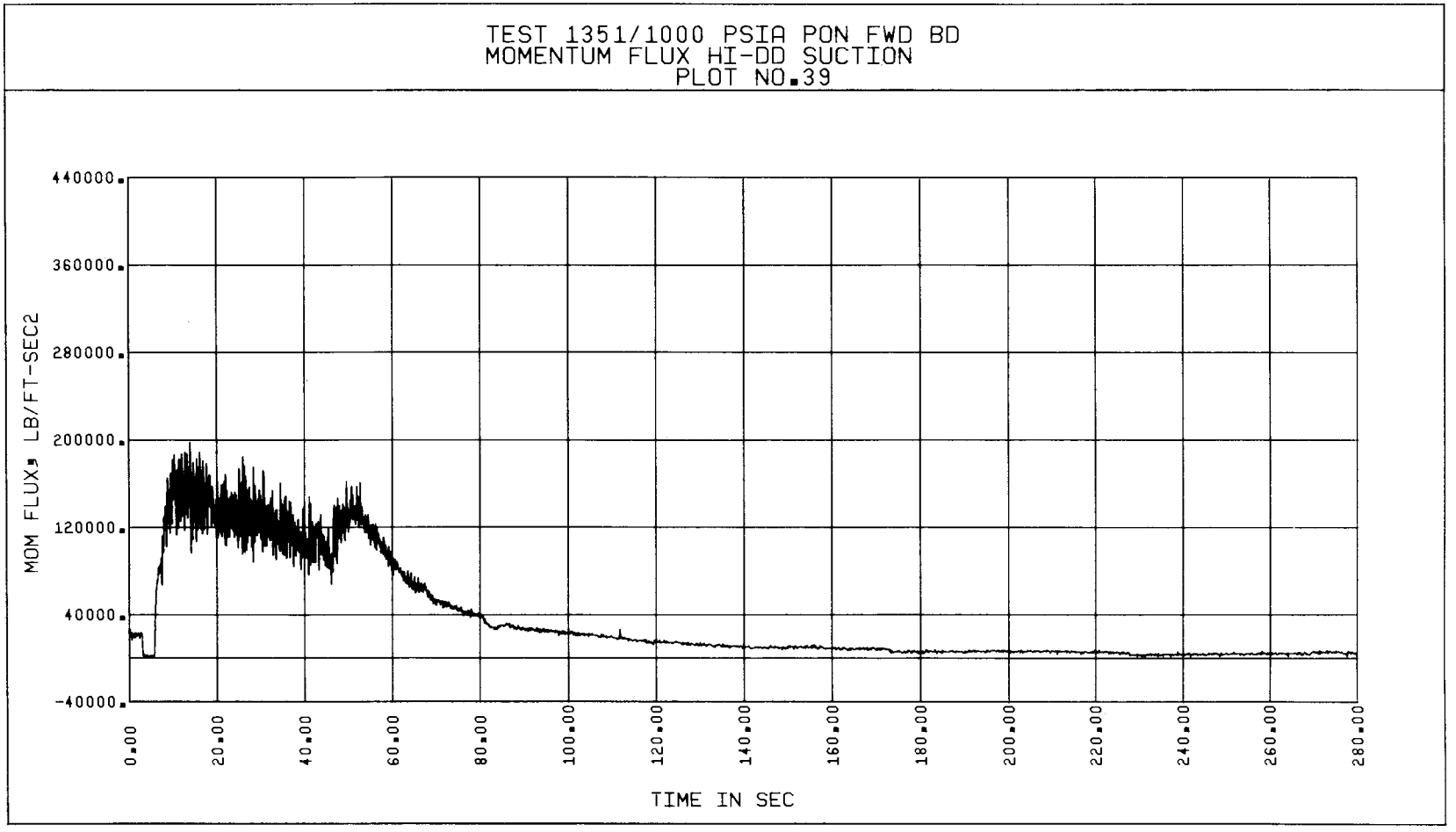

Figure 5-4. Test 1351, Typical Plot of Drag Disc Output

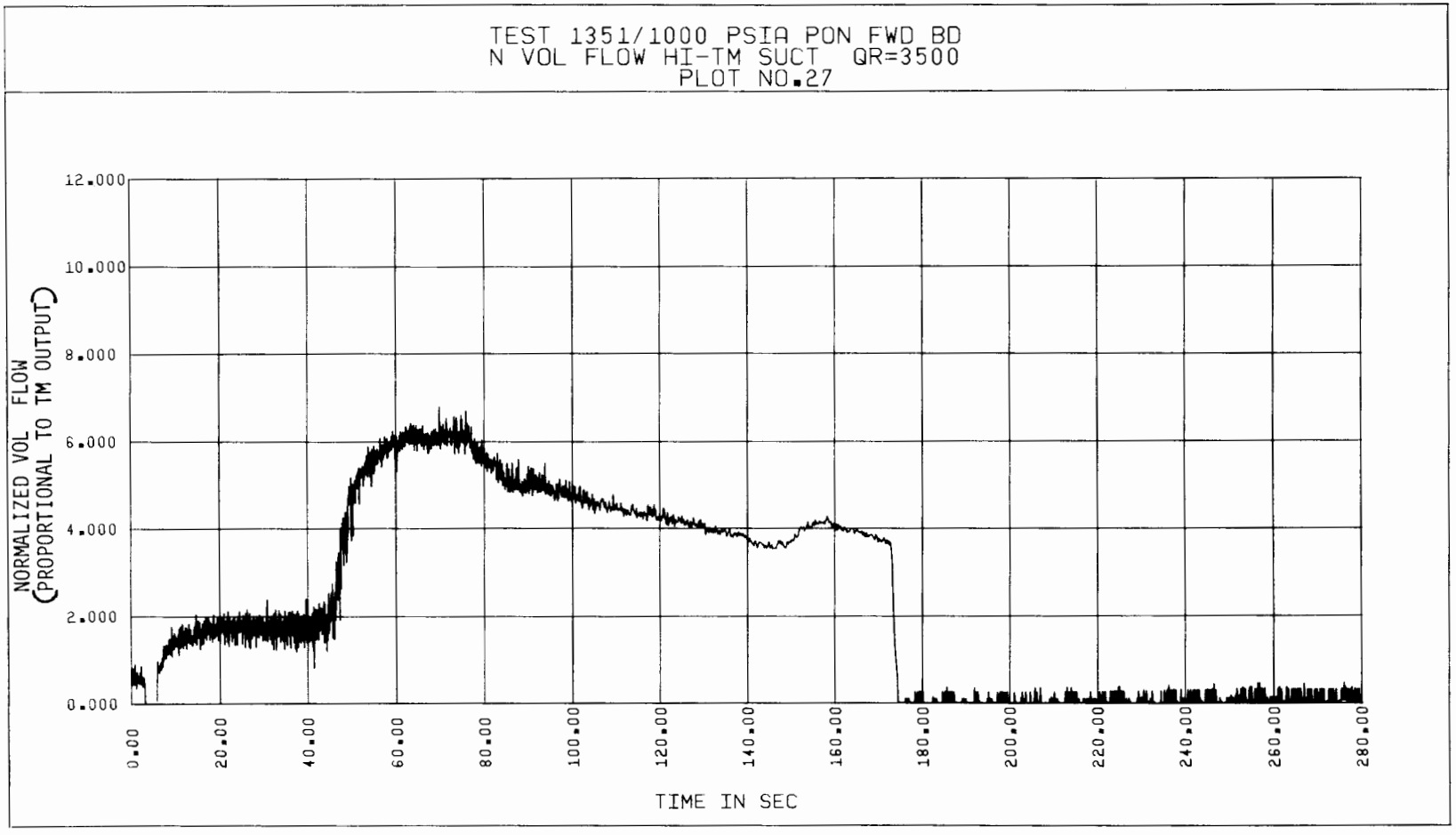

Figure 5-5. Test 1351, Typical Plot of Turbine Meter Output

To check the overall consistency of the transient data, various measurements for each test were compared against corresponding measurements for other tests to determine if the data followed expected trends. For example, the speed trace for a free-wheeling, intermediate size break blowdown test was compared against the same parameter trace for a free-wheeling, full-size break blowdown test. Since the pump speed is directly dependent on the volumetric flowrate for this type of blowdown, the full-size break speed trace is expected to be substantially higher than the trace for the intermediate size break. Similar comparisons were made for the pressures, temperatures, normalized volumetric flow rates, mass flow rates, torques, and pump heads.

Another means of assessing the validity and quality of the reduced FM transient data on measured parameters is by comparing plots from the Transient Data Reduction (TDR) program with plots generated from the scanner data. For almost all the blowdown parameters, raw data was recorded by the scanner data acquisition system for every five second interval. Some of this data was later reduced independently of the TDR program by means of another data reduction program which employed corresponding appropriate data conversion equations. The reduced data thus developed was plotted by means of a Hewlett-Packard XY plotter. Although these plots do not give a detailed description of the transient behavior of any parameter (due to low data point density), these are sufficient to provide general trends of each blowdown parameter. The time-plots generated from the results of the TDR program described in Section 4.2 are spot checked against these plots as a means of ensuring the overall quality of the reduced measured data. Typical scanner data plots are presented as Figures 5-6 through 5-9. Additional scanner data plots are provided in Volume VI, Transient Data.

Repeatability of results for one blowdown test versus another, similar, blowdown test is expected to add credence to the transient data presented in this report. With this thought in mind two similar blowdown tests were conducted, one in Phase I and the other in Phase II. These are Tests 701 and 1156, both of which were 57 percent orifice size, free-wheeling forward flow blowdown tests. The initial pressures and flows were slightly different for these tests (See Figure 5-10 through 5-13). From Figure 5-10 and 5-11 it is seen that the pressure decay rates are similar for the two tests (Note that the steady-state plot duration for Test 1156 is slightly longer than that for Test 701). Transient measurement comparisons for density and momentum flux are provided

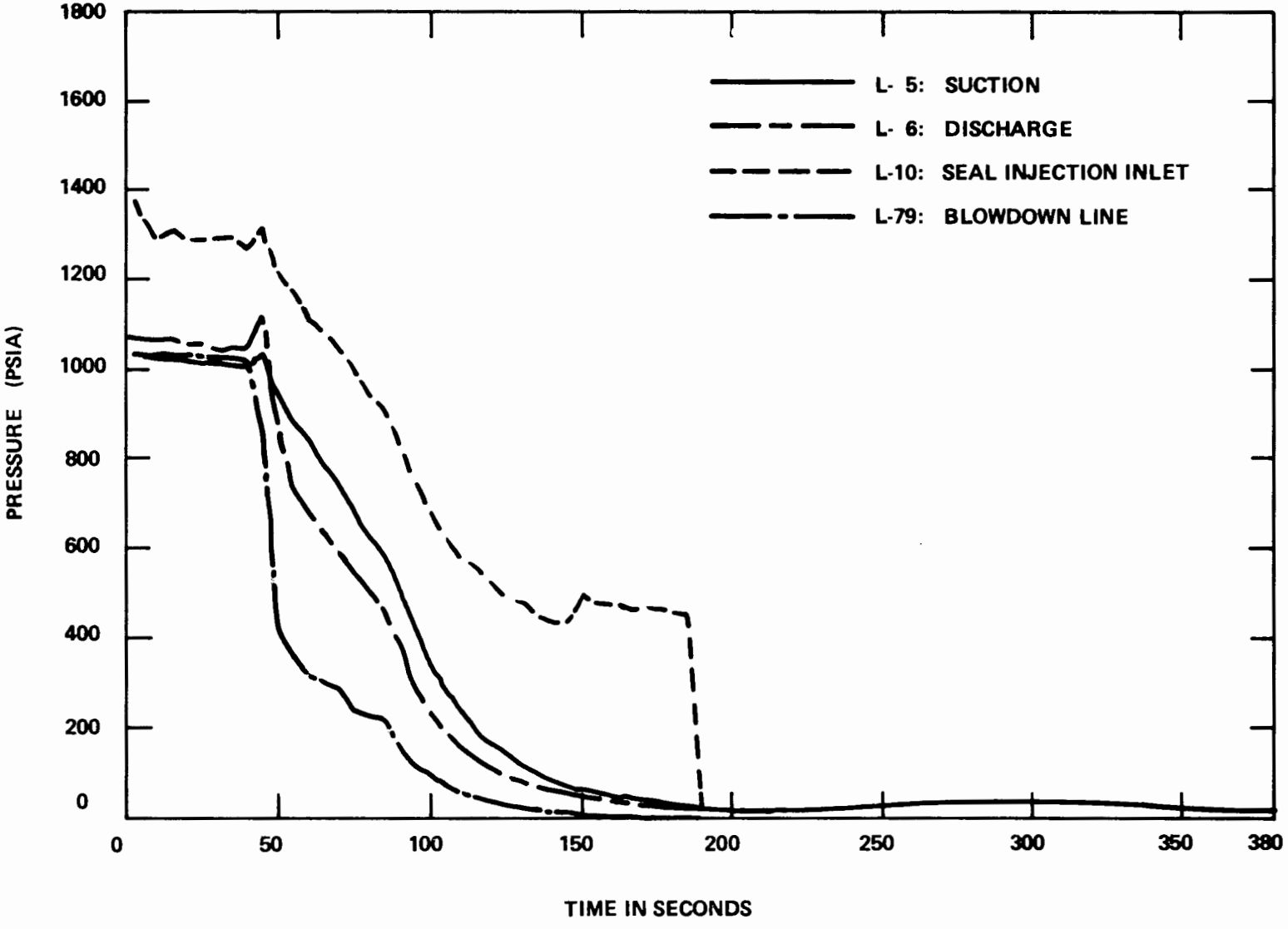

Figure 5-6. Test 1351, Scanner Data Plot of Test System Pressures vs Time

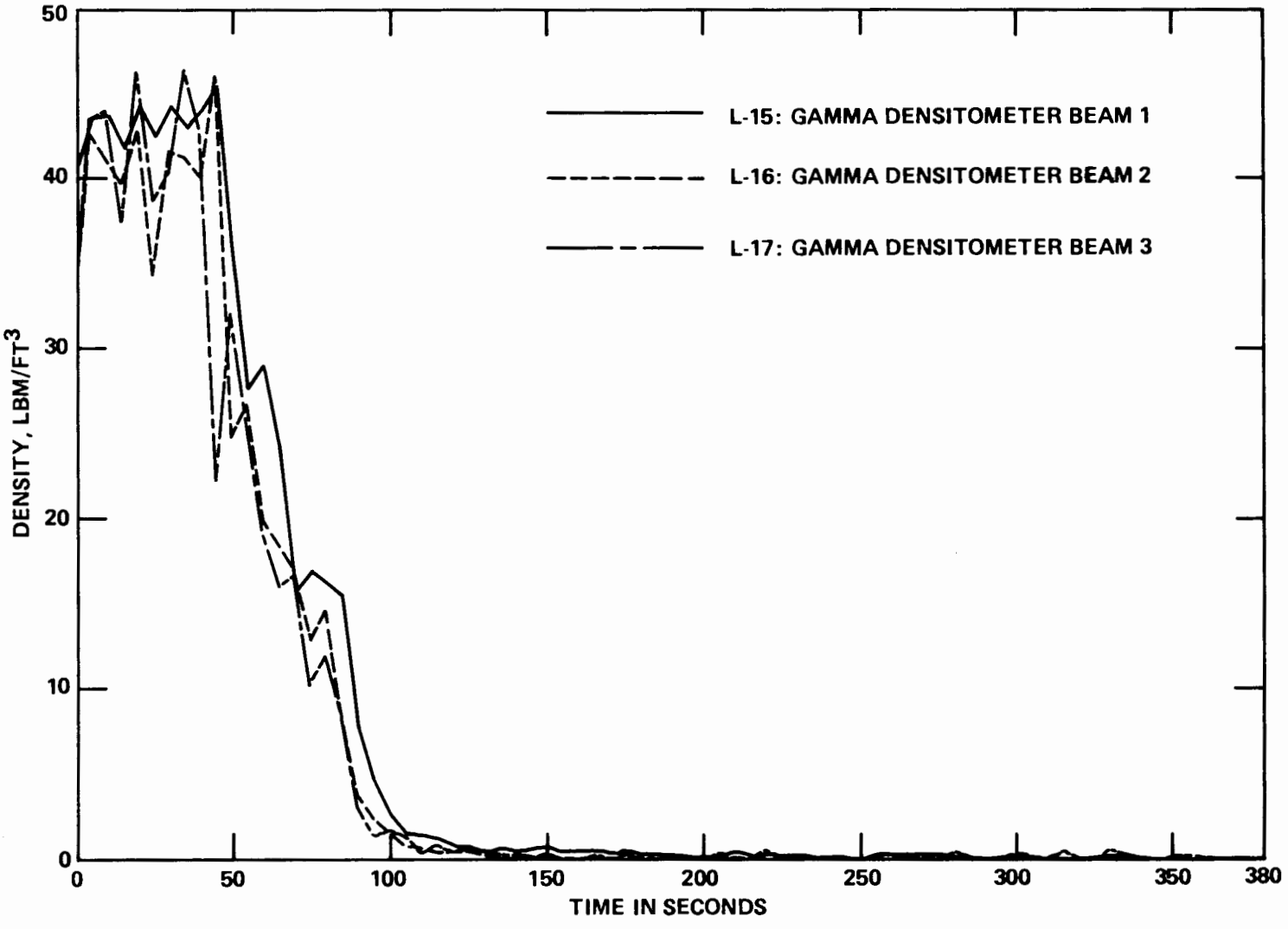

Figure 5-7. Test 1351, Scanner Data Plot of Suction Densities vs Time

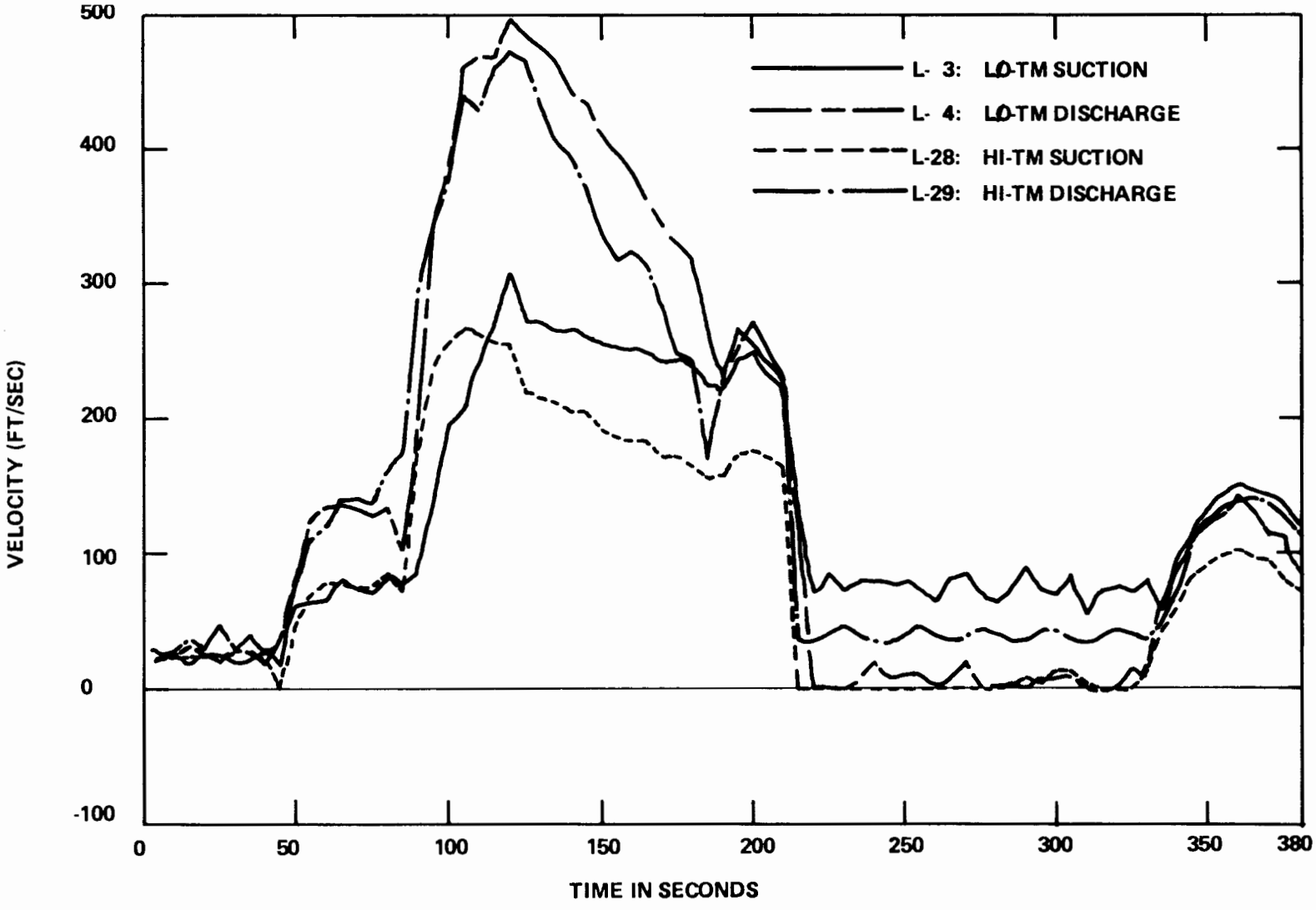

Figure 5-8. Test 1351, Scanner Data Plot of Turbine Meter Velocities vs Time

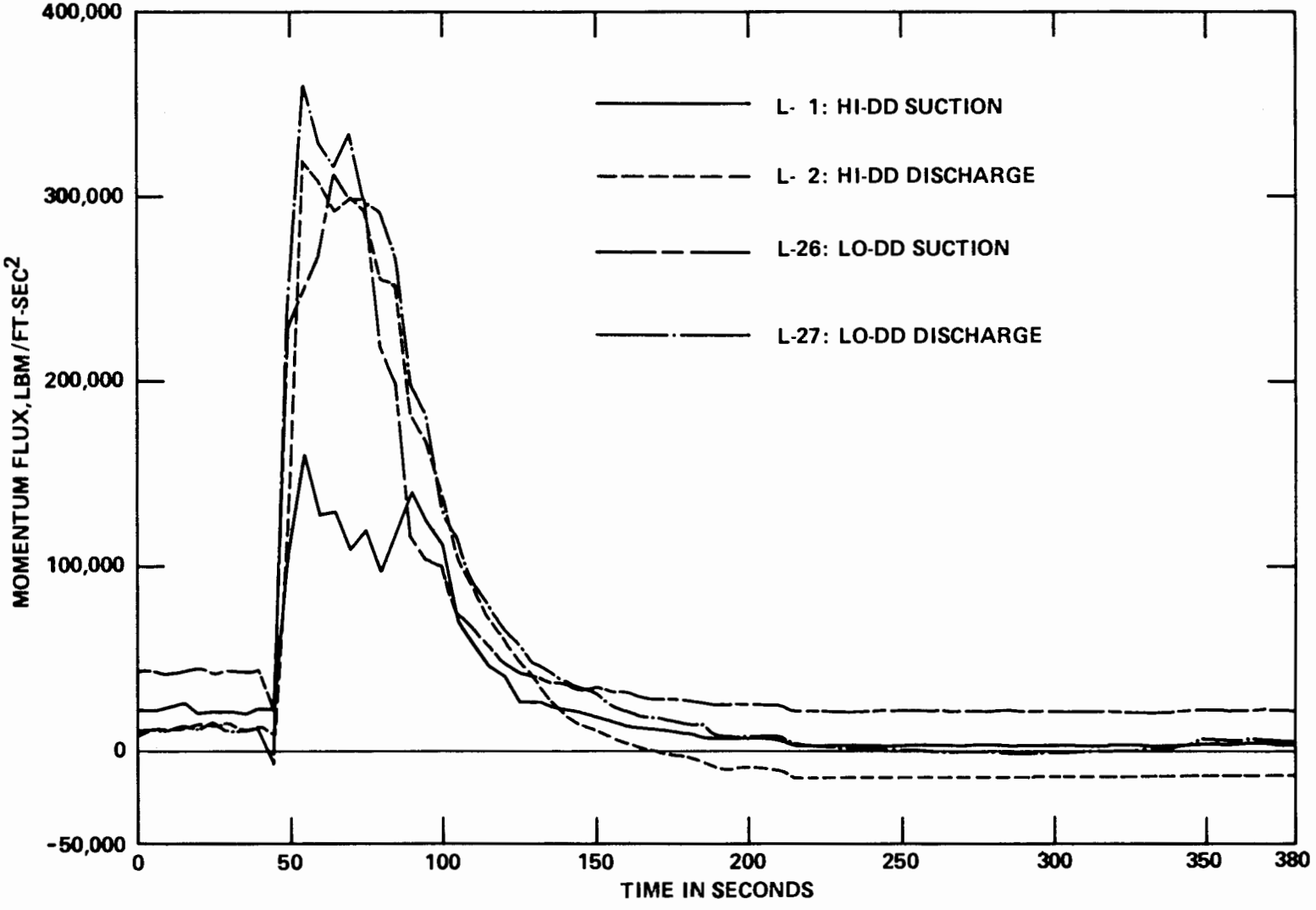

Figure 5-9. Test 1351, Scanner Data Plot of Drag Disc Momentum Fluxes vs Time

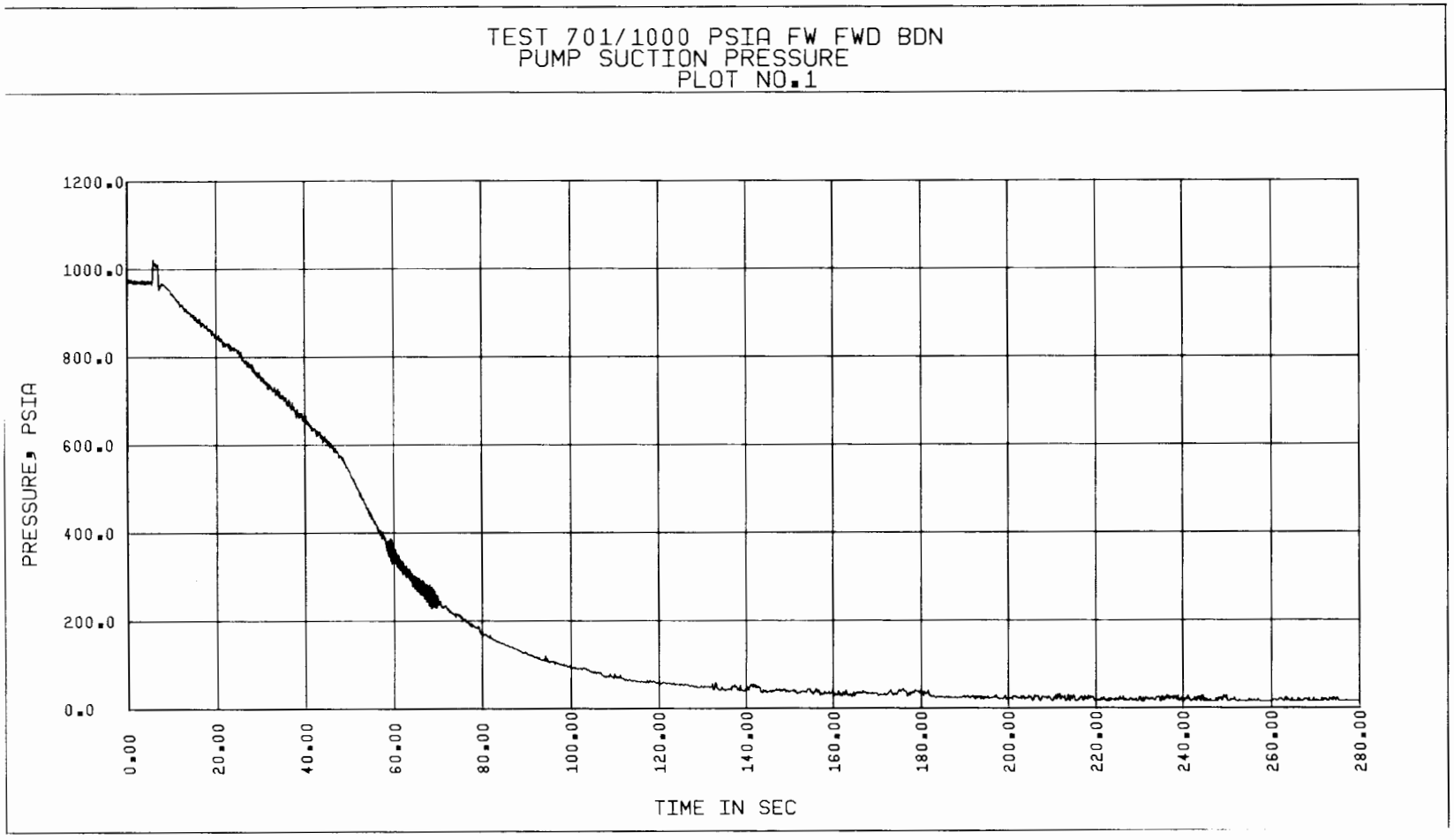

Figure 5-10. Test 701, Suction Pressure vs Time

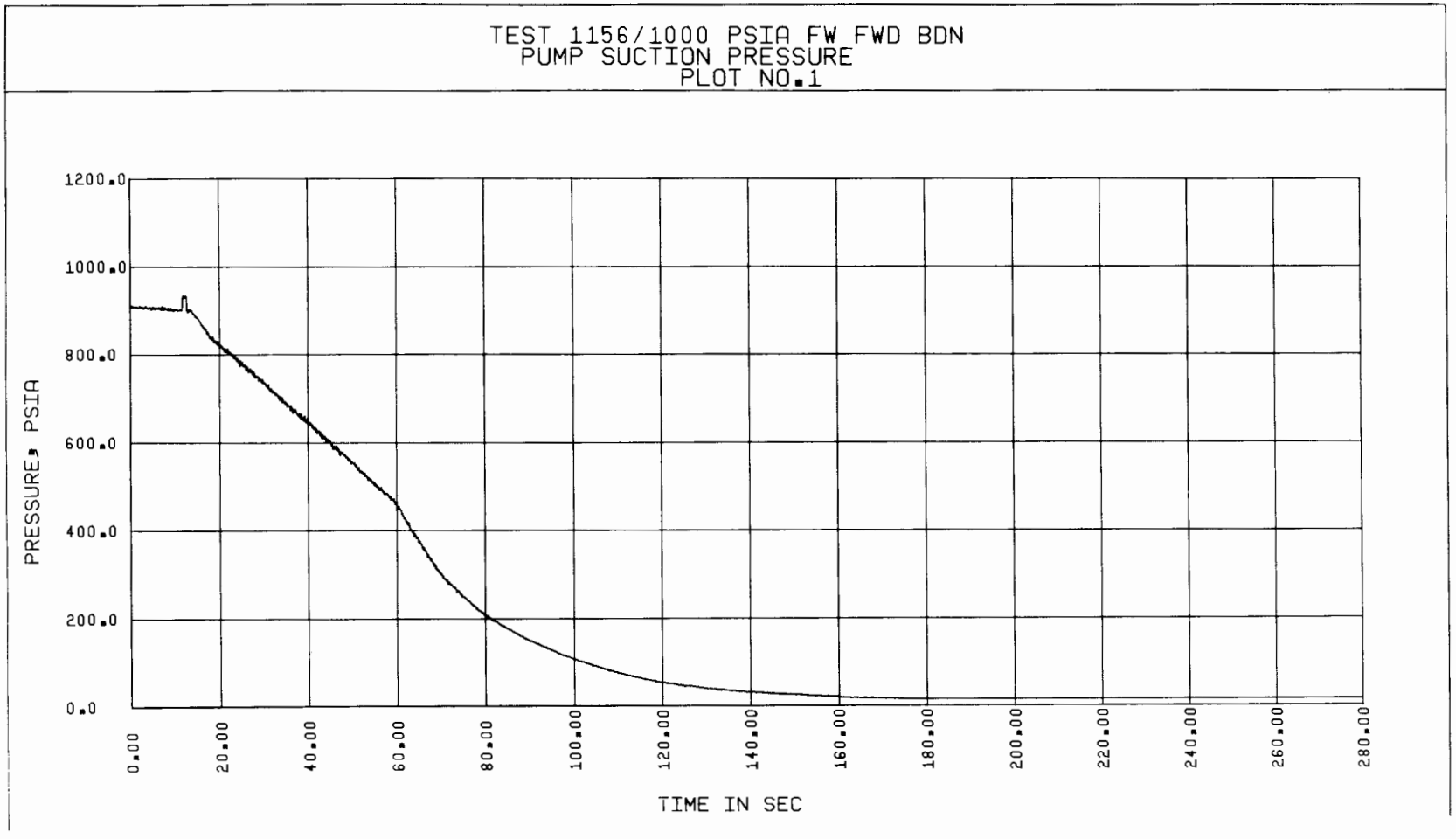

Figure 5-11. Test 1156, Suction Pressure vs Time

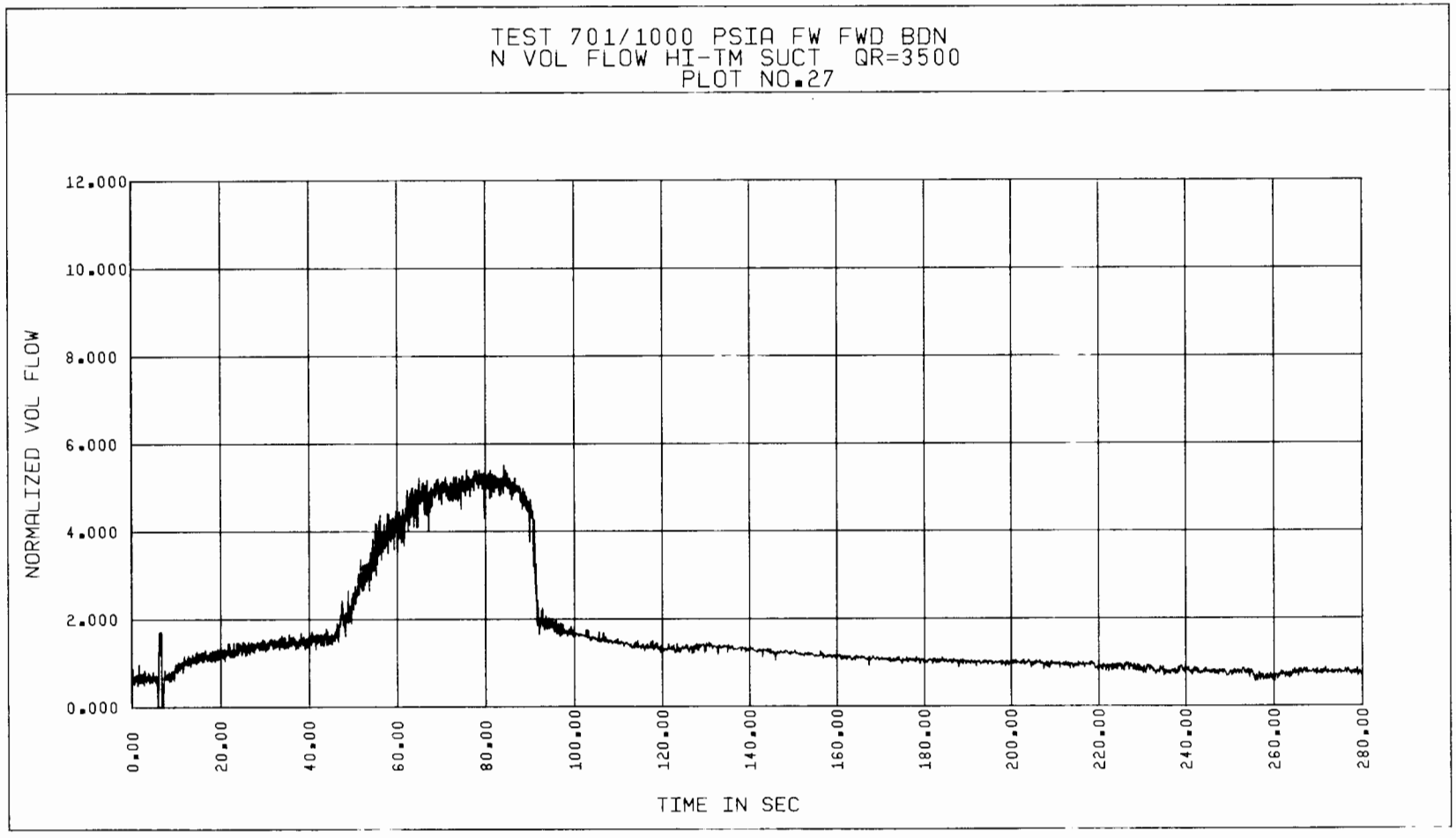

Figure 5-12. Test 701, Normalized Suction Volumetric Flow Rate vs Time

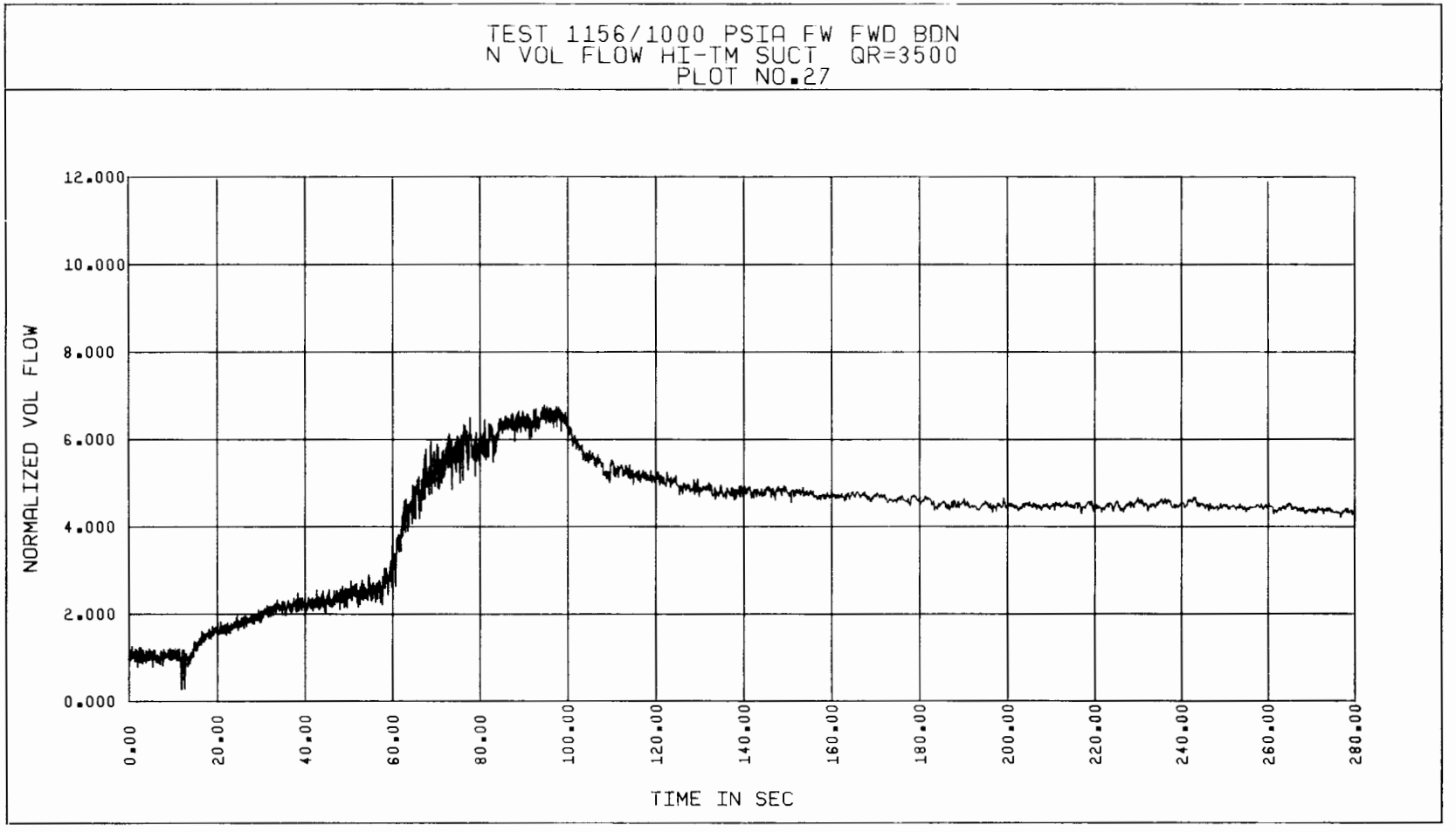

Figure 5-13. Test 1156, Normalized Suction Volumetric Flow Rate vs Time

in Figure 5-14 through 5-19. The values for the densities are seen to be similar, except towards the end of the blowdown when mostly steam flows through the test loop. The disagreement between long term densities may be partially attributable to the calibration procedure, and the uncertainties associated with the measurement of very low densities (steam densities). Comparison of the suction momentum fluxes indicates that the momentum flux measured by the high drag disc for Test 1156 is considerably lower than that for Test 701. As seen from Figure 5-17, the plotted ρV^2 values for Test 1156 becomes zero and then negative towards the end of the blowdown test. Consequently, it is believed that the high suction drag disc calibration constants for Test 1156 are incorrect, leading to ρV^2 values considerably lower than those for Test 701. The comparisons between ρV^2 values measured by the high drag discs at discharge for both tests appears to be quite good as indicated in Figure 5-18 and 5-19. The pump performance parameters for both tests are provided in Figures 5-20 through 5-25. It is seen that both the pump head and torque values are similar for both tests. Although the pump speed variation is similar for the two tests, for Test 1156, the peak speed does not reach a value as high as the one obtained for Test 701. This may be due to the higher initial pressure and flow rate values realized for Test 701. In general, the repeatability of transient measurements and pump performance is considered good based on the results of these two transient tests.

In the results of the transient tests presented, it is seen that random fluctuations are present in most of the measured transient parameter plots, except in those for suction and discharge pressures and temperatures, and pump speed. The reason for these fluctuations may be in part noise from the measuring instruments, as well as that physically generated by non-homogeneity in the two-phase mixture as it flows past these instruments. It is a sizable task to assess the noise contribution due to each of these sources, and it is beyond the scope of this report. Another source of random fluctuations in some reduced parameters is mathematical division of a relatively large parameter value by a very small parameter value, to develop a derived parameter. An example is the drag disc-gamma densitometer determined volumetric flow rate (See Figure 5-26). As the fluid becomes almost all steam the density value reaches a minimum. The measured value of the density fluctuates around this minimum value. These fluctuations are due to the uncertainty in the gamma densitometer measurements. The value of this fluctuation could be of the

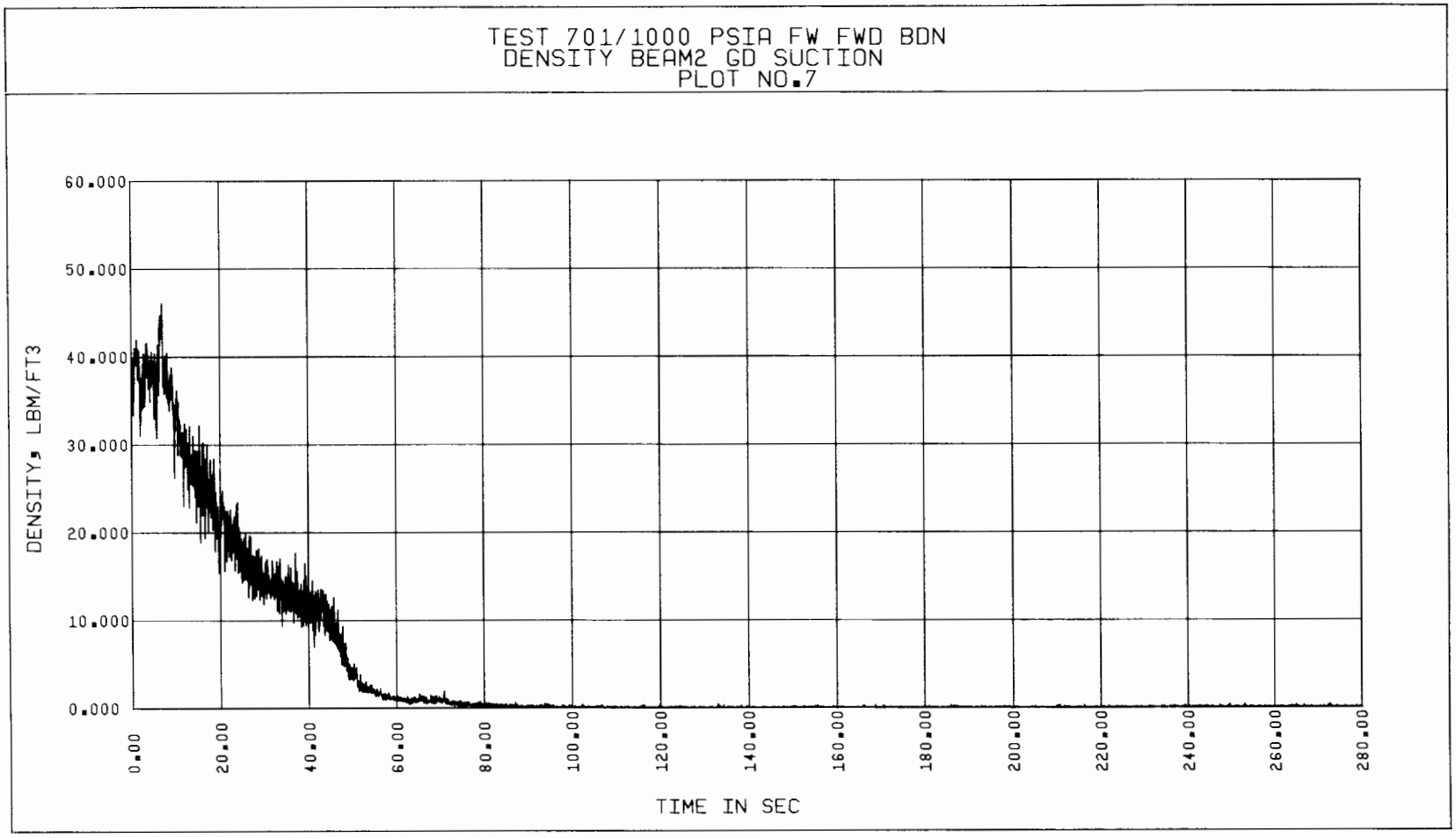

Figure 5-14. Test 701, Suction Density vs Time

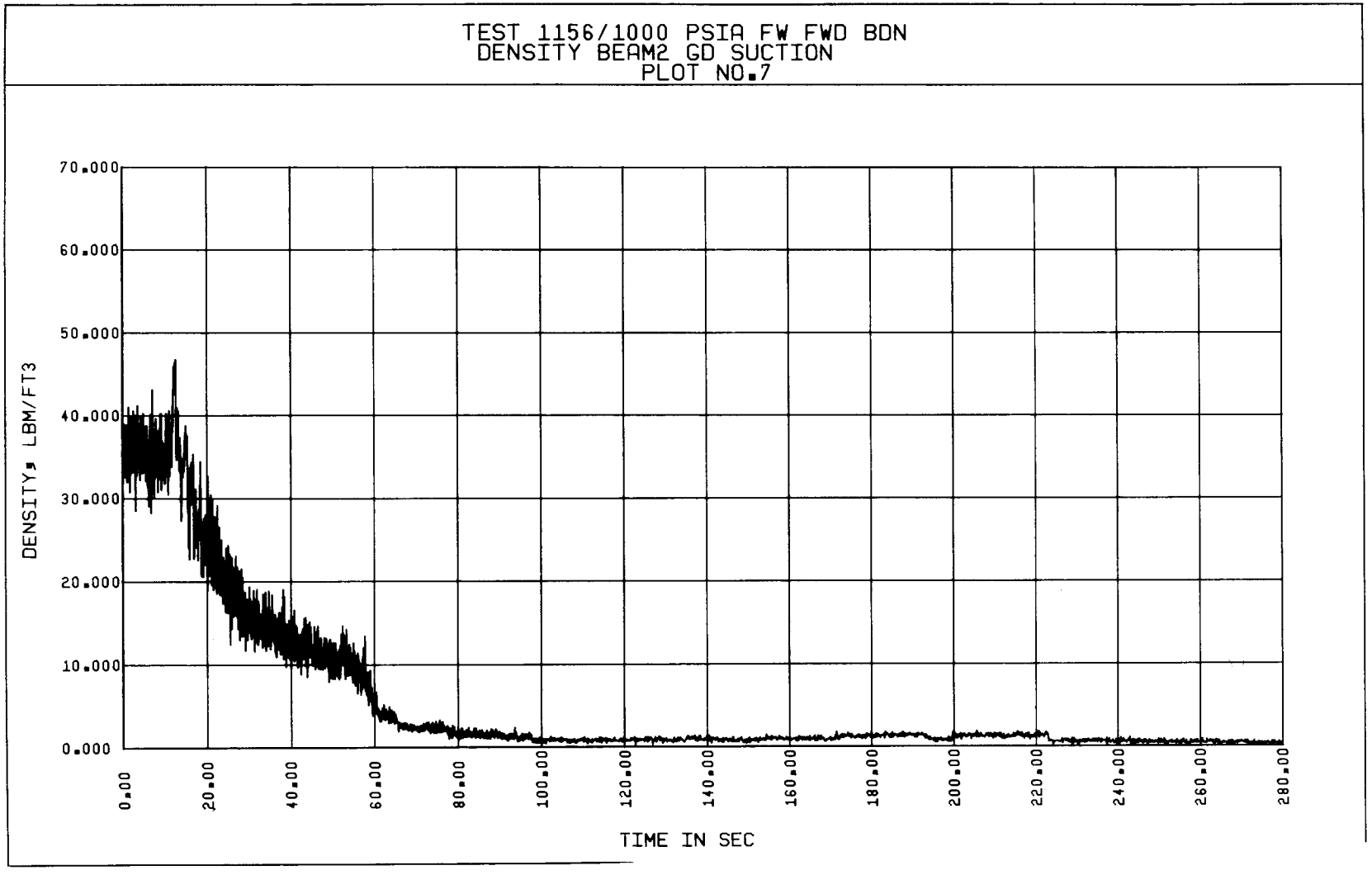

Figure 5-15. Test 1156, Suction Density vs Time

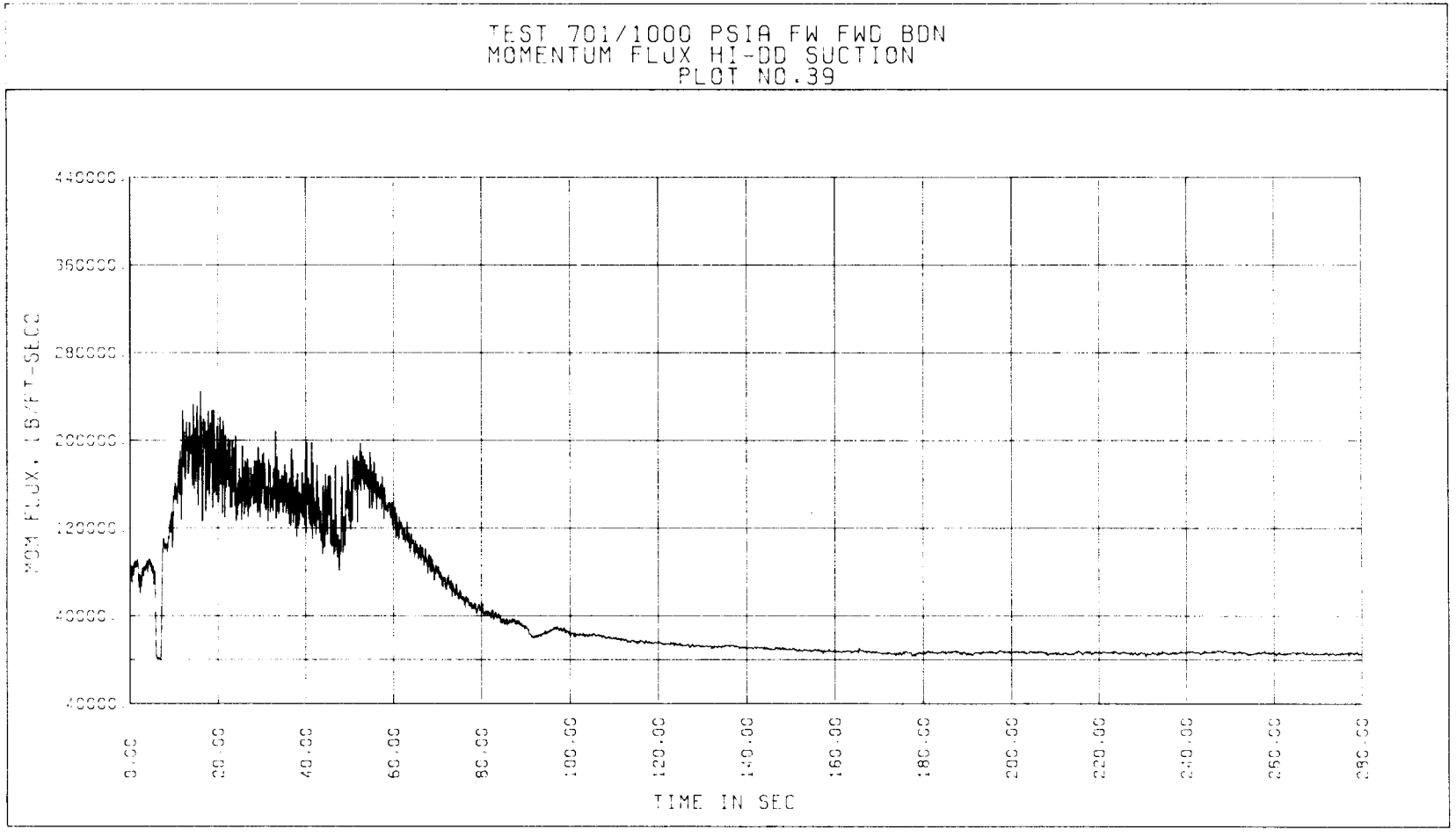

Figure 5-16. Test 701, Suction Momentum Flux vs Time, Based on High Drag Disc Data

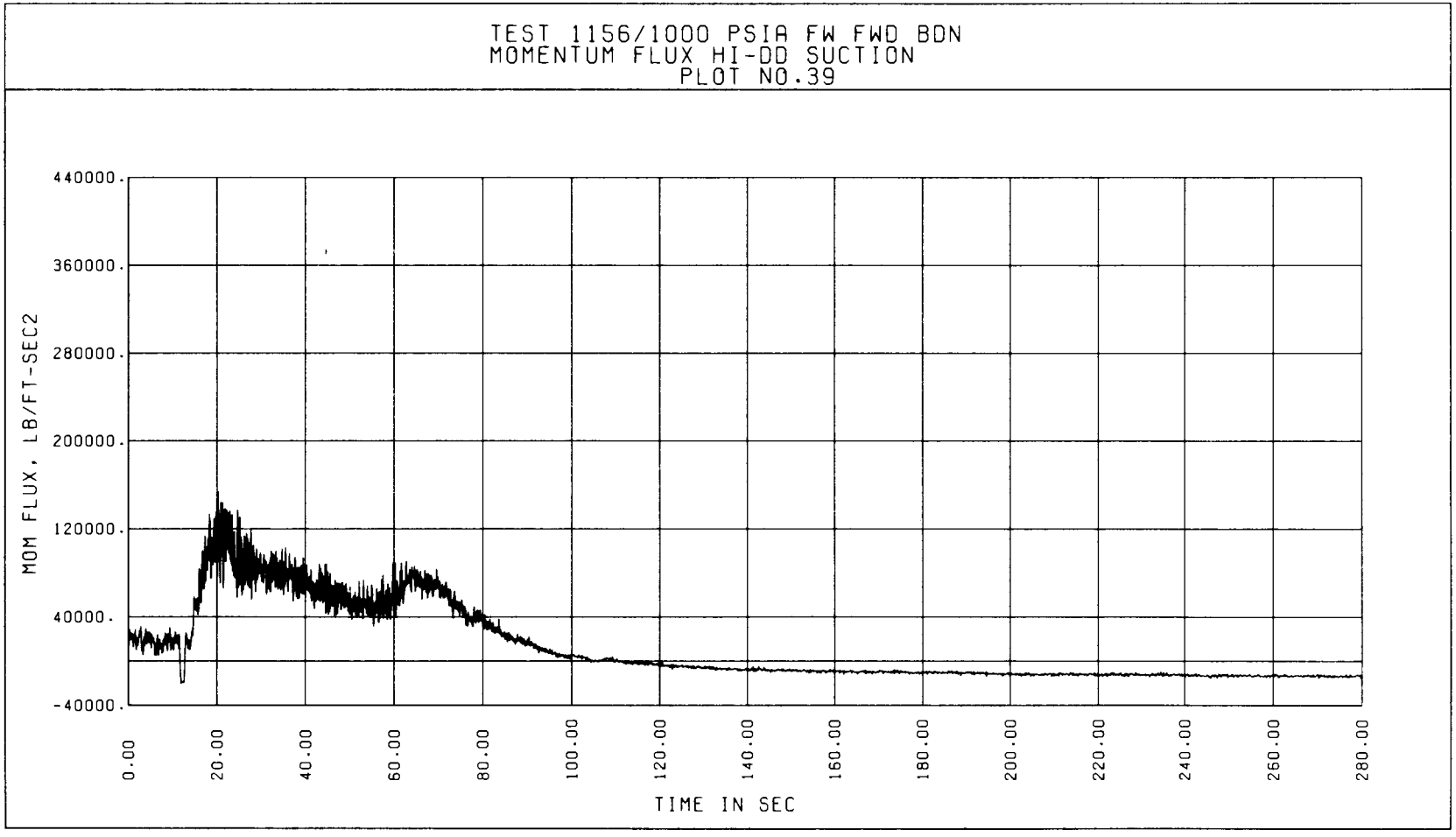

Figure 5-17. Test 1156, Suction Momentum Flux vs Time, Based on High Drag Disc Data

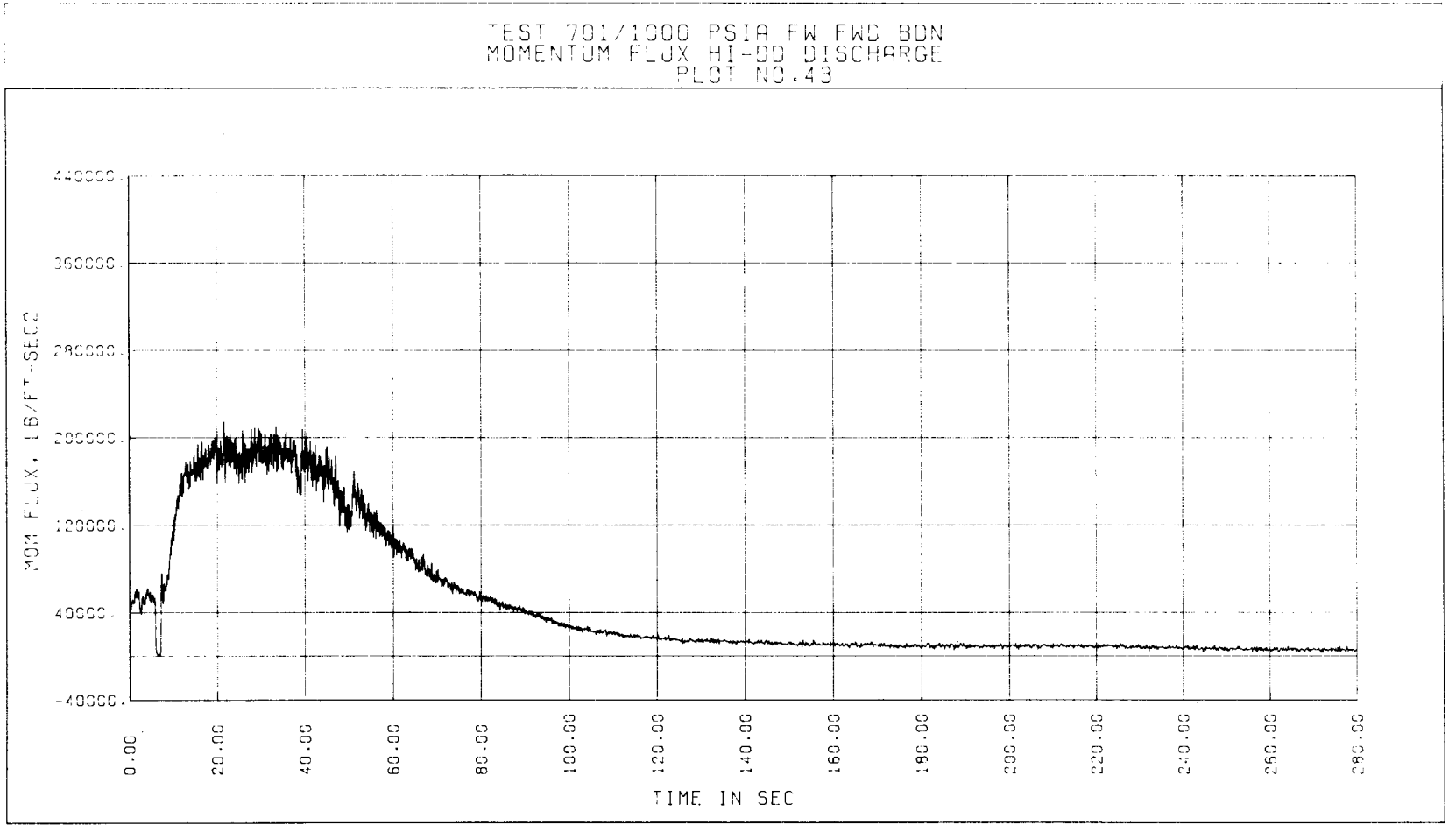

Figure 5-18. Test 701, Discharge Momentum Flux vs Time, Based on High Drag Disc Data

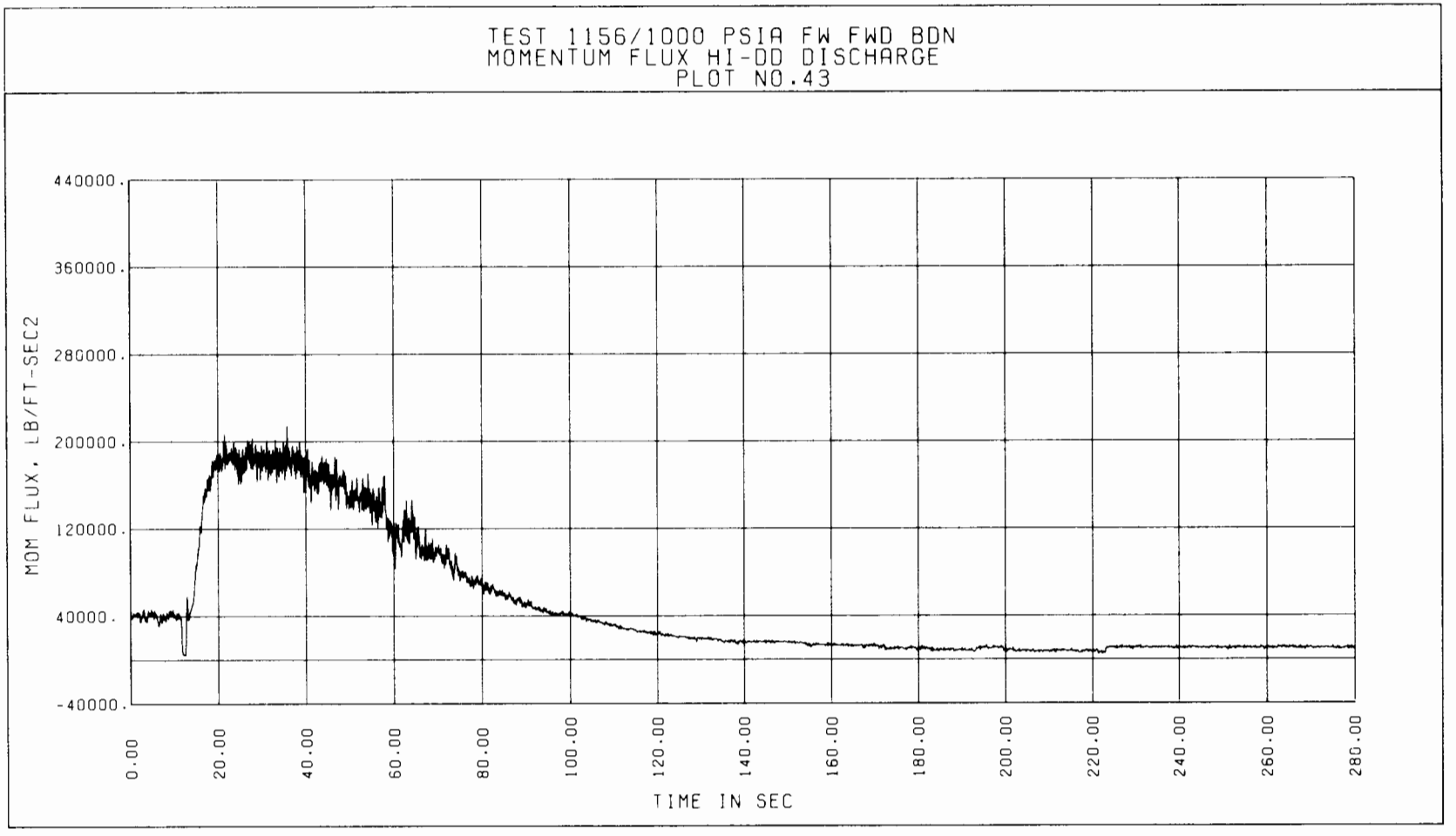

Figure 5-19. Test 1156, Discharge Momentum Flux vs Time, Based on High Drag Disc Data

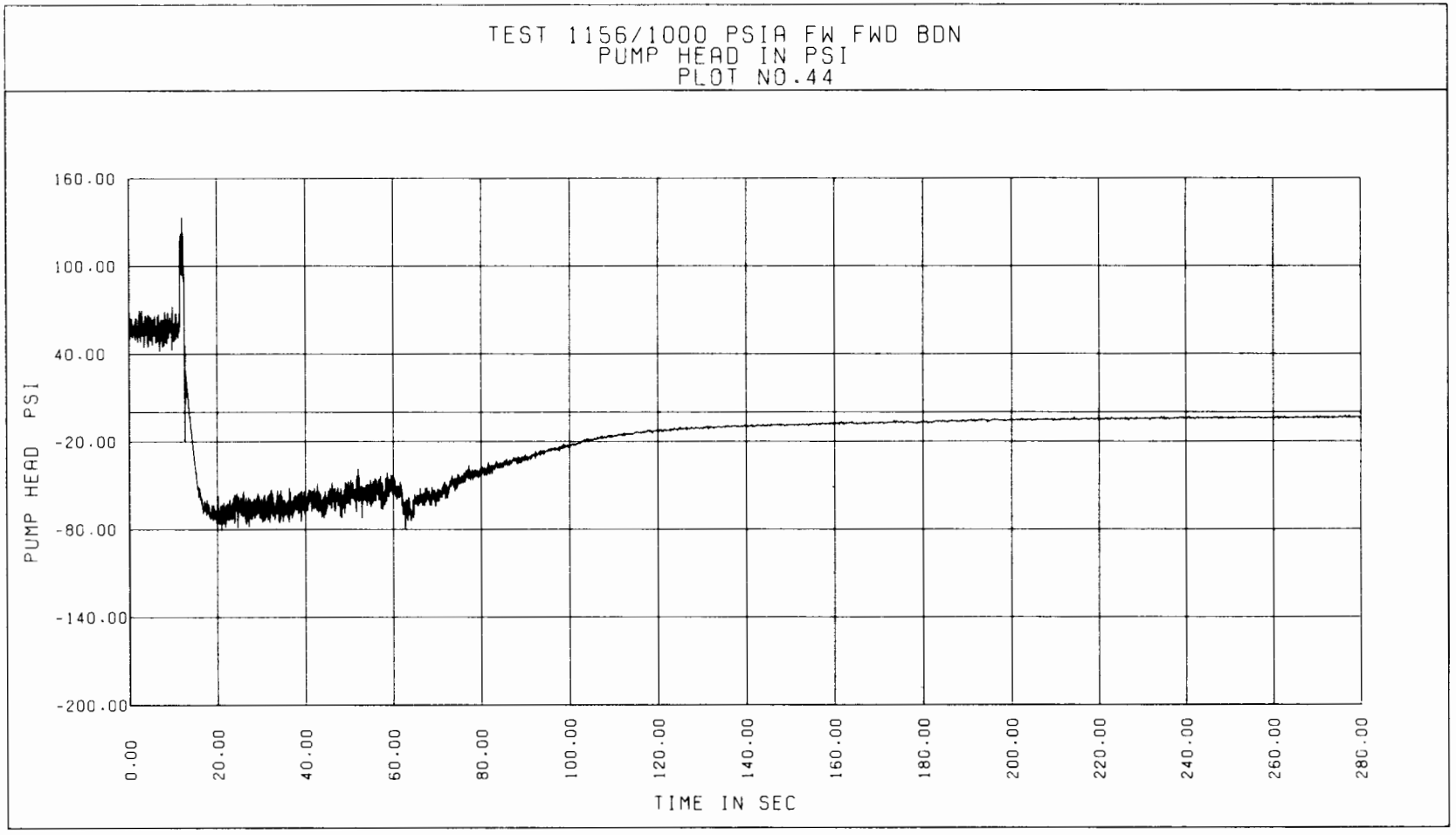

Figure 5-20. Test 1156, Pump Head vs Time

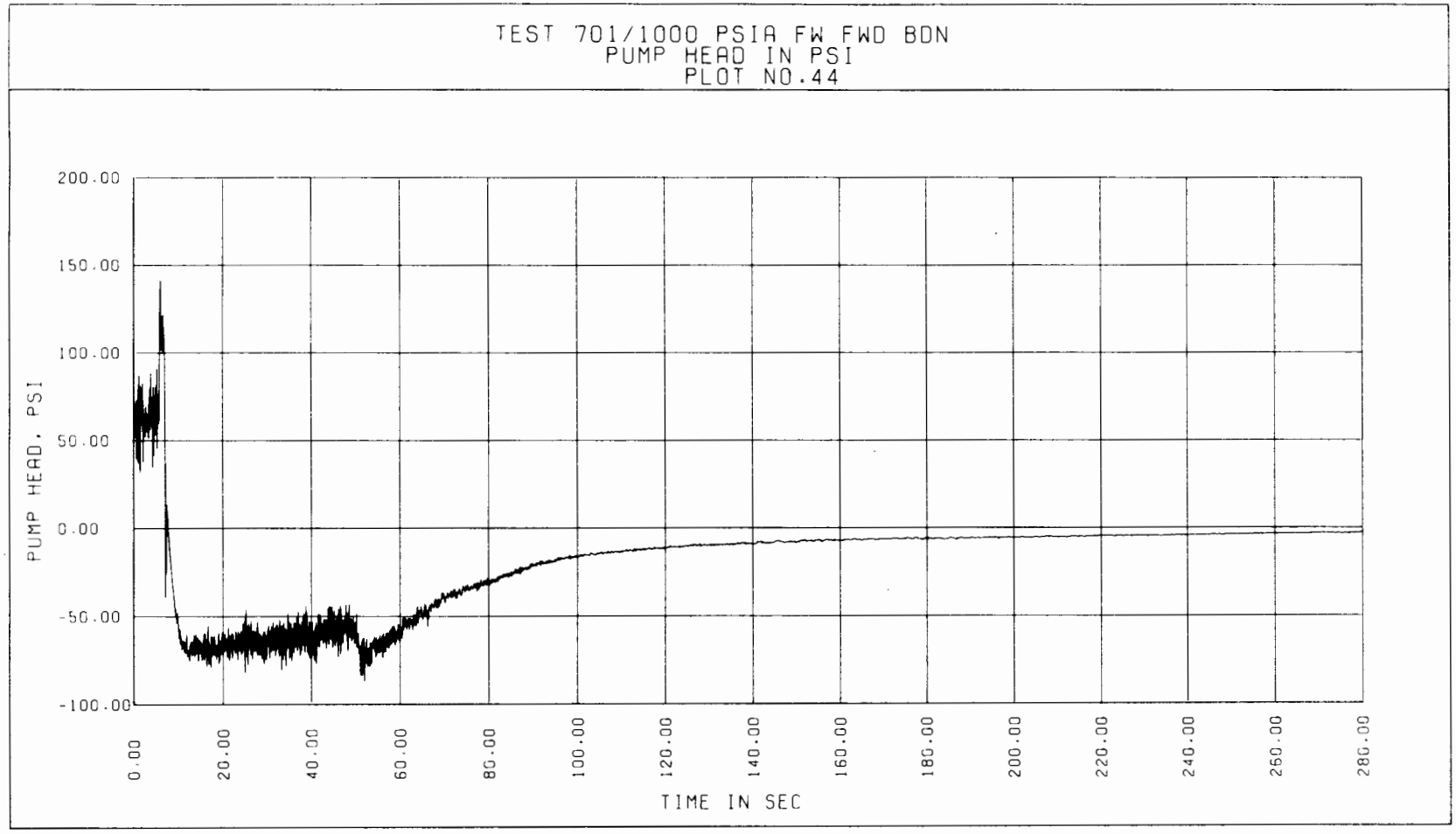

Figure 5-21. Test 701, Pump Head vs Time

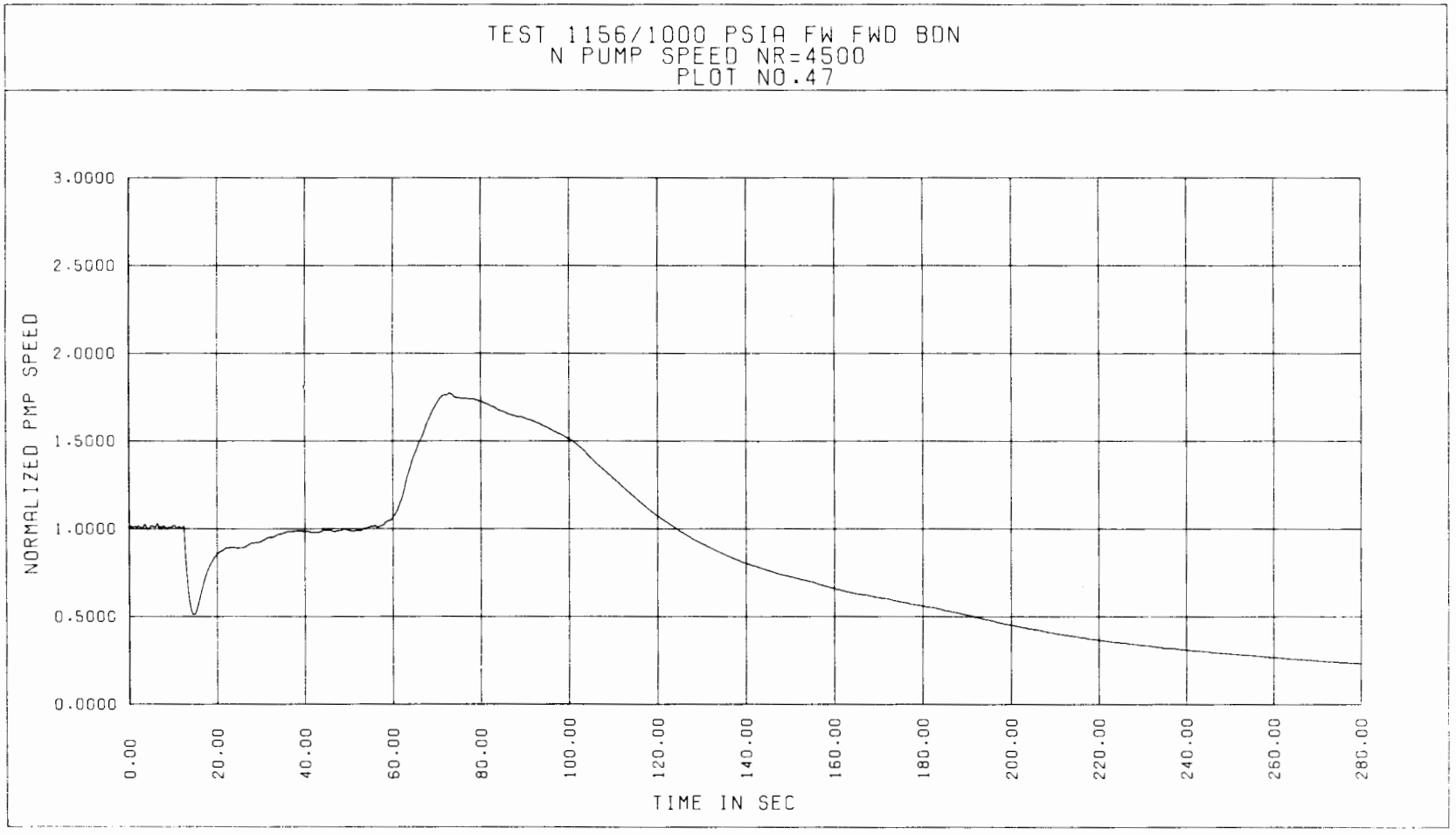

Figure 5-22. Test 1156, Normalized Pump Speed vs Time

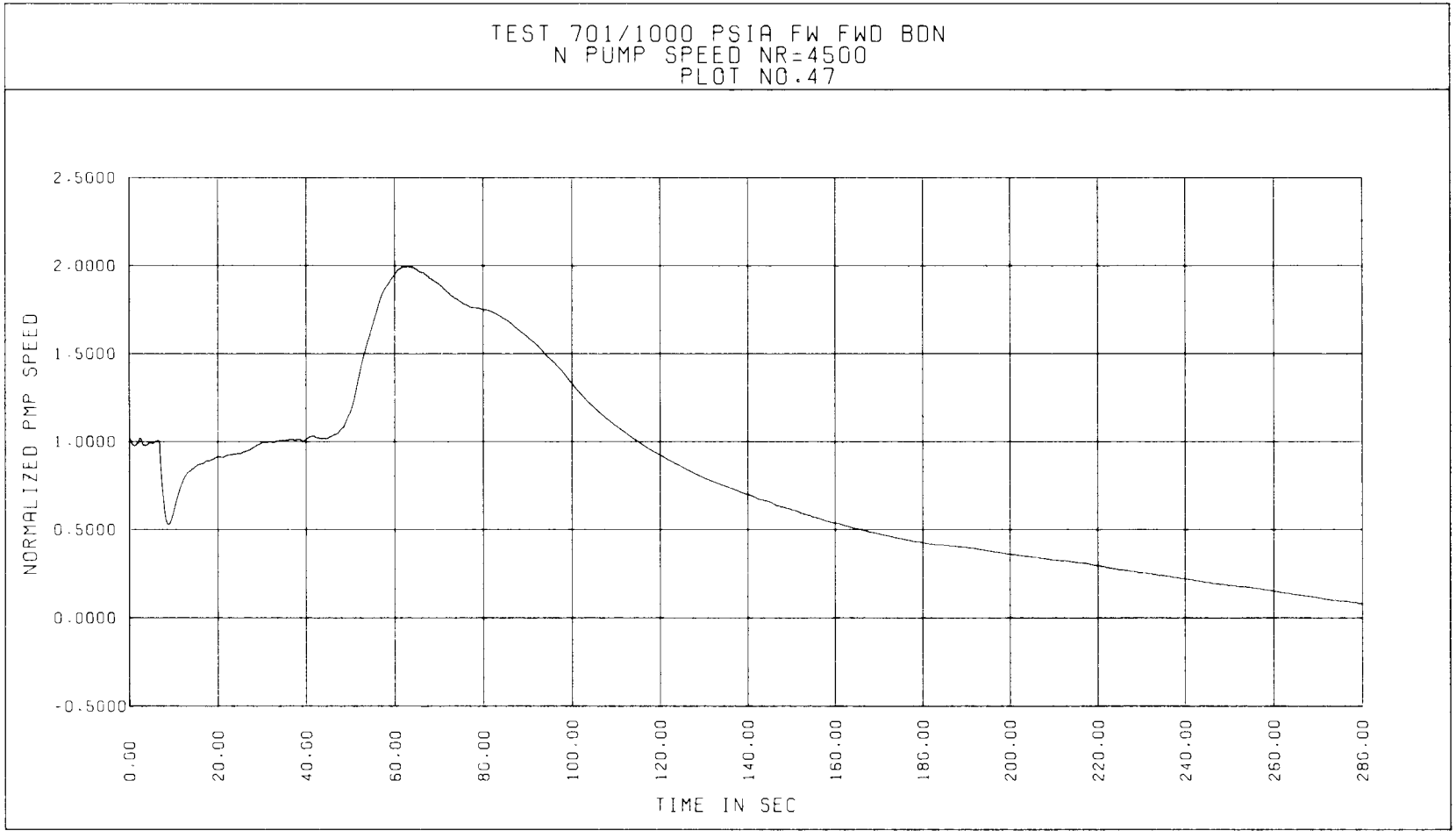

Figure 5-23. Test 701, Normalized Pump Speed vs Time

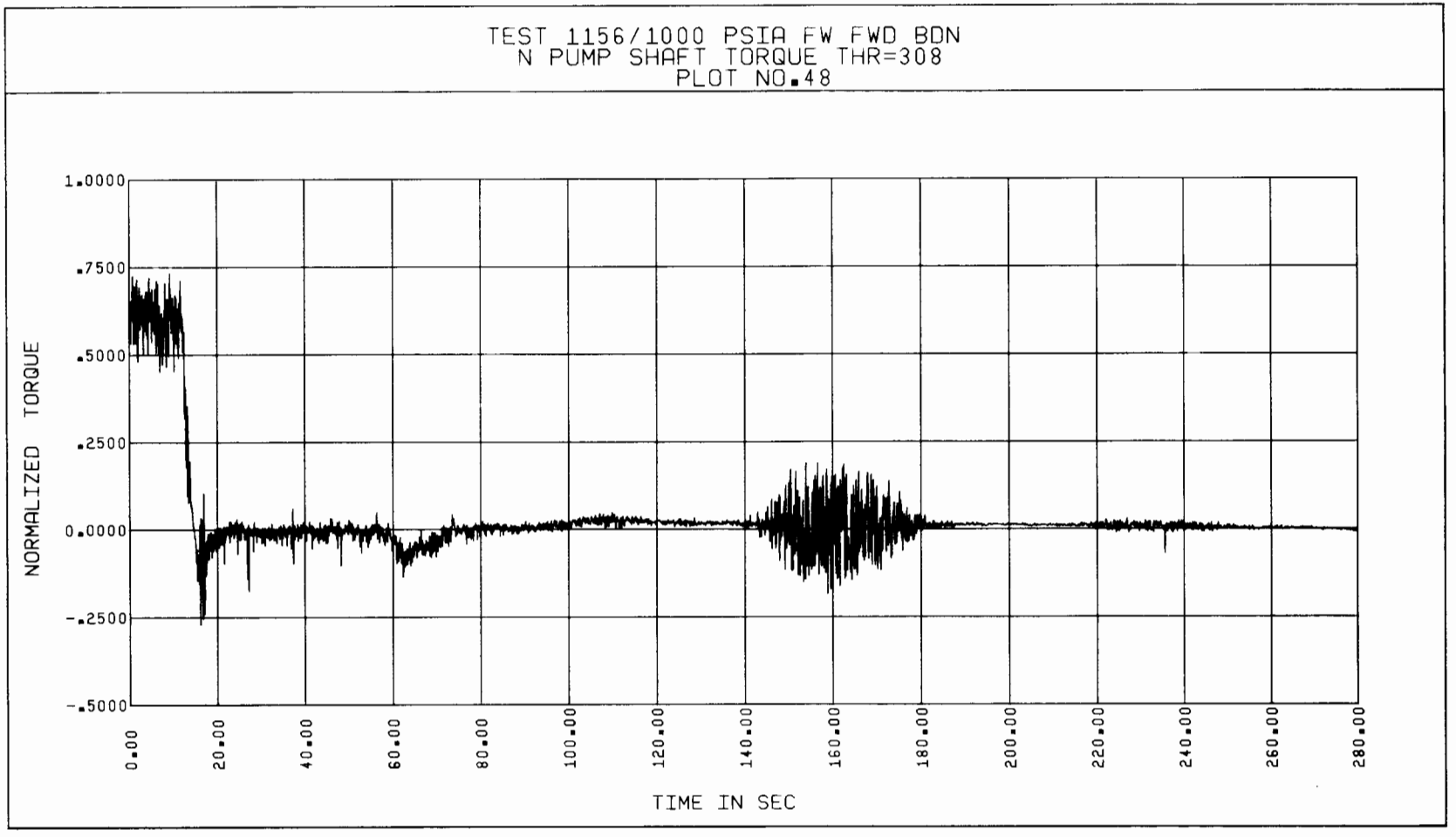

Figure 5-24. Test 1156, Normalized Pump Shaft Torque vs Time

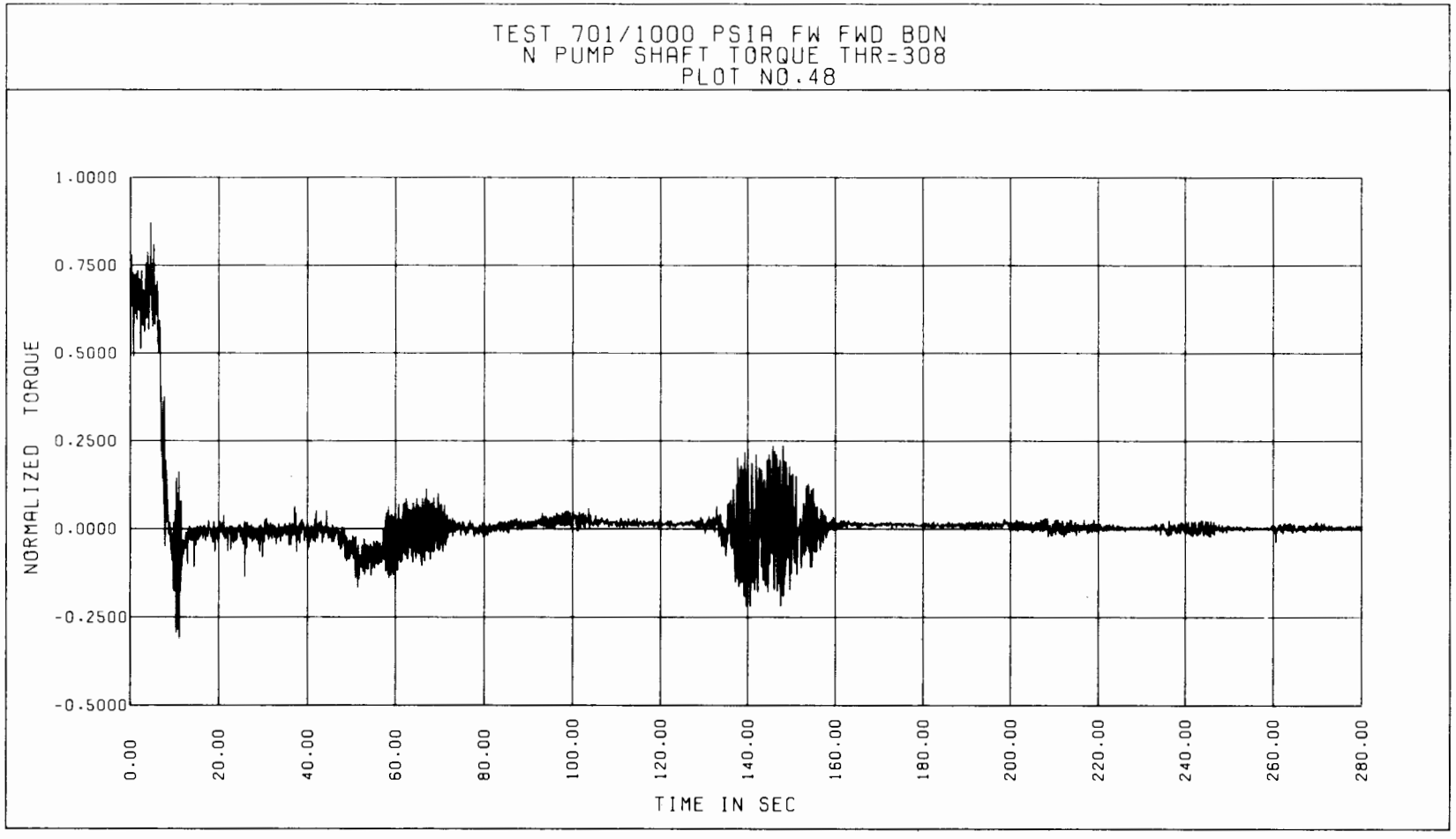

Figure 5-25. Test 701, Normalized Pump Shaft Torque vs Time

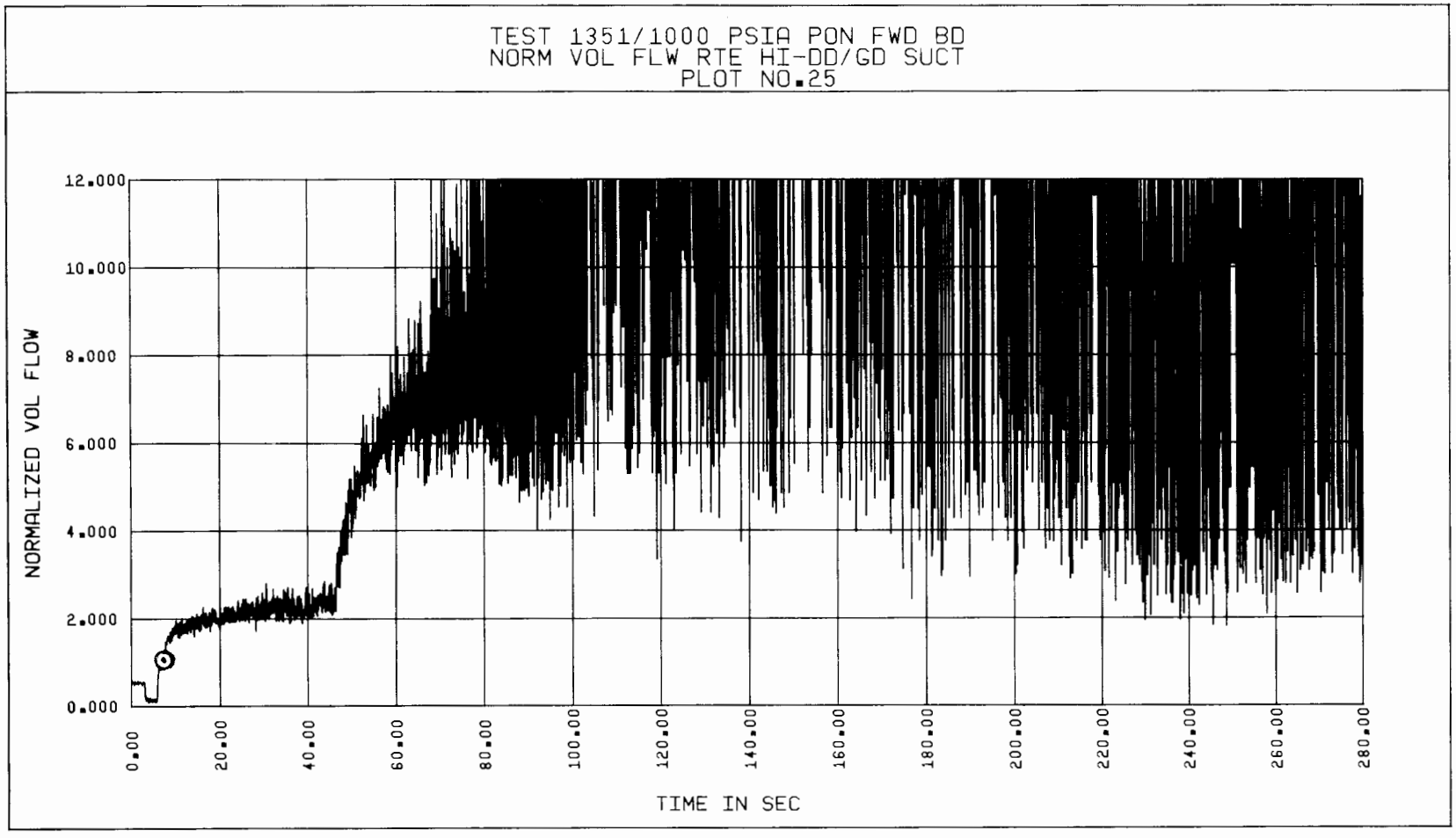

Figure 5-26. Test 1351, Normalized Volumetric Flow Rate vs Time

order of ±30% of the mean value for gamma densitometer measurements. Dividing the momentum flux values measured by the drag disc by the highly oscillatory low values of density generates the large amplitude oscillations seen in Figure 5-26 for the particular derived parameter.

An extensive analysis of the measurement uncertainties in the transient data will not be completed in this report. These are expected to be at least as large as those for steady-state data. The primary parameter uncertainties for steady-state measurements are provided in Volume VII, Test Facility Description, and the equations for generating the uncertainties for derived parameters are given in Volume VIII, Data Processing Methods. Further discussion of the transient measurement uncertainties will be provided in subsequent sections on data analysis.

In Section 5.2 below, overall observations and trends of the transient data are discussed, and additional qualification of the transient data is provided as data for various tests are analyzed.

5.2 OVERALL OBSERVATIONS AND TRENDS

In this section general observations on pump and test system behavior and processes involved during representative blowdowns will be described in detail. The pump and test system behavior will be described in terms of variations in pressures, void fractions, fluid densities and temperatures, volumetric and mass flow rates, momentum fluxes, pump speed, pump head, and pump hydraulic torque. Computer generated plots of these parameters are provided to aid in the discussion of this behavior. Some of these plots were developed using several different methods involving appropriate combinations of instrument measurements. In the discussion of the behavior of the blowdown parameters, typical curves generated on the basis of only one specific method will be considered, since the trends of the curves developed on the basis of other methods are similar. General descriptions of the blowdown behavior for each mode of testing will be followed by a discussion of various processes involved during the blowdowns. Homogeneity of flow, flow regime, and parameter oscillations during the blowdowns will also be considered in some detail.

5.2.1 Pump And Test System Blowdown Behavior

As indicated in Sections 2 and 3.2, the transient tests were conducted with either initially zero loop flow or non-zero loop flow. The modes of operation of the pump rotor during the blowdown were:

- rotor allowed to free wheel-motor power off
- rotor locked-motor power off, and
- motor power on

The location of the break was either at the suction side or the discharge side of the test pump. The blowdown behavior of the test system and the pump was dependent on the initial operating conditions and the mode of operation of the pump rotor. Therefore, the general behavior during the blowdown tests is discussed first, and then the differences in behavior between blowdown test cases are pointed out.

The test system depressurizes rapidly during the initial seconds after rupture indicating a subcooled blowdown period (see Figure 5-27). Then the pressure decays at a nearly constant rate during the saturated blowdown period. A mixture of saturated water and steam is expelled from the loop through the break during this time period. Typically this time period may be of the order of 40 to 200 seconds, for the spectrum of break sizes employed in the transient tests. After this time period, a sharp change in the slope of the pressure-time curve takes place. This is noticeable as a knee in the pressure curve of Figure 5-27. This change in slope is thought to be due to a change in the fluid condition from mostly liquid to mostly steam. Soon afterwards, the suction side as well as the discharge side of the test pump is voided of liquid, and the void fraction reaches a value of approximately 1.0 as indicated by the gamma densitometer. The void fraction curve of Figure 5-28 supports this observation. Eventually the pressure decays at a very low rate indicating that the fluid is all steam, either saturated or superheated.

The suction and discharge fluid temperatures during the blowdown are at saturation conditions until the loop piping is voided of liquid and the temperature sensing instrument is heated by the hot wall due to radiative heat transfer. The temperature curves of Figure 5-29 show this behavior. Note that the fluid thermocouple at discharge can be affected by the test pump seal injection inward leakage, and consequently may not show radiation heatup until at a later time, as seen from this figure. The suction and discharge density curves (Figure 5-30 and 5-31) also show a behavior similar to the pressure

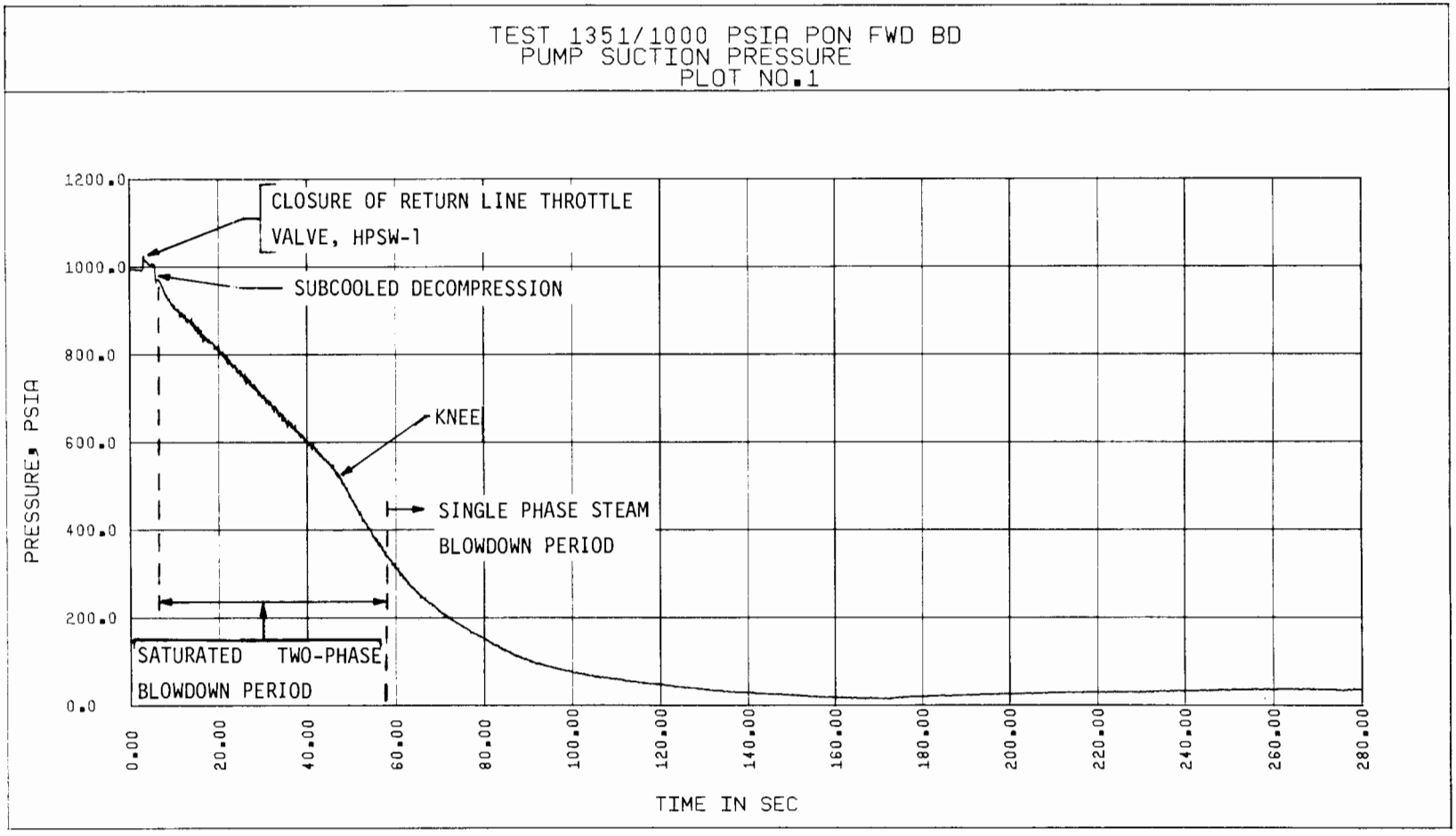

Figure 5-27. Test 1351, Suction Pressure vs Time

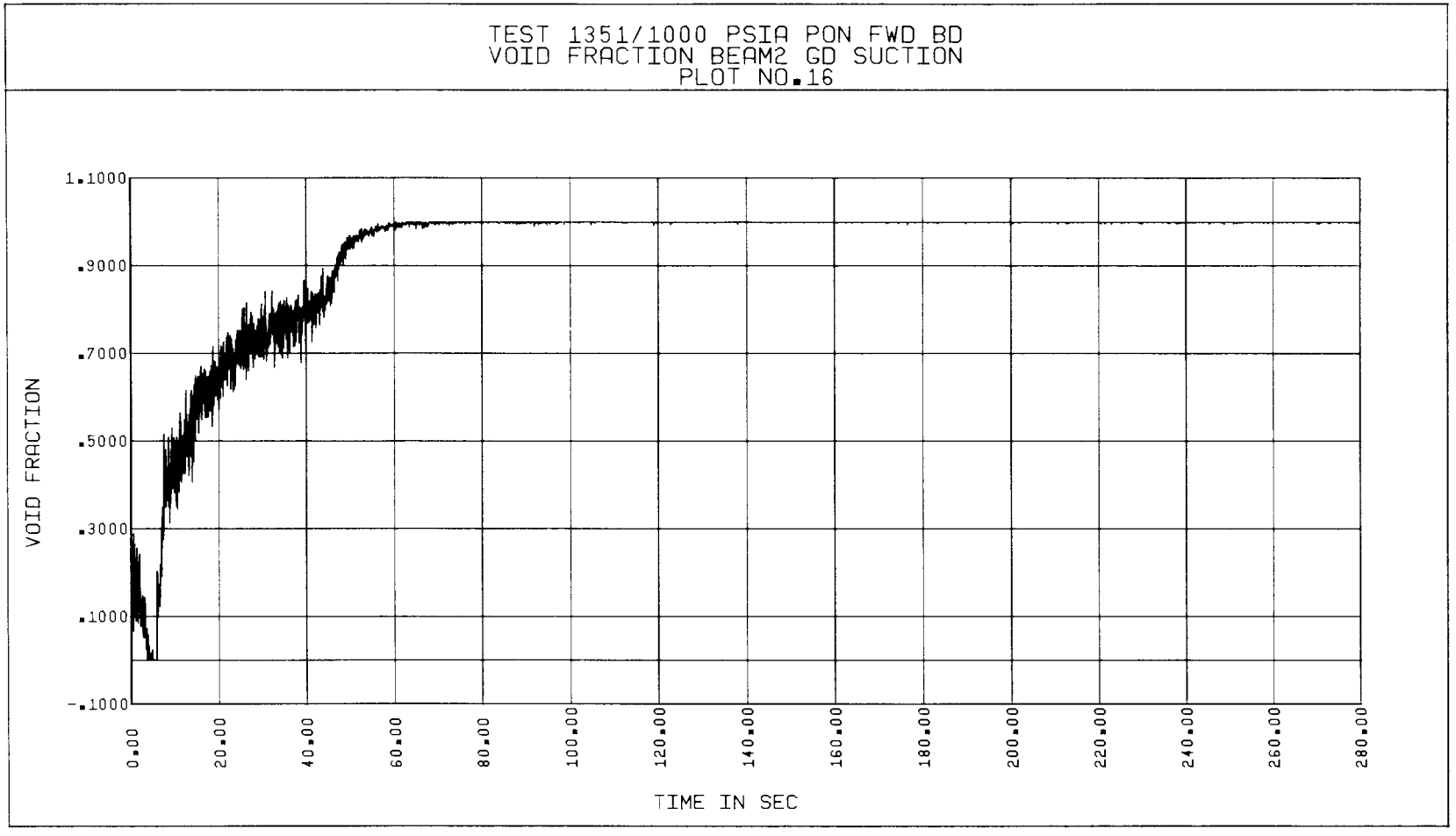

Figure 5-28. Test 1351, Void Fraction vs Time

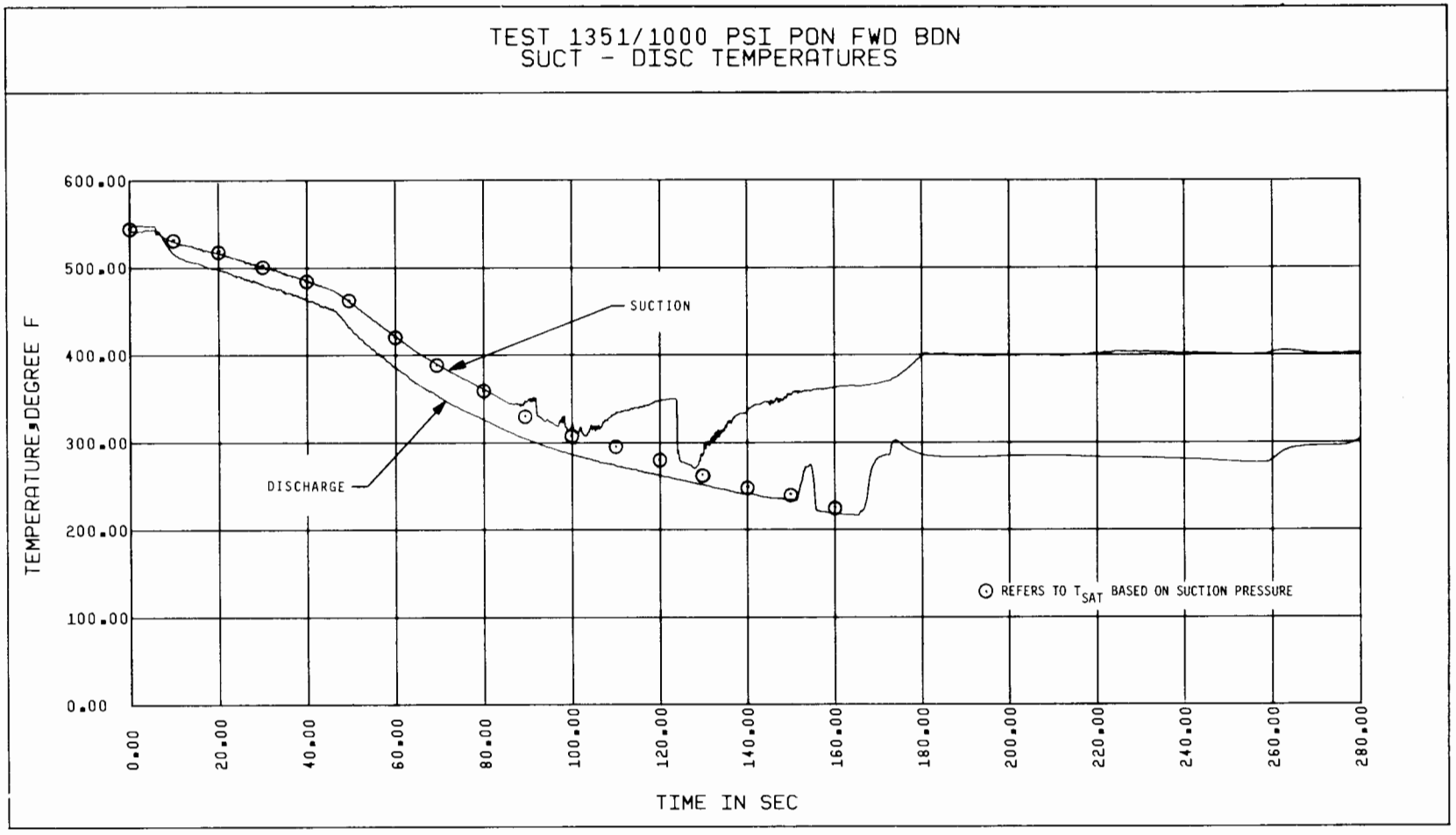

Figure 5-29. Test 1351, Suction and Discharge Temperature vs Time

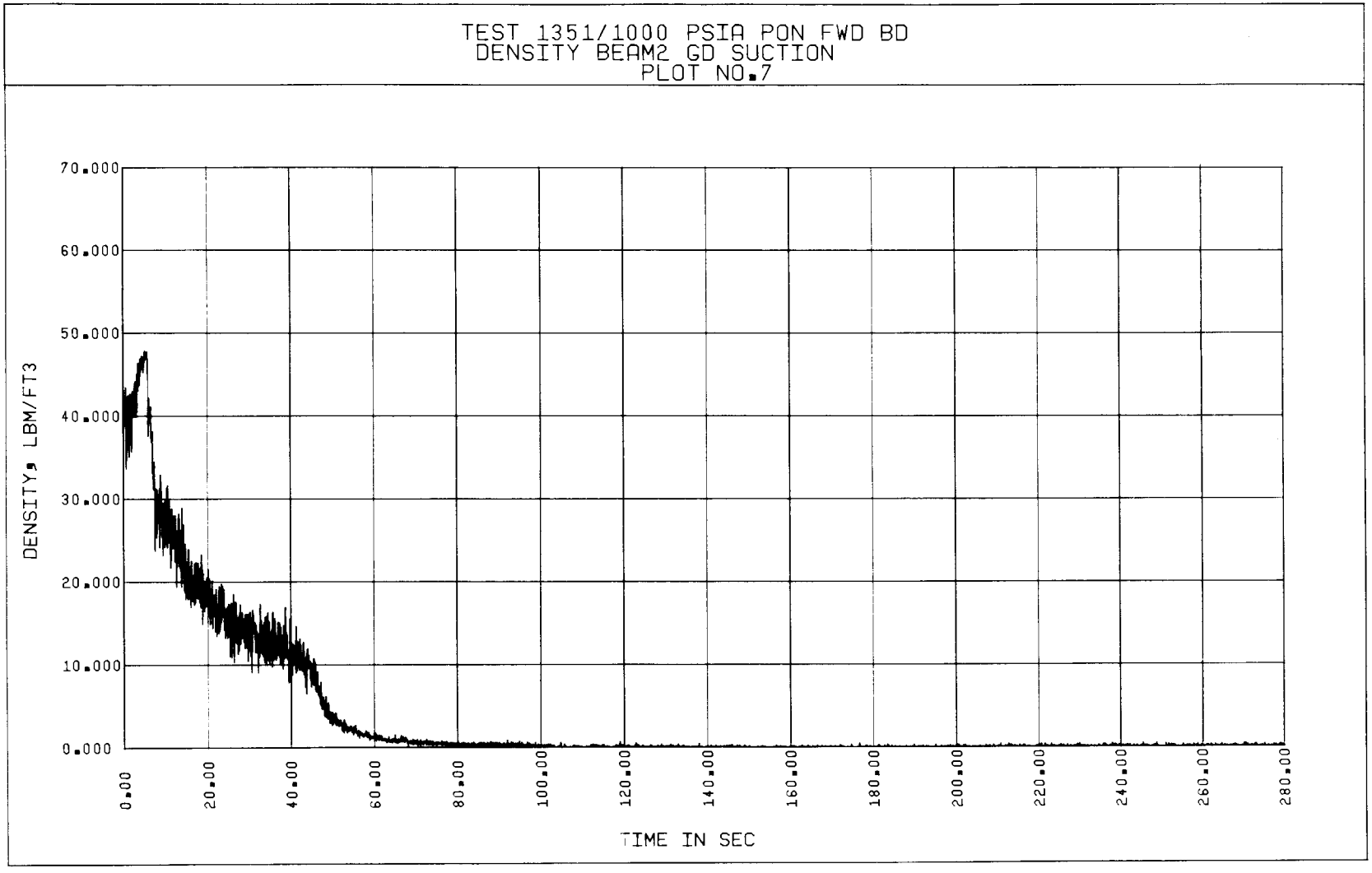

Figure 5-30. Test 1351, Suction Density vs Time

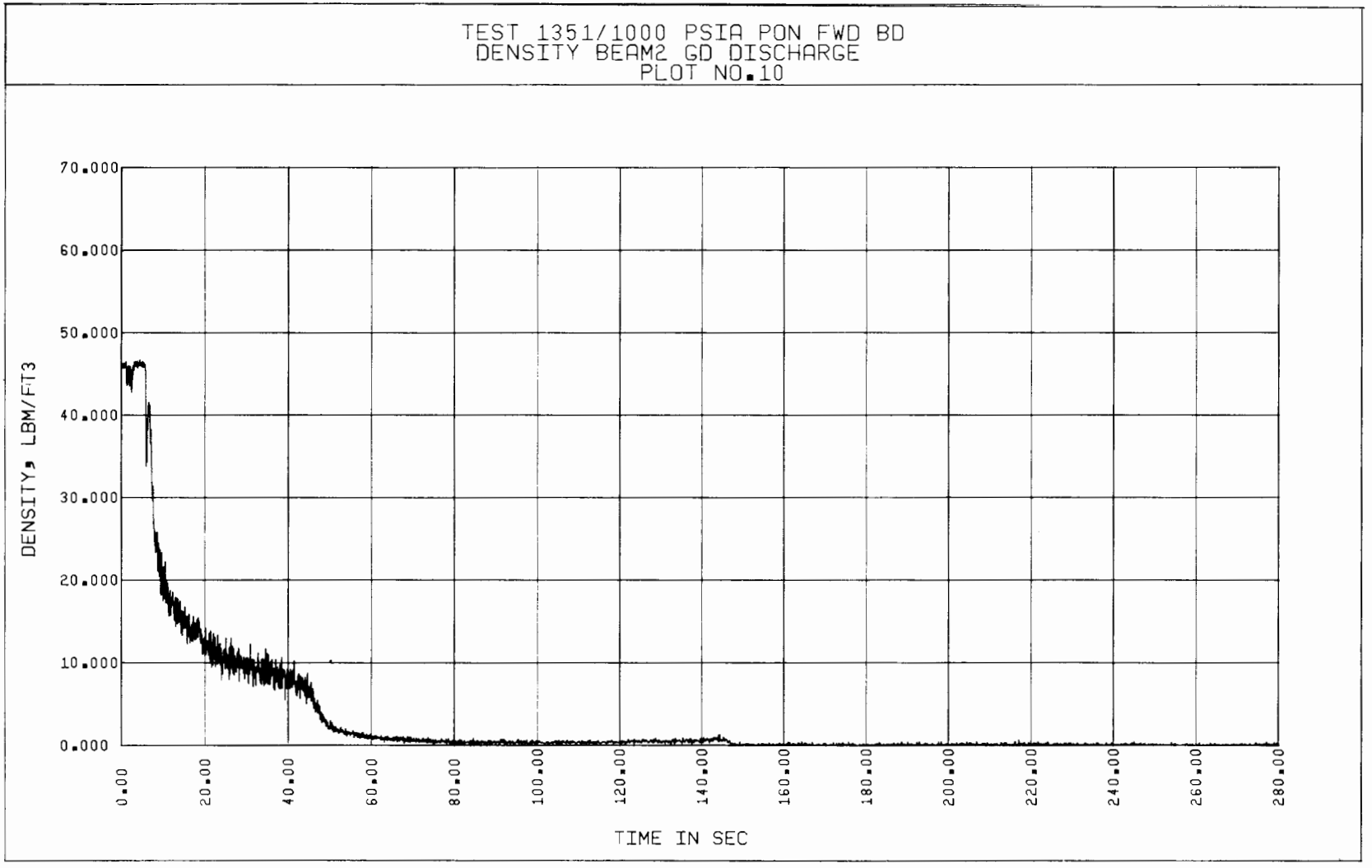

Figure 5-31. Test 1351, Discharge Density vs Time

curves. These densities approach single-phase subcooled water density ($\sim$47 lbm/ft^3) at the time the return line valve is shut and rapidly decay to the saturated two-phase density, eventually reaching single-phase saturated or superheated steam density.

The volumetric flow rate behavior as determined from the drag disc-gamma densitometer measurements or the turbine meter measurements (See Figures 5-32 or 5-33) shows an initial rapid increase in its value from the steady-state near-rated volumetric flow rate value. This time period is referred to as the "initial surge" (Period I). Within a few seconds after rupture, the volumetric flow rate reaches a quasi-steady value and remains at that value for several seconds ($\sim$40 to 90 seconds duration). This time period is labelled the quasi-steady state time period (Period II). As the piping becomes voided of liquid, the volumetric flow rate again increases rapidly, reaching a peak value and eventually falls off to lower values as seen from Figure 5-33. This time period is referred to as the "second surge" (Period III).

Typical mass flow rate variations during the blowdown are illustrated by the curve of Figure 5-34. It is seen that the mass flow rate is nearly constant during the steady-state time period and approaches zero value just after the closure of the return line throttle valve. After blowdown rupture takes place, the mass flow rate increases rapidly for few seconds and reaches a peak value. Then it falls off at a constant rate, until the loop piping is voided of liquid. At that time the mass flow rate decreases more rapidly, and then diminishes as the blowdown driving pressure and energy are expended.

The integral of the mass flow rate curve calculates the cumulative total of mass that has flowed through the measuring section and out through the break at any time during the blowdown. The mass flow integral curve of Figure 5-35 illustrates the transient behavior of this parameter. Due to the large mass flow rates realized at the beginning of the blowdown, this integral increases rapidly during the initial few seconds of the transient and then gradually levels off to a maximum value as seen in Figure 5-35. Due to the effect of seal injection inward leakage at the test pump, the slope of this curve towards the end of the blowdown can be slightly positive, instead of zero. Note that the mass flow integral prior to rupture is zero, since there is no mass flow out of the test loop during the steady-state time period. In Figure 5-35, the mass of

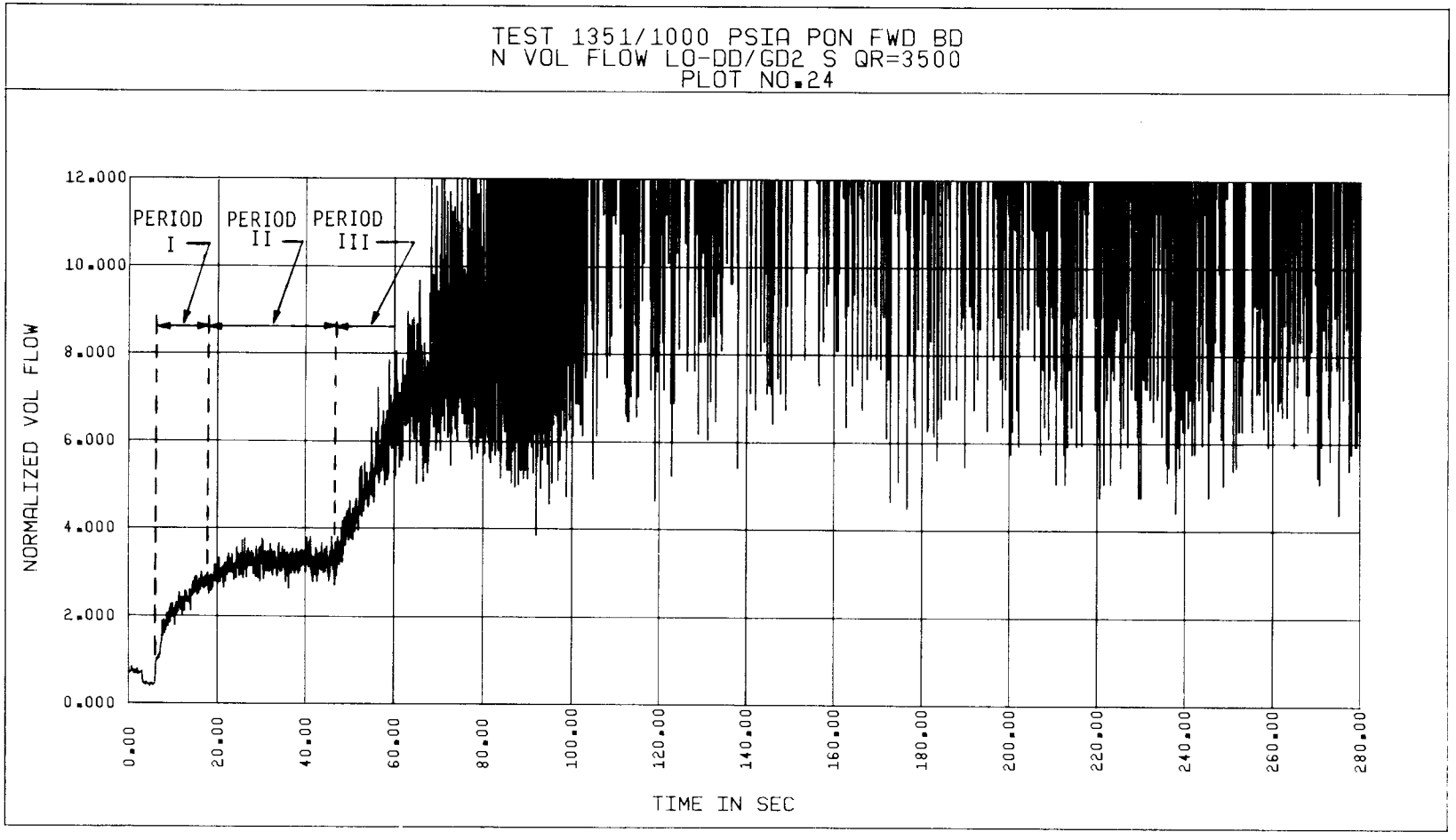

Figure 5-32. Test 1179, Normalized Suction Volumetric Flow Rate vs Time for Three Periods

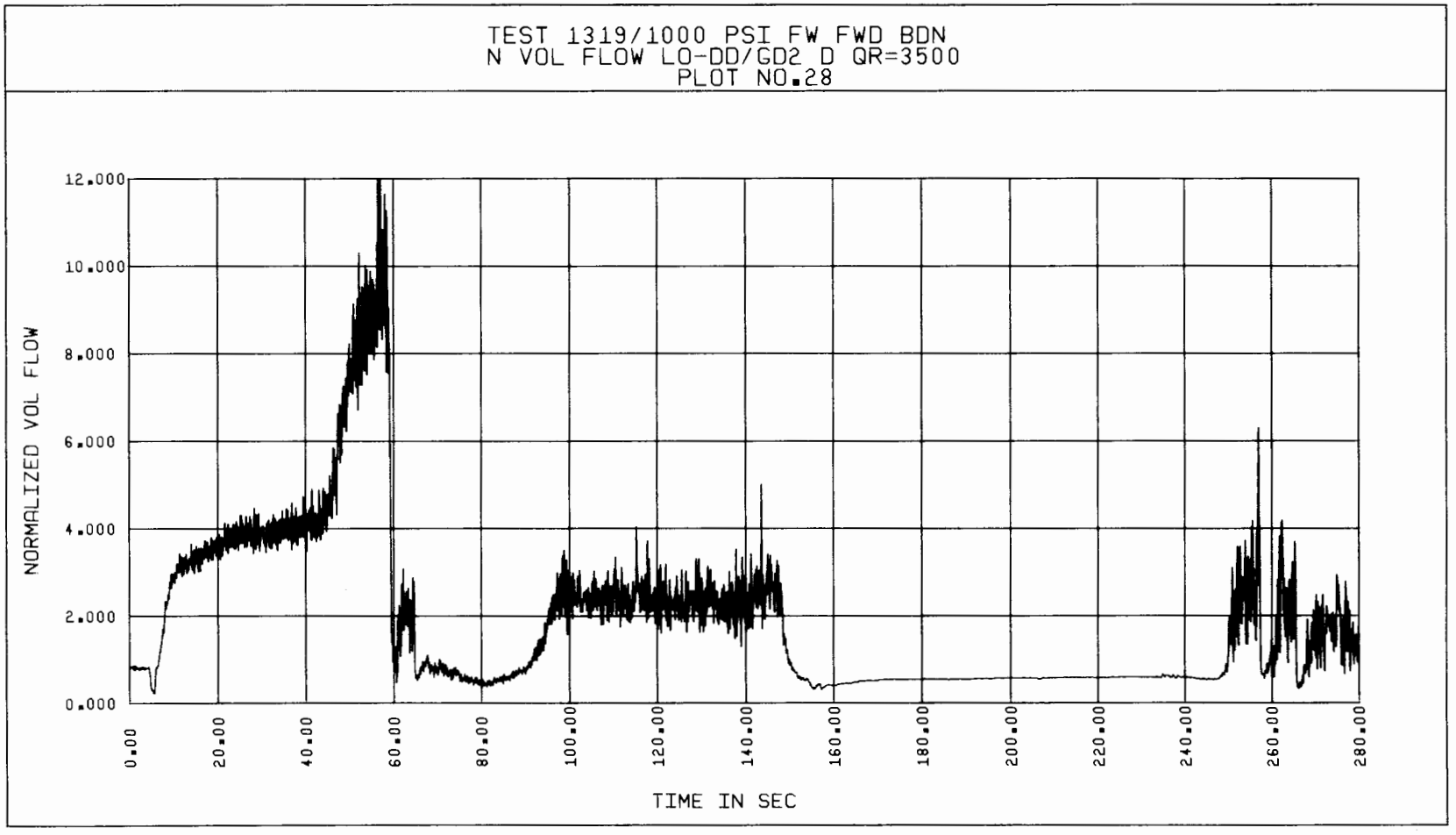

Figure 5-33. Test 1179, Normalized Suction Volumetric Flow Rate vs Time for Three Periods

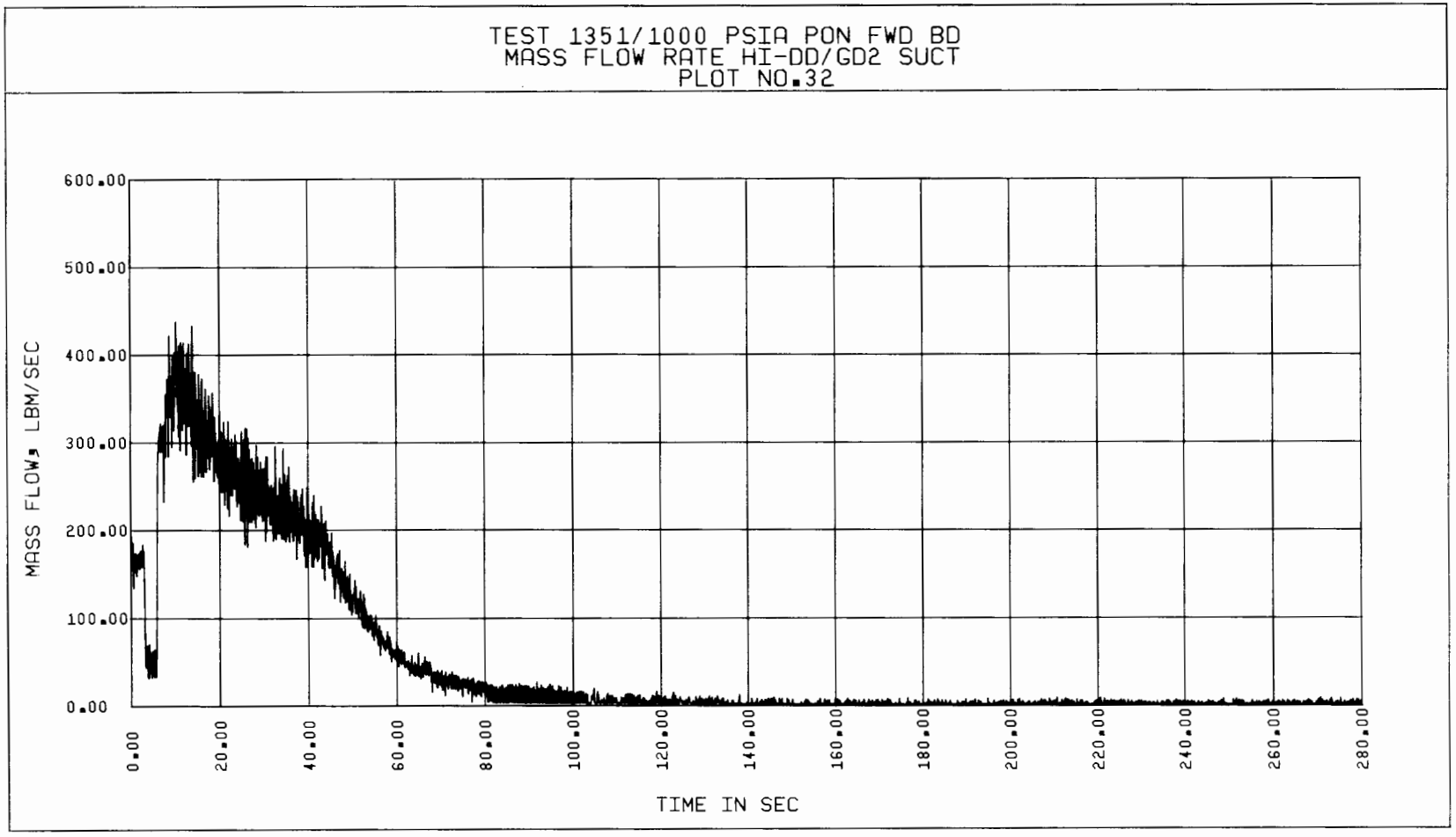

Figure 5-34. Test 1351, Suction Mass Flow Rate vs Time

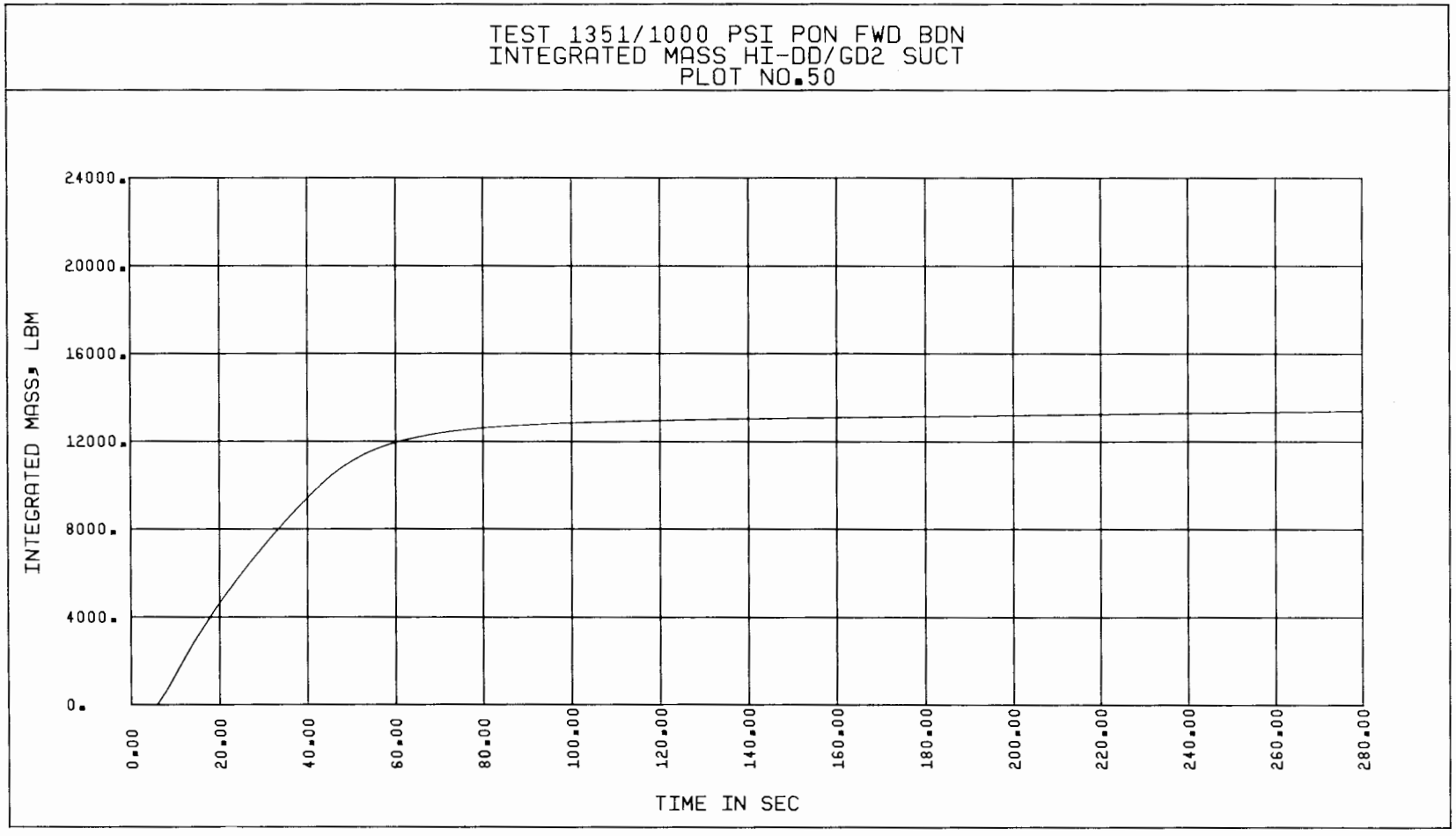

Figure 5-35. Test 1351, Integrated Suction Mass Flow vs Time

fluid initially in the piping sections from which the fluid can flow through the suction measuring section and out through the break is 13,900 lbm for comparison purposes. Details of the computation of this value are provided in Appendix A.

The test pump seal injection flow (cold water at about 160°F) into the pump cavity behind the impeller is shown in Figure 5-36. This flow is measured by an orifice flow meter in the inlet injection line. It is seen that the flow remains essentially constant during most of the transient. The seal injection flow out of the pump cavity as measured by the magnetic flow meter decreases with time during the blowdown and is plotted as a function of time in Figure 5-37. Comparison of the curve of Figure 5-36 with that of Figure 5-37 indicates that the net seal injection leakage flow was into the mainstream during the transient.

The momentum flux directly measured by the drag disc (Figure 5-38) starts out at relatively small values (corresponding to the initial density and near-rated volumetric flow rate) and rises rapidly to a peak value and eventually falls off to lower values, as both the flow rate and the density decrease. Both the low and high drag discs at discharge and the low drag disc at suction showed gradual varying momentum flux values, whereas the momentum flux measured by the high drag disc at suction had two distinct peaks and was substantially lower than that measured by the low drag disc at suction. This pattern of behavior was repeated for almost all the blowdown runs. Implications of this behavior with regard to flow homogeneity is discussed in Section 5.2.3.

Typical pump speed variation during the blowdown for the free-wheeling case is shown in Figure 5-39. It is seen that the speed is near-rated initially, and as the pump motor power is turned off, it first decreases. Then the fluid volumetric flow rate surges up (Period I), the speed also increases rapidly and remains at the quasi-steady value for several ($\sim$49 to 90) seconds (Period II). It again rapidly rises, as the fluid condition changes to almost all steam, and reaches a peak value. It then levels off and eventually drops off to lower values, as the volumetric flow rate also diminishes to final steam values (Period III). It is seen that for the most of the duration of the blowdown, the speed trace follows the trends of the volumetric flow rate curve (See Figures 5-32 and 5-39).

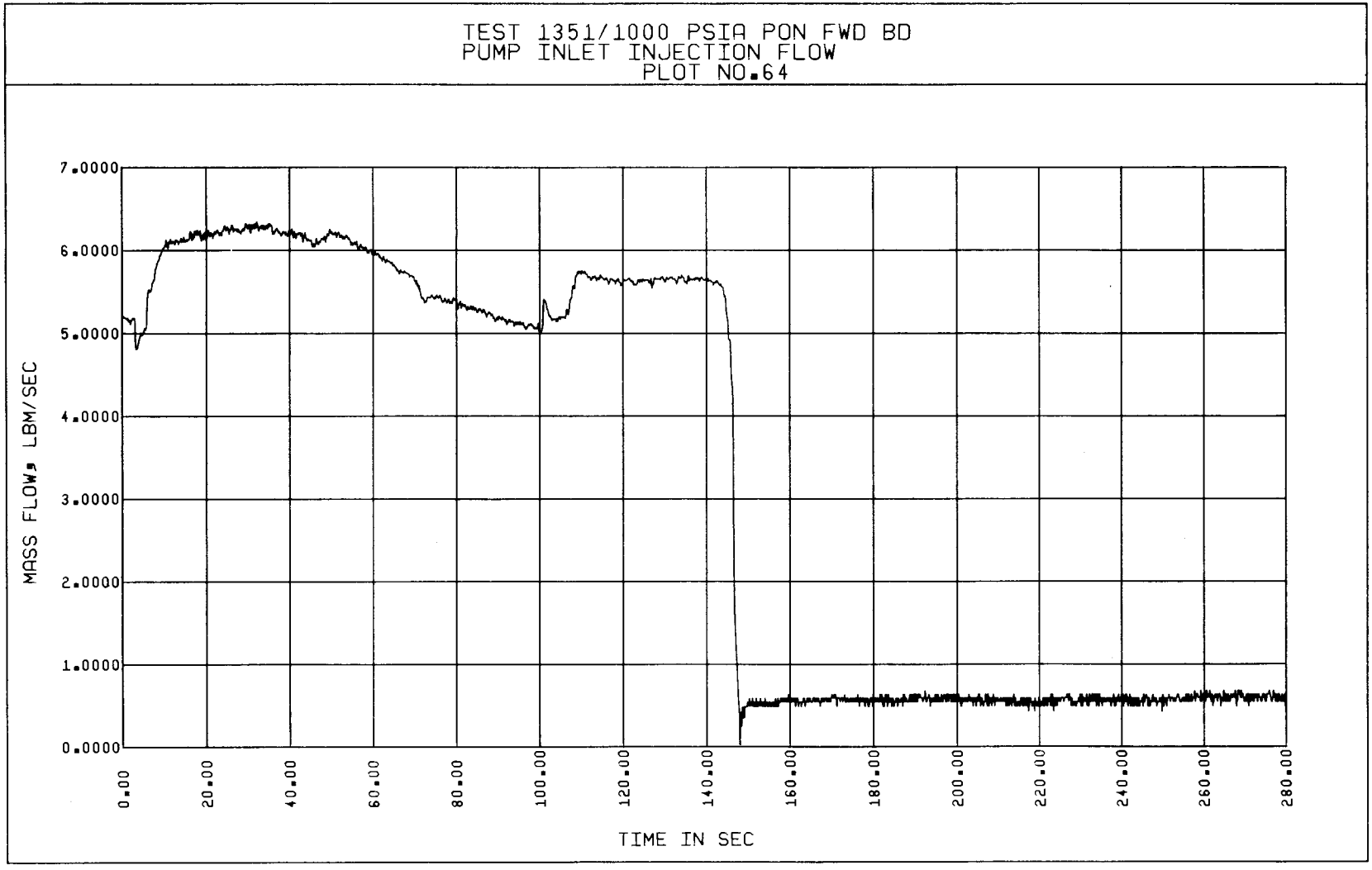

Figure 5-36. Test 1351, Pump Seal Injection Inlet Flow vs Time

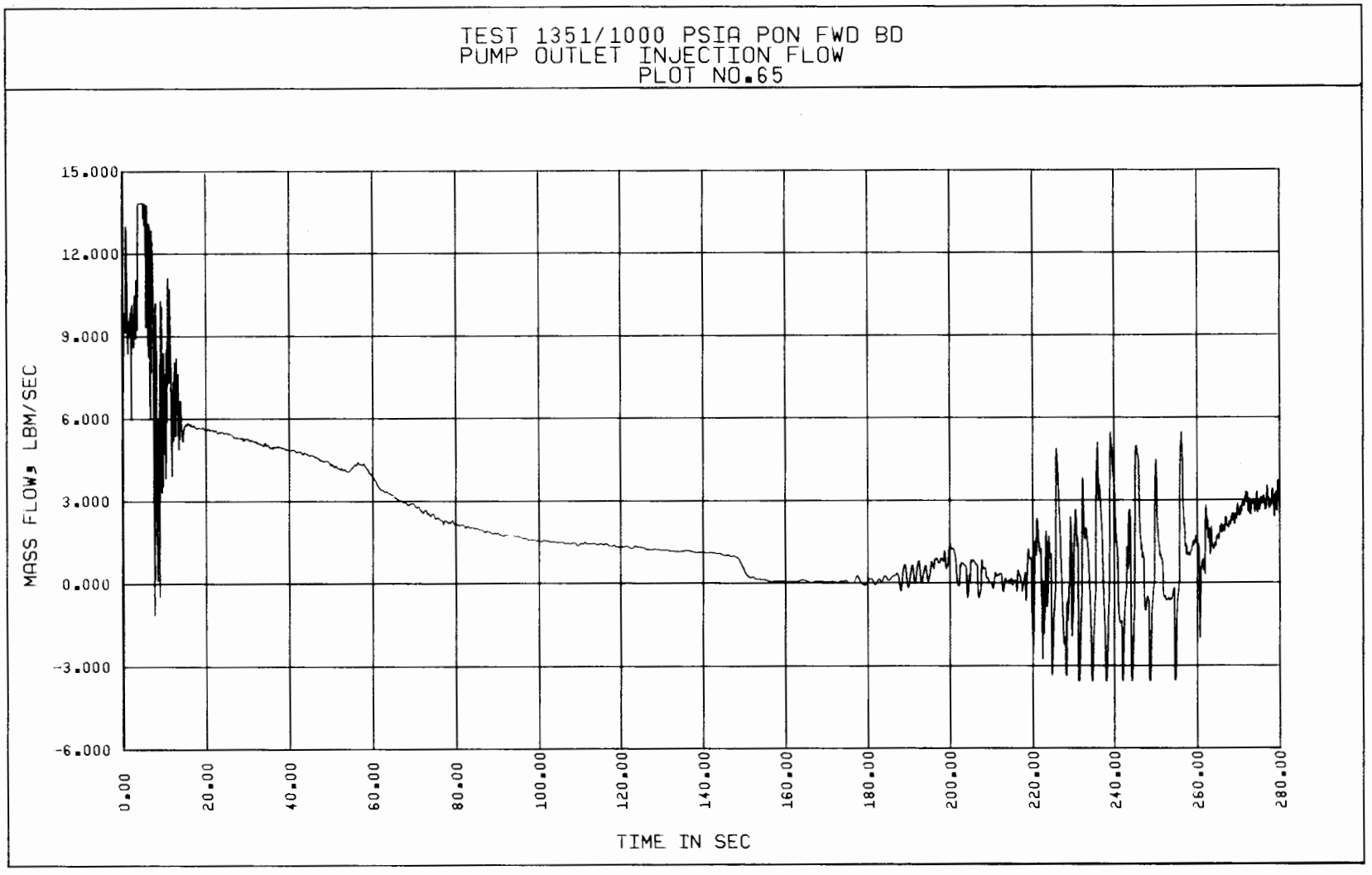

Figure 5-37. Test 1351, Pump Seal Injection Outlet Flow vs Time

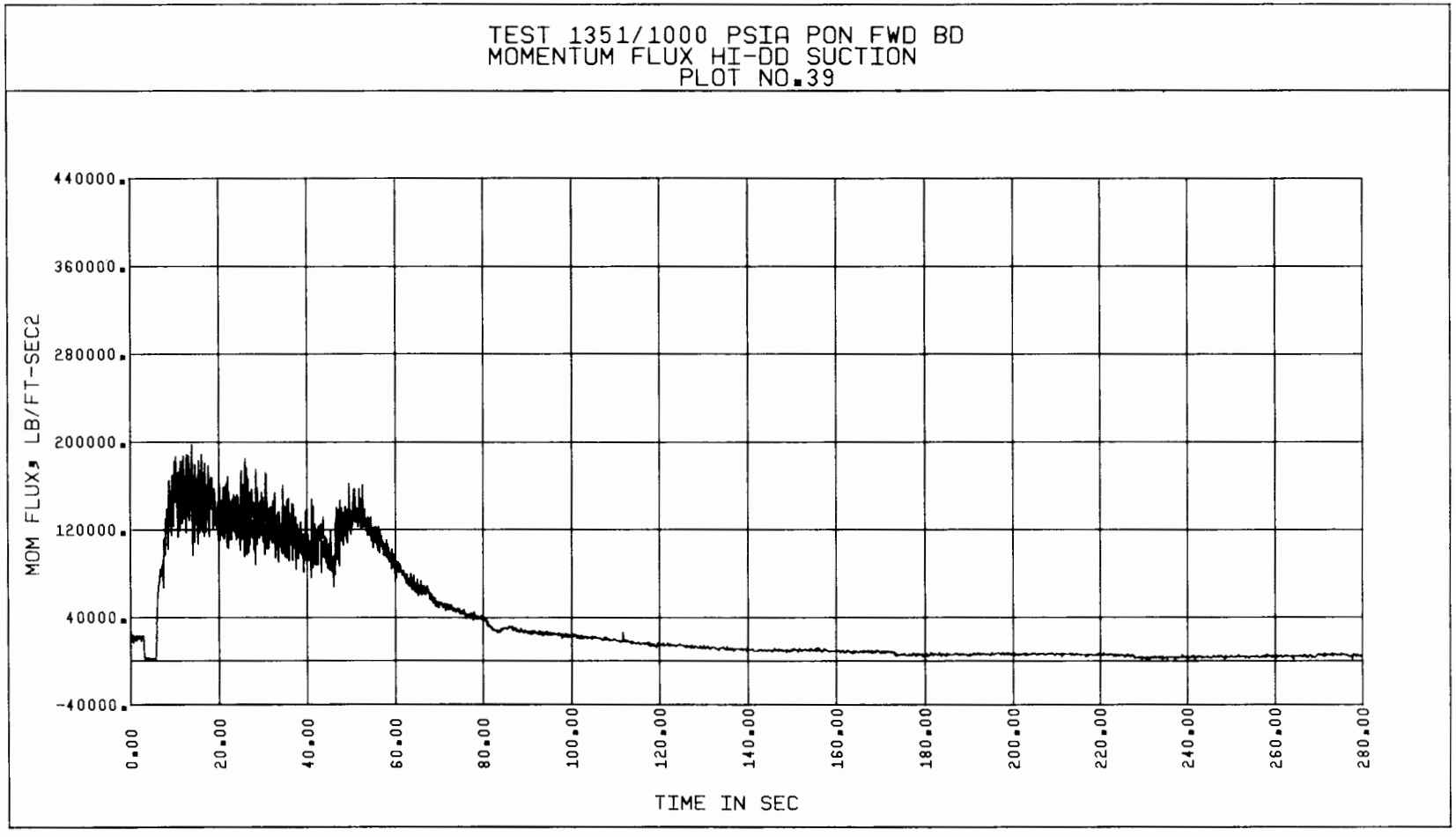

Figure 5-38. Test 1351, Suction Momentum Flux vs Time

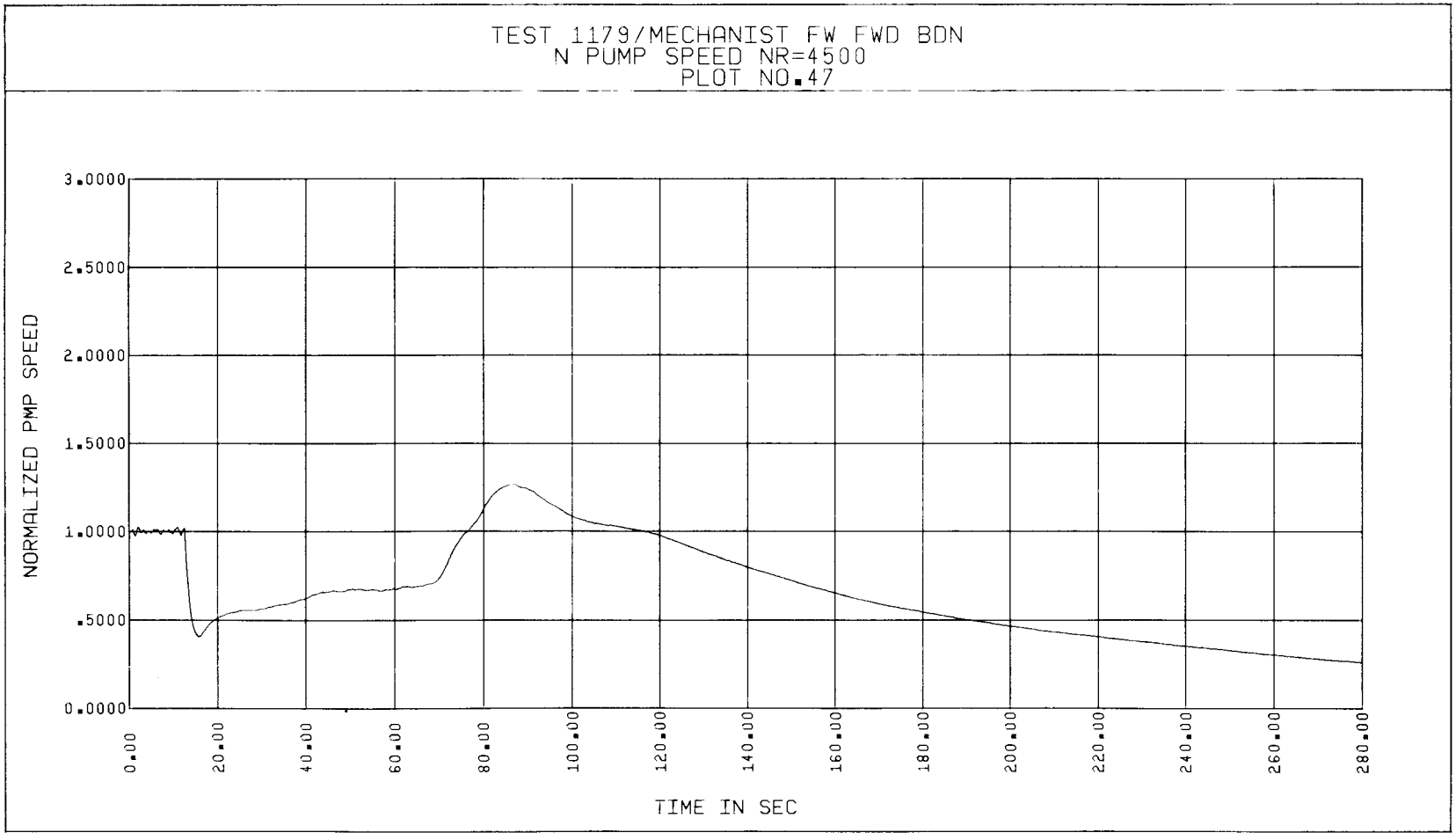

Figure 5-39. Test 1179, Normalized Pump Speed vs Time

The pump blowdown performance parameters, such as the pump head and torque, are also dependent on the volumetric flow rate variation. At steady-state conditions immediately prior to the rupture of the diaphragms, the pump head has a positive value corresponding to the steady-state single-phase or two-phase volumetric flow rate and speed (See Figure 5-40). As closure of the return line throttle valve is effected, the pump head momentarily reaches the shut-off head, and when rupture occurs, the pump head drops off to negative values (indicating lower discharge pressures than suction pressures) reaching a maximum negative pump head value within a few seconds. The pump head (psi) trace also exhibits a pattern similar to the momentum flux curve of Figure 5-38, in that two distinct peaks (negative) are noticeable in it. As all the fluid in the test system changes into steam, the pump head became very small and asymptotically approaches the zero value.

The measured pump shaft torque (Figure 5-41) for free-wheeling forward flow tests starts out positive initially and becomes negative within a few seconds after the pump motor is turned-off. It crosses the zero torque line approximately at the time that the pump speed reaches a minimum value after the power trip. The torque becomes more negative as the pump rotor is accelerated forward by the fluid due to the increased volumetric flow through the pump. Eventually as the speed and the flow rate become quasi-steady, the shaft torque approaches zero value and remains there until the speed is increased due to the second surge in volumetric flow rate. At that time, the shaft torque becomes more negative again. Generally, after the peak speed is reached, the shaft torque should return to near zero and remain there during final steam flow through the test pump. For Test 1319 (Figure 5-41) however, the blowdown line valve was closed at about 59 seconds and the pump was developing positive torque during coastdown pumping.

The hydraulic torque variation during the transient is illustrated by the curve of Figure 5-42. It is a derived parameter from the shaft torque and the friction and windage torque, which is dependent on the pump speed and the average pressure within the pump. It is also affected by the angular acceleration of the pump. Trends similar to those discussed above for the shaft torque hold true for the hydraulic torque during the transient, even though the magnitude of the hydraulic torque is somewhat different from those for the shaft torque.

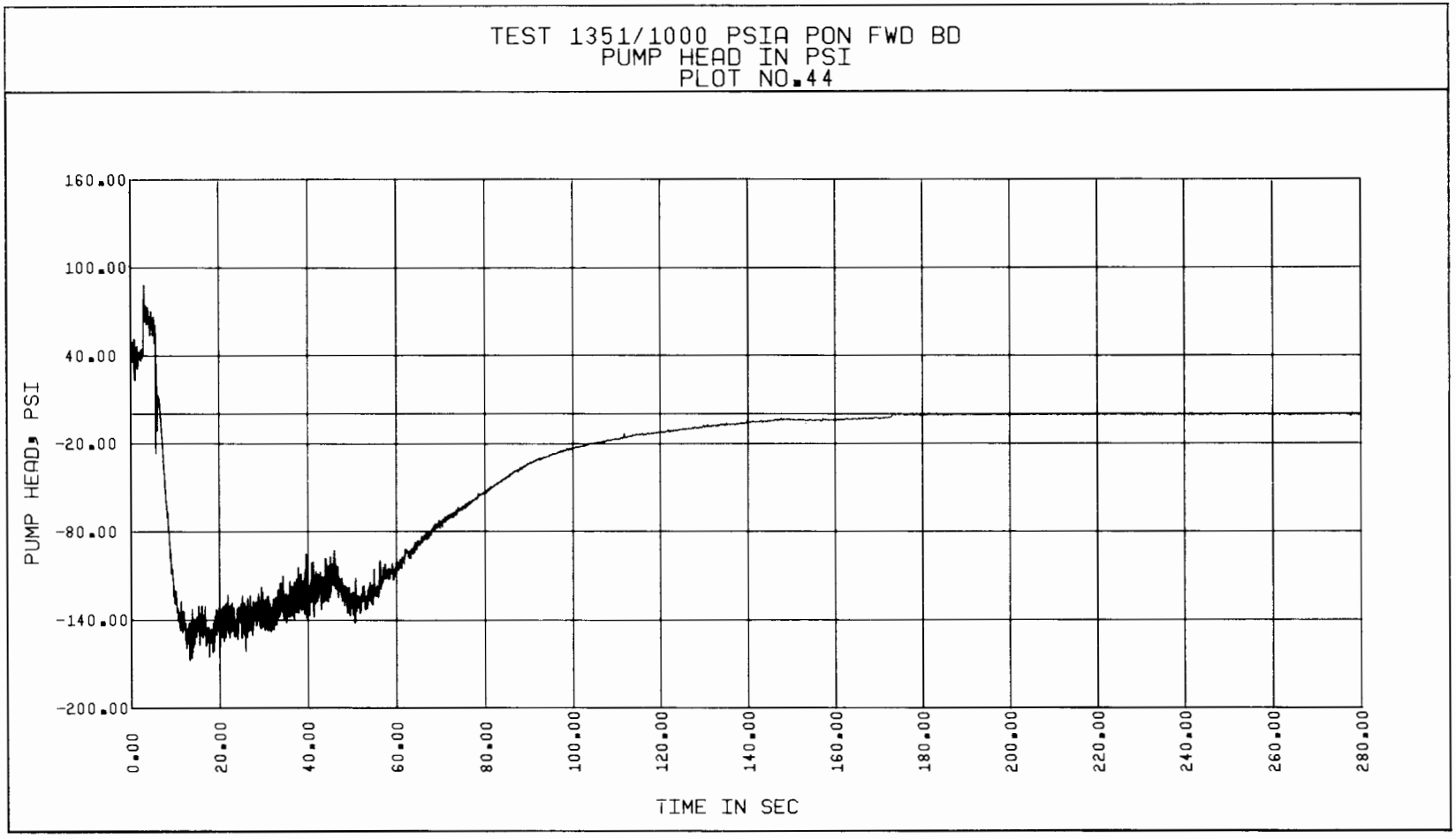

Figure 5-40. Test 1351, Pump Head vs Time

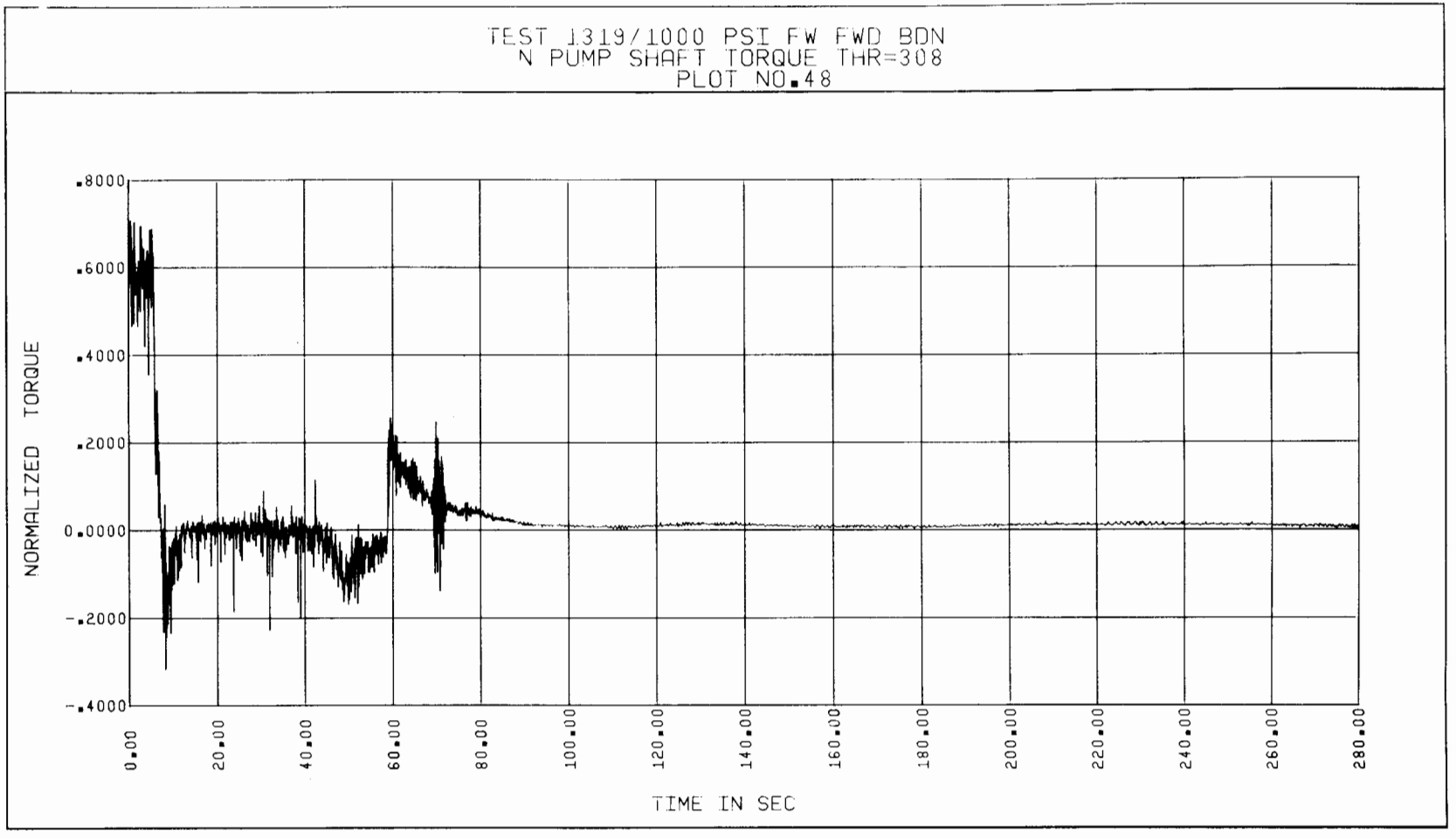

Figure 5-41. Test 1319, Normalized Pump Shaft Torque vs Time

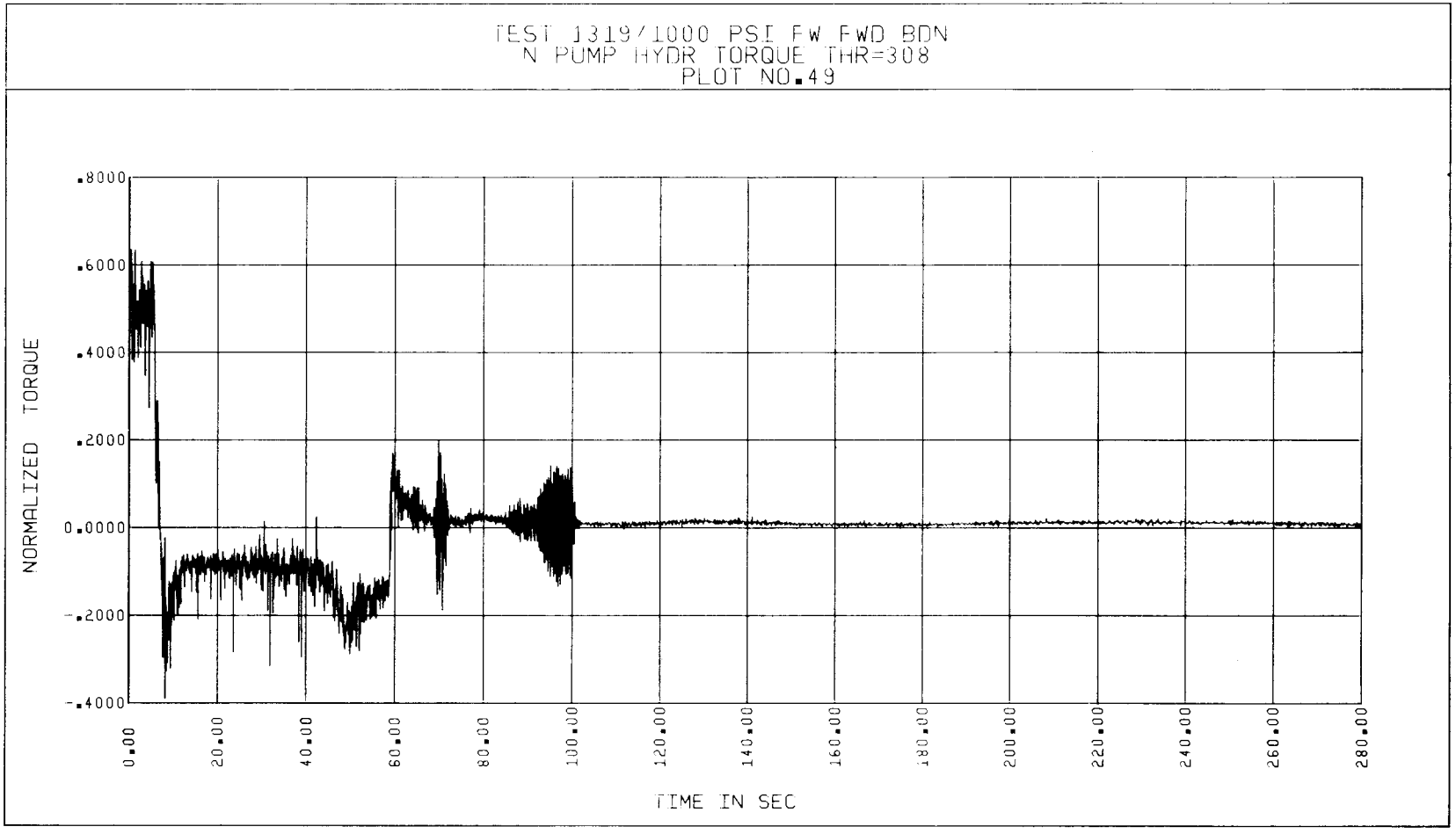

Figure 5-42. Test 1319, Normalized Pump Hydraulic Torque vs Time

Variations in general test system and pump behavior discussed above exist among various blowdown tests, and these shall be briefly looked at below relative to the location of the break and the mode of testing.

Case I. Locked Rotor Forward Blowdown Test

For this mode of testing, the break is located at the discharge side of the pump, and the pump rotor is prevented from rotating in either the forward or the reverse direction during the transient as well as during a few seconds prior to rupture. The blowdown starts from initially stagnant fluid conditions, and the fluid is subcooled during steady-state. Thus, the initial fluid volumetric flow rate, pump speed and the void fraction are essentially zero. The initial mass flow rate, momentum flux, pump head and torque are similarly zero. During the transient with pump speed zero, the pump head and the torques remain negative (See Figures 5-43 and 5-44). The hydraulic torque values are identical to those for the shaft torque, since the pump shaft and rotor are not rotating. For all other parameters, the general behavior described above is applicable.

Case II. Free-Wheeling Forward Blowdown Test

The location of the break for this case is also at the discharge side of the pump. However, the initial flow and speed are not zero for this case. There is circulation through the loop initially, and a positive head is developed by the test pump during steady-state operation. The initial shaft and hydraulic torque are also positive due to the near-rated volumetric flow rate and speed condition. For most of the blowdown tests using this mode of testing, the pump initial flow and speed were adjusted to be as close as possible to the rated flow (3500 gpm) and speed (4500 rpm).

During the blowdown, the pump volumetric flow rate and the pump speed variations follow the trends described in the general behavior section above. That is, the three distinct time periods - initial surge, quasi-steady state time period, and second surge - were noticeable also for the speed trace as seen from Figure 5-39. The initial void fraction at the suction side of the pump was non-zero for this case due to the fact that the fluid circulation through the loop was maintained only by the test pump. The test pump cavitated because of the high vapor pressure of the fluid at the suction side and the pressure loss

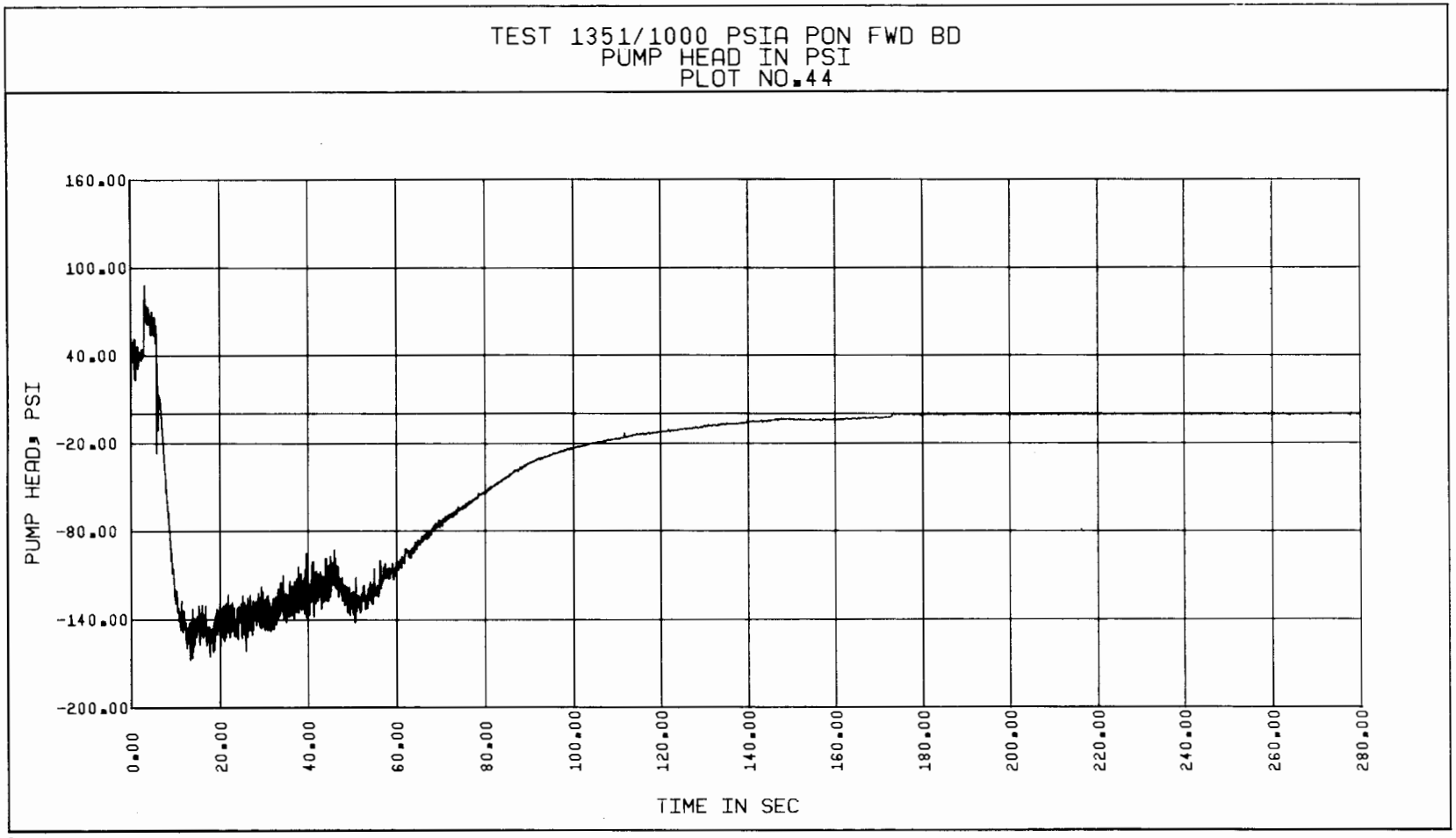

Figure 5-43. Test 1267, Pump Head vs Time

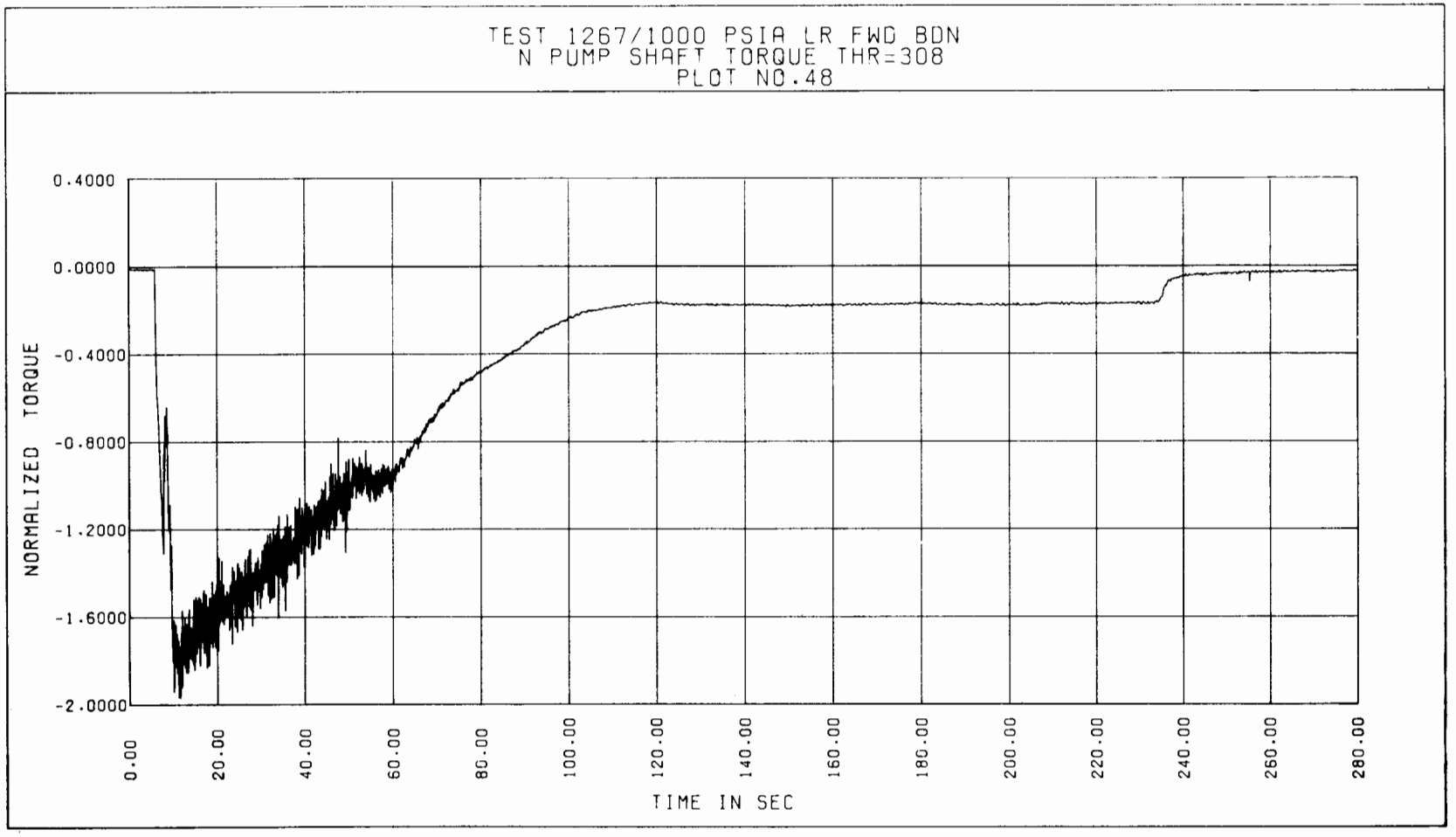

Figure 5-44. Test 1267, Normalized Pump Shaft Torque vs Time

which occurred with no booster pump head between the high pressure drum and the test pump. The initial suction side void fraction momentarily reached slightly subcooled fluid condition when the return line throttle valve was closed and the test pump achieved the shut-off head (See Figure 5-45). The fluid flow rate approached the zero value at this time. In general, the overall trends of the blowdown plots presented in Figure 5-28 through 5-42 are typical of the transient behavior of the test system and pump for this case.

Case III. Power-On Forward Blowdown Test

Again the location of the break for this case is the discharge side of the pump. The initial flow, speed, void fraction, torque, pump head, and momentrum flux are similar to those realized for Case II. In fact, the general blowdown behavior is also similar to that for Case II, except for the behavior of the pump speed and torque curves. The pump speed during the blowdown is maintained constant at the initial value by keeping the motor power on throughout the test (See Figure 5-46). The variable frequency speed control system described in Volume VII, Section 3, is used to maintain this constant speed by providing electrical braking during the transient, when the pump impeller attempts to accelerate as a result of turbining action by the fluid. Consequently, the shaft torque remains at large negative values during most of the transient as seen from Figure 5-47. Eventually, as the fluid is mostly turned into steam, the shaft torque becomes smaller, and even positive. The hydraulic torque curve follows the same trends as those for the shaft torque curve since the speed is held constant during the transient. All other parameters behave in the same manner as described for Case II blowdown tests.

Case IV. Locked Rotor Reverse Blowdown Test

For this mode of testing, the break is located at the suction side of the pump, and the pump rotor is prevented from rotating in either the forward or reverse direction during the transient as well as the few seconds immediately prior to rupture. The fluid is subcooled initially, and the blowdown starts from initially stagnant fluid conditions. Thus the steady-state fluid volumetric flow rate, pump speed and the void fraction are zero. Furthermore, the pump speed during the transient is also zero. The initial mass flow rates, momentum flux, pump head and torques are similarly zero. During the transient, the pump flow is in the reverse direction. The pump head and the shaft torque

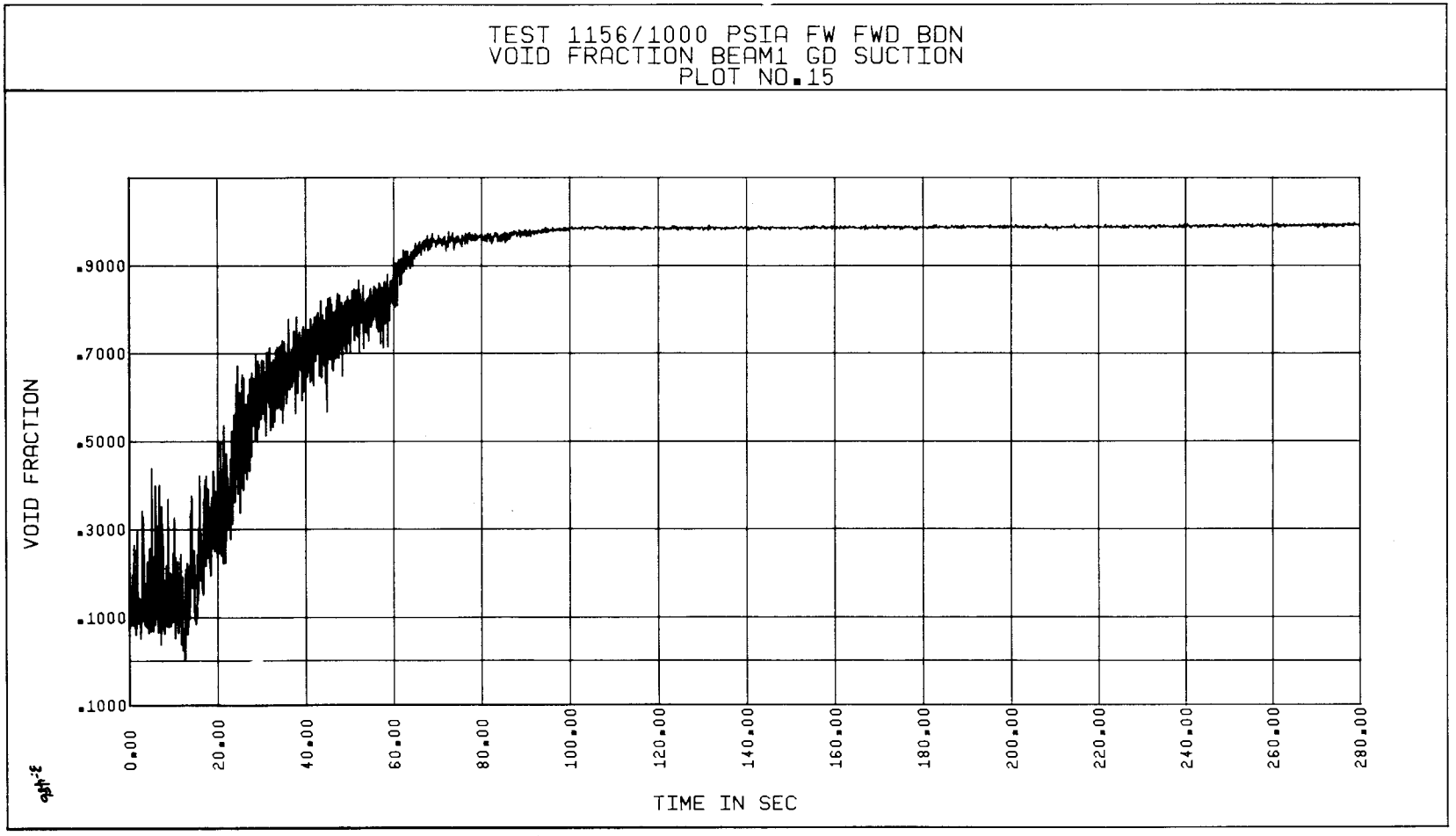

Figure 5-45. Test 1156, Suction Void Fraction vs Time

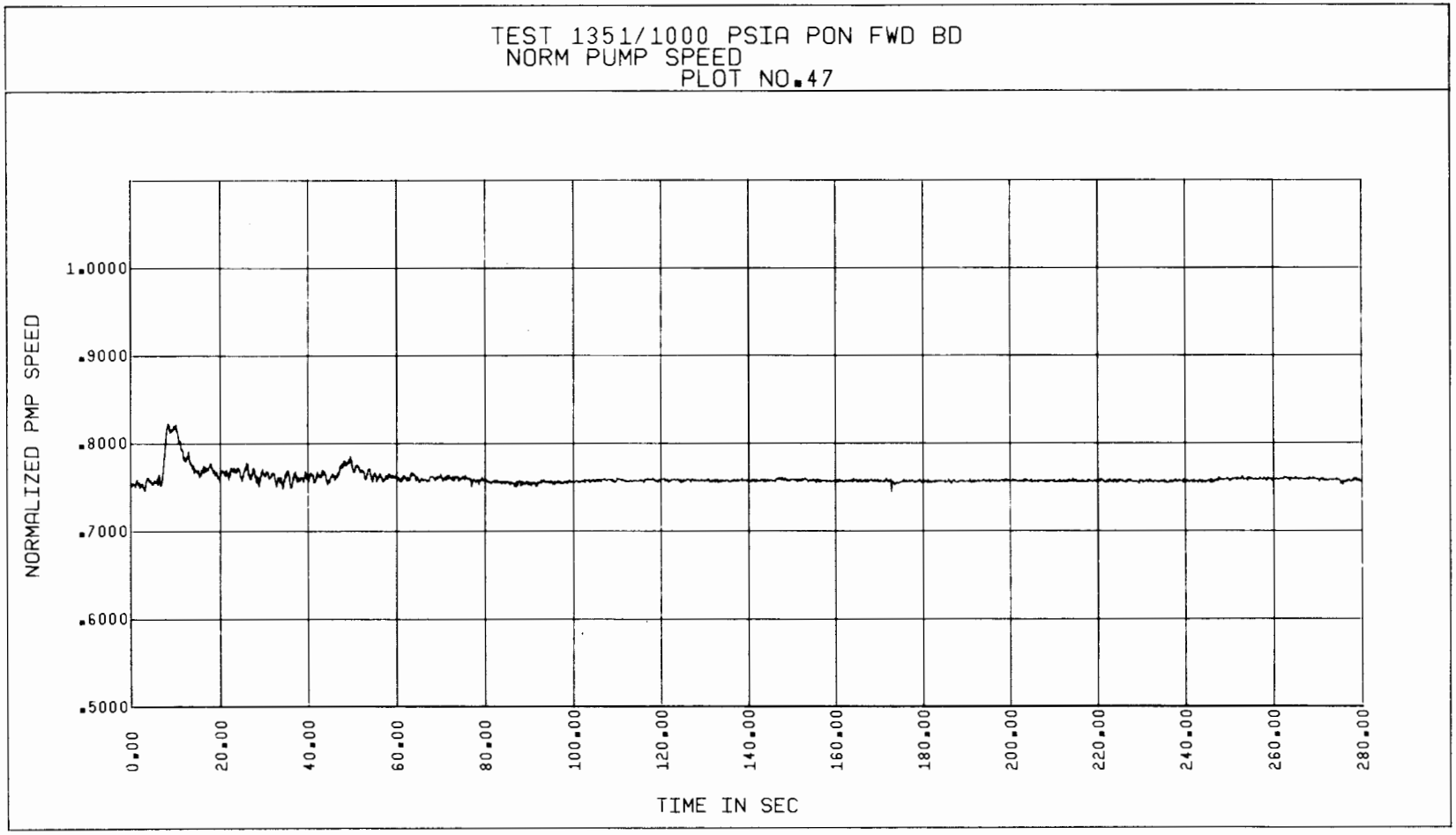

Figure 5-46. Test 1351, Normalized Pump Speed vs Time

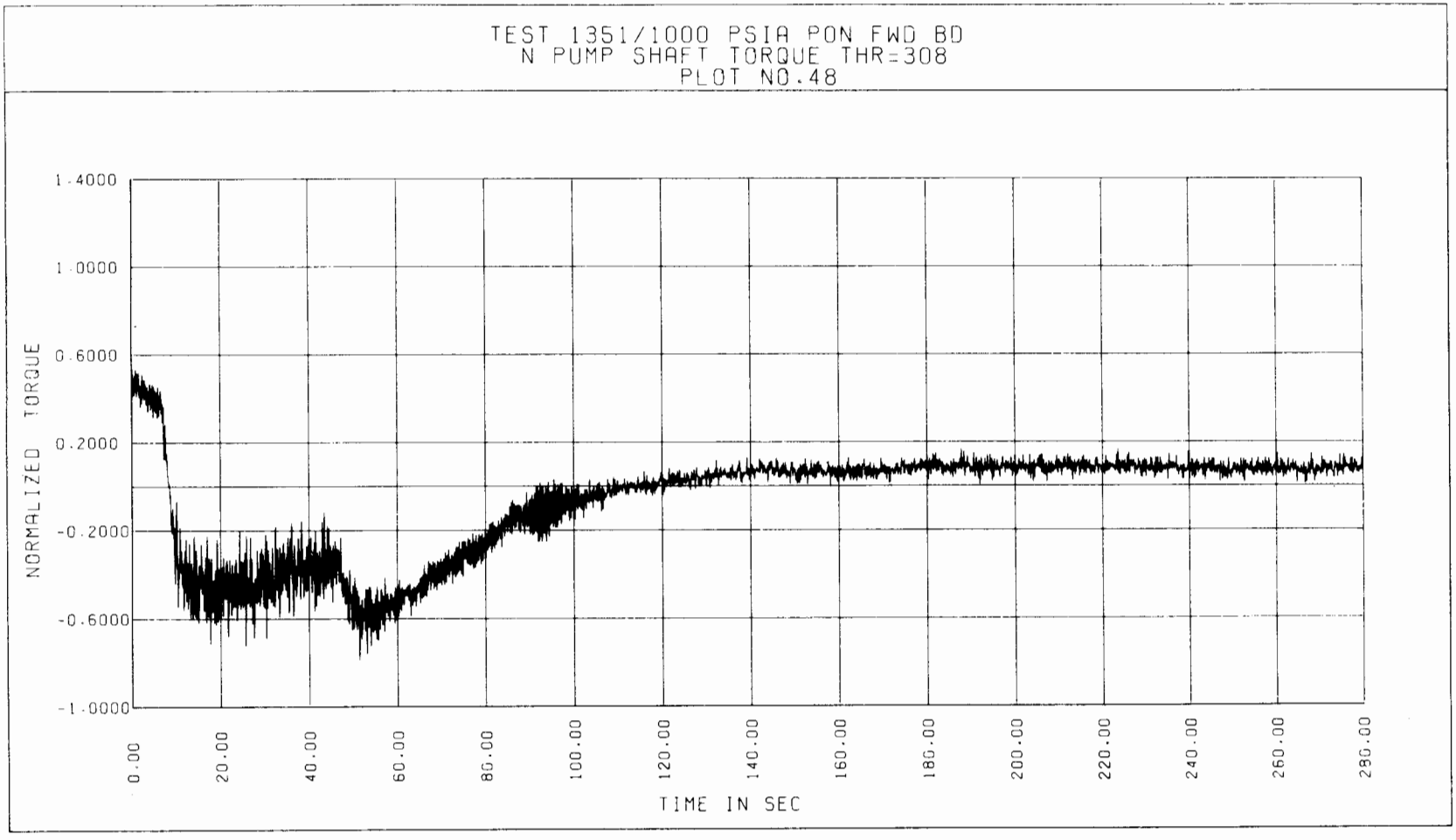

Figure 5-47. Test 1351, Normalized Pump Shaft Torque vs Time

remain positive during the blowdown (See Figures 5-48 and 5-49) due to the higher discharge side pressure and the turbining hydraulic torque developed by the fluid, respectively. The shaft torque values are identical to those for the hydraulic torque since the pump rotor is locked. (See Figures 5-49 and 5-50). For all other blowdown parameters the general behavior described earlier is applicable.

Case V. Free-Wheeling Reverse Blowdown Test

The break location for this case is also the suction side of the pump. The initial flow rate and pump speed are not zero, however, for this case. During steady-state operation just prior to rupture, the flow rate and speed are in the forward direction, either at or below rated values. Since the initial flow is developed by the test pump alone, the void fraction at the suction side of the pump is greater than zero during steady-state operation. When the return line throttle valve is closed, the void fraction approaches zero. A positive pump head is developed by the test pump during steady-state operation, and the initial loop circulation is in the forward direction.

During the transient, the pump flow direction is reversed from positive to negative. The duration of the positive flow time period is very short (See Figure 5-51). After the power is turned-off, the test pump slows down and crosses the zero speed line within a few seconds, and stays negative during most of the duration of the blowdown (Figure 5-52). The three distinct time periods -- initial surge, quasi-steady state time period, and second surge -- described in the general behavior section are noticeable in the speed trace for this case also. Similar trends hold true for the volumetric flow rate as seen from Figure 5-51. However, there are many more oscillations in this curve than there are in the speed trace. The pump head variation during the transient is shown in Figure 5-53. It is seen that the pump head remains positive during the blowdown, that is, the discharge pressure was higher than the suction pressure throughout the transient. The pump shaft torque values are positive during most of the duration of the transient, since the pump is in the reverse turbining operating mode during most of the test. For this operating mode, the hydraulic torque is considered positive and its magnitude is large enough to overcome the friction and windage torque and accelerate the pump rotor during part of the transient. The net effect therefore, is a

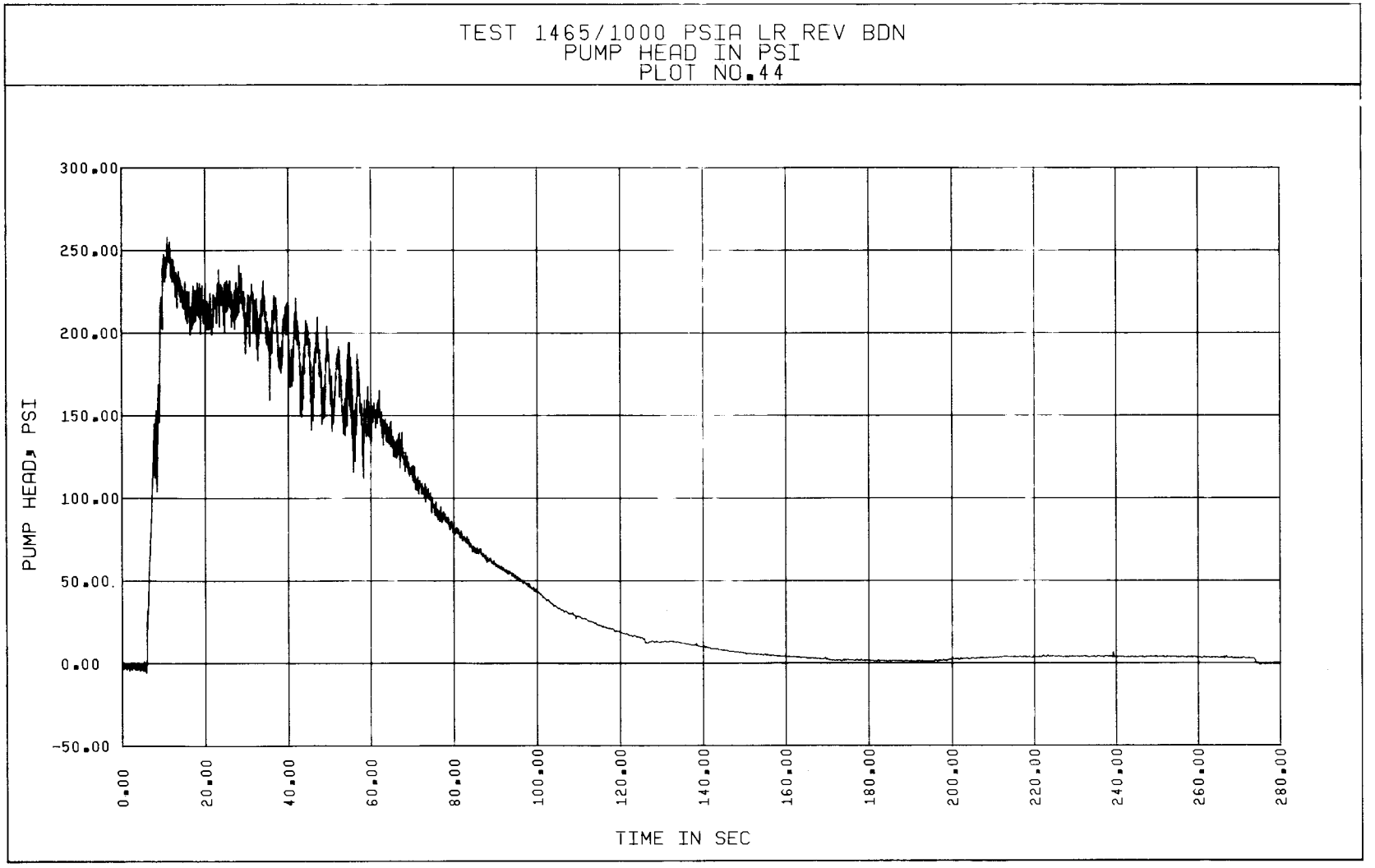

Figure 5-48. Test 1465, Pump Head vs Time

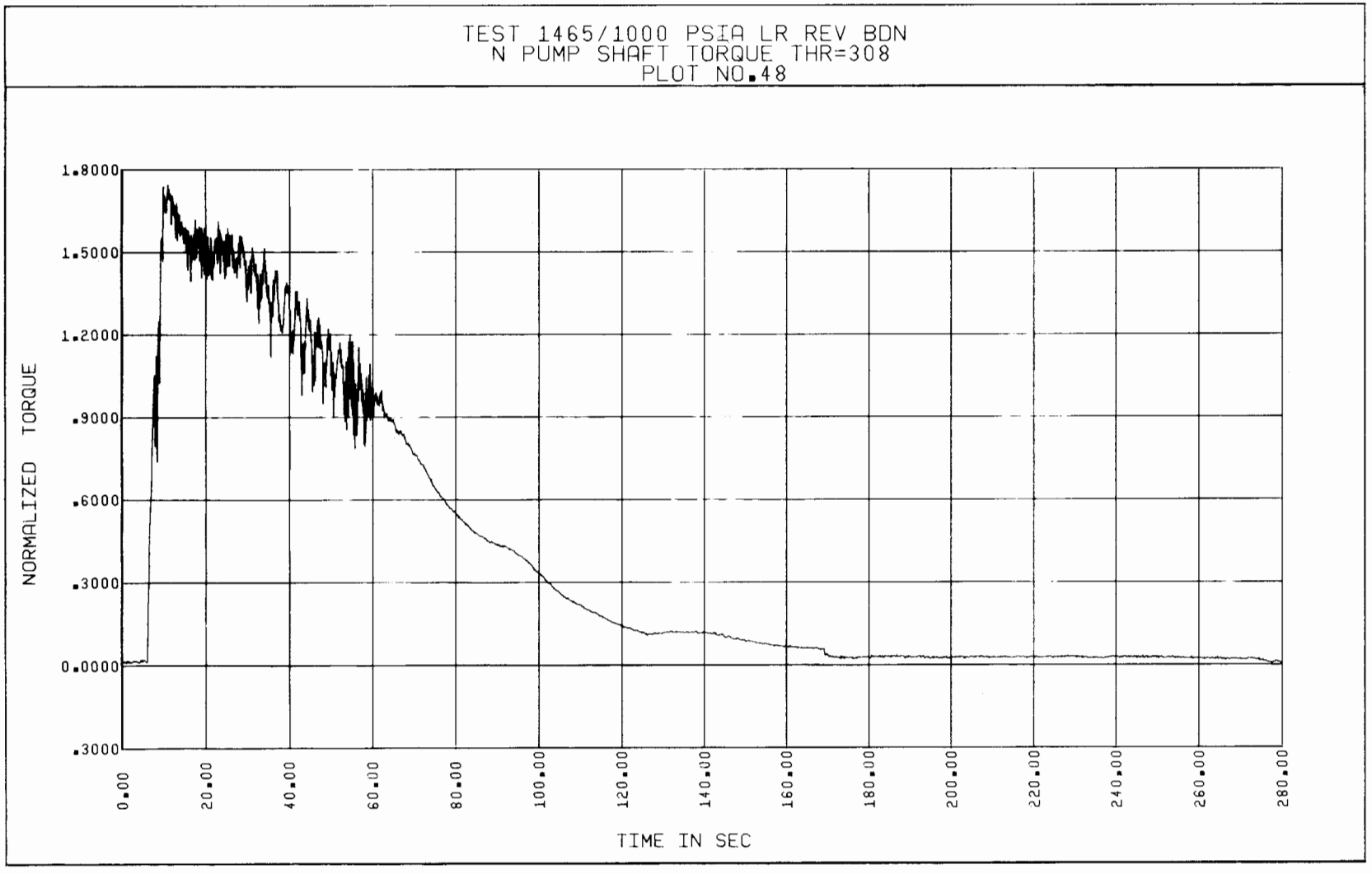

Figure 5-49. Test 1465, Normalized Pump Shaft Torque vs Time

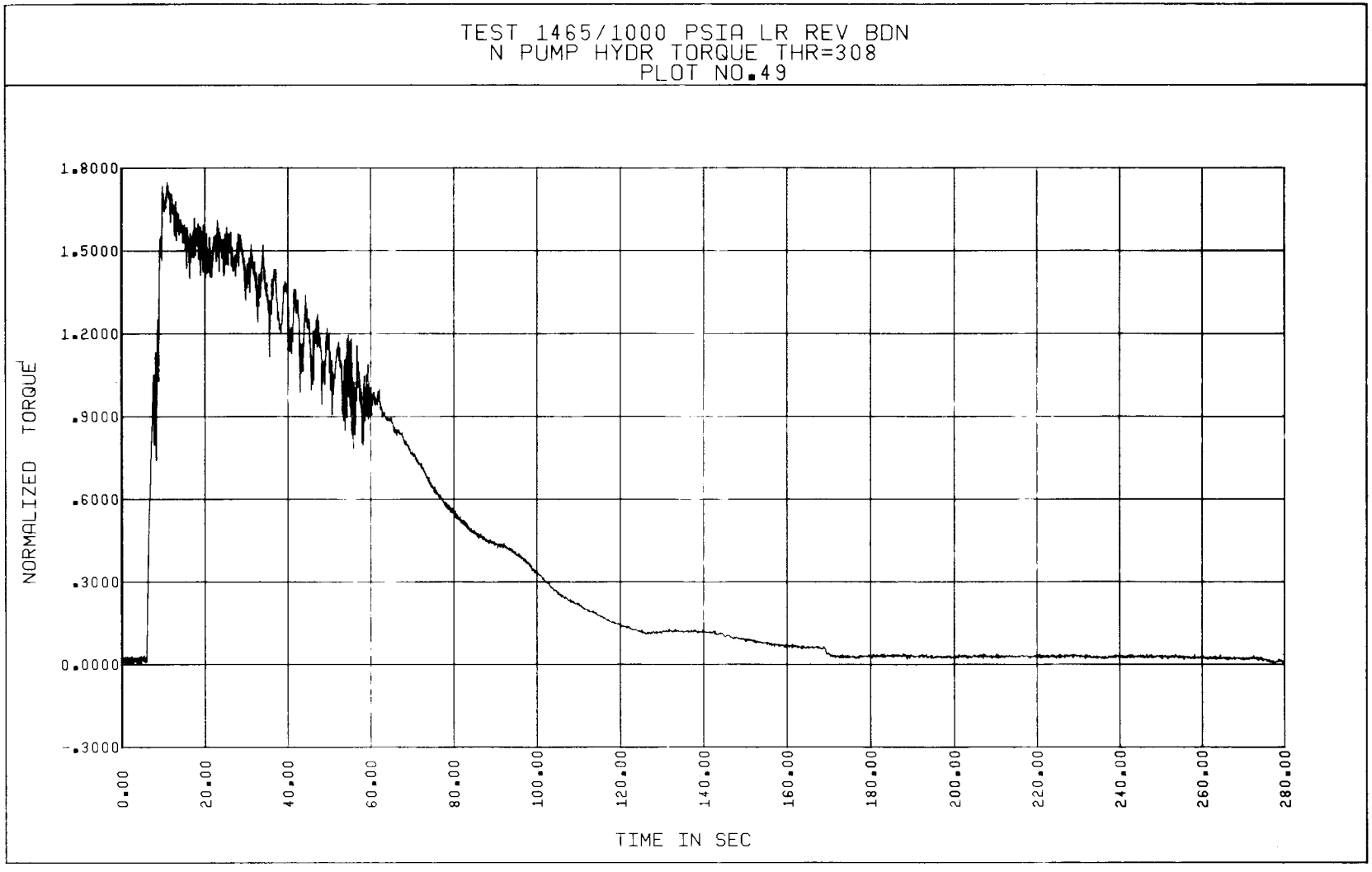

Figure 5-50. Test 1465, Normalized Pump Hydraulic Torque vs Time

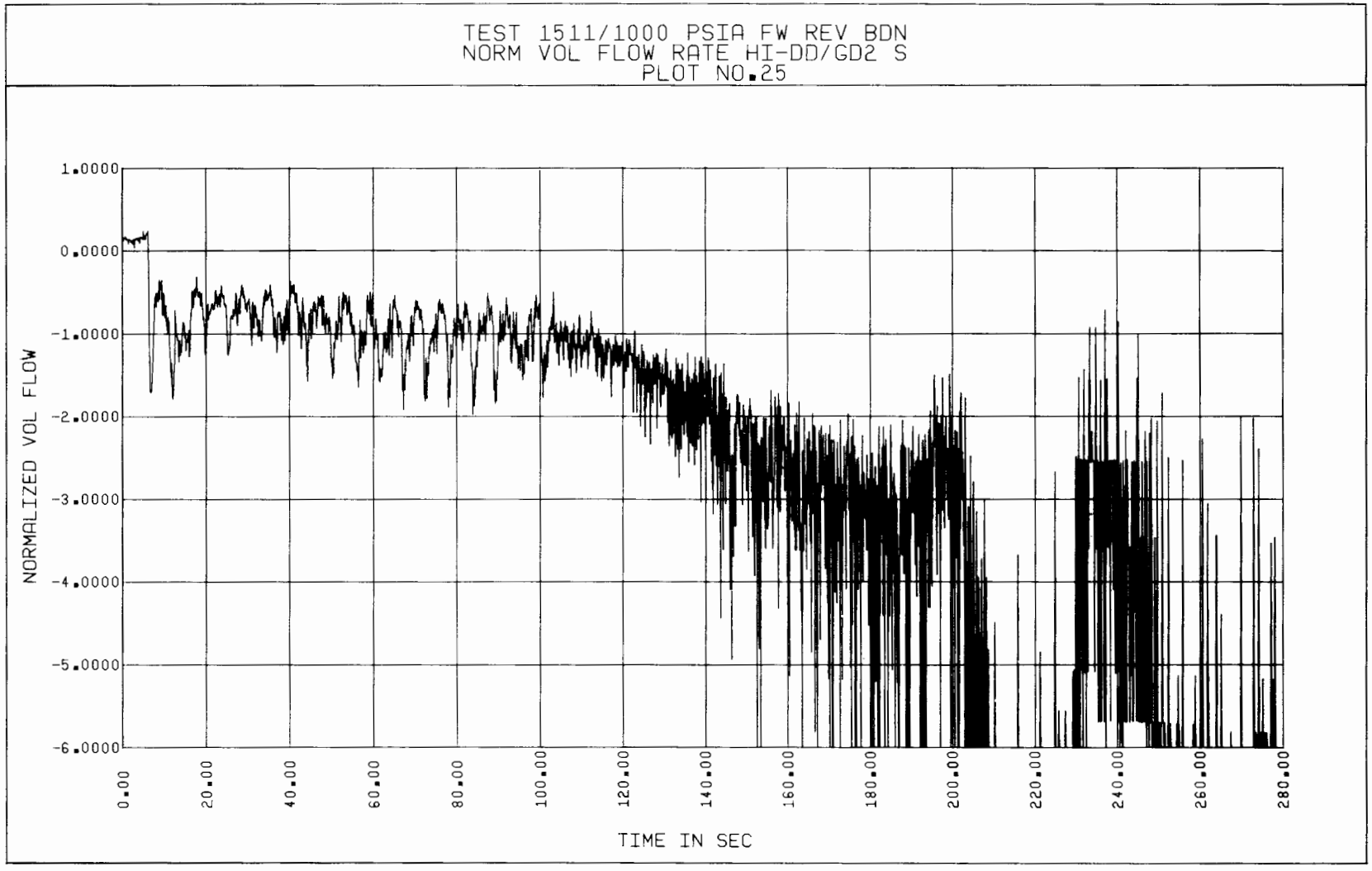

Figure 5-51. Test 1511, Normalized Suction Volumetric Flow Rate vs Time

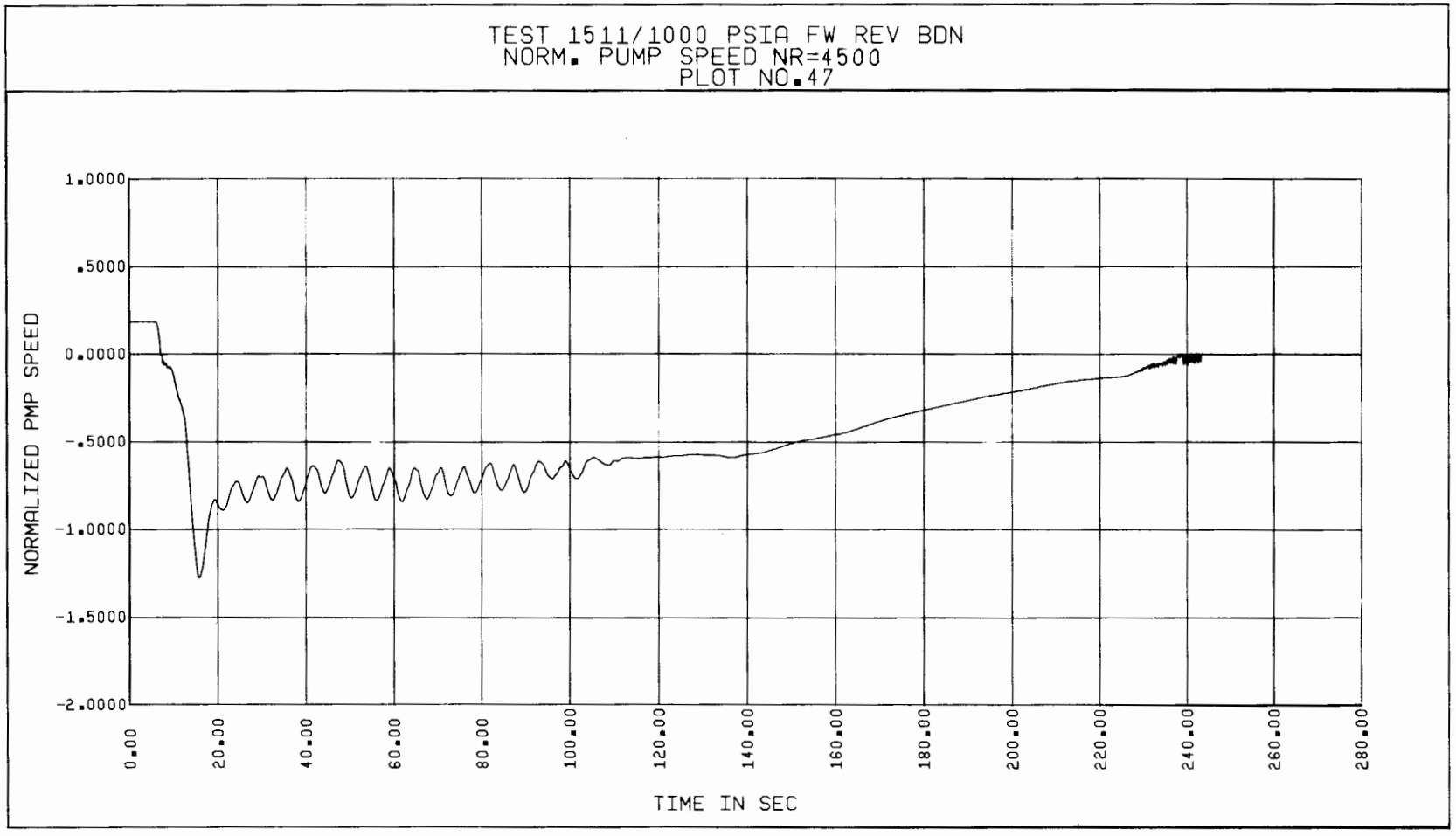

Figure 5-52. Test 1511, Normalized Pump Speed vs Time

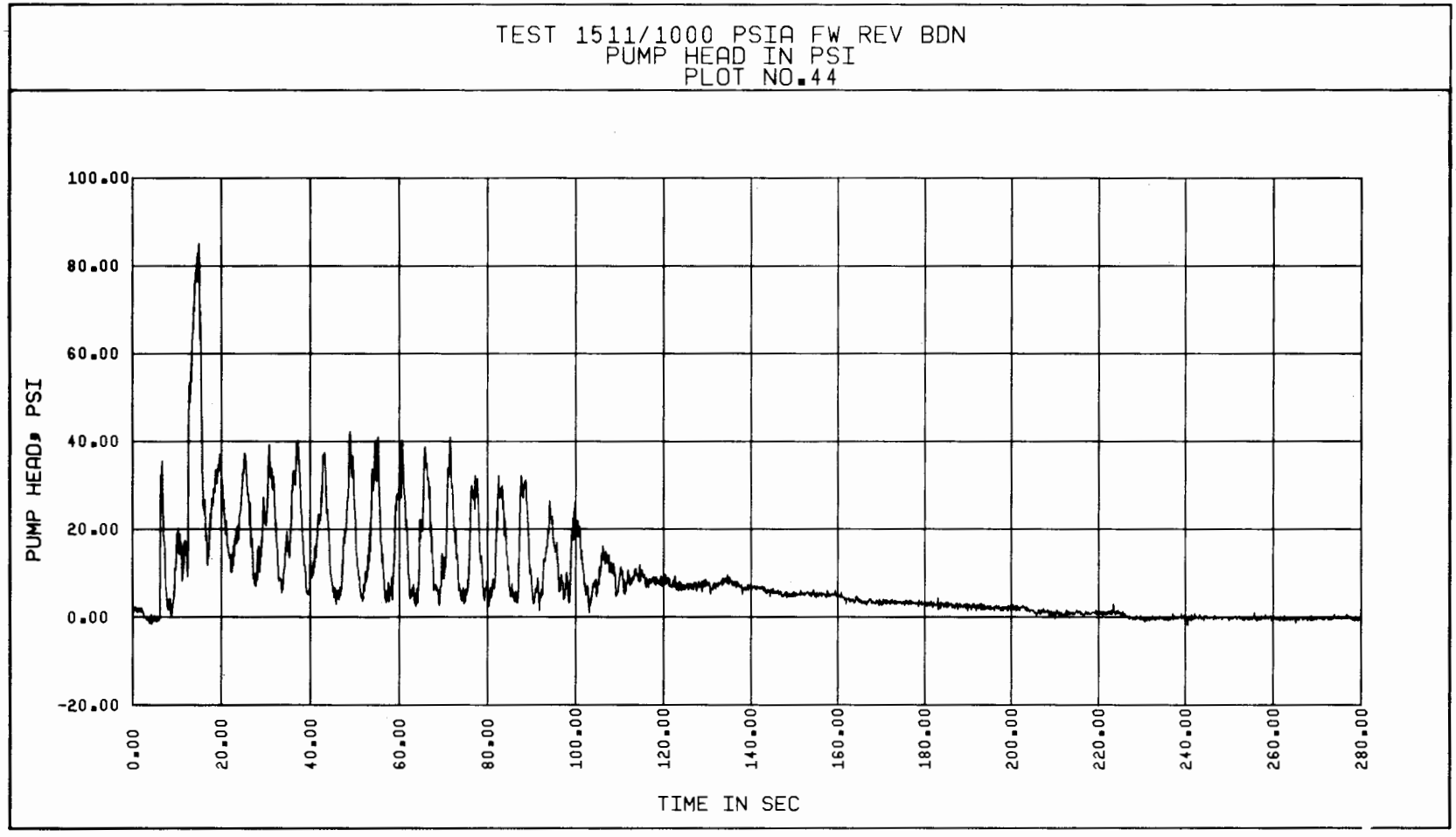

Figure 5-53. Test 1511, Pump Head vs Time

positive shaft torque which overcomes the friction and windage and any acceleration in the drive system during most of the transient as seen from Figure 5-54. All other blowdown parameters behave in the manner described in the general behavior discussion above.

5.2.2 Peak Flows And Speeds

The general behavior of the volumetric flow rate and the pump speed variation, for a free-wheeling case, realized during the transient was discussed in the subsection above. For almost all the blowdowns, the variations of these parameters were dictated by the break size and the break location. As indicated earlier, the general behavior of the volumetric flow rate curve was that it increased sharply (in the forward or reverse direction) just after rupture, reaching a quasi-steady state intermediate value. It remained at this value for several seconds, and then it rapidly increased again and eventually fell off to lower values. Similar trends were also seen in the pump speed traces for the free-wheeling blowdown tests.

Both the volumetric flow rate and the speed parameters eventually reach peak values, during the second surge. In Figure 5-55 the normalized volumetric flow rates measured by the high suction turbine meter for several blowdown tests are plotted as functions of time. These curves were developed by hand-smoothing the normally noisy machine plots for the volumetric flow rates. The spectrum of break sizes covered ranges from 34 percent to 100 percent of the full pipe area. The peak normalized volumetric flow rates (normalization based on Q_R = 3500 gpm) realized ranged between 4.5 (for Test 1179, 34% break size) and 6.3 (for Test 1351, 100% break size) as seen from Figure 5-55.

The normalized pump speeds for several tests are plotted in Figure 5-56 as functions of time. The break sizes ranged between 5 percent and 100 percent. For the 5 percent break size blowdown test (Test 1380), the pump speed does not rise during the transient, as the transient volumetric flow rate is not large enough to accelerate the pump. For the other break sizes, the peak normalized speeds ranged between 1.27 (for Test 1179) and 2.25 (for Test 1319). It was also realized that larger overspeeds would be obtained for reverse flow, free-wheeling blowdowns than for forward flow, free-wheeling blowdowns for the same break sizes, based on the pump speed plots of Figures 5-56 and 5-57. Figure 5-57 shows the pump speed variations for the two free-wheeling, reverse flow blowdowns, Test 497 and 1511, as a function of time.

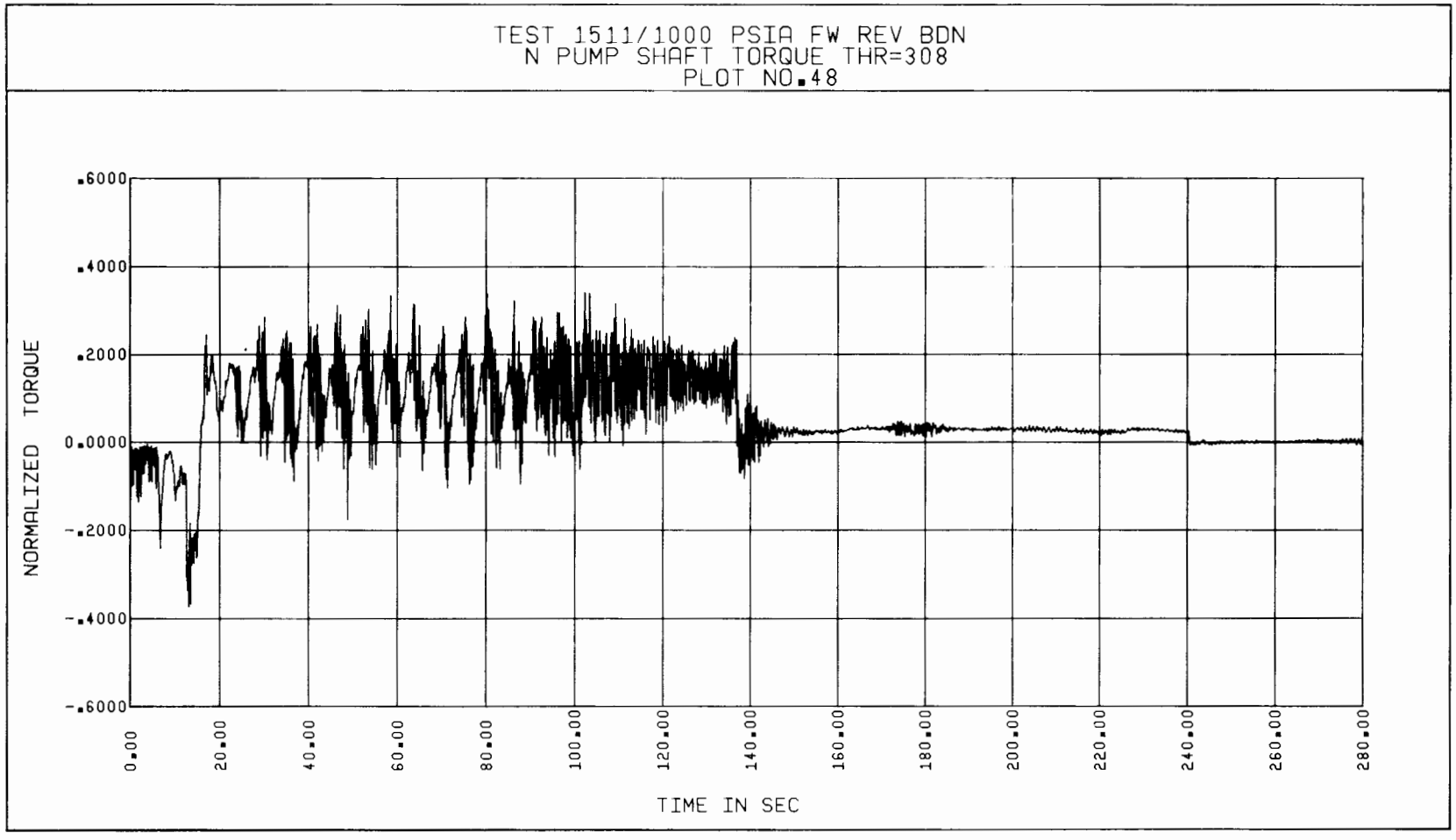

Figure 5-54. Test 1511, Normalized Pump Shaft Torque vs Time

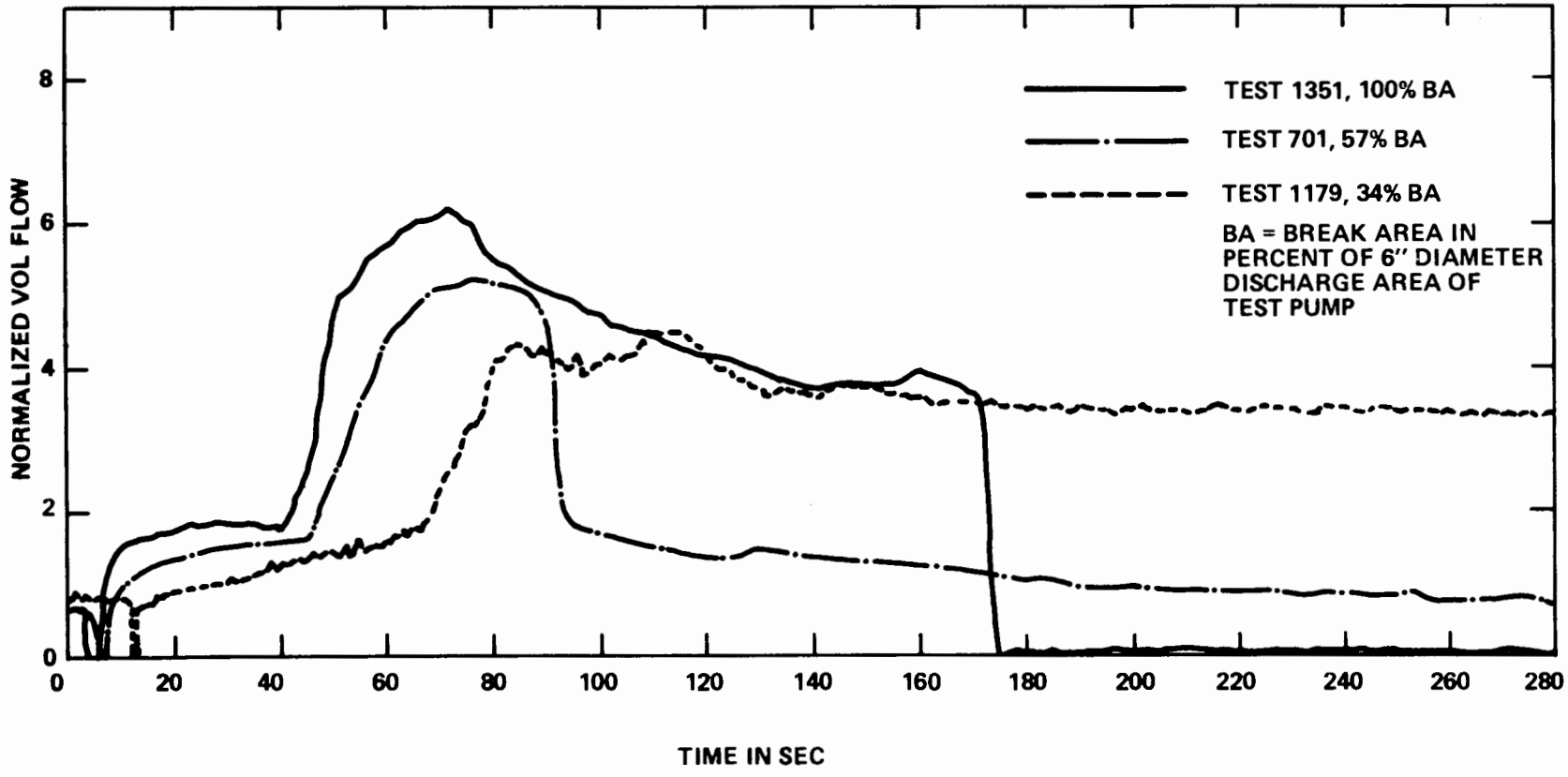

Figure 5-55. Normalized Suction Volumetric Flow Rate vs Time for a Spectrum of Break Sizes

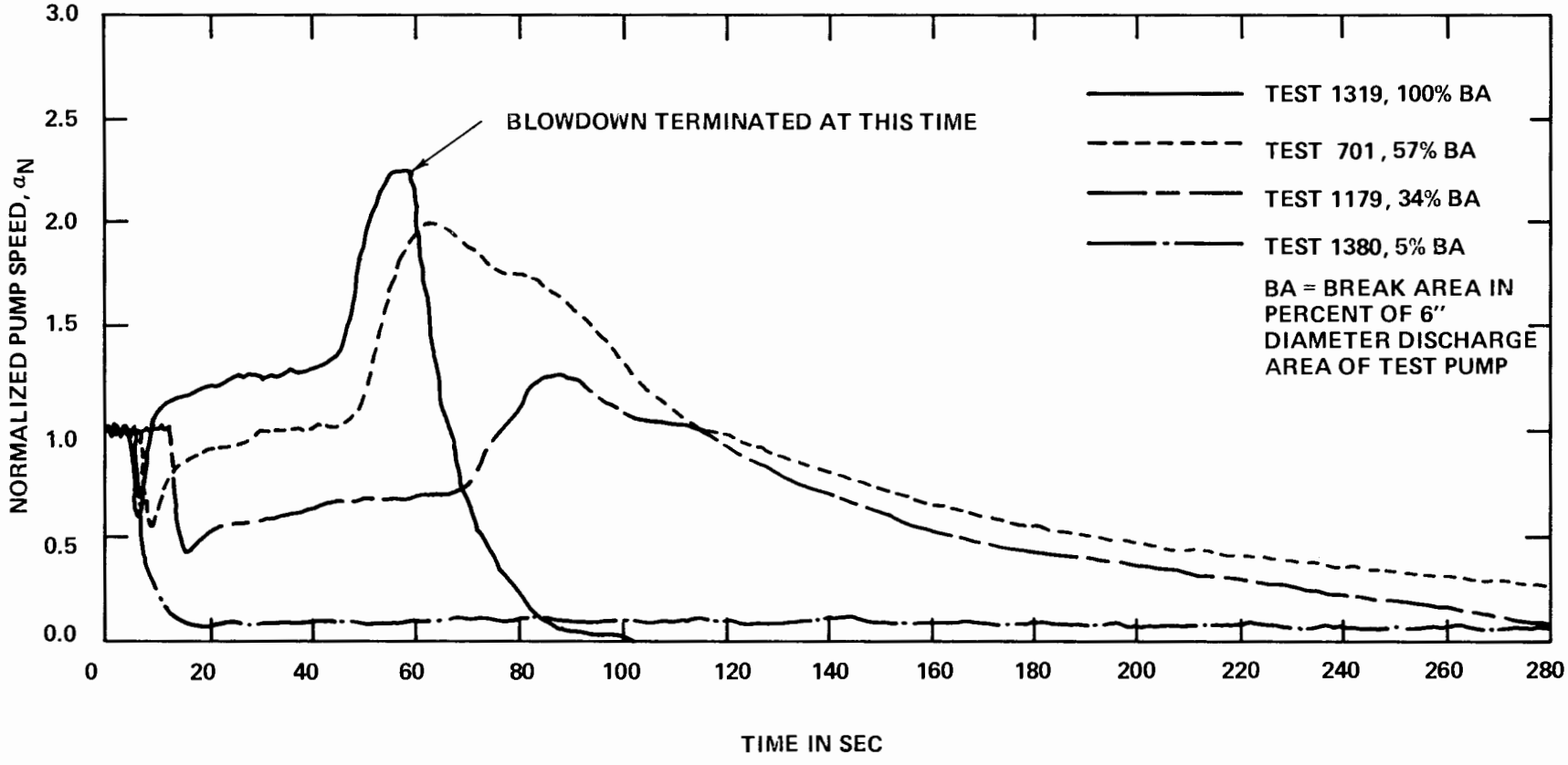

Figure 5-56. Speed vs Time for a Spectrum of Discharge Break Sizes

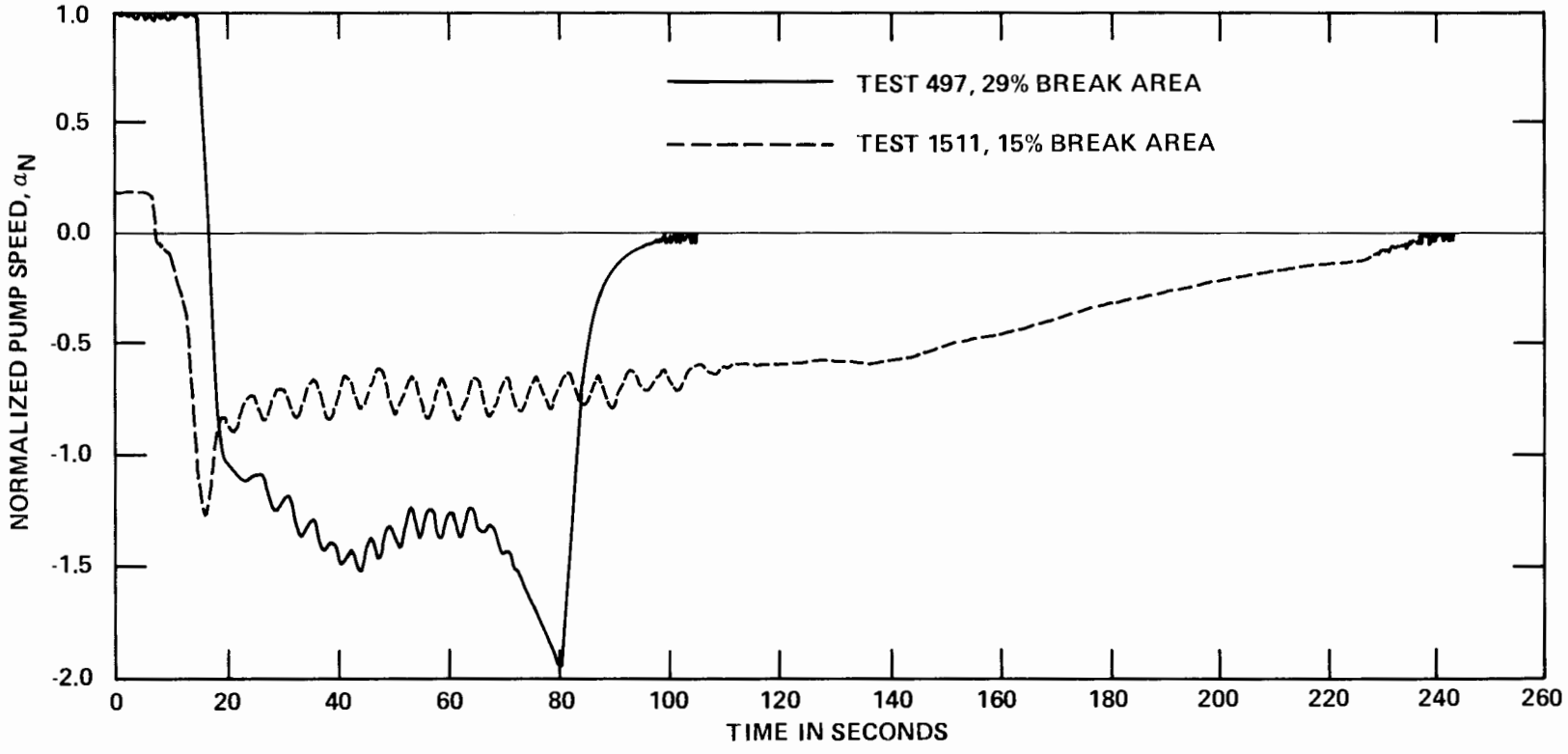

Figure 5-57. Speed vs Time for Different Suction Break Sizes

The maximum normalized pump speed realized for Test 497 (29% break size) was approximately 1.9. However, for the free-wheeling, forward flow blowdown Test 1179 (34% break size), the peak normalized speed is only 1.27 (Figure 5-56). This operating characteristic is partially attributable to the fact that the pump would be more efficient as a normal turbine, which is the mode of operation during a reverse flow, free-wheeling blowdown test.

5.2.3 Homogeneity of Flow

For further analysis using the transient data (Section 5.5 and Volume IV) it is important to know the transient pump operating condition at suction as well as at discharge for representative blowdown tests. These operating conditions include: pressure, volumetric flow rate, pump speed, and void fraction (or density). If the two-phase flow through the instrument spools is truly homogeneous, then any of the volumetric flow rates, directly measured or derived, at a measuring location and any of the gamma densitometer measurements at the same location may be employed to uniquely characterize the flow and the void fraction.

Homogeneous two-phase flow is defined as a flow in which the two phases are uniformly distributed at any cross-section in the pipe with no slip between phases. Dispersed flow is defined as a flow in which the two phases are uniformly distributed at any cross-section in the pipe but slip occurs between phases. To gain additional insight into the discussion of flow homogeneity, consider Figures 5-58 and 5-59, which present the suction and discharge instrumentation, respectively, applicable to most of the blowdown tests. At each instrument spool, there are three gamma densitometer beams and four flow measuring instruments (two turbine meters and two drag discs).

A composite plot of gamma densitometer beam density measurements at suction for Test 1351 is provided in Figure 5-60, and individual beam density plots for the same test are provided in Volume VI. Interpretation of beam 3 measurements of the SIS and DIS gamma densitometers is considered uncertain due to the proximity of this beam to the pipe wall. Additionally, due to its location, the reading obtained from beam 3 represents only a small percentage of the flow through the pipe. Thus, if beam 3 measurements are neglected, the density distribution at the SIS can be considered uniform. The fluid velocities directly measured by the turbine

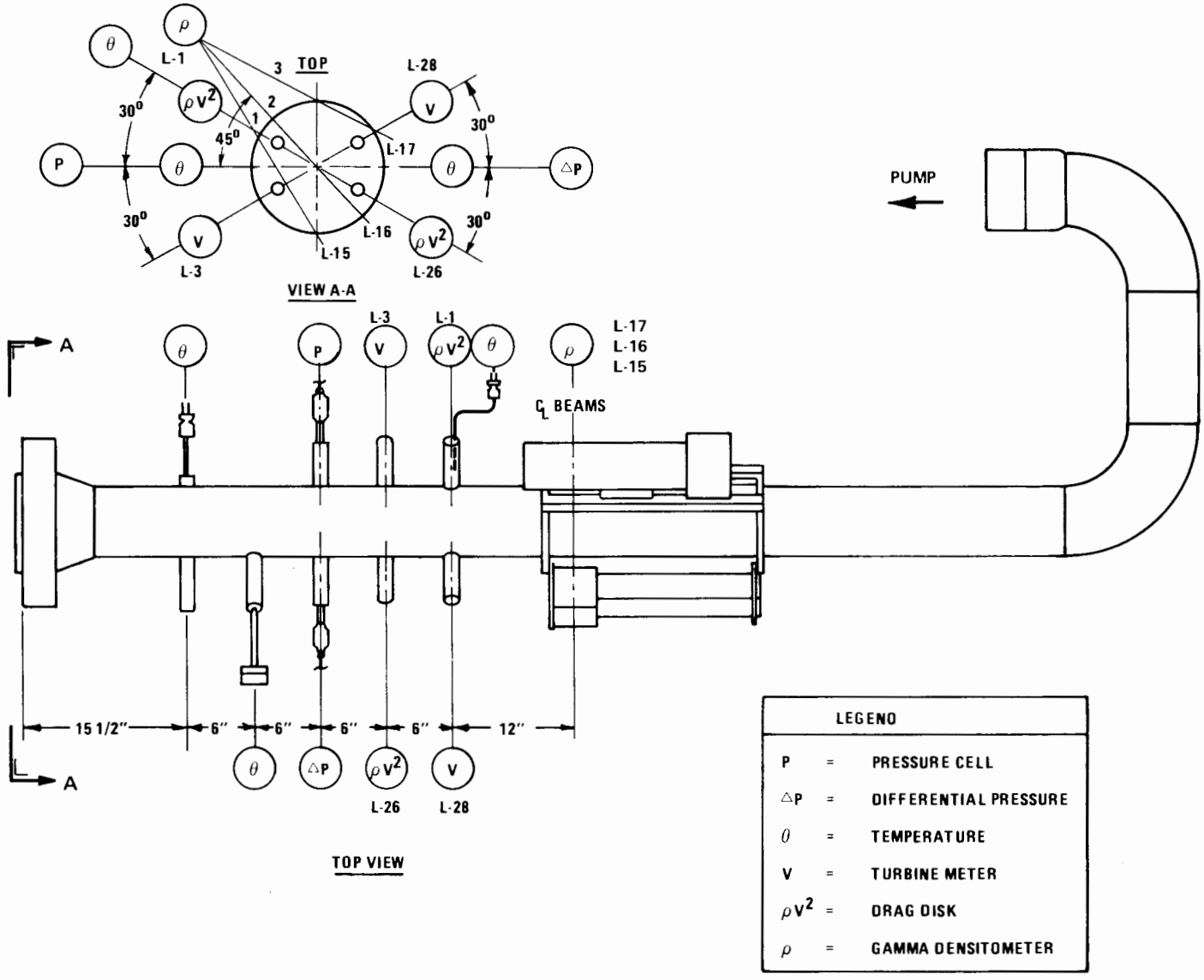

Figure 5-58. Test 1351, Pump Suction Instrument Spool

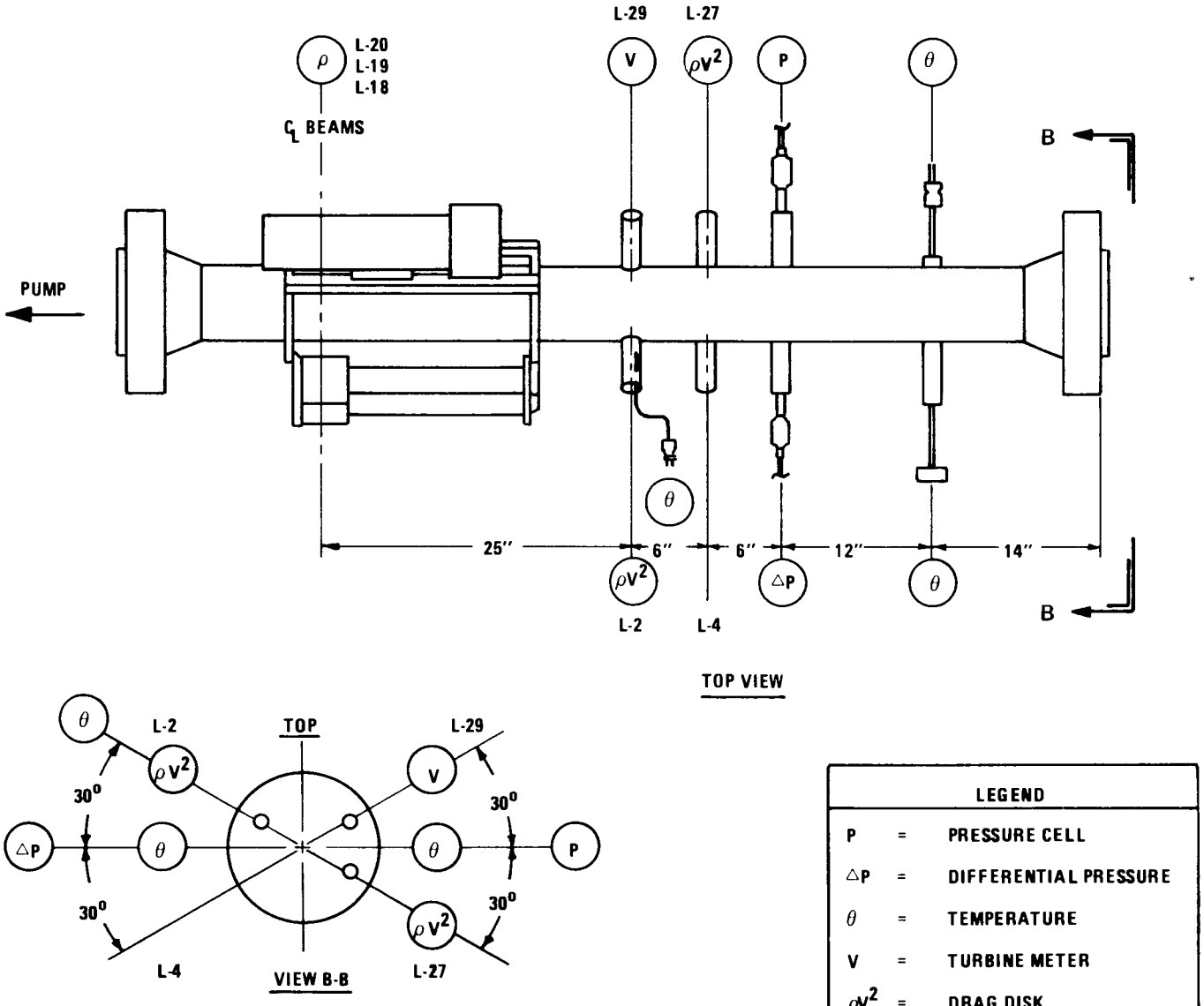

LEGEND		
P	=	PRESSURE CELL
△P	=	DIFFERENTIAL PRESSURE
θ	=	TEMPERATURE
V	=	TURBINE METER
ρV^2	=	DRAG DISK
ρ	=	GAMMA DENSITOMETER

TEST 246 DISCHARGE INSTRUMENT SECTION

Figure 5-59. Test 1351, Pump Discharge Instrument Spool

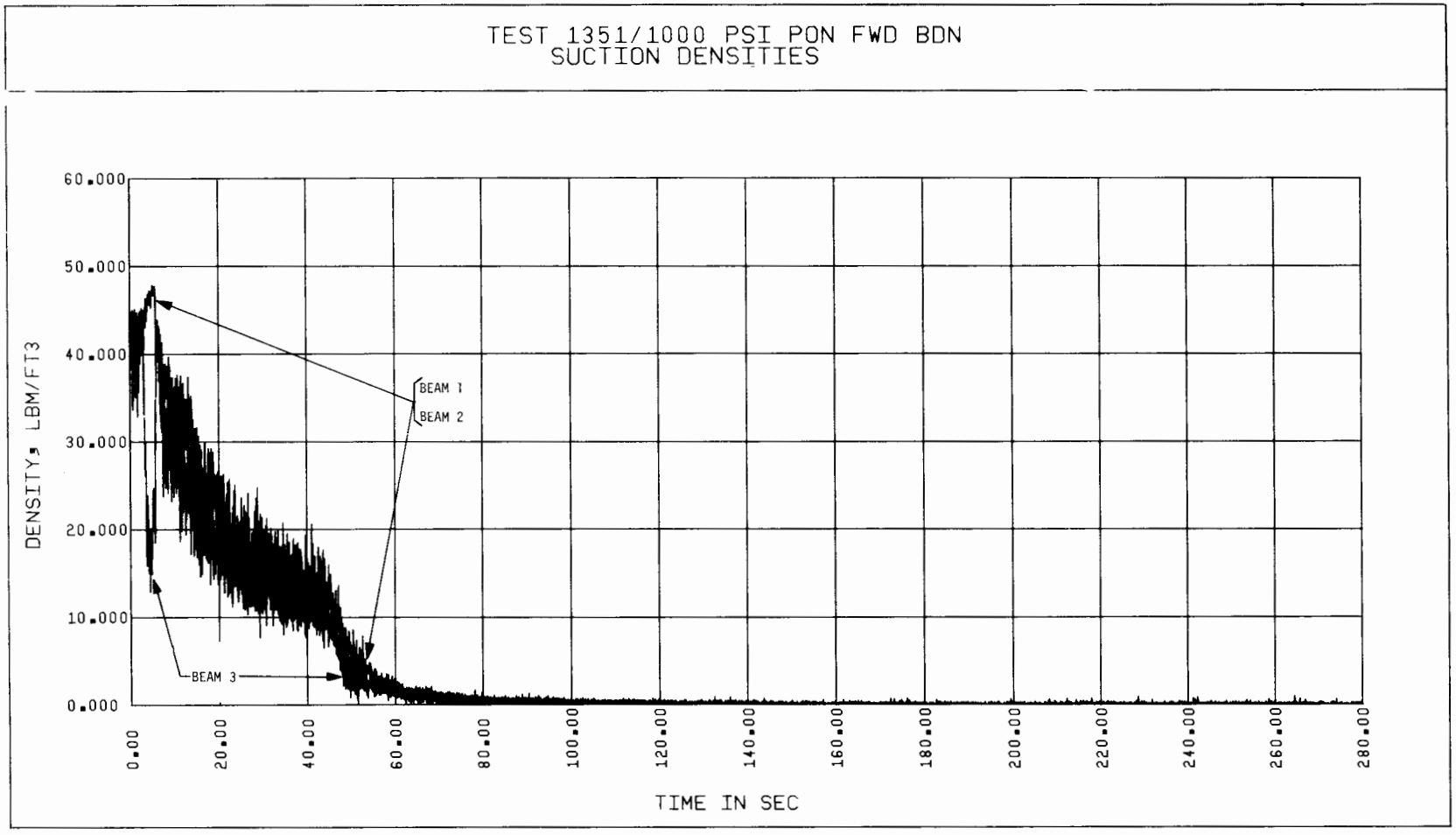

Figure 5-60. Test 1351, Composite Plot of SIS Gamma Densitometer Beam Density Measurements

meters are shown in Figure 5-61 and 5-62. Figure 5-62 indicates that the low turbine meter at suction malfunctioned towards the end of the blowdown, when the blowdown isolation valve (HPSW-2) was closed. At that instant in time the fluid in the test loop is expected to reach stagnant conditions. However, the low turbine meter read large positive values, even after HPSW-2 was closed, as seen from Figure 5-62. Although these turbine meter measurements show some unusual features, the normalized volumetric flow rates of Figures 5-61 and 5-62 appear to be similar during the initial surge and quasi steady-state time periods (40-60 seconds). During the second surge, the high turbine meter curve has a convex shape and remains at higher values than the low turbine meter curve, which exhibits a ramp variation. The disagreement between the measurements of these turbine meters during the second surge may be attributed to the fact that single-phase calibration, which formed the basis for this data, may not be applicable at high void fractions, particularly if the velocity distributions differ. The blowdown behavior described above for the suction turbine meters is applicable to almost all the blowdown tests. Based on this behavior, it may be postulated that the fluid flow at the SIS was essentially uniform up to the beginning of the second surge.

The momentum flux variations measured by the drag discs at the SIS are presented in Figures 5-63 and 5-64 for the high and the low drag discs, respectively. It is seen that the ρV^2 values for the low drag discs are substantially higher (by a factor of 2) than those for the high drag disc most of the transient. As indicated earlier, this behavior for the SIS drag discs repeated for almost all the tests. It is believed that instrument uncertainties alone cannot account for the large disagreement in measurements between the two drag discs. Consequently, the momentum flux distribution is considered non-uniform during the transient. Since it was established earlier that the SIS density distribution was uniform, the reason for the non-uniformity in ρV^2 must be attributed to a non-uniformity in velocity, and consequently the volumetric flow rate. Thus, the conclusions from the turbine meter measurements and the drag disc measurements are contradictory. Whereas the turbine meter and gamma densitometer data support a homogeneous SIS flow field during the initial surge and quasi steady time period, the drag disc and gamma densitometer data support non-homogeneous fluid flow during the transient. It is evident that the interpretation of the fluid flow rate related data at the SIS is complex. Simplifying assumptions and additional analysis will be employed for estimating volumetric flowrates at the SIS for initial data presentation and evaluation.

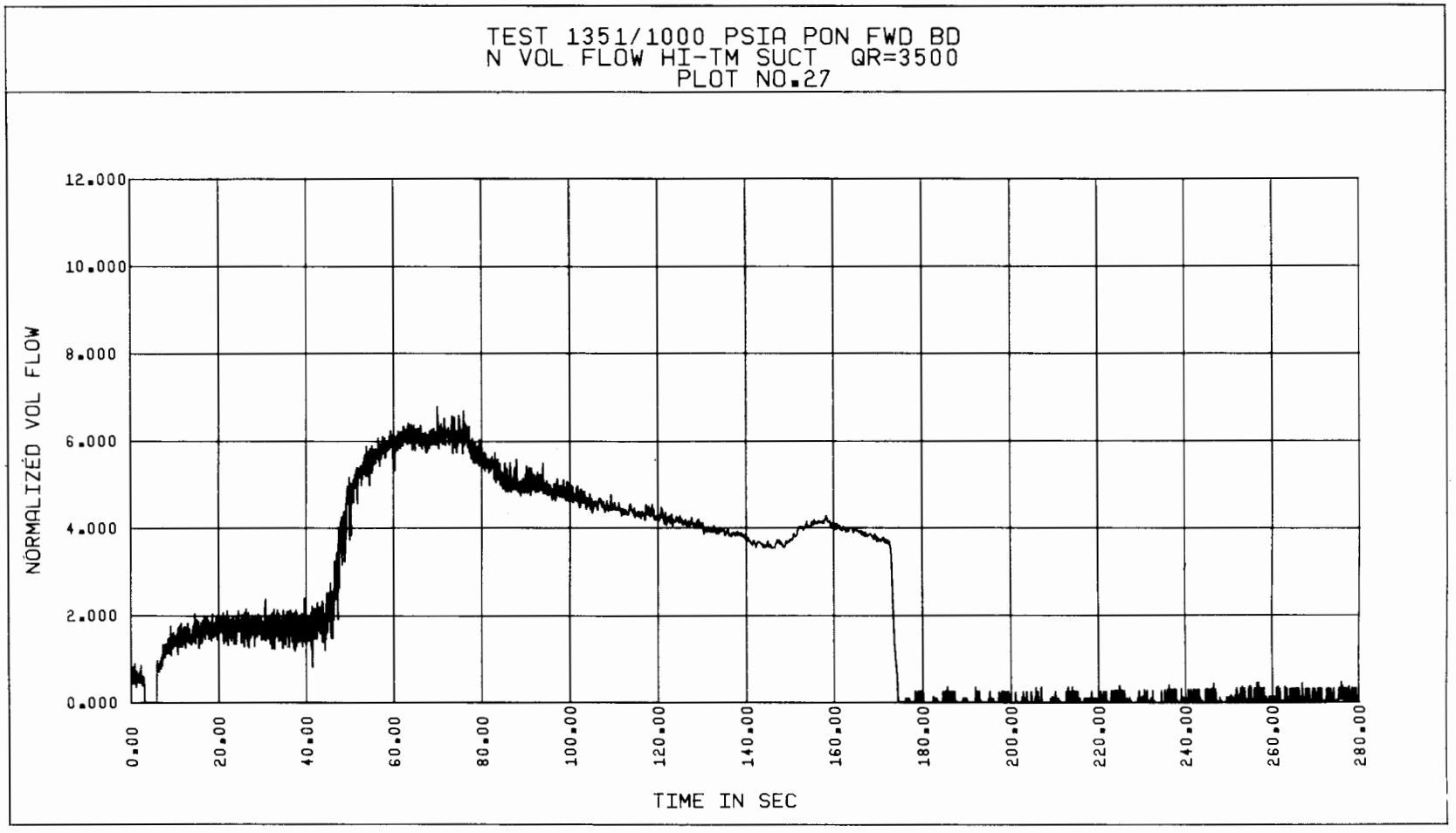

Figure 5-61. Test 1351, Normalized Suction Volumetric Flow Rate vs Time, Based on High Turbine Meter Data

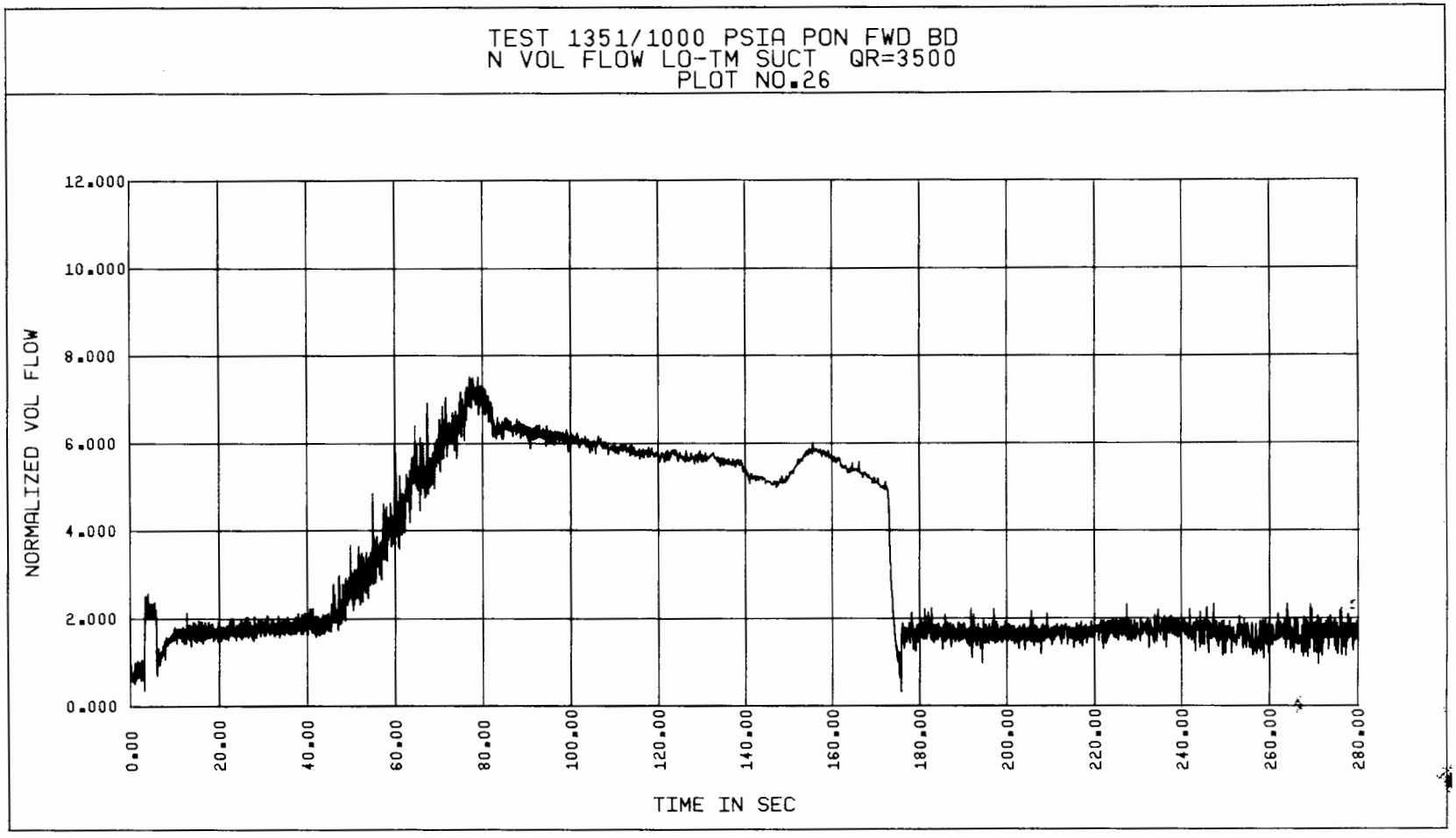

Figure 5-62. Test 1351, Normalized Suction Volumetric Flow Rate vs Time, Based on Low Turbine Meter Data

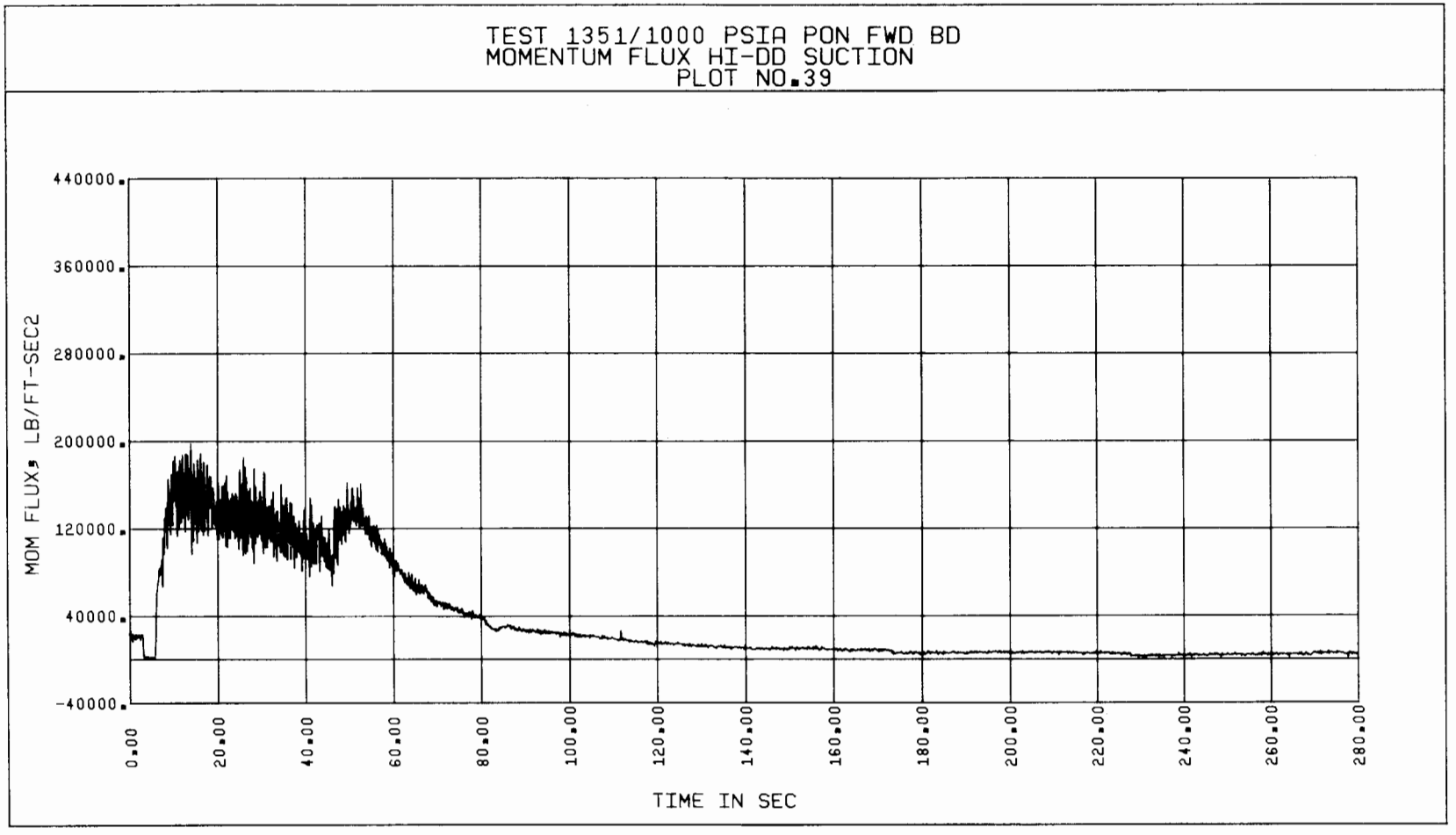

Figure 5-63. Test 1351, Suction Momentum Flux vs Time, Based on High Drag Disc Data

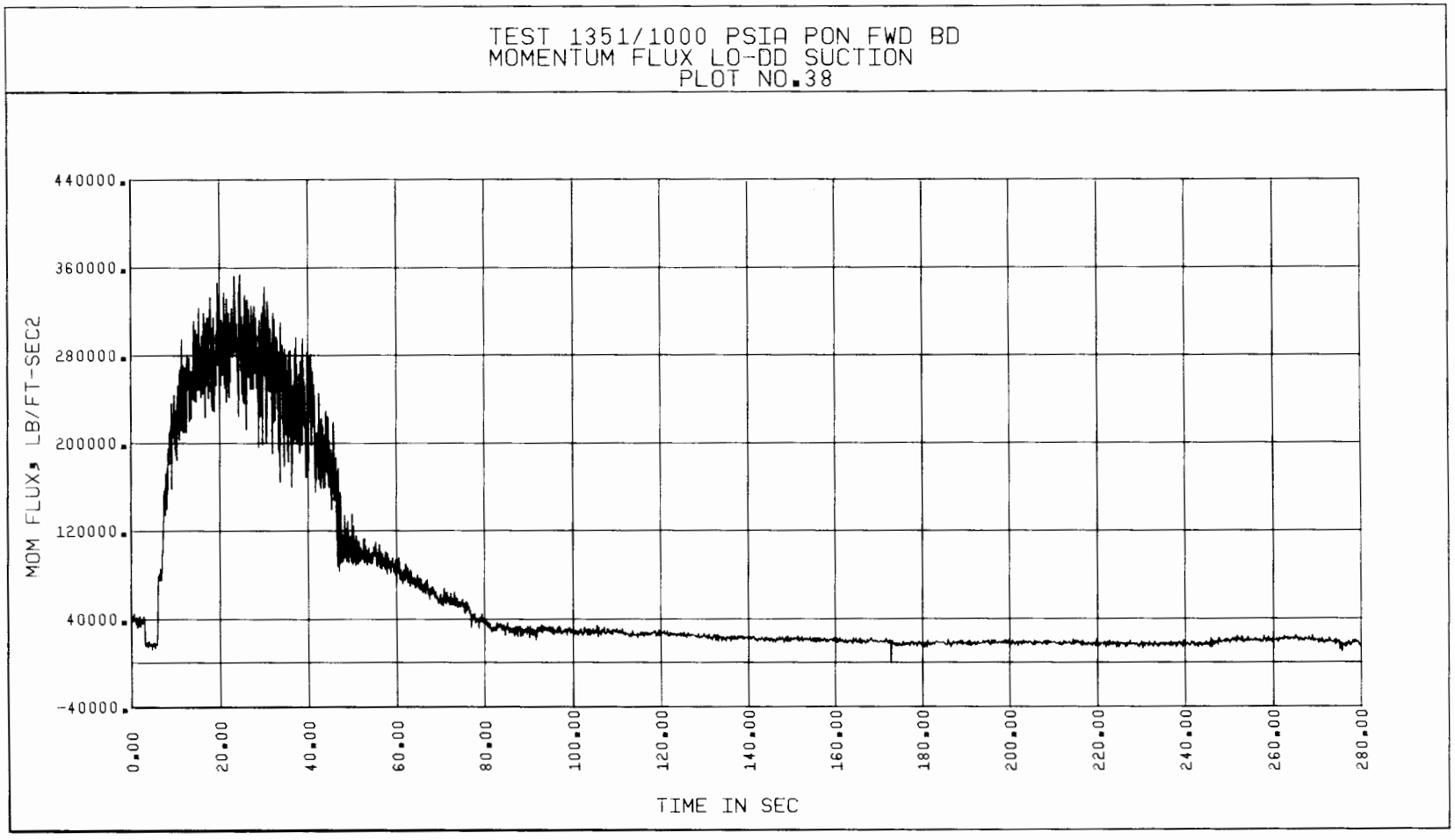

Figure 5-64. Test 1351, Suction Momentum Flux vs Time, Based on Low Drag Disc Data

A composite plot of DIS densities as measured by the gamma densitometer beams is shown in Figure 5-65. Again, if the measurements of beam 3 are disregarded for the reason mentioned earlier, it may be concluded that the DIS density is uniform. The DIS velocity data and the momentum flux data measured by the turbine meters and the drag discs are provided in Figures 5-66 through 5-69. Although the higher turbine meter curve in Figure 5-66 does not return to zero for zero flow condition, it is seen that there is more uniformity in velocity at the DIS than at the SIS. The DIS momentum flux distribution also appears to be more uniform than the SIS ρV^2 distribution, within instrument uncertainties. This pattern of behavior was observed for most of the forward flow transient tests, and it is postulated that the fluid flow is more homogeneous at the DIS than at the SIS for forward flow blowdown tests. The implication here is that within the test pump the two phases get well-mixed, resulting in essentially homogeneous flow at the DIS.

Additional discussion of flow homogeneity and three-instrument flow rate interpretation are provided in Section 5.5.

5.2.4 Parameter Fluctuations

Parameter fluctuations seen in most of the blowdown plots can be of two types. The first type is random fluctuations as a result of noise, either from the measuring instruments themselves or generated by the two-phase mixture as a result of formation, collapse, and motion of bubbles. This type of fluctuations was briefly discussed in Section 5.1.

The other type of fluctuations is periodic oscillations. The small break area (5 percent orifice size) forward flow blowdowns exhibited this phenomenon (Figure 5-70). In addition, results of both of the free-wheeling reverse flow blowdown tests (497 and 1511) also exhibited this phenomenon (Figures 5-71 and 5-72). The break sizes for these blowdown tests (15-29 percent) were somewhat larger than those for the forward flow blowdown tests mentioned above. In the case of the forward flow blowdowns, these periodic fluctuations, or oscillation may be associated with the small break sizes. However, for the reverse flow blowdowns, it is not clear whether the size of the break is the dominating effect, since the break sizes are not that small. It would require further testing and analysis to indicate whether the oscillations are caused by the test system independent of the pump, by the test pump independent of the system, or by the interaction between the test system and the test pump.

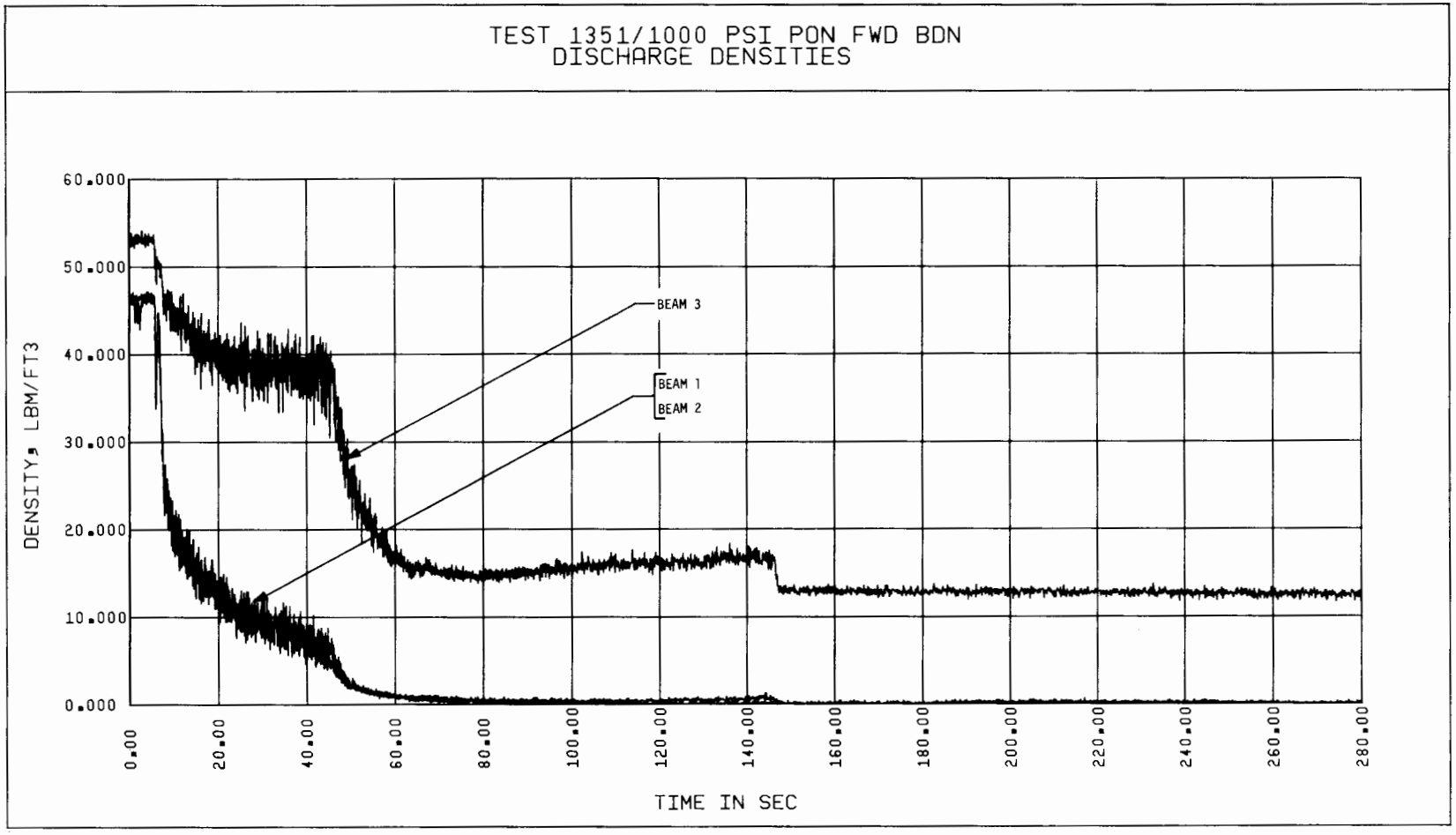

Figure 5-65. Test 1351, Composite Plot of DIS Gamma Densitometer Beam Density Measurements

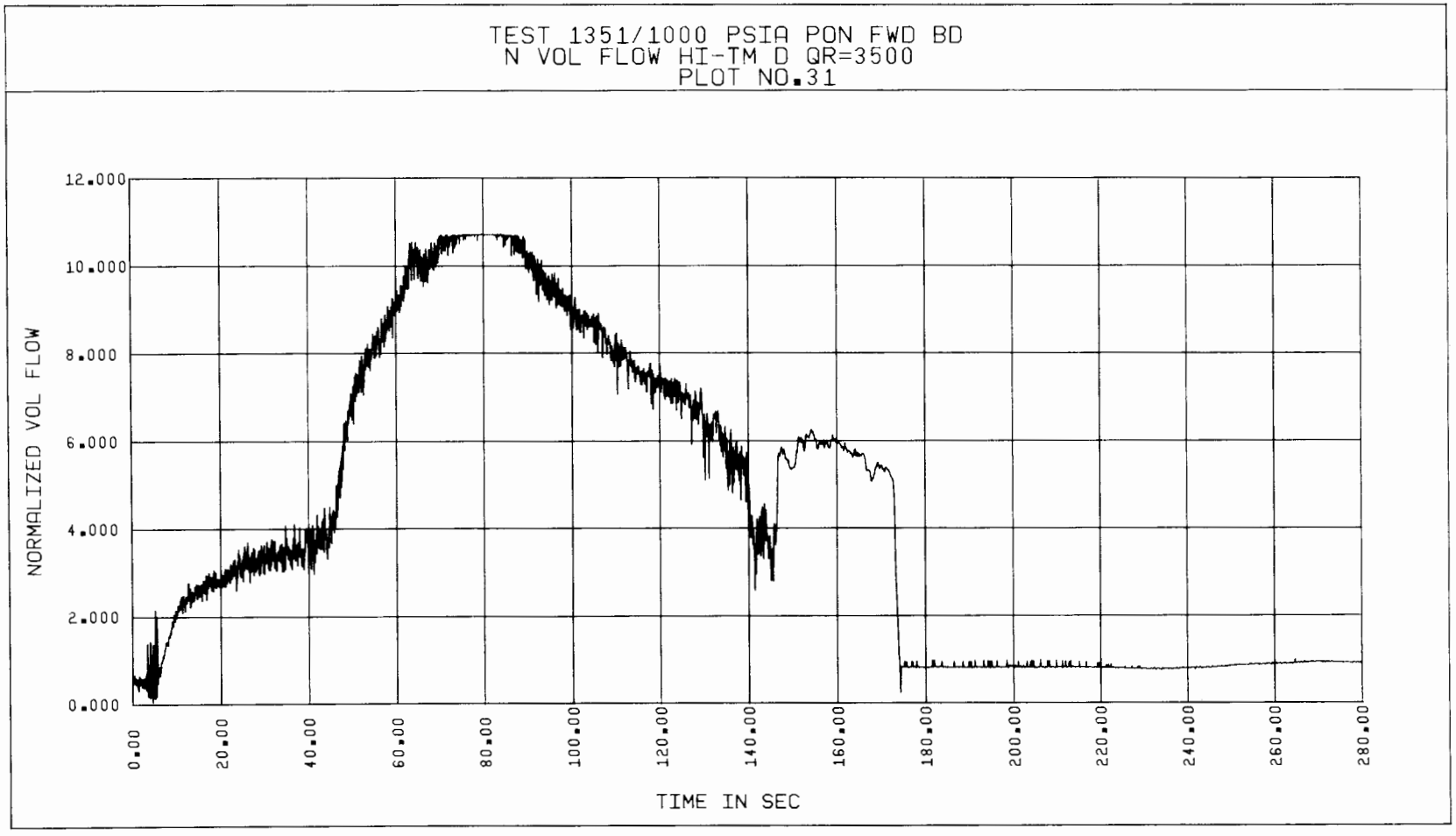

Figure 5-66. Test 1351, Normalized Discharge Volumetric Flow Rate vs Time, Based on High Turbine Meter Data

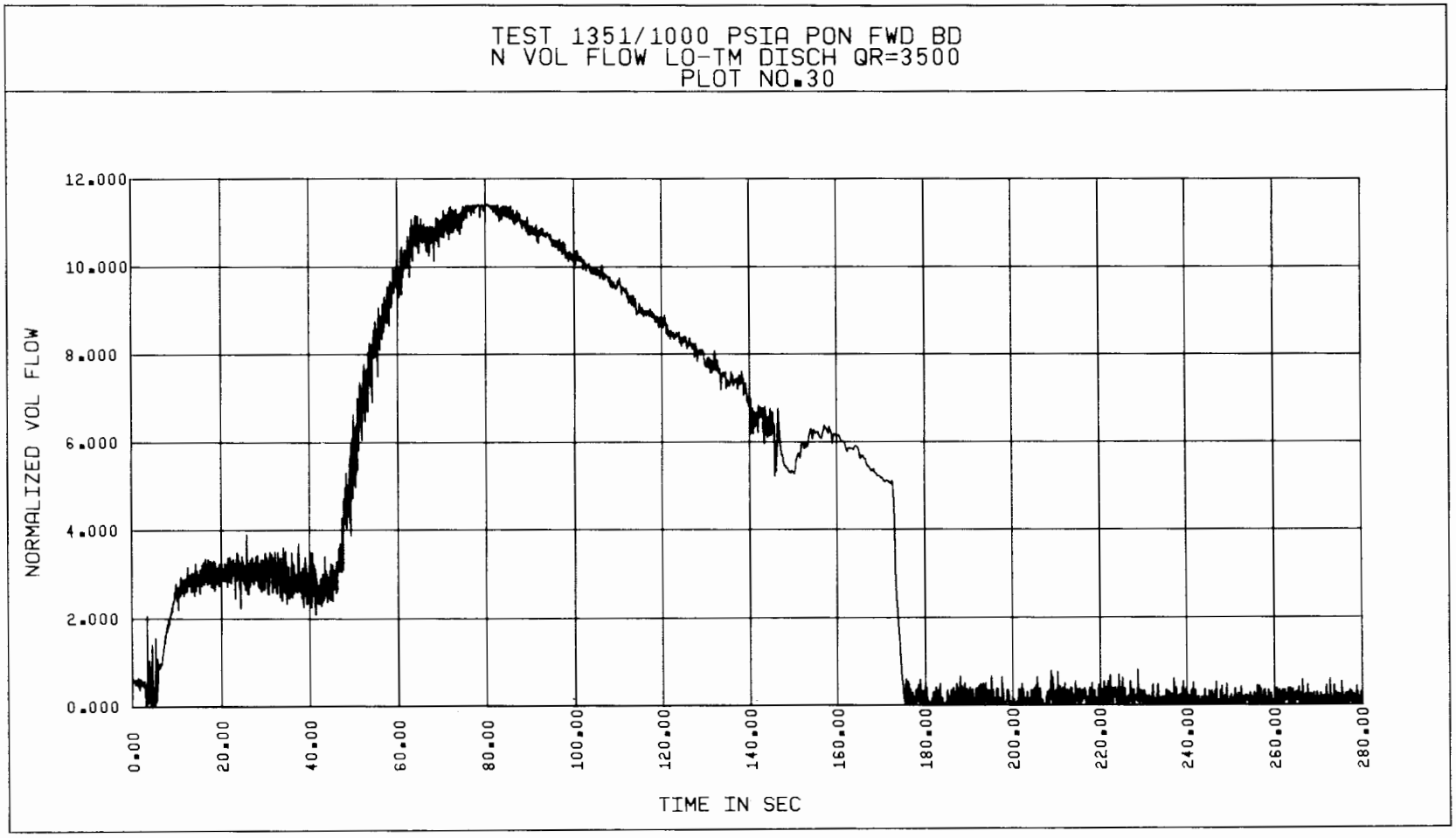

Figure 5-67. Test 1351, Normalized Discharge Volumetric Flow Rate vs Time, Based on Low Turbine Meter Data

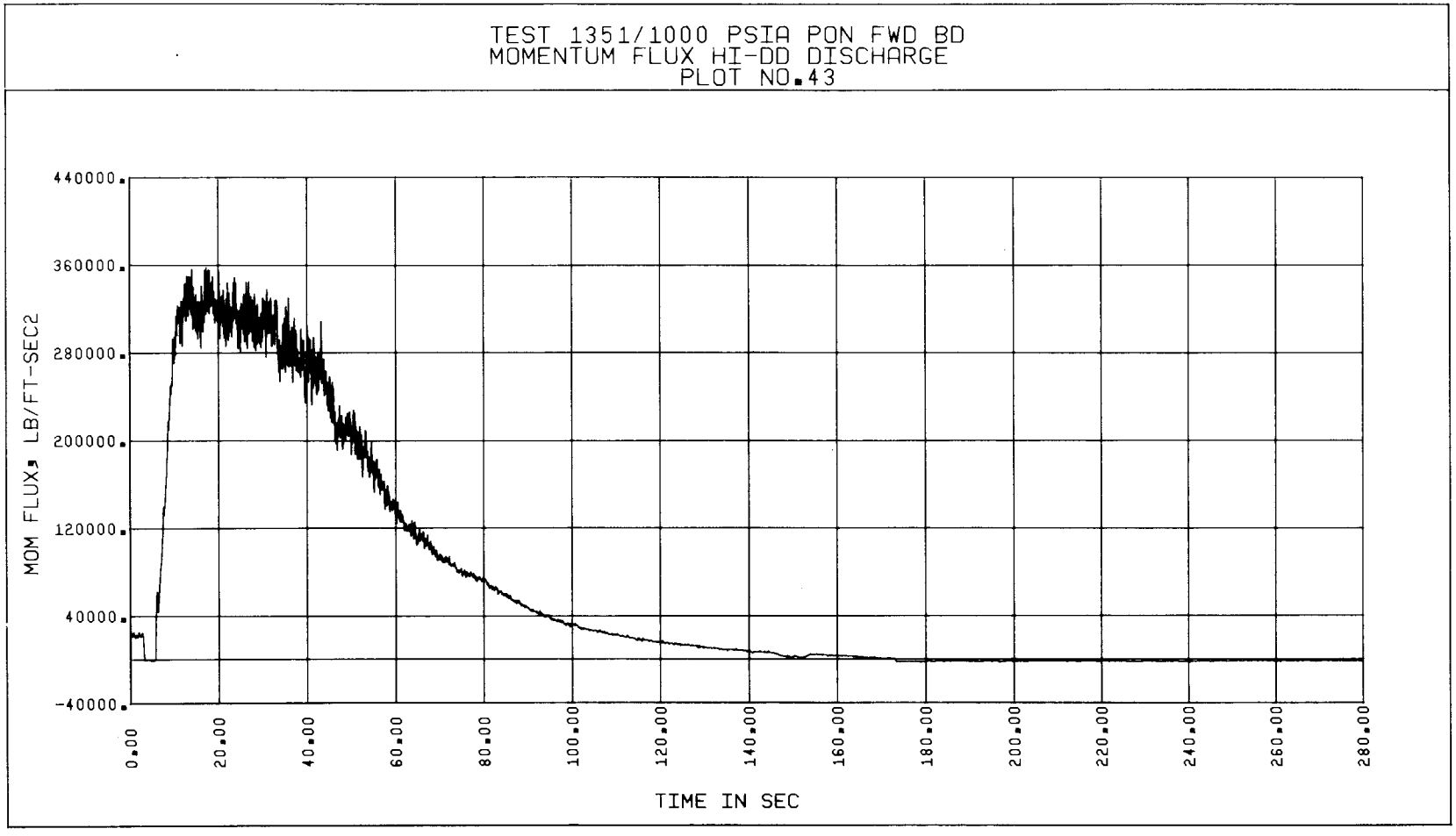

Figure 5-68. Test 1351, Discharge Momentum Flux vs Time, Based on High Drag Disc Data

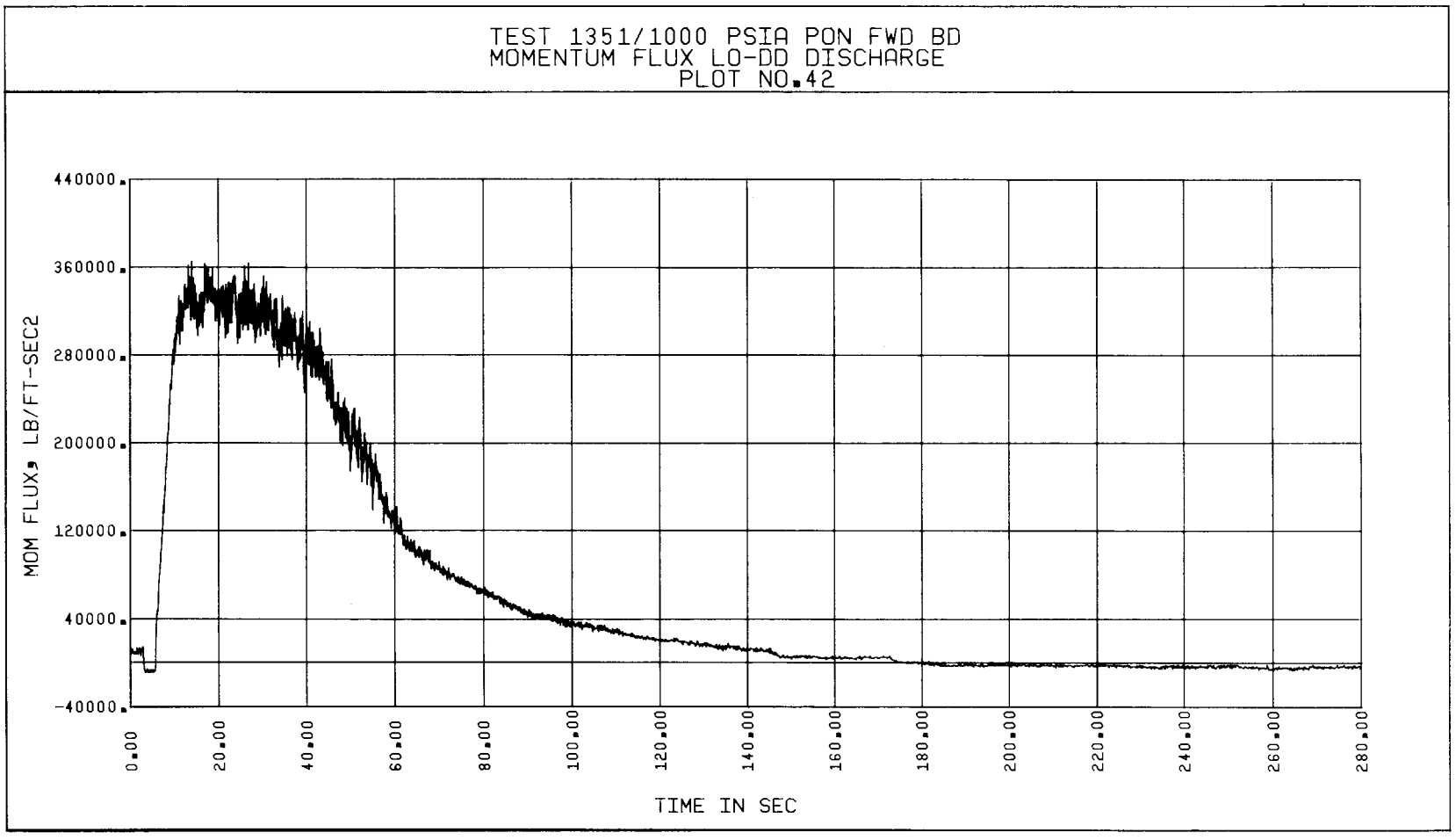

Figure 5-69. Test 1351, Discharge Momentum Flux vs Time, Based on Low Drag Disc Data

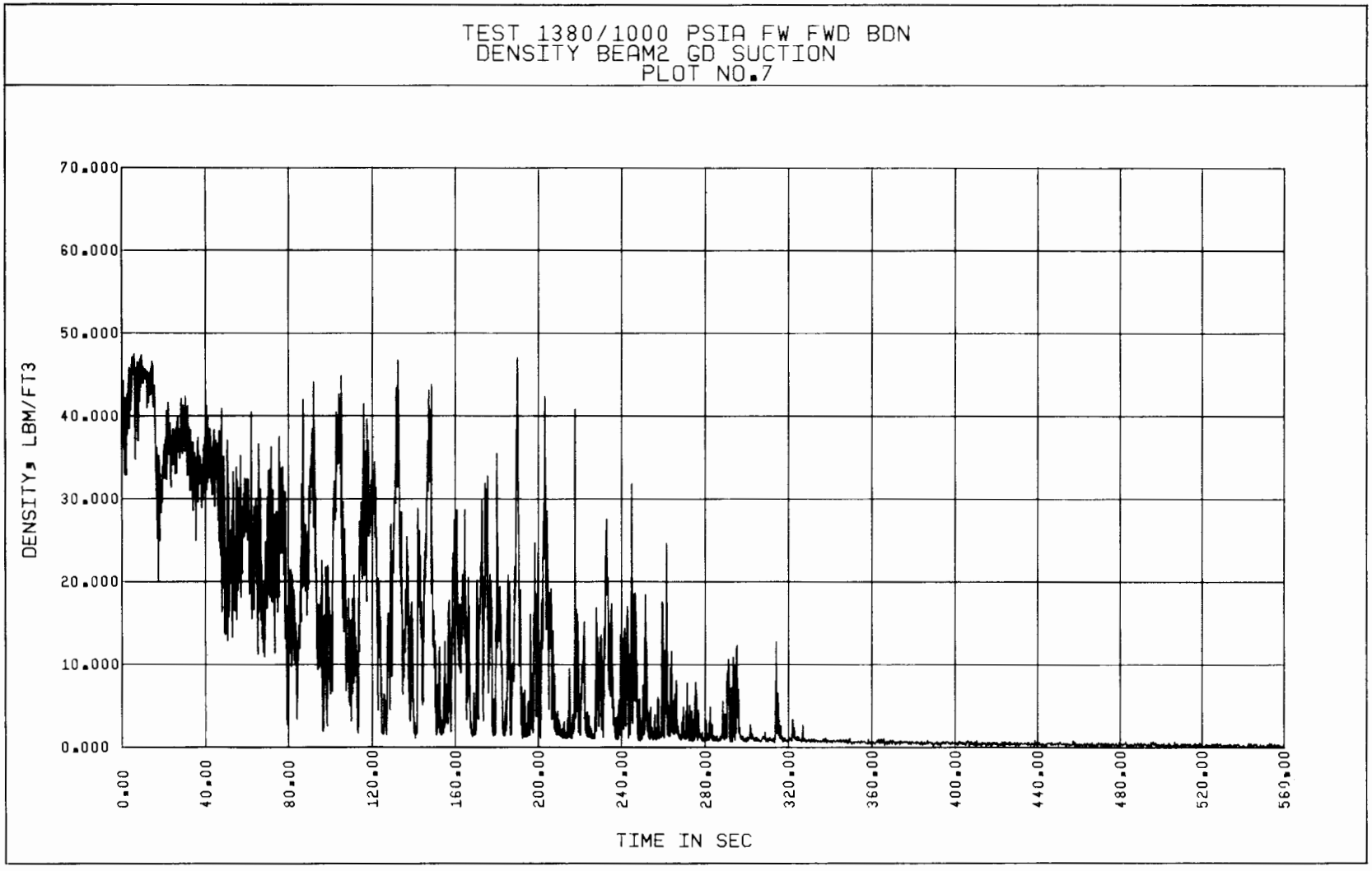

Figure 5-70. Test 1380, Suction Density vs Time

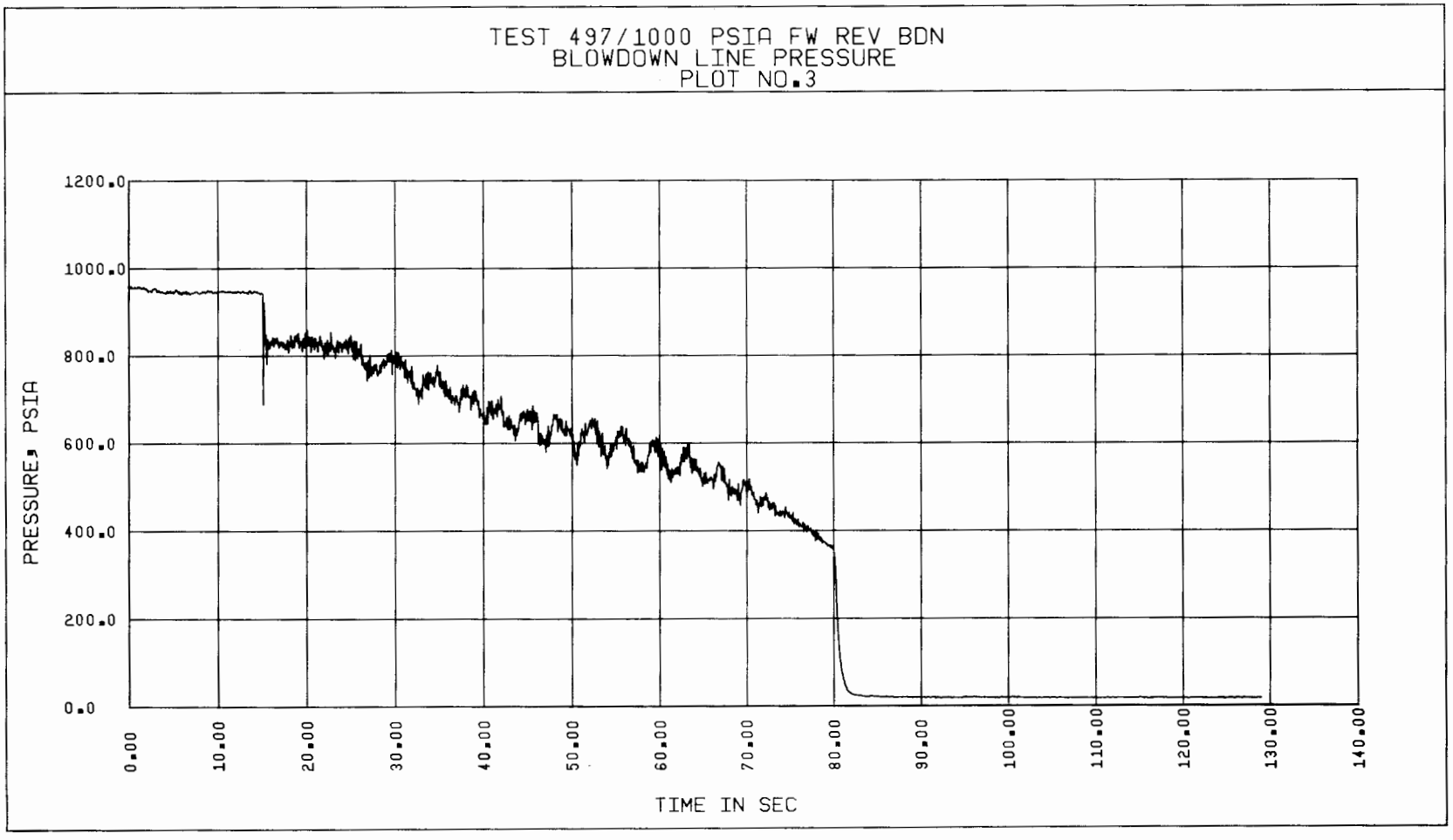

Figure 5-71. Test 497, Blowdown Line Pressure vs Time

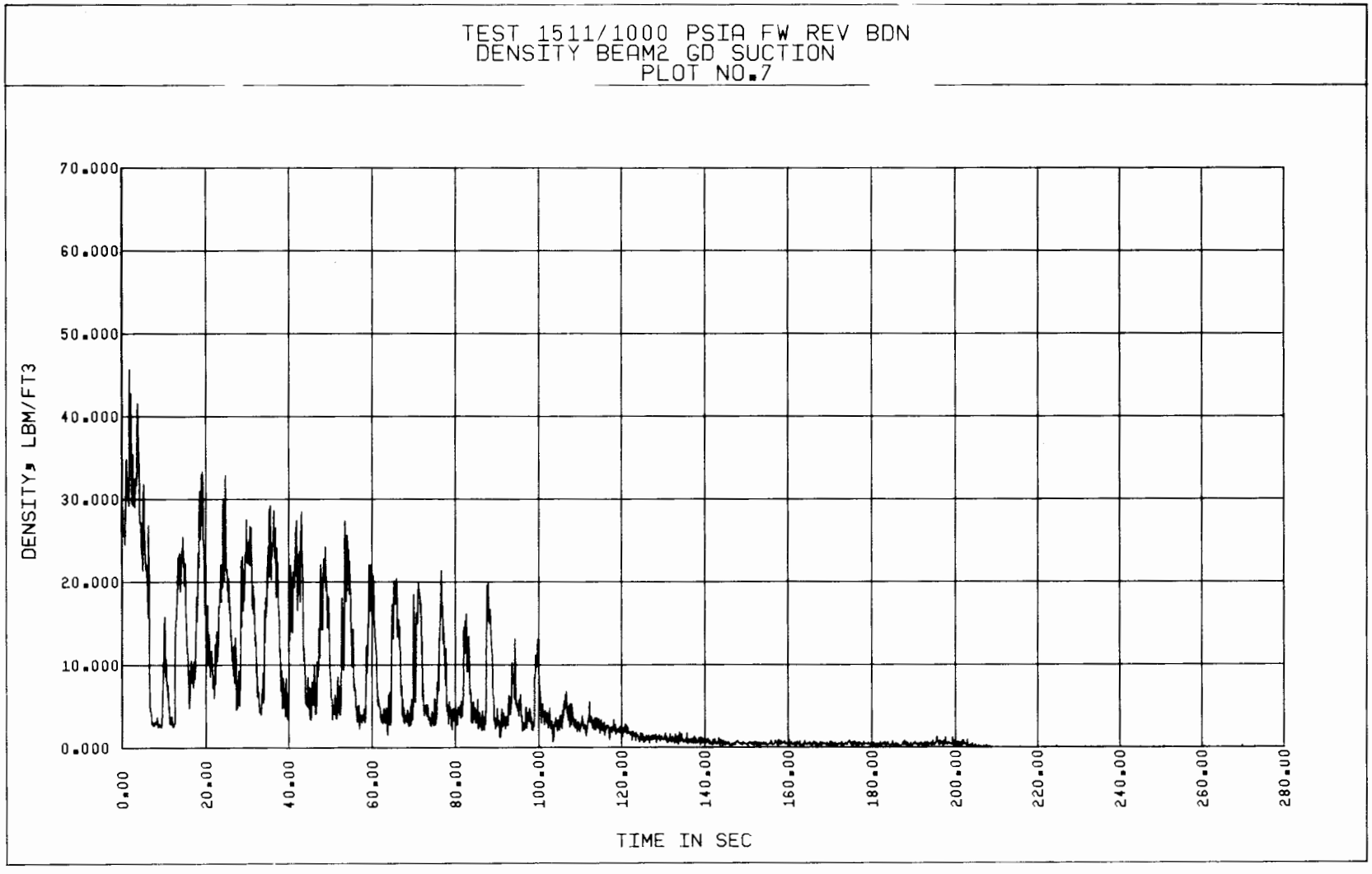

Figure 5-72. Test 1511, Suction Density vs Time

5.3 TEST RANGE VERSUS RANGE OF INTEREST

It is worthwhile to learn how well the parameter ranges covered by the transient tests compare with the range of parameters of interest. To accomplish this it is appropriate to compare some of the transient test results with those obtained from NSSS LOCA blowdown calculations. As discussed in Section 3.2, it is not required that the test blowdowns reproduce the time histories of calculated NSSS LOCA blowdowns. It is sufficient that:

1. somewhere in the assortment of test system blowdowns there are a number of times when the test pump operating conditions momentarily pass through the range of conditions typical of NSSS LOCA blowdowns, and

2. at these times, the severity of the transient tests is sufficiently representative of the LOCA's to check the applicability of a calculational model based on data from steady-state tests.

There are several ways of checking the transient data to determine whether the above conditions are satisfied. The key pump operating conditions to be considered in this context are, pressure, void fraction, normalized volumetric flow rate and normalized pump speed. It is important that when the test system operating conditions are compared against those from NSSS blowdown calculations, similar locations (relative to the test pump) be employed for both cases. Since pump path average properties were used in available curves showing the results of NSSS LOCA calculations (Reference 1), the void fraction and the normalized volumetric flow rate are referenced to average conditions within the pump for these comparisons.

The occurrence of any differences between transient and steady-state pump performance, even when the same upstream or pump average conditions exist momentarily, depends on whether there are any significant inertial or non-equilibrium phase change effects. Analyses by others in the field (e.g. Reference 6) suggest that except during extreme transients (more rapid than the main saturated decompression portion of blowdowns), the fluid inertia in the pump itself is of little effect and a more likely source of nonequilibrium is lag in phase change effects. This is the basis for using $d\alpha_F/dt$ as a criterion for severity of a transient.

Thus, the variations of pump average void fraction, α_F, versus time after start of vaporization are employed to indicate the severity of either NSSS or

test system blowdowns. In Figure 3-2, these variations are shown for typical NSSS and test system blowdown calculations. A similar plot showing the pump average void fraction variation during representative transient tests is shown in Figure 5-73. Superimposed on this plot are the same void fraction variations presented in Figure 3-2 for typical NSSS blowdown calculations. A comparison of the criterion $d\alpha_F/dt$ can be derived from the curves of Figure 5-73. This figure indicates that the test system produced blowdowns with $d\alpha_F/dt$ up to one-half of that for large break LOCA rates in the 0 to 40 percent void fraction range, and up to one-third of that for large break LOCA rates in the 75 to 85 percent void fraction range. If the large break LOCA rates might cause significant differences between steady-state and transient performance, then it is expected that the comparison between steady-state data and data for a test system blowdown with $d\alpha_F/dt$ up to one-half of that for large break LOCAs would indicate some appreciable deviations although not to the same degree. Thus, the rate of change of void fraction realized for the 100 percent break area test system blowdowns is considered adequate to check the steady-state performance data to derive a dynamic pump calculation model.

Another means of checking the adequacy of the range of operating conditions achieved during the test system blowdowns is by comparing variations of the homologous flow to speed ratio ν/α_N versus the void fraction α_F for NSSS blowdowns with those obtained from test system blowdowns. These variations are plotted in Figure 5-74 for typical NSSS discharge leg break blowdown calculations and representative transient tests. It is seen that the test system curves start out at the zero flow and zero void fraction point, whereas the NSSS curves start out at the zero void fraction and $\nu/\alpha_N = 1.0$ point. This is because both the test void fraction and the flow rate approach zero when the return line throttle valve is suddenly closed prior to rupture. For the NSSS blowdowns, there are substantial amounts of flow through the pump during the subcooled decompression period, and the flow does not stagnate when the fluid reaches saturation condition. In general the representative blowdown traces shown in Figure 5-74 span a wide range of combinations of NSSS void fractions and homologous flow to speed ratios during the blowdowns. These combinations are considered sufficient to check the applicability of steady-state data to the dynamic pump calculation model and to give adequate sampling of the ranges of prime interest for broken leg forward flow blowdowns. Other blowdown tests can be shown similarly as relating to large-break locked rotor

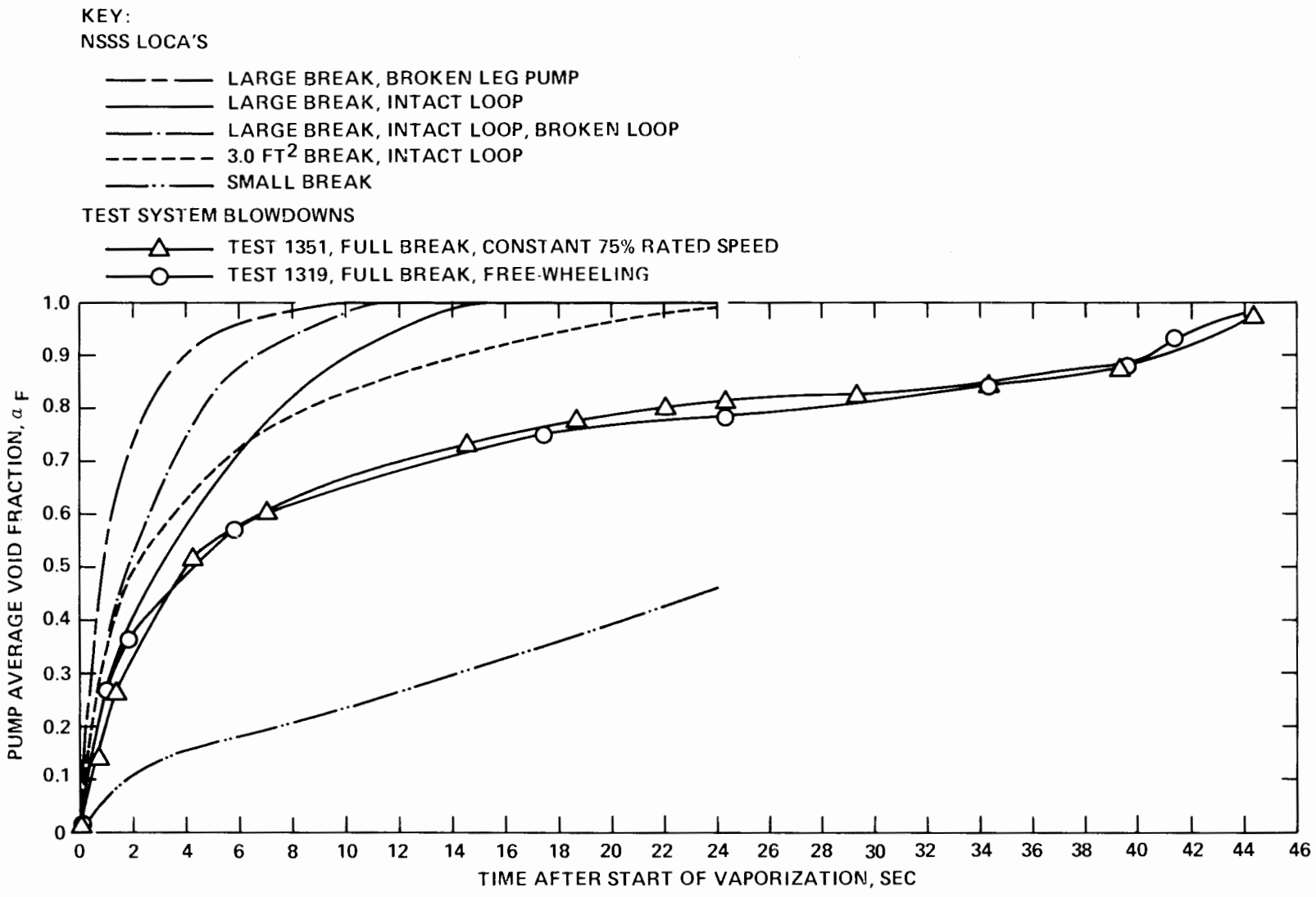

Figure 5-73. Comparison of Transient Test Results with a Range of Typical NSSS Blowdowns, Pump Average Void Fraction vs Time

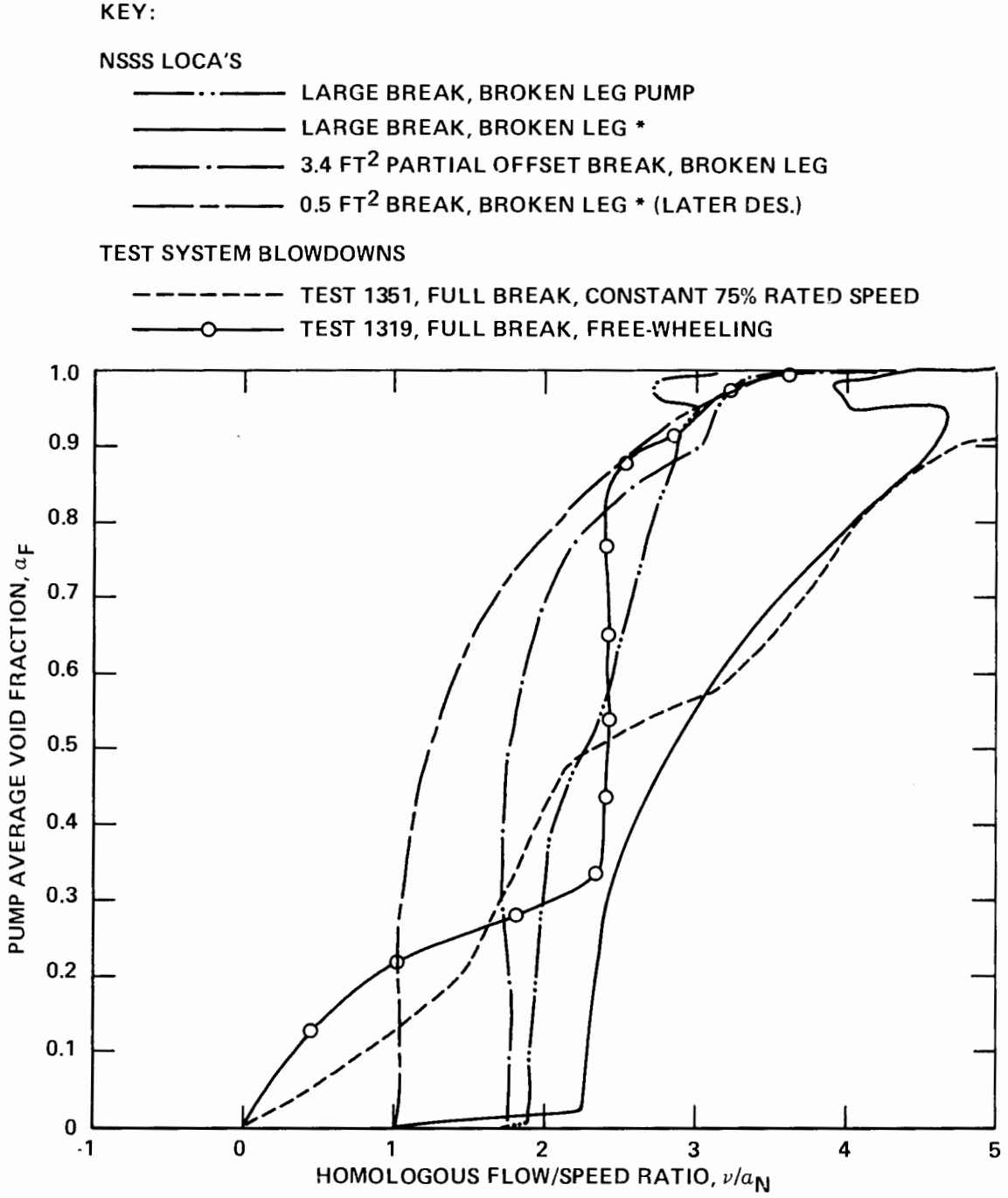

Figure 5-74. Comparison of Transient Test Results with Typical NSSS Blowdowns for Discharge Leg Breaks, ν/α_N vs α_F

and medium-break free-rotor blowdowns with reverse flow, as well as a variety of smaller-break blowdowns in which transient effects are less severe and not expected to be significant to performance.

The variation of pump suction pressure with respect to void fraction may also be employed to check the range of operating conditions realized during the test system blowdowns versus the NSSS LOCA range. In Figure 5-75 the pump suction pressure versus void fraction is presented for both Tests 1319 and 1351, together with the upper and lower ranges for the same parameter variation for the NSSS blowdown calculations. It is seen the test system curves have trends similar to those for NSSS curves, and lie in the middle of the NSSS ranges. This range of combinations of pressure and void fraction for the test system blowdowns appears to be adequate, since the effect of pressure is considered secondary on pump performance from steady-state data analysis (Volume II).

It is evident from the discussions above that the operating conditions, such as pressure, void fraction, volumetric flow rate and pump speed for the 100% break area test system blowdowns span a wide range of NSSS LOCA operating conditions of prime interest. These include transients severe enough to check the applicability of steady-state data to a calculation model for analyzing transient performance.

5.4 SELECTION OF KEY SAMPLE BLOWDOWN TESTS

As indicated earlier, one of the purposes of generating transient two-phase pump performance data is to compare the model pump transient performance against steady-state test results at similar pump operating conditions. A total of 16 blowdown tests were performed on the model pump (See Section 3). Not all the data generated during the transient tests are equally suitable or useful for analysis and comparison with the steady-state data collected. Some of the transient tests were exploratory in nature. Also, data from some tests involved inconsistencies, were more complex to interpret, and covered a more limited portion of the range of interest as discussed in Section 5.3. For the initial analysis and presentation included in this report, certain criteria were developed for selecting blowdown tests to provide primary comparisons against steady-state test results. These criteria are summarized as follows:

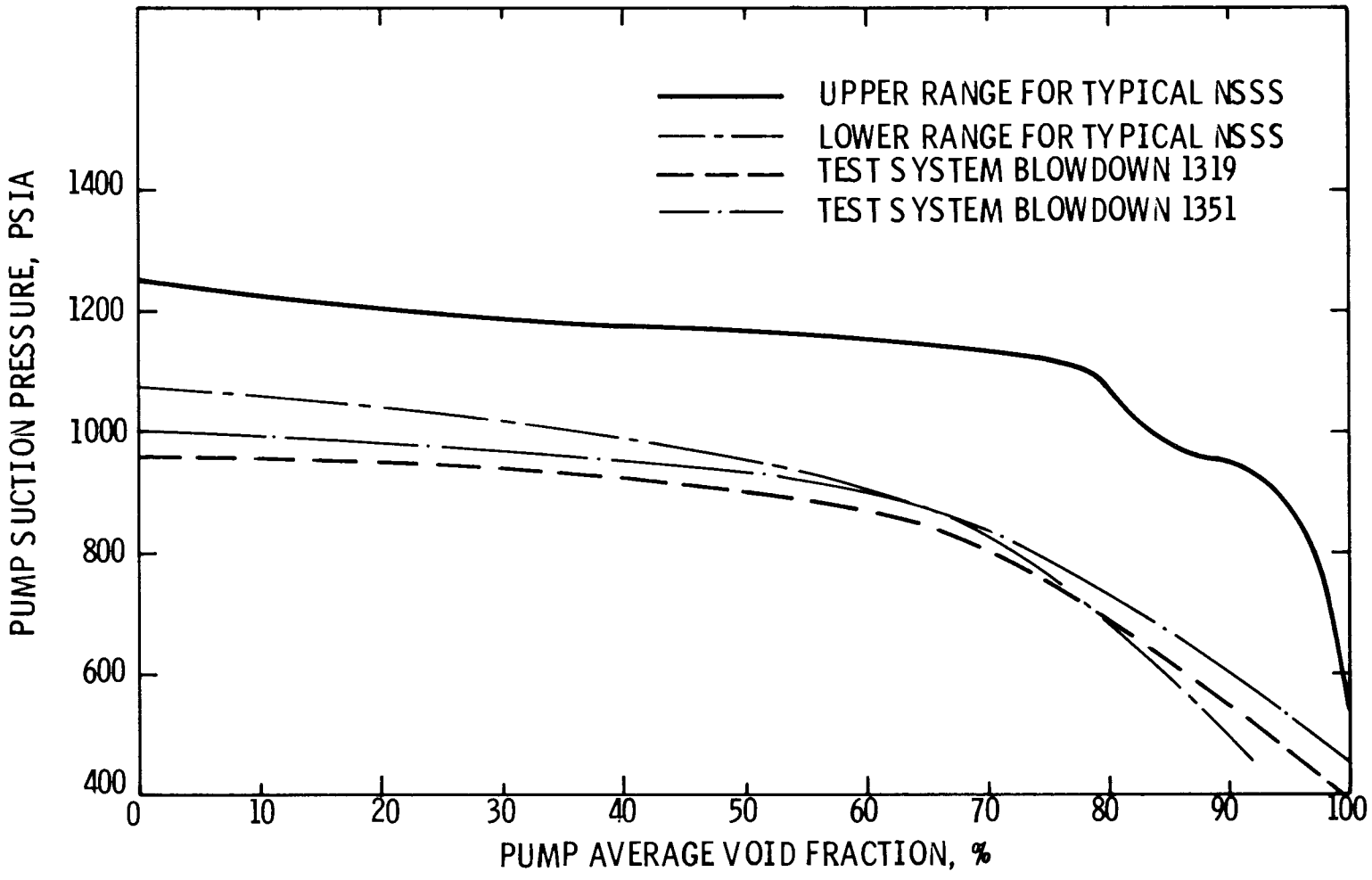

Figure 5-75. Comparison of Transient Test Results with a Range of Typical NSSS Blowdowns, Pump Suction Pressure vs Void Fraction

1. The operating condition, such as volumetric flow rate, speed, void fraction, and pressure, encountered during the selected test system blowdowns should span much of the range of values for the same parameters obtained for a spectrum of NSSS LOCA blowdown calculations. Since the pump performance is being correlated on the basis of homologous parameters based on flow similarity (as derived in Volume II), the homologous flow-to-speed ratio, ν/α_N, can be employed as an operating condition alternative to flow and speed individually.

2. The selected blowdown tests should include operation up to the maximum $d\alpha_F/dt$ achieved in the transient test program.

3. The data from the selected blowdown tests should not exhibit appreciable periodic fluctuations which overly complicate the interpretation of various transient measurements.

4. The magnitude of the pump performance parameters (such as pump head and hydraulic torque) in the range of prime interest should be adequately large (greater than 5 percent of rated values) to minimize the effect of measurement uncertainties.

From Figure 5-73, it is evident that the rate of change of voiding the fluid with respect to time, $d\alpha_F/dt$, varies directly as the break size. Thus, the largest $d\alpha_F/dt$ ratio is obtained for the 100 percent break area blowdowns, namely Tests 1267, 1319 and 1351. Note that the above discussion excludes the free-wheeling reverse flow blowdowns, since appreciable periodic fluctuation are present in almost all the measured parameters for these tests.

In Figure 5-74, the variation of the homologous flow to speed ratio for representative test system blowdowns are compared against those obtained from typical NSSS blowdown calculations. Specifically, curves for two test system blowdowns (Tests 1319 and 1351) are provided in this figure. Test 1319 was a 100 percent break area, free-wheeling forward flow blowdown, and Test 1351 was a 100 percent break area "power-on" forward flow blowdown. It is seen that the curve for Test 1351 covers a wider range of ν/α_N ratio than that for Test 1319. This is because the normalized volumetric flow rate variation and normalized speed variation for Test 1319 are similar to each other, as seen from Figure 5-76 and 5-77. Consequently, the ratio ν/α_N covers only a small range (1.5 to 3.0) during most of the transient for this test.

The pump speed and volumetric flow rate variation for Test 1351 are shown in Figures 5-46 and 5-61 of Section 5.2. It is seen that the pump speed is essentially invariant for this test, and consequently, the normalized flow to

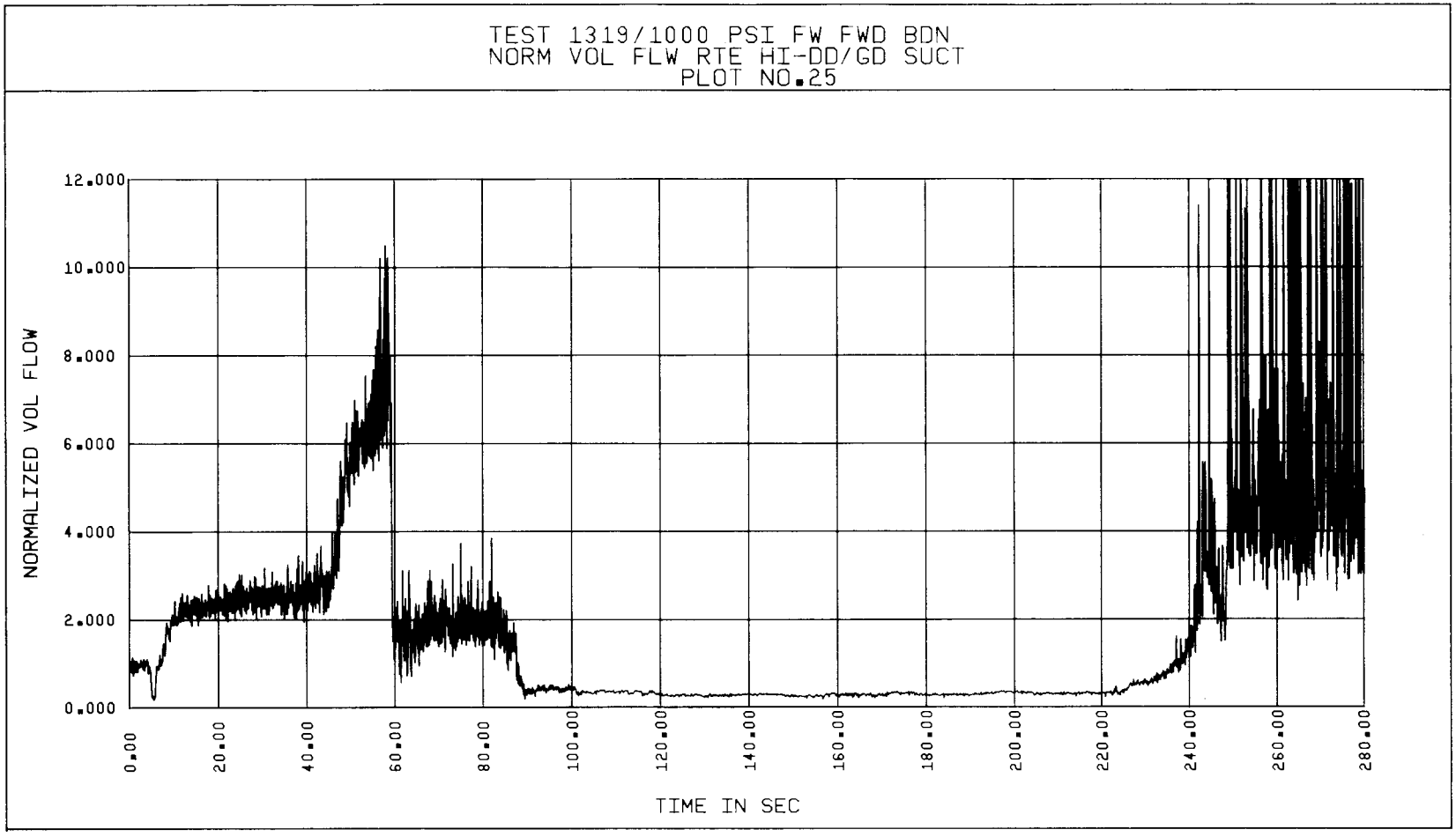

Figure 5-76. Test 1319, Normalized Suction Volumetric Flow Rate vs Time

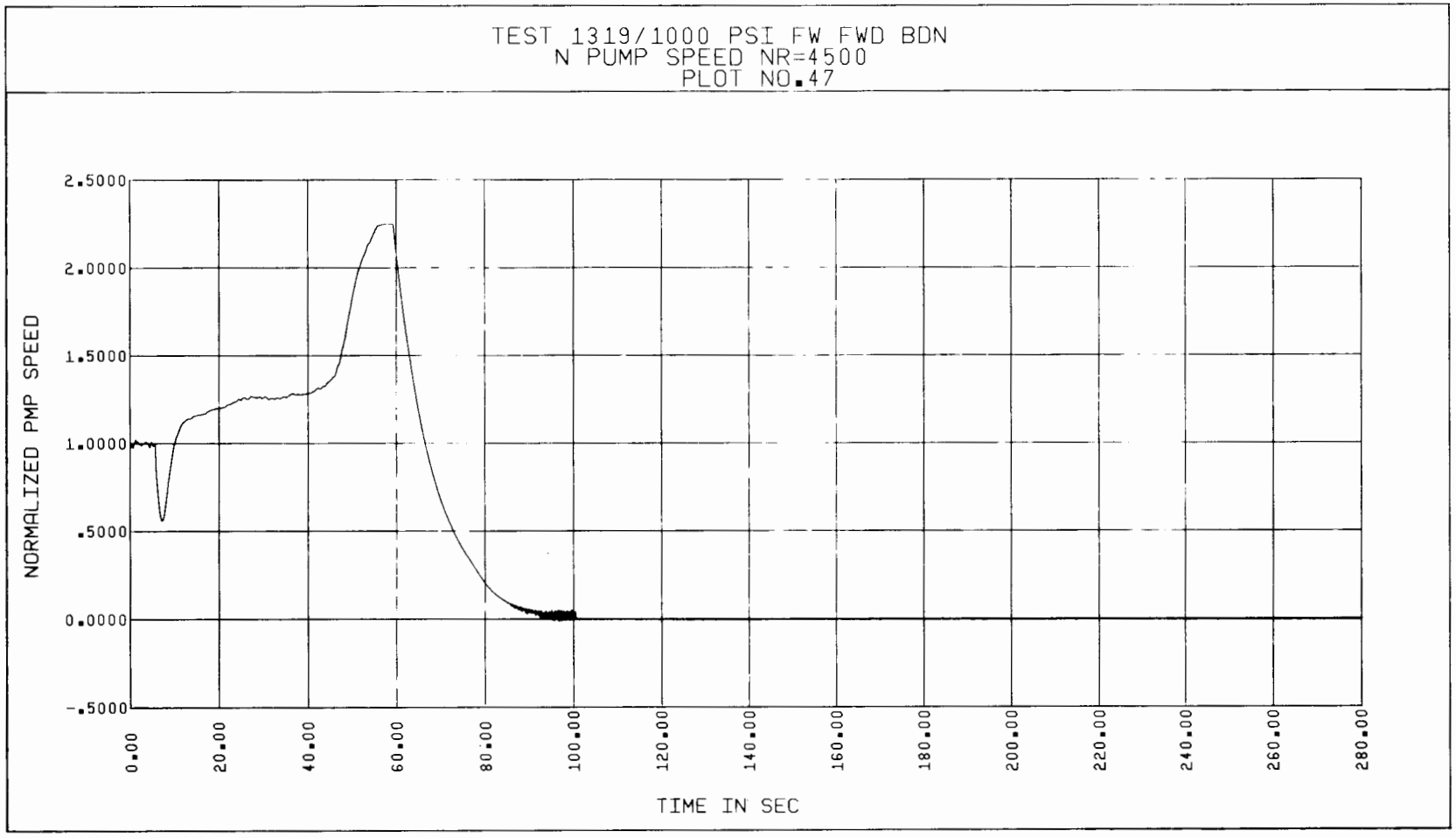

Figure 5-77. Test 1319, Normalized Pump Speed vs Time

speed ratio varies with time in a manner similar to the volumetric flow rate of Figure 5-61. This variation is illustrated in Figure 5-74.

For Test 1267, the pump rotor was locked, and consequently ν/α_N is infinite and α_N/ν is zero at all times during the blowdown. Thus, data from Test 1267 offers only a restricted comparison with steady-state data.

The homologous flow to speed ratios for both Tests 1319 and 1351 cover a wide range of values. For Test 1319, the pump speed is allowed to vary during the blowdown, and consequently the hydraulic torque values (Figure 5-78) are somewhat lower than those obtained for Test 1351. These hydraulic torque values are considered large enough for comparison with steady-state data, without clouding the comparison due to measurement uncertainties. The pump performance parameters (head and hydraulic torque) for Test 1351 are presented in Figures 5-40, and 5-79. It is seen that the magnitudes of these parameters are substantially large during most of the blowdown. The measurement uncertainties associated with these parameters are also considered minimal, thereby satisfying the requirements of criterion 4.

It is clear from these discussions that Tests 1319 and 1351 are proper choices for key blowdown tests whose results can be employed to make direct comparisons with steady-state data over a range of prime interest. Analysis of flow data from these tests is provided in Section 5.5 and in Volume IV. Details of extracting transient performance "snapshots" and comparisons of transient and steady-state performance are also covered in Volume IV.

5.5 DETERMINATION OF TRANSIENT VOLUMETRIC FLOW RATE

In order to facilitate comparisons between transient and steady-state test results, it is important that the suction volumetric flow rate be uniquely determined. As indicated in Section 5.2.3, the interpretation of the two-phase flow rate related data (gamma densitometer, turbine meter, and drag disc measurements) at the SIS is rather difficult, and some simplifying assumptions were made for the initial estimate of SIS volumetric flow rates used in this report. The conversion constants used in the reduction of turbine meter and drag disc measurements are based on single-phase calibration tests. Flow patterns at higher void fractions may deviate from single-phase patterns and reduce the applicability of these constants. However, the general behavior

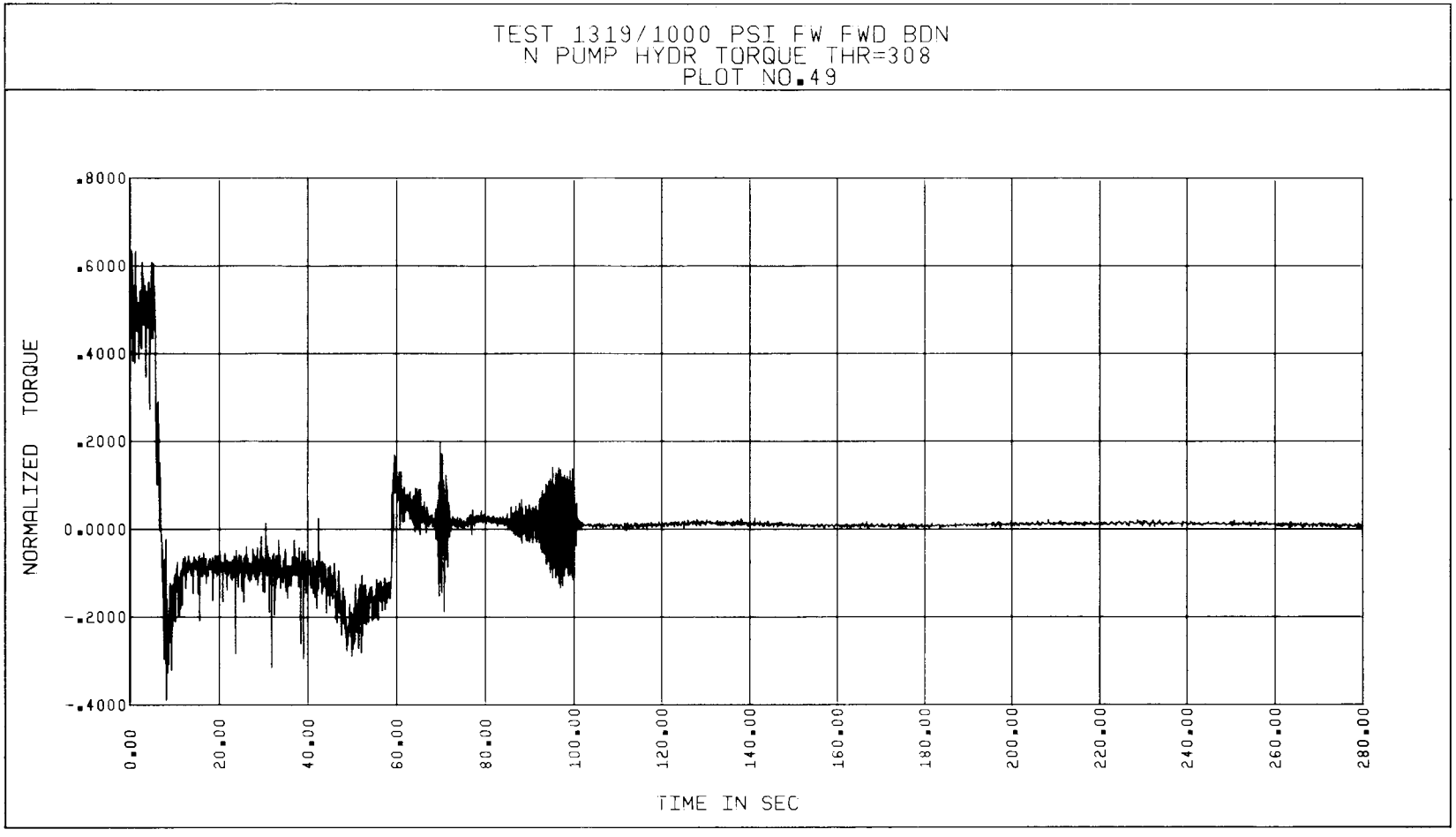

Figure 5-78. Test 1319, Normalized Pump Hydraulic Torque vs Time

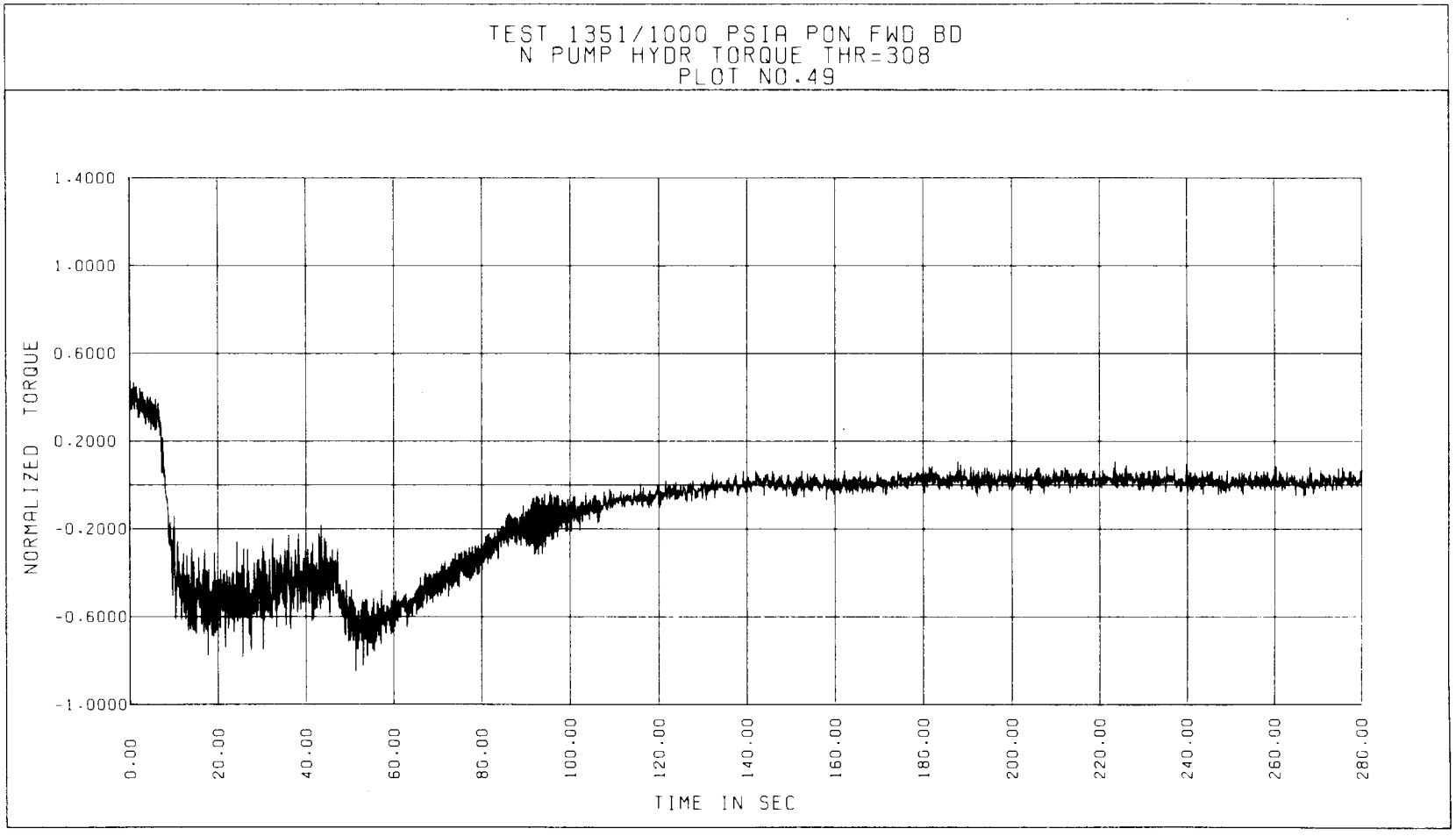

Figure 5-79. Test 1351, Normalized Pump Hydraulic Torque vs Time

and interrelationships between the gamma densitometer, turbine meter, and drag disc data at the SIS and DIS repeat from test to test for similar modes of testing. The use of simplistic (homogeneous) methods for interpretation of the three type of measurements to yield a volumetric or mass flow rate gives inconsistent results, especially at the SIS. The drag disc and turbine meter data presented as plots are for "point" measurements (small sensor targets) in large pipes during a transient two-phase phenomenon. Optimum methods for interpreting these point measurements in terms of average momentum flux or average fluid velocity in the pipe have not been identified or developed within the limited analysis in this project.

For use in initial data analysis and evaluations of results, simplistic calculations based on homogeneous flow shall be used to establish criteria for selecting portions of the data to apply in estimating volumetric flow rates. Other interpretations of flow data (e.g. Reference 6 and 7) are possible and could have advantages for analyzing dispersed flow with slip between the phases.

The description of the procedure employed in the determination of the volumetric flow rate is provided below. Sample blowdown test data are subjected to this procedure to arrive at the volumetric flow rate estimates. The following steps are involved in the process.

1. Using the Transient Data Reduction (TDR) code (See Section 4.2), develop the volumetric flow rate, momentum flux, mass flow rate, and the integrated mass curves for the suction and discharge instrumentation spools (SIS and DIS). These curves are based on the data from four turbine meters (TM's) and four drag discs (DD's) combined with the data from two gamma densitometers (GD's). There are generally two TM's, two DD's and one GD located at the SIS and a like number located at the DIS. Although there are three individual beam measurements available for each GD (See Figure 5-80), only the middle beam (beam 2) measurements are employed in the appropriate calculations. For the flow parameters mentioned above, four individual curves for momentum flux and eight curves for each of the other parameters are generated involving different combinations of instrument types (TM-GD, DD-GD, etc. as described in Section 4.2).

2. The curves generated for individual instrument measurments (drag disc momentum fluxes, turbine meter volumetric flow rates and gamma densitometer densities) are reviewed to verify the functional performance of the measuring instruments. Improper functioning of the instruments can be due to instrument damage, such as turbine meter bearing failure or damage to drag disc targets. Some of these instrument malfunctions result in atypical curve shapes relative to the others. The measurements by those instruments which fail this "mechanical performance test" should be disregarded in the analysis that follows.

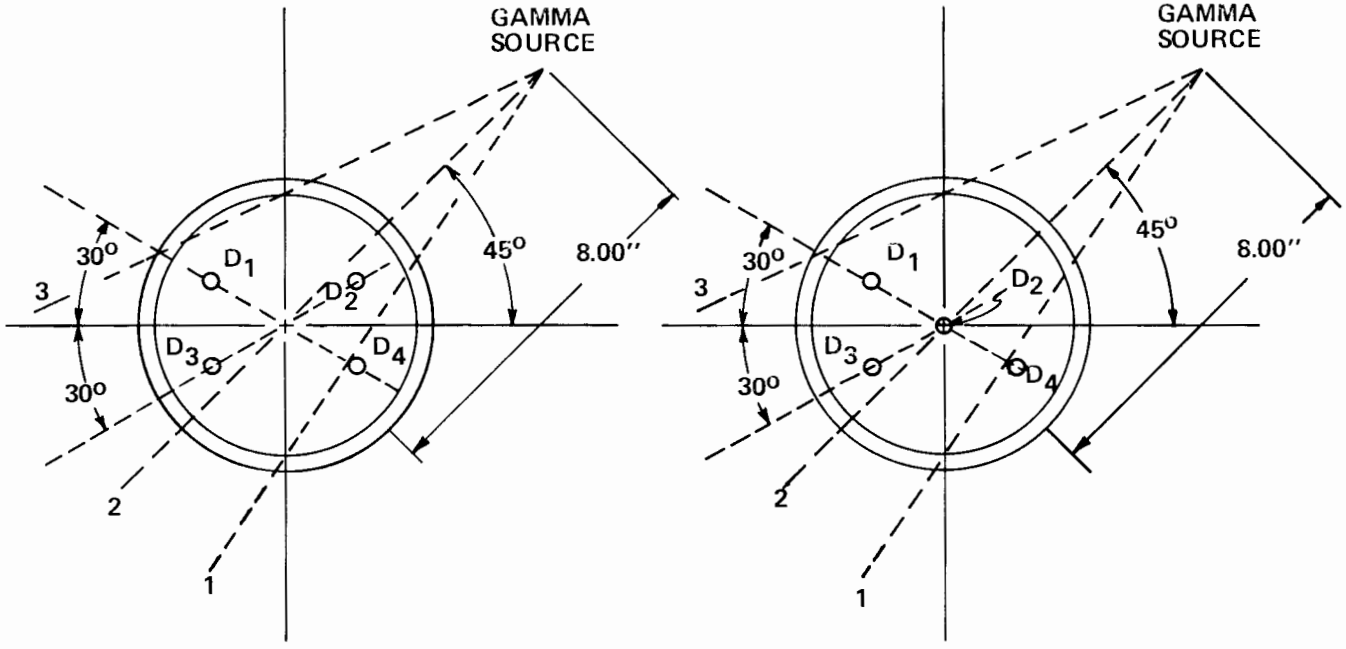

D_1: HI-TM (TURBINE METER), L-28

D_2: HI-DD (DRAG DISC), L-1

D_3: LO-DD (DRAG DISC), L-26

D_4: LO-TM (TURBINE METER), L-3

SUCTION SIDE INSTRUMENT SPOOL-
LOOKING AWAY FROM PUMP

D_1: HI-DD (DRAG DISC), L-2

D_2: HI-TM (TURBINE METER), L-29

D_3: LO-TM (TURBINE METER), L-4

D_4: LO-DD (DRAG DISC), L-27

DISCHARGE SIDE INSTRUMENT SPOOL-
LOOKING TOWARD PUMP

Figure 5-80. Suction and Discharge Instrumentation For Test 1351

3. After the proper functioning of the measuring instruments has been assessed, generate flow parameter curves based on averages for the suction TM's, discharge TM's, suction DD's and discharge DD's. The term average refers to an arithmetric average of the individual measurements by similar instruments at a particular measuring location. A maximum of four such curves can be developed for each flow parameter mentioned in Step 1 above, using the TDR code.

4. As a means of further qualifying the flow rate curves developed in Step 3 a "mass balance test" is performed on them. This test amounts to checking the mass balance across the pump using the average TM mass flow rate curves, and then the average DD mass flow rate curves. In each case the difference between the suction and discharge mass flow rate values should be accounted for by the seal injection leakage flow rate into the pump during the test as derived from the curves for seal injection inflow and outflow.

5. The final test for qualifying the flow rate curves involves the "mass flow integral test". This test pertains to the integrated mass curves, and compares the measured total mass that flowed through a measuring section during a particular time period of the transient with that calculated from the piping fluid inventory based on measured densities at the beginning and end of this time period and from the seal injection mass flow leakage into the pump during the same time period.

Based on the above tests and calculations using the measured data, the volumetric flow rate at the suction side of the pump is estimated. This flow rate may be provided by one instrument combination for part of the transient and by another for the rest of the transient.

In order to illustrate the application of the above method, consider the determination of the volumetric flow rate at pump suction for two of the forward blowdown tests, Tests 1319 and 1351. First, the data for Test 1351 is analyzed. The volumetric flow rate, momentum flux, mass flow rate, and the integrated mass curves generated per Step 1 for this test are shown in Figures 5-81 through 5-102. The volumetric flow rates indicated by the SIS TM's are uniform up to about 45 seconds. The LO-TM shows smaller volumetric flow rates than the HI-TM during the second state, and has a different shape (ramp instead of convex). Furthermore, the LO-TM curve does not approach zero values after termination of the blowdown (closure of HPSW-2 at about 173 seconds). Possible explanations for this behavior may be inapplicability of single-phase calibrations at very high void fractions, or eccentric response of electronic circuity to noise when there is no TM rotation input signal.

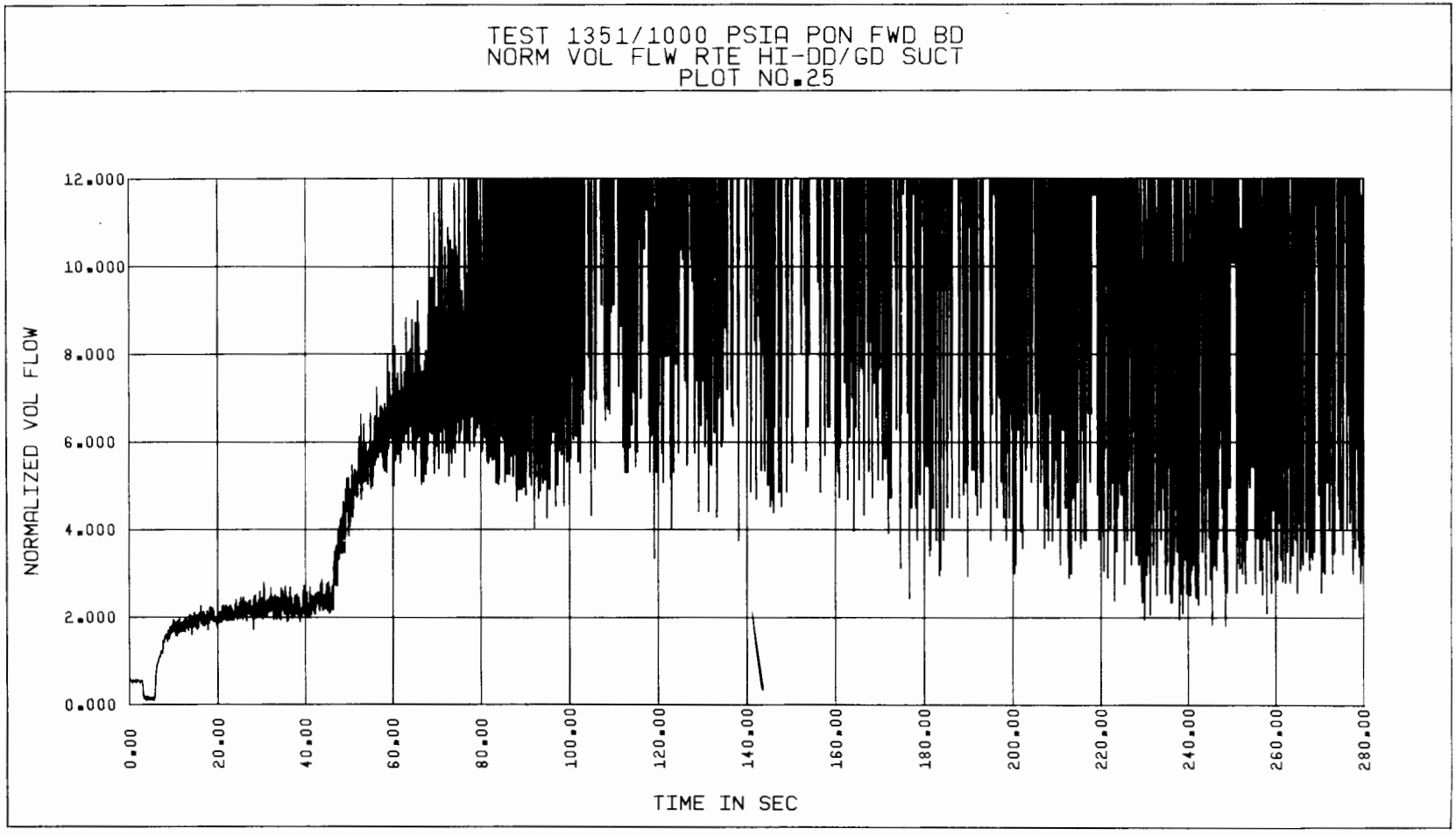

Figure 5-81. Test 1351, Normalized Suction Volumetric Flow Rate vs Time, Based on Suction Gamma Densitometer and High Drag Disc Data

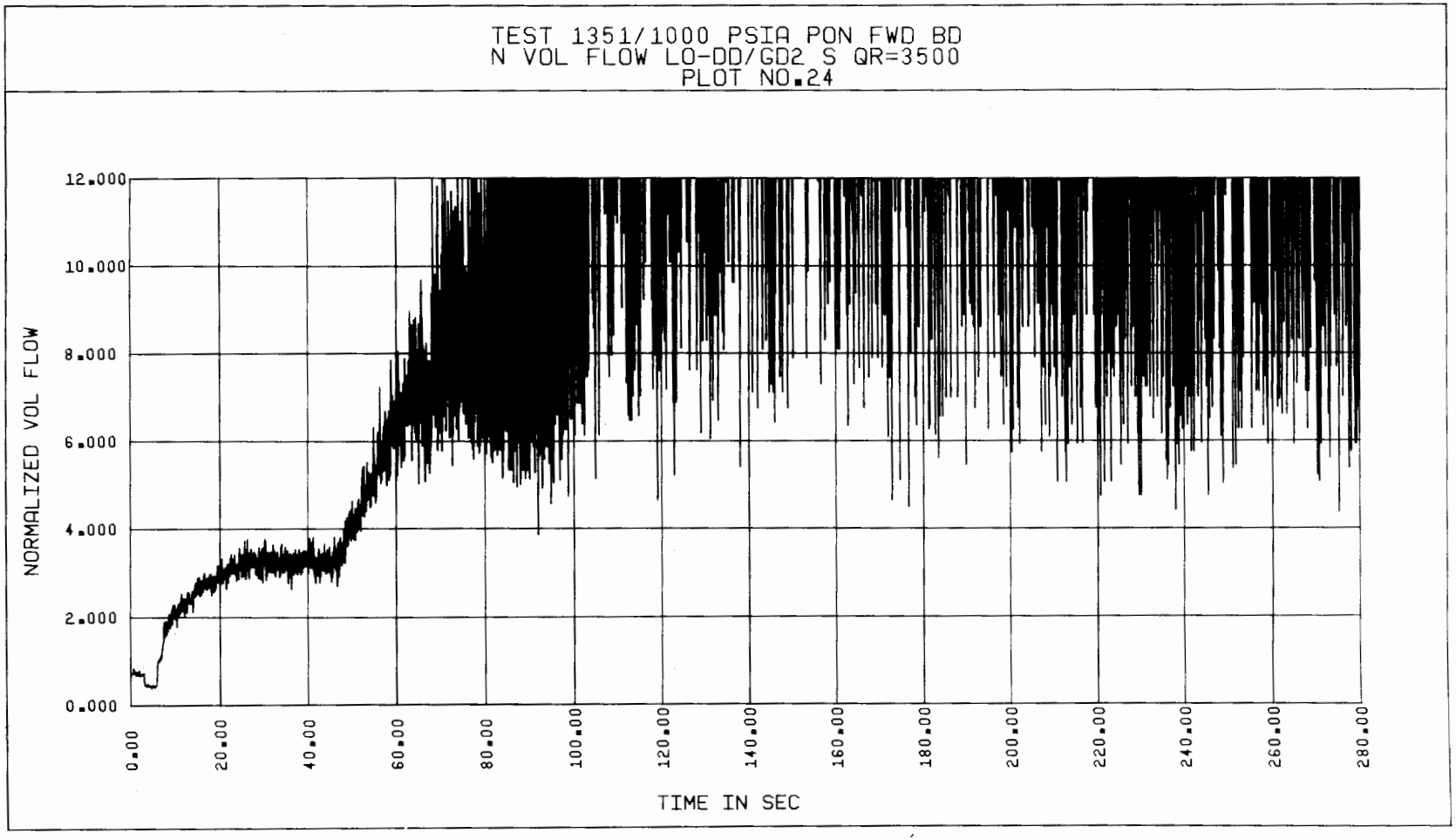

Figure 5-82. Test 1351, Normalized Suction Volumetric Flow Rate vs Time, Based on Gamma Densitometer and Low Drag Disc Data

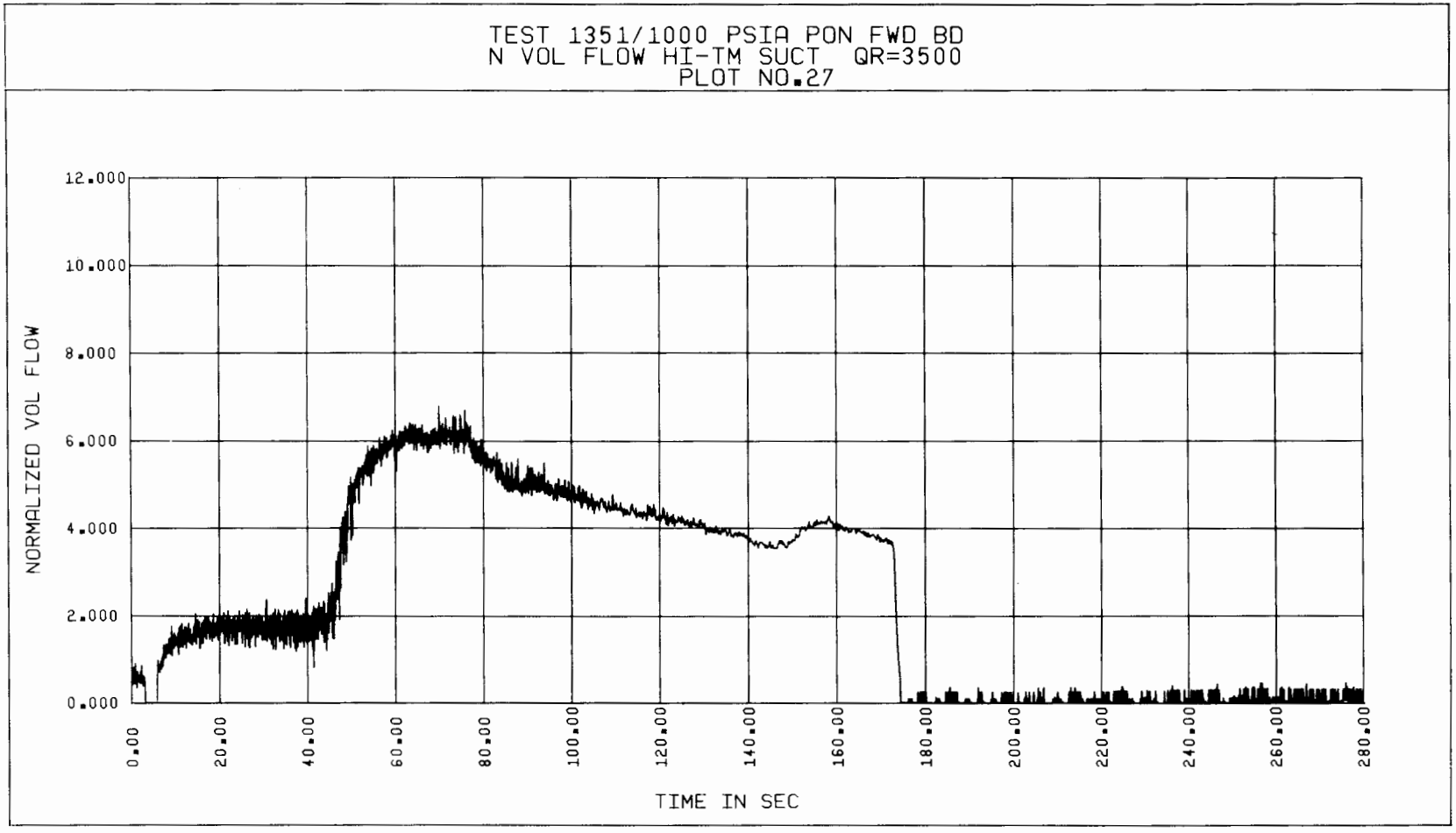

Figure 5-83. Test 1351, Normalized Suction Volumetric Flow Rate vs Time, Based on High Turbine Meter Data

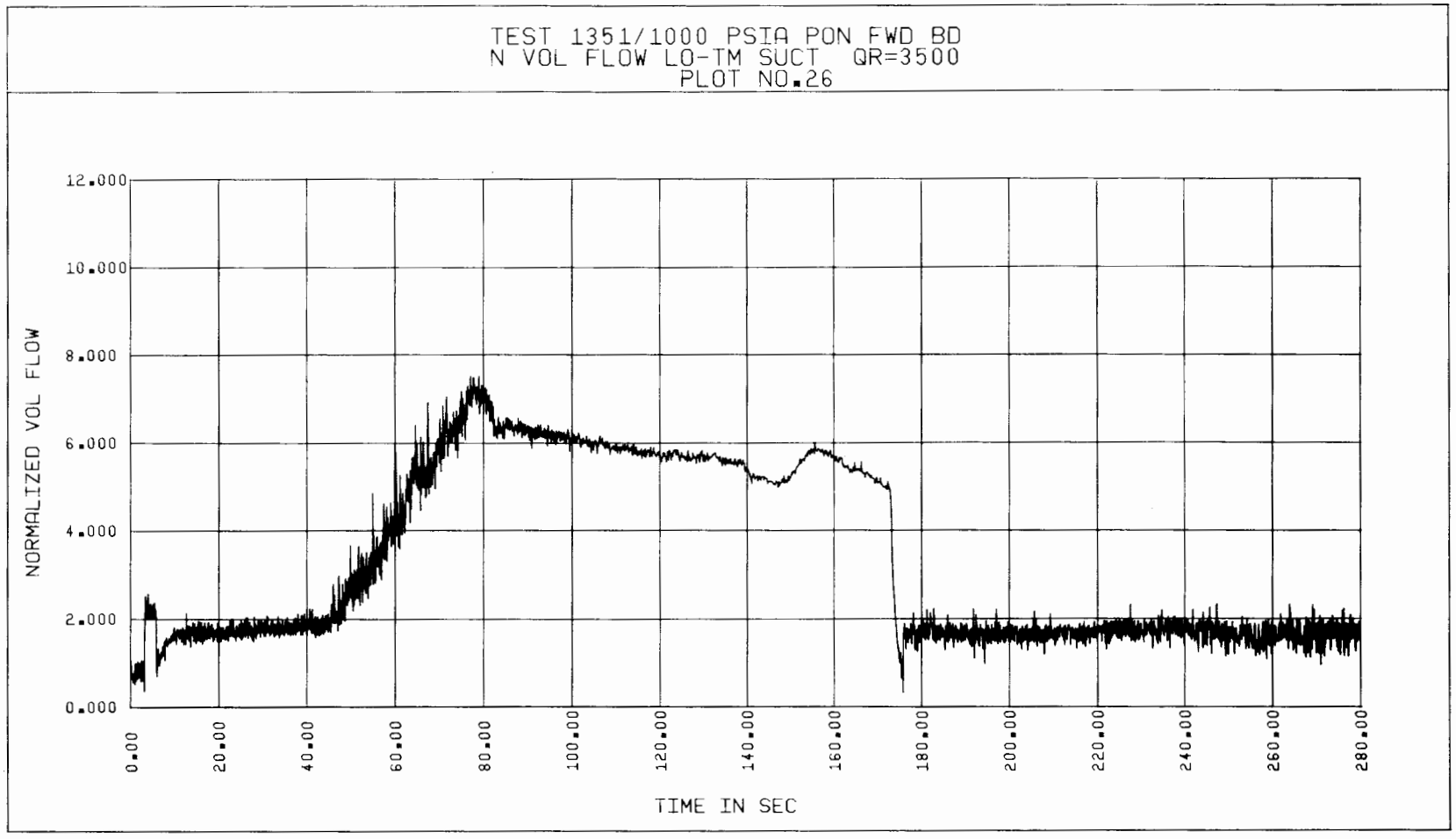

Figure 5-84. Test 1351, Normalized Suction Volumetric Flow Rate vs Time, Based on Low Turbine Meter Data

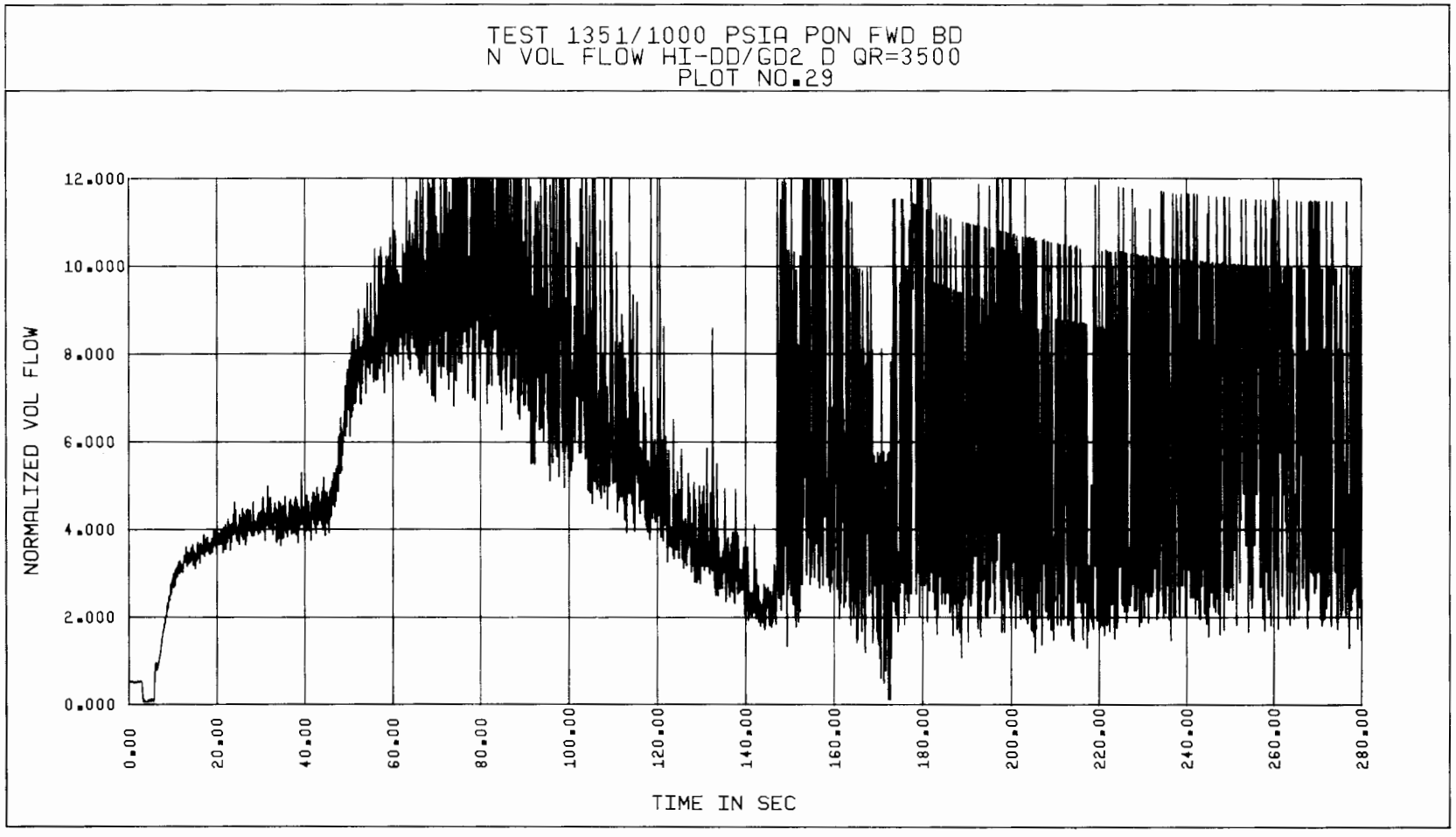

Figure 5-85. Test 1351, Normalized Discharge Volumetric Flow Rate vs Time, Based on Gamma Densitometer and High Drag Disc Data

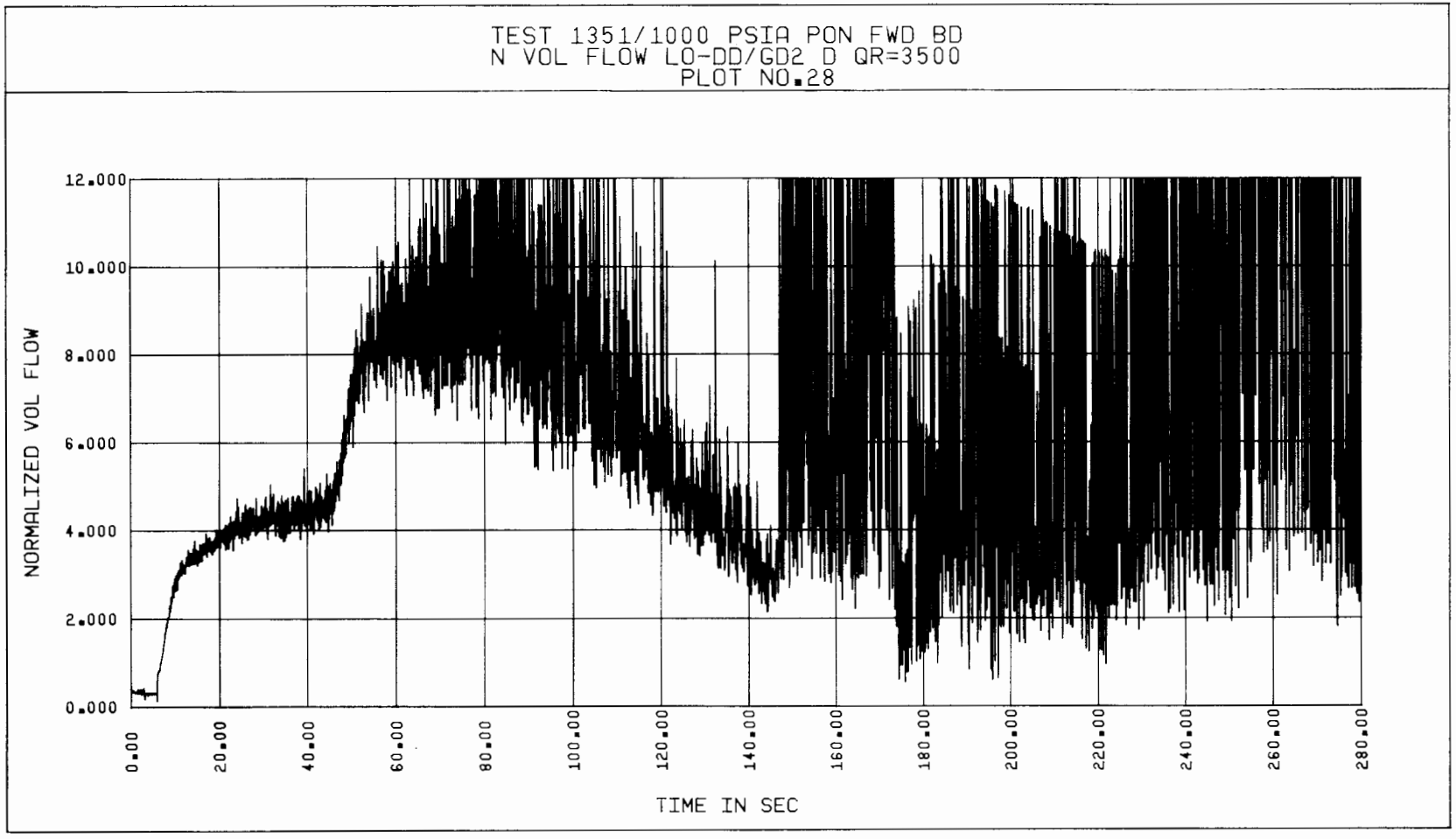

Figure 5-86. Test 1351, Normalized Discharge Volumetric Flow Rate vs Time, Based on Gamma Densitometer and Low Drag Disc Data

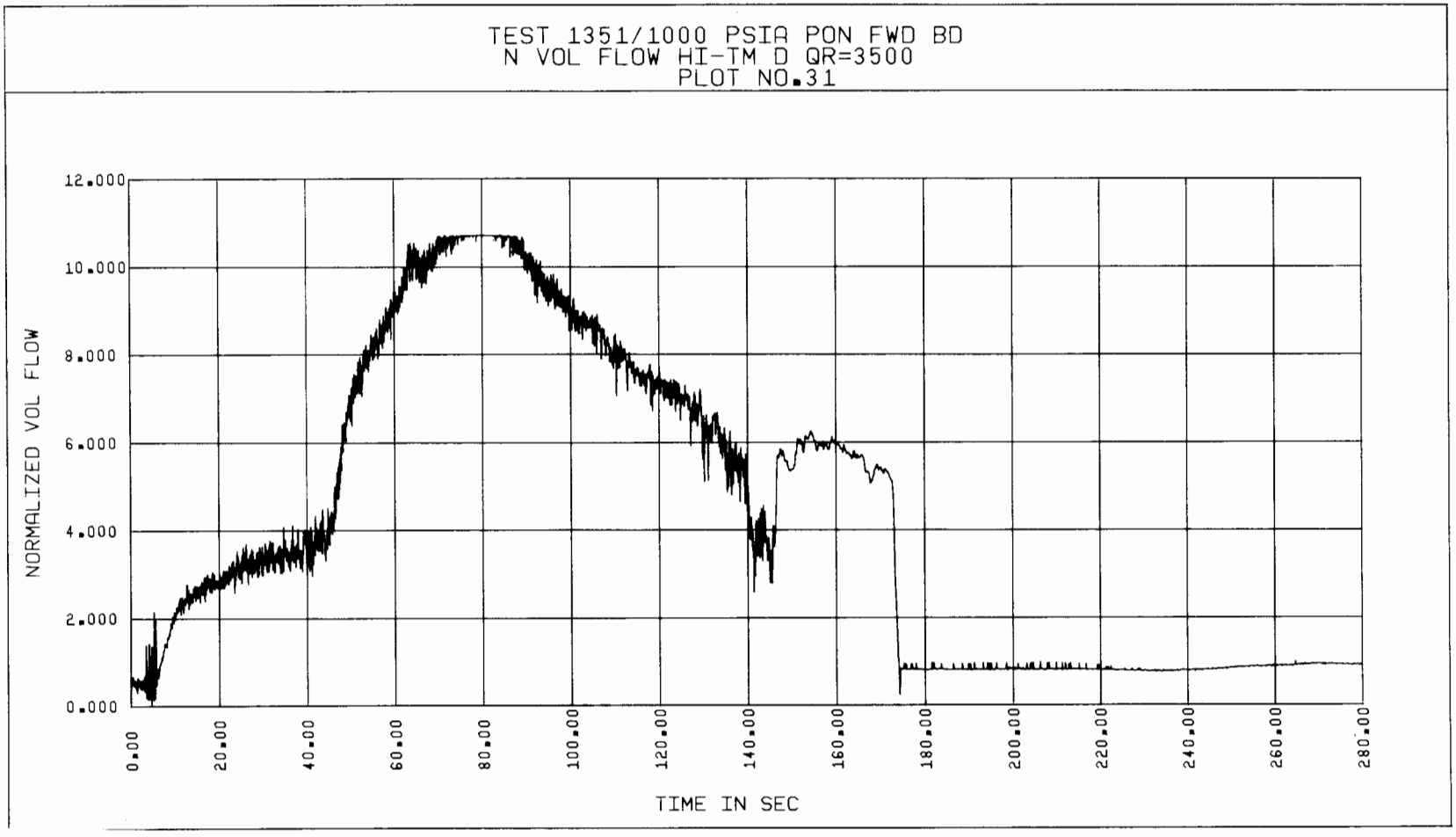

Figure 5-87. Test 1351, Normalized Discharge Volumetric Flow Rate vs Time, Based on High Turbine Meter Data

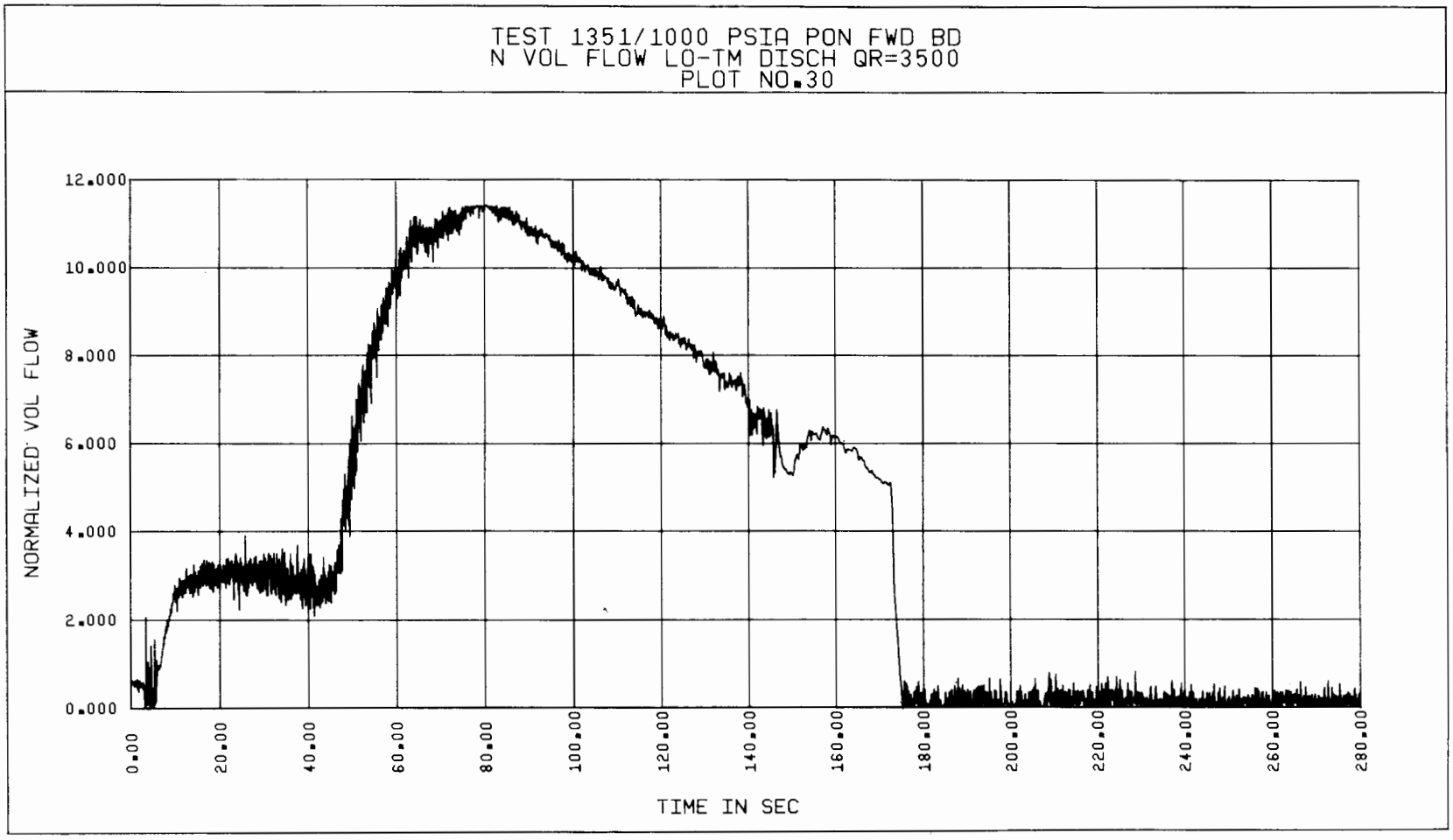

Figure 5-88. Test 1351, Normalized Discharge Volumetric Flow Rate vs Time, Based on Low Turbine Meter Data

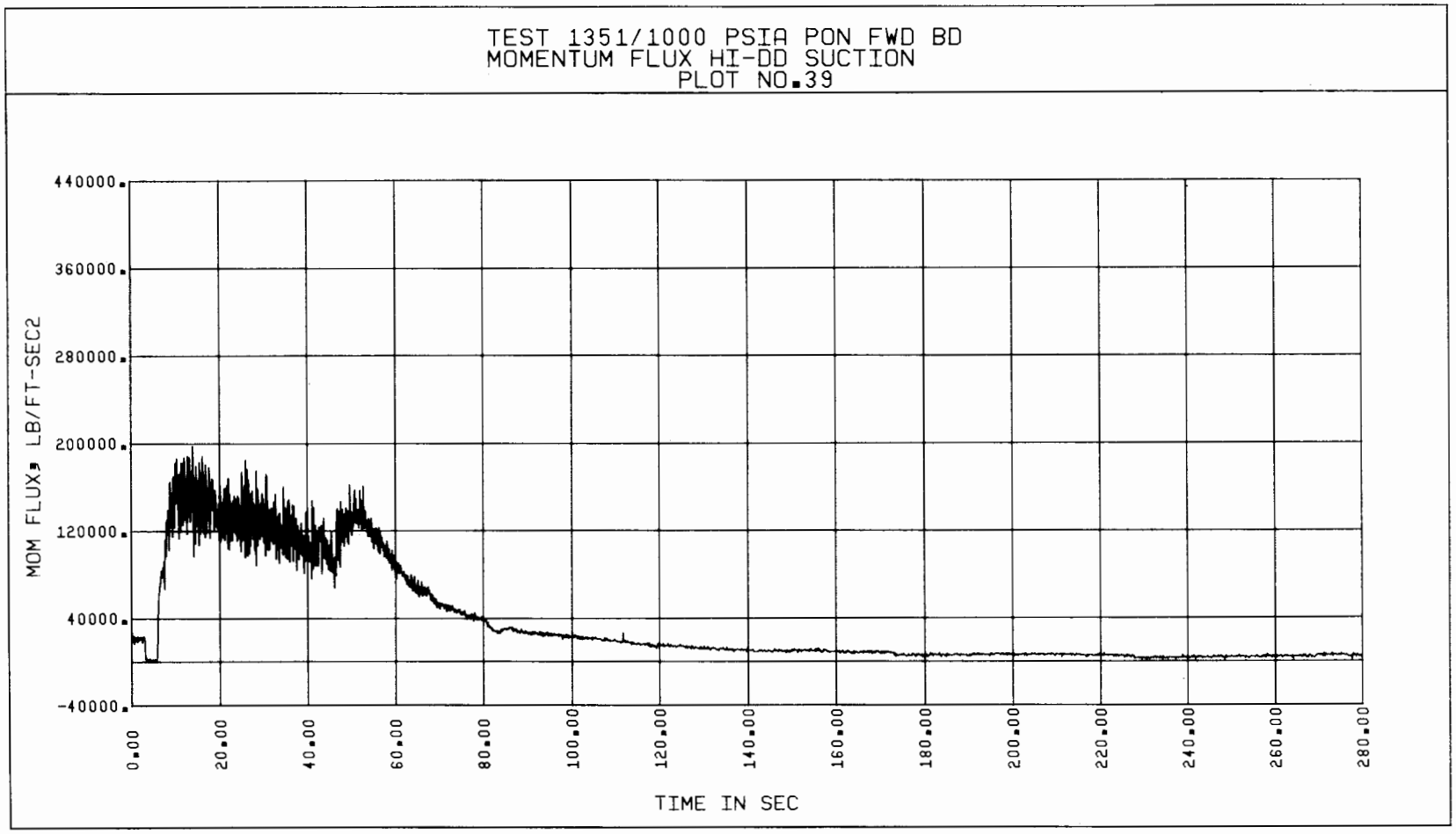

Figure 5-89. Test 1351, Suction Momentum Flux vs Time, Based on High Drag Disc Data

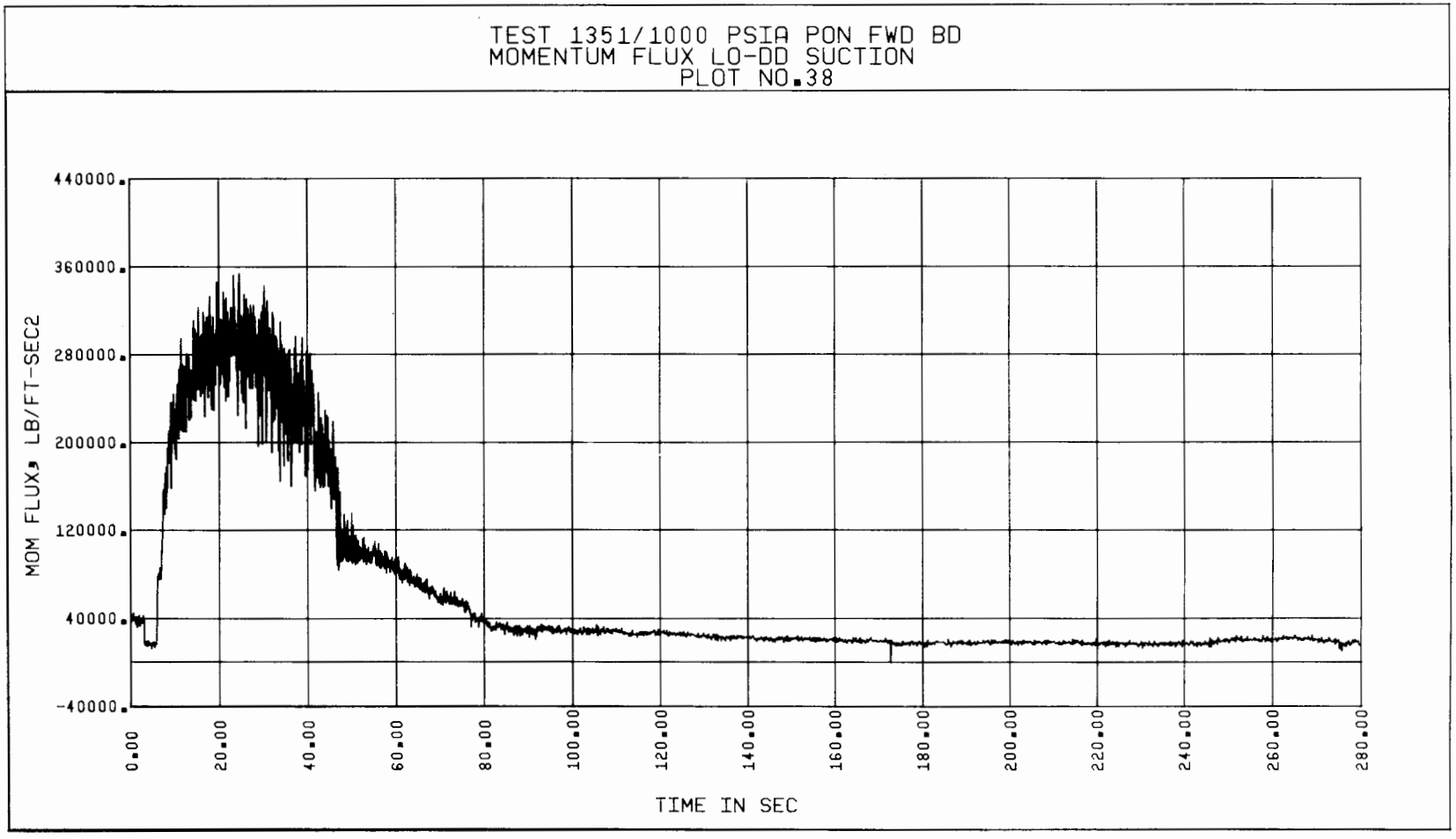

Figure 5-90. Test 1351, Suction Momentum Flux vs Time, Based on Low Drag Disc Data

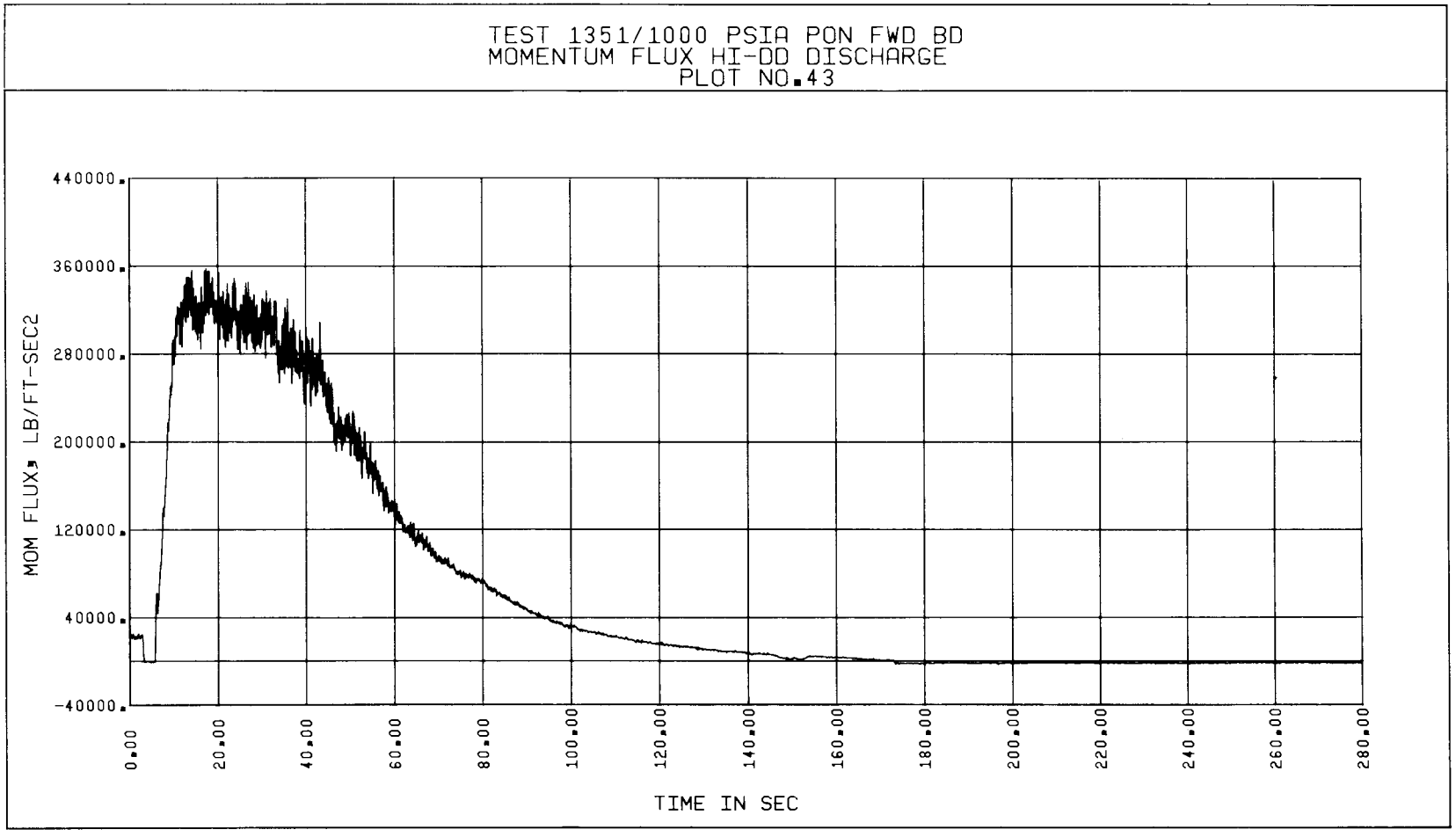

Figure 5-91. Test 1351, Discharge Momentum Flux vs Time, Based on High Drag Disc Data

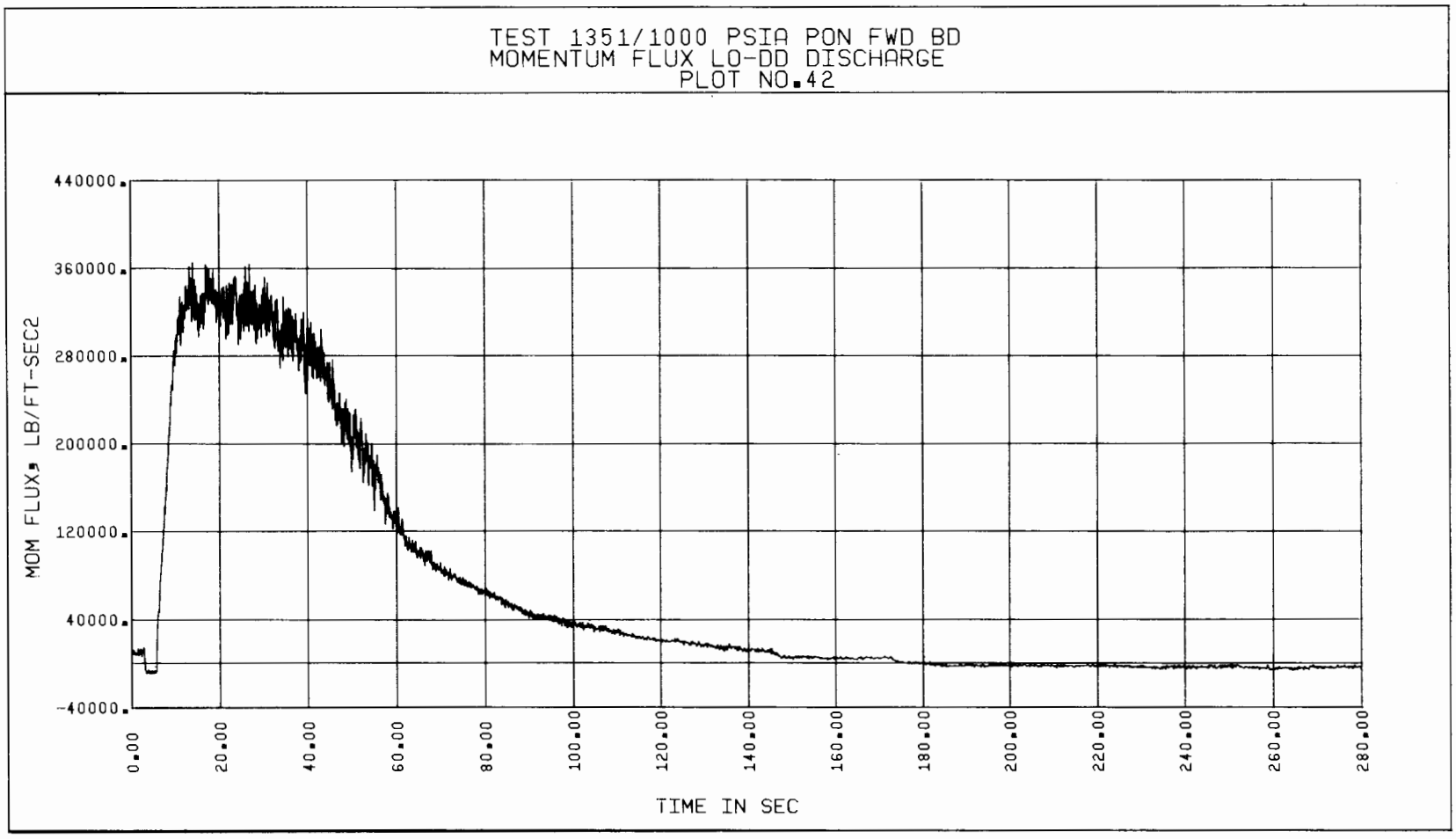

Figure 5-92. Test 1351, Discharge Momentum Flux vs Time, Based on Low Drag Disc Data

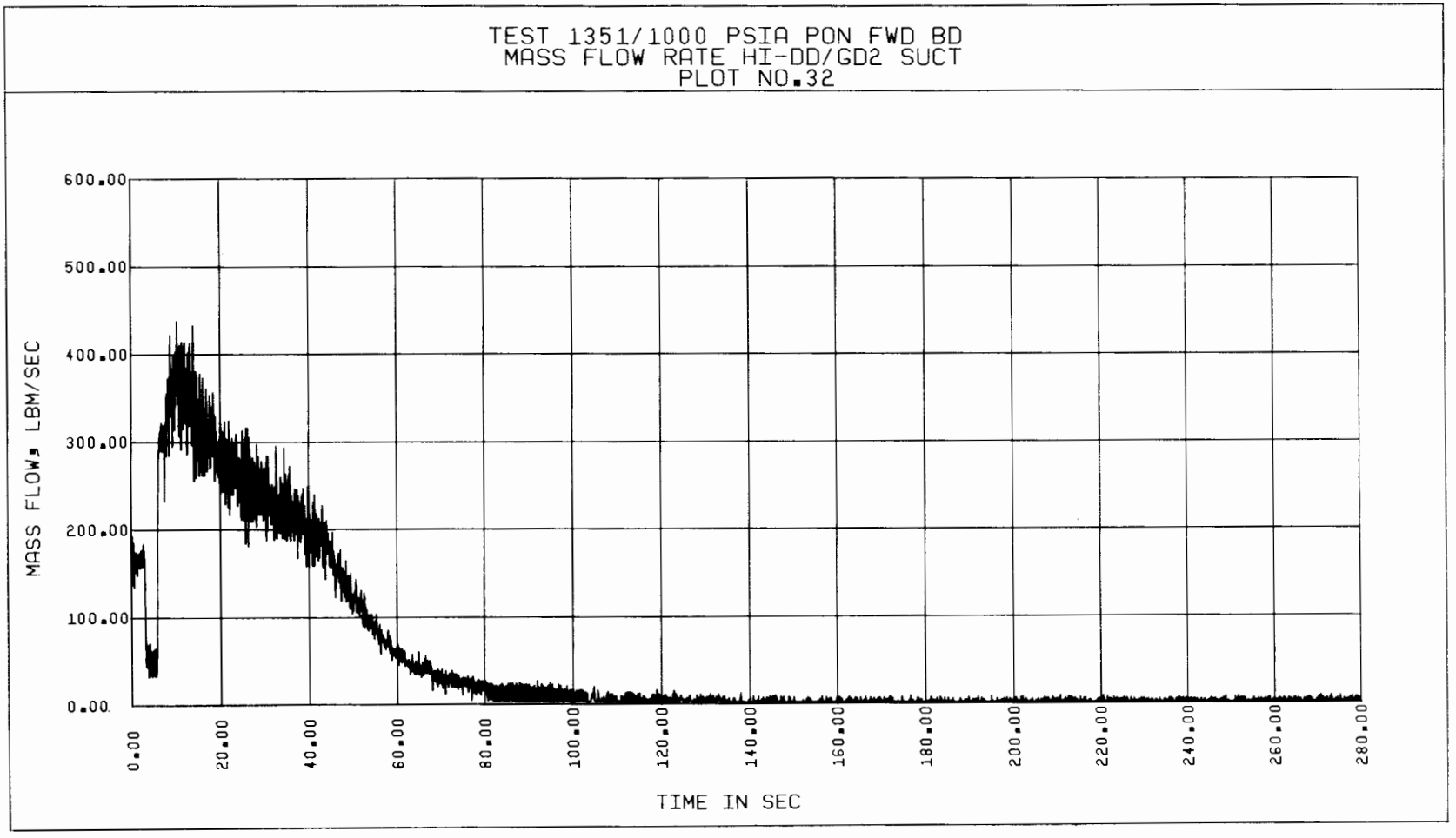

Figure 5-93. Test 1351, Suction Mass Flow Rate vs Time, Based on Gamma Densitometer and High Drag Disc Data

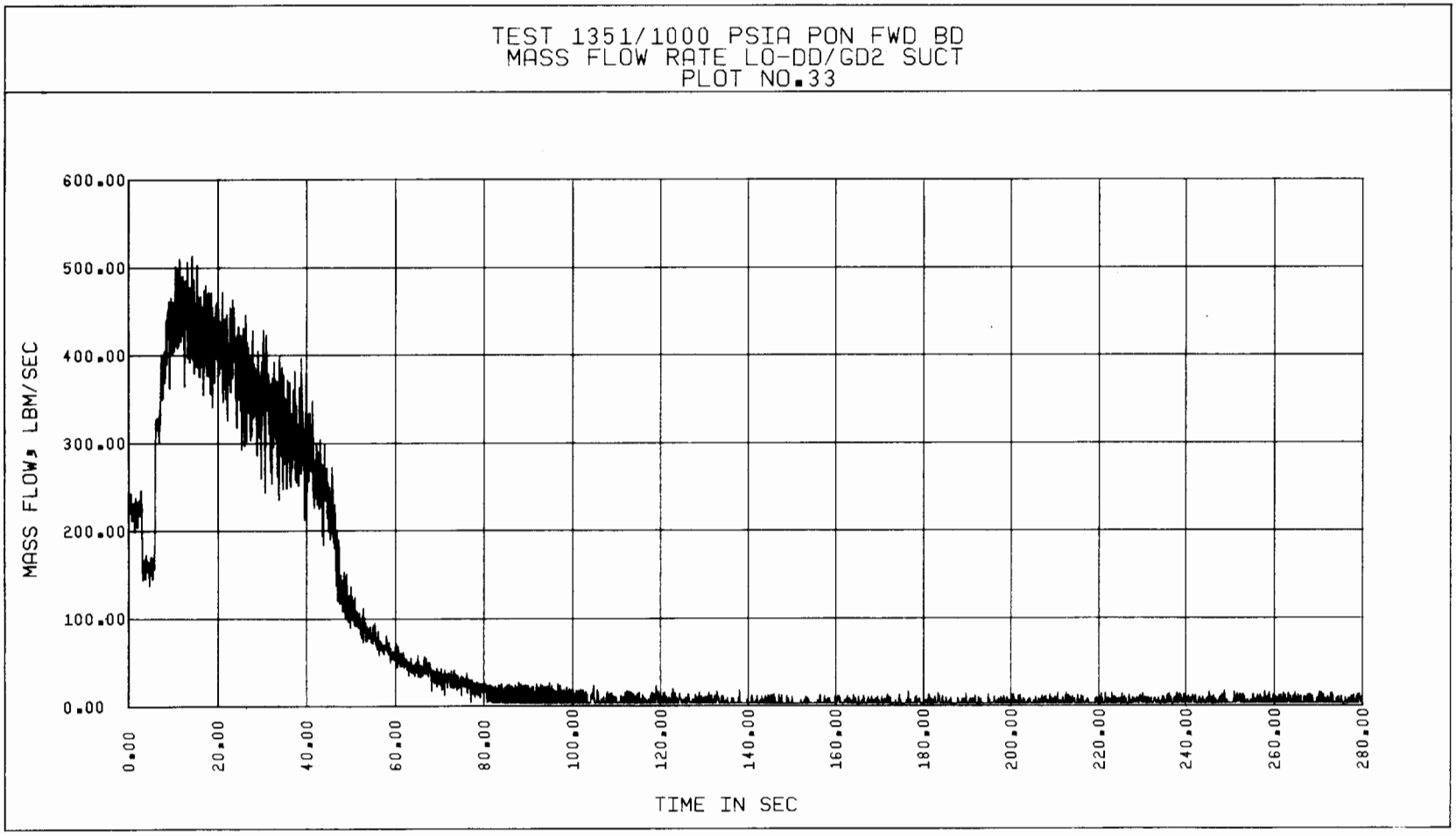

Figure 5-94. Test 1351, Suction Mass Flow Rate vs Time, Based on Gamma Densitometer and Low Drag Disc Data

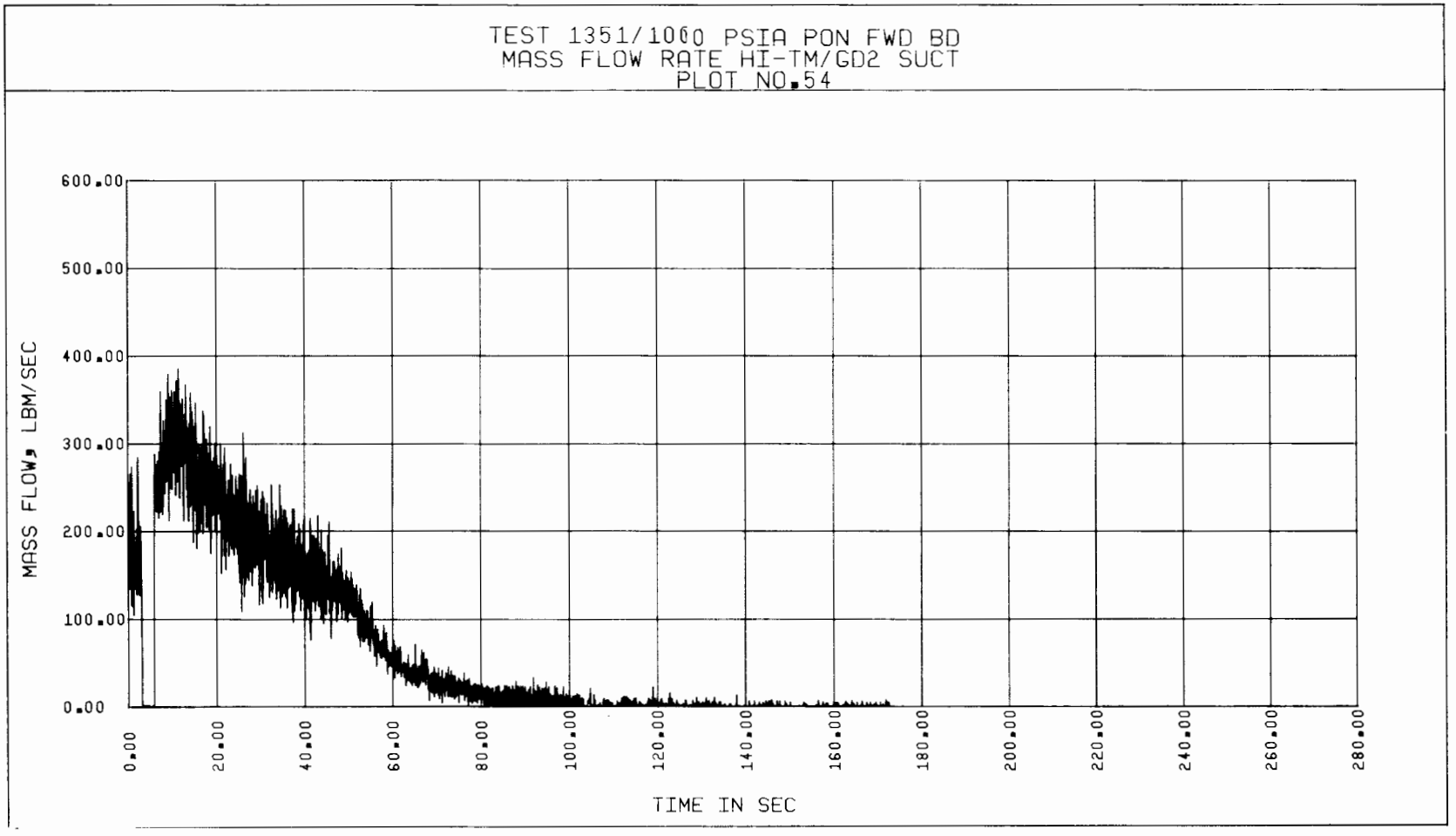

Figure 5-95. Test 1351, Suction Mass Flow Rate vs Time, Based on High Turbine Meter and Gamma Densitometer Data

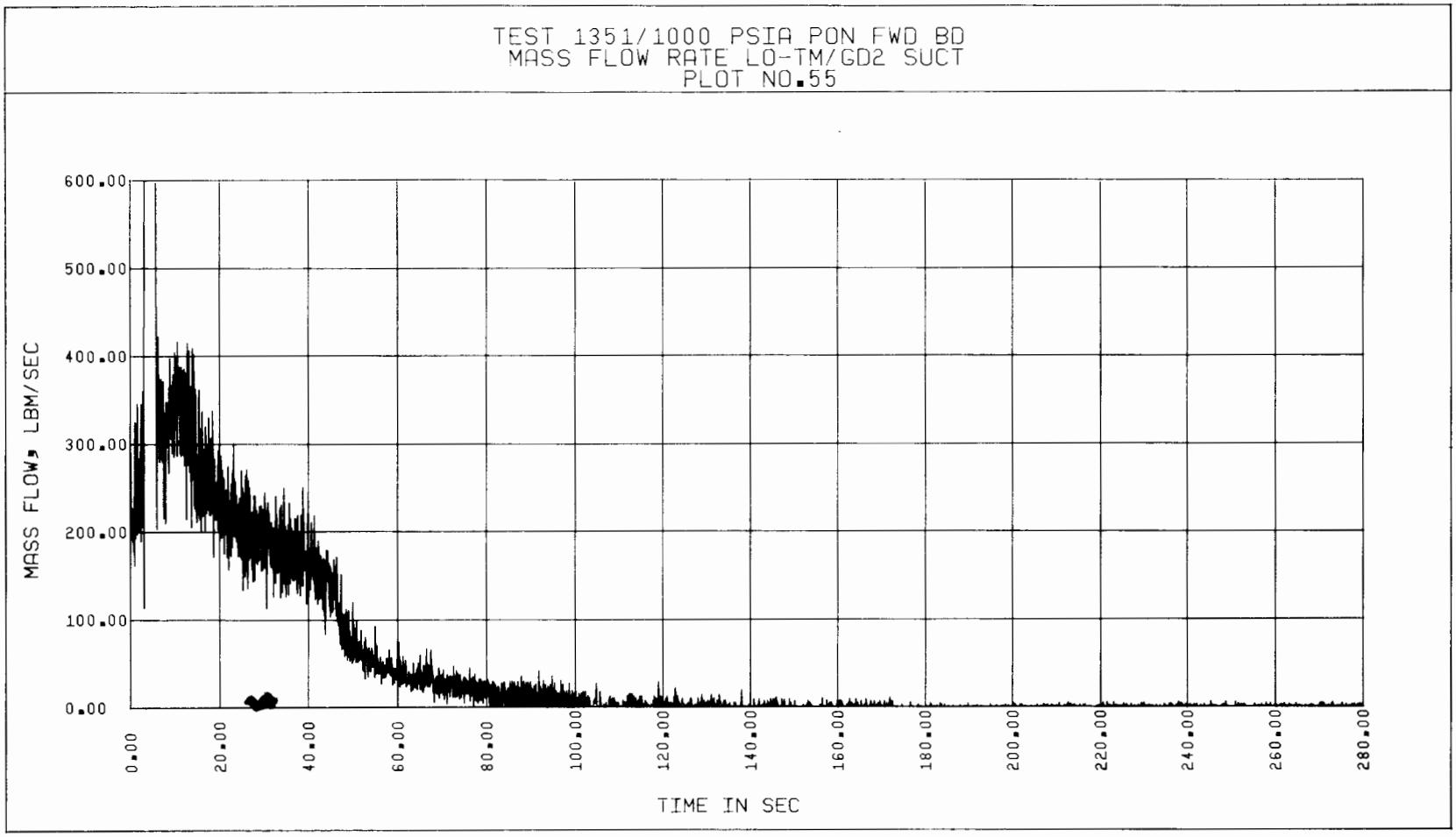

Figure 5-96. Test 1351, Suction Mass Flow Rate vs Time, Based on Gamma Densitometer and Low Turbine Meter Data

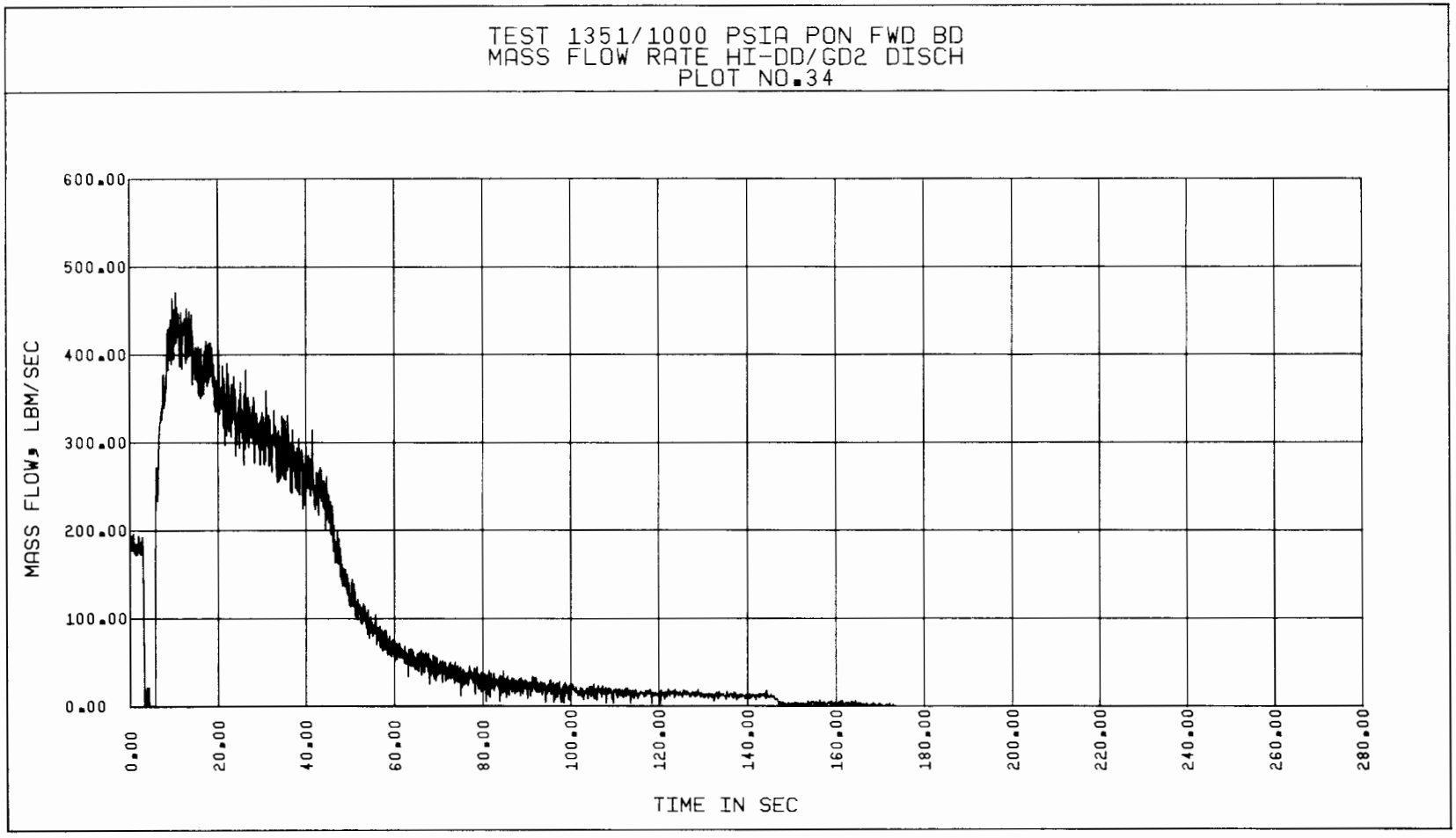

Figure 5-97. Test 1351, Discharge Mass Flow Rate vs Time, Based on Gamma Densitometer and High Drag Disc Data

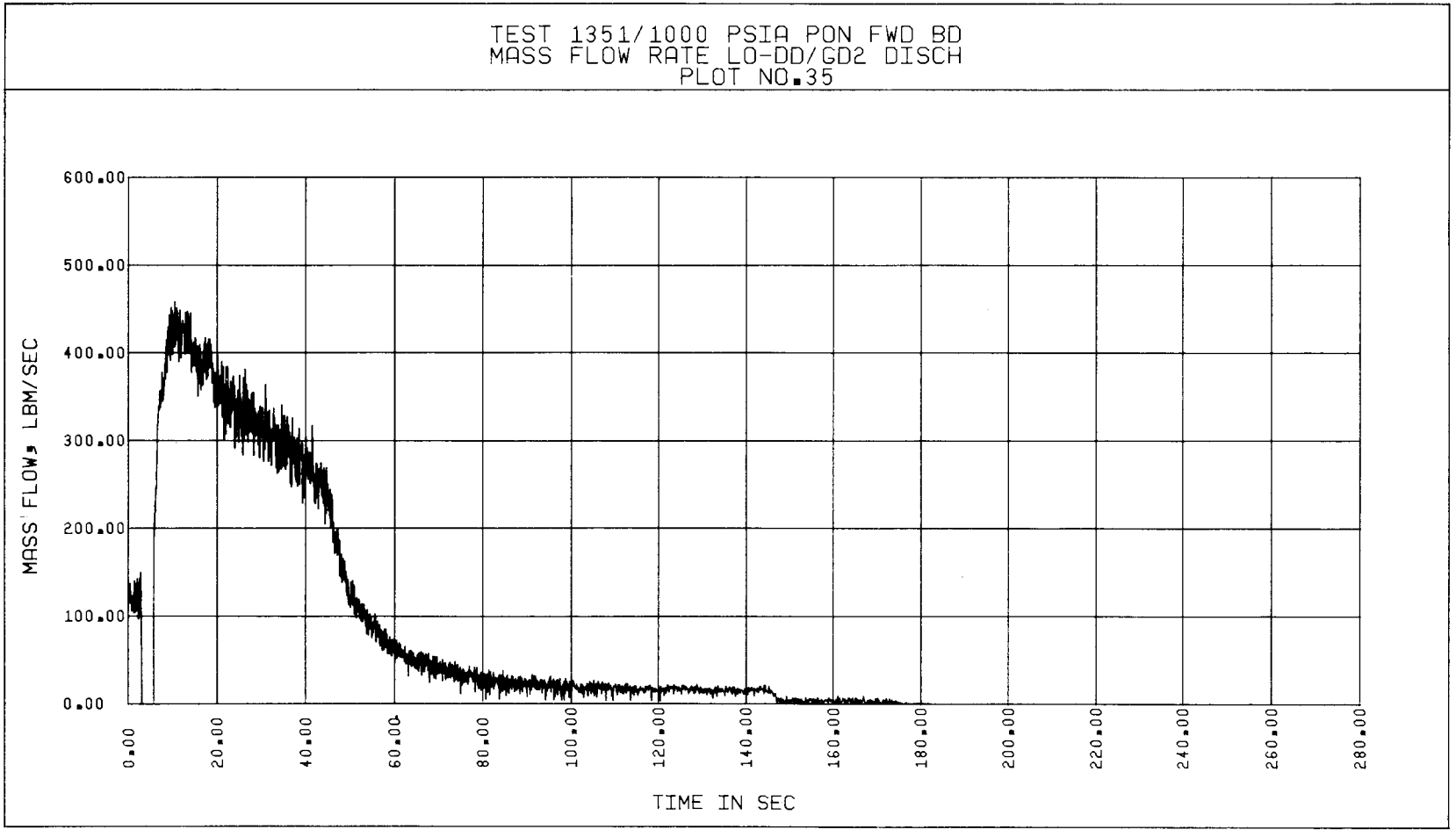

Figure 5-98. Test 1351, Discharge Mass Flow Rate vs Time, Based on Gamma Densitometer and Low Drag Disc Data

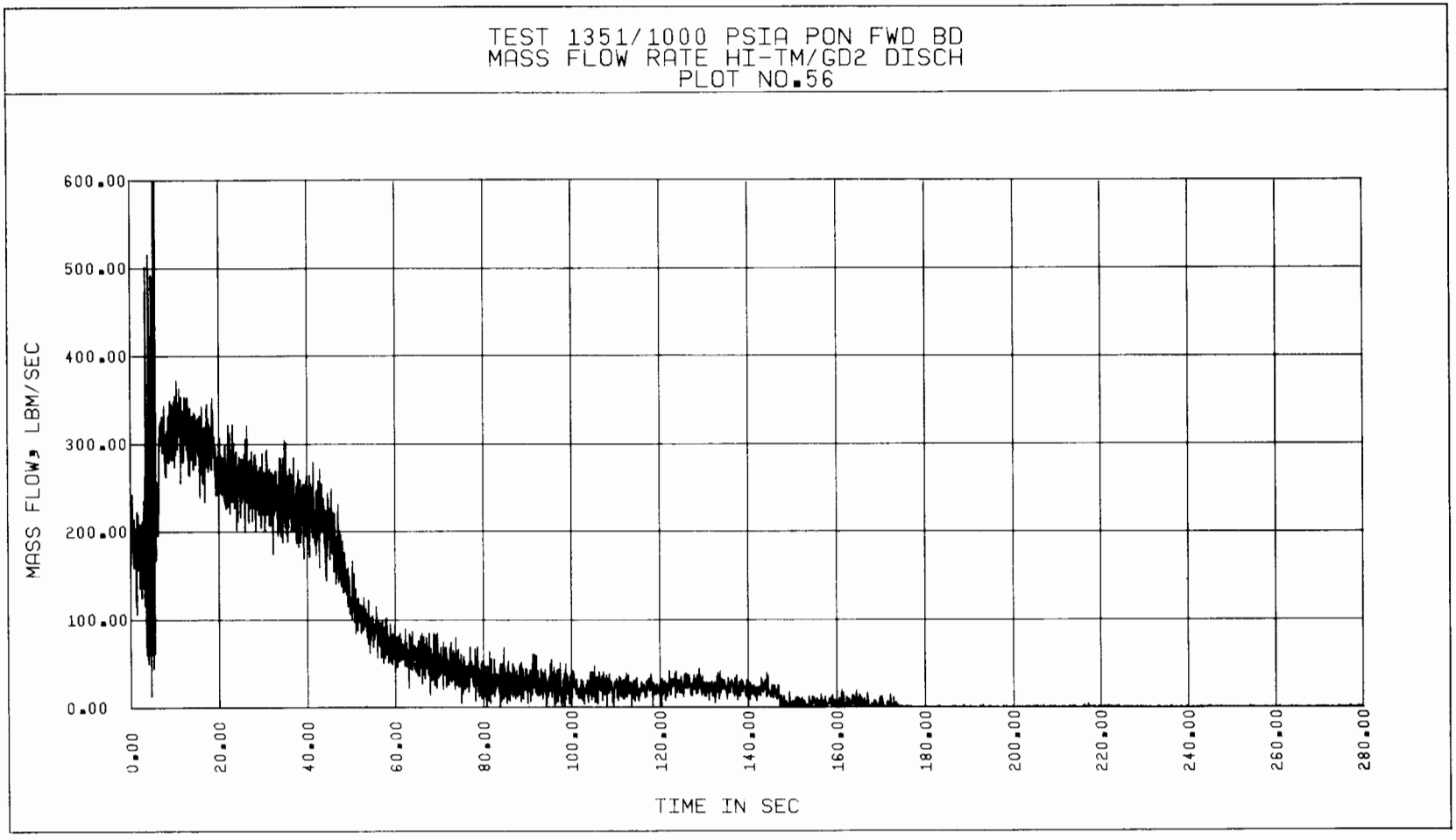

Figure 5-99. Test 1351, Discharge Mass Flow Rate vs Time, Based on Gamma Densitometer and High Turbine Meter Data

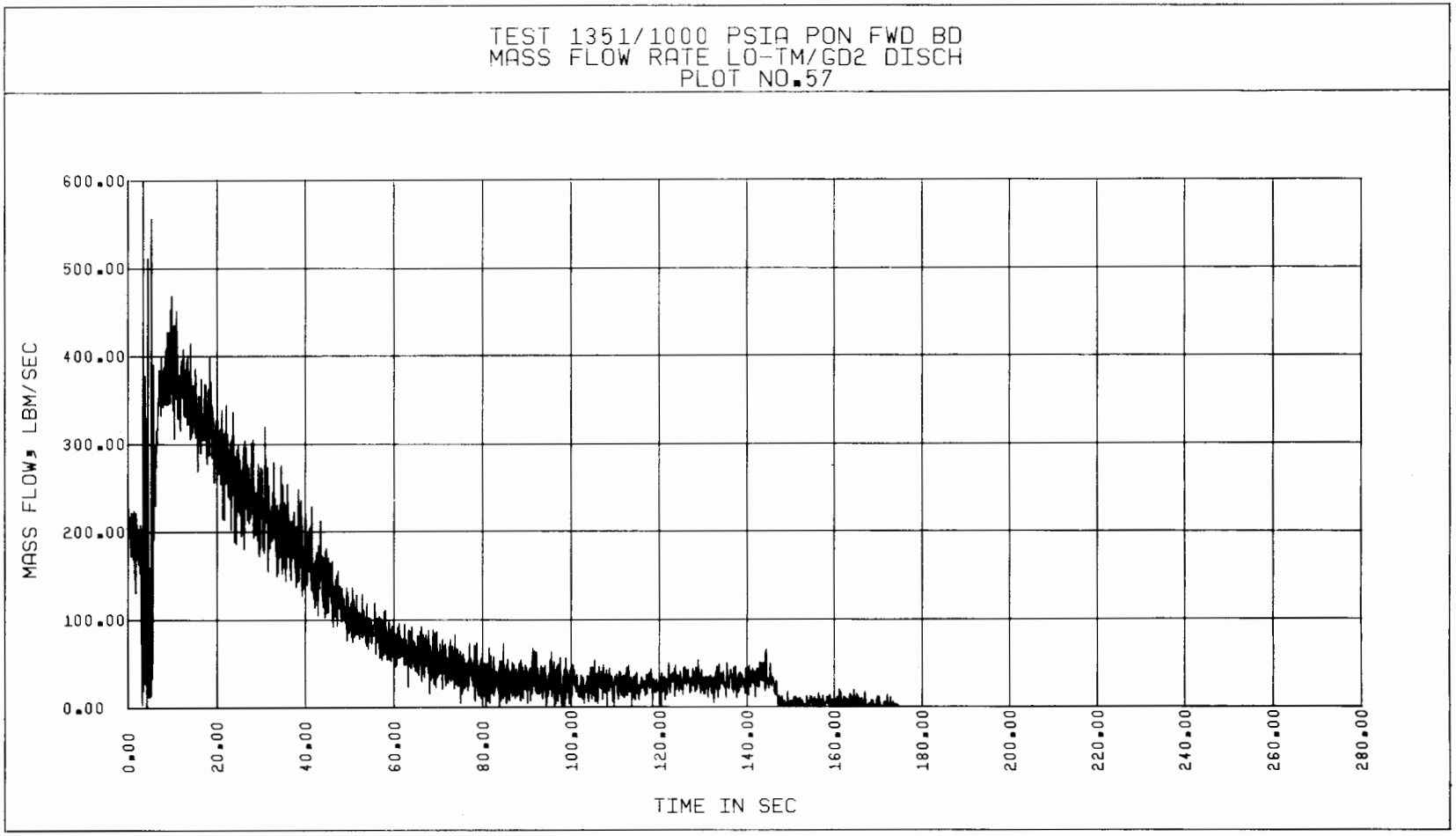

Figure 5-100. Test 1351, Discharge Mass Flow Rate vs Time, Based on Gamma Densitometer and Low Turbine Meter Data

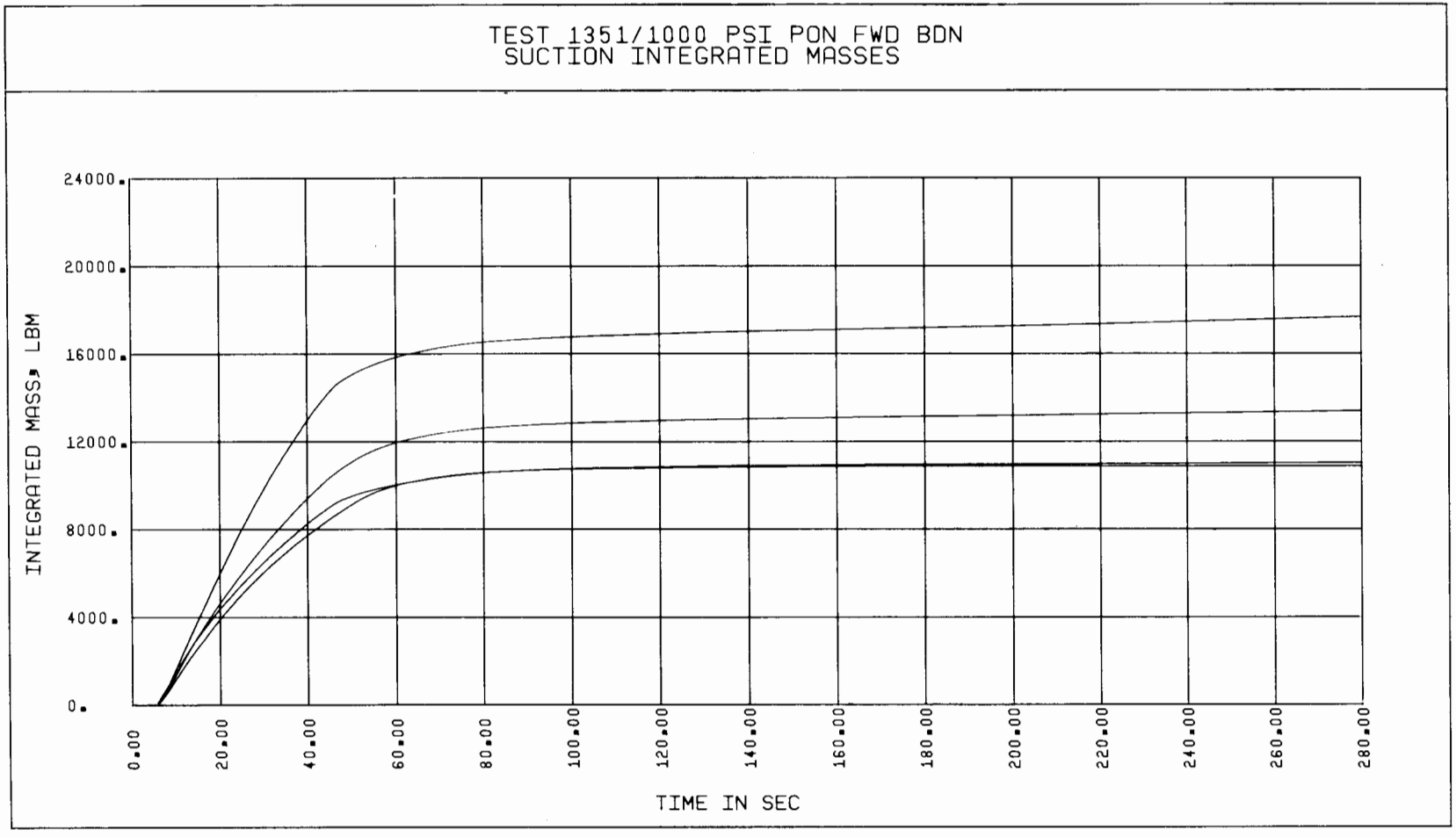

Figure 5-101. Test 1351, Suction Integrated Masses vs Time

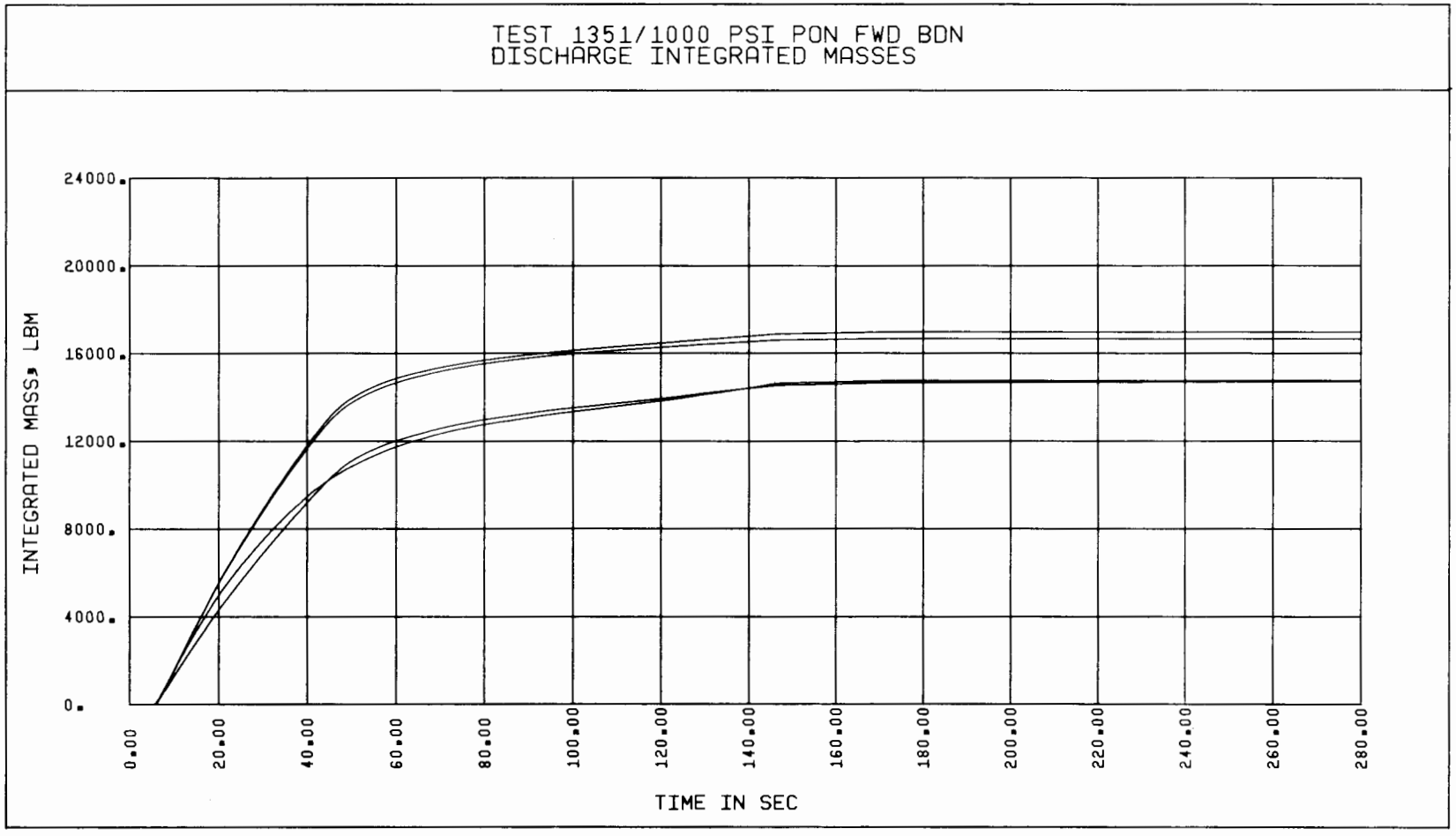

Figure 5-102. Test 1351, Discharge Integrated Masses vs Time

The SIS momentum flux values for Test 1351 as shown in Figure 5-89 and 5-90 are seen to be quite different. The peak value measured by the LO-DD is about twice as large as those measured by the HI-DD. Since the density distribution is uniform, this may imply a non-uniform velocity field at the SIS. The HI-DD indicates near-zero momentum flux values (within instrument uncertainty) after the blowdown is terminated. However, the LO-DD does not fully approach zero values at this time. Pre-blowdown calibrations indicated this drag disc to have a large uncertainty which may be partially responsible for the large deviations from the zero value. Averaged parameter curves were then generated as shown in Figure 5-103 through 5-112. On the average mass flow rate curves, the mass balance test of Step 4 was applied. It is seen that the average mass flow rate curves generated for the DD-GD combination (see Figure 5-107 and 5-109) differ only by a small amount of mass flow rate. This difference is attributed to the seal injection leakage flow into the pump (see Figure 5-36 and 5-37). Comparison of the average mass flow rate curves generated for the TM-GD combination shows larger differences between the two curves (See Figure 5-108 and 5-110). These differences are not explainable by the small amounts of seal injection leakage (Figures 5-36 and 5-37), and hence these curves fail the mass balance test.

In order to perform the mass flow integral test of Step 5, the time period to be considered is the duration from rupture time to about 170 seconds after rupture. The choice of the final time of 170 seconds was not completely arbitrary. By this time most of the loop piping became voided of liquid, and the fluid density reached substantially lower values. The errors in estimating the mass of the low density fluid in the loop piping are considered small, and hence the choice of this time value. Note also that the blowdown isolation valve (HPSW-2) was closed at about 173 seconds.

In order to identify the sections of the loop piping from which the fluid can flow through the measuring sections during the transient, the loop schematic of Figure 5-113 is employed. It is seen that the mass of fluid in the piping between the return line throttle valve and the drum, in the high pressure drum, and in the piping between the drum and the SIS can flow through the SIS during the blowdown. For the DIS, the additional mass of fluid between the SIS and DIS should be considered. The initial and final masses are calculated from the appropriate loop volumes indicated above, and from the fluid densities

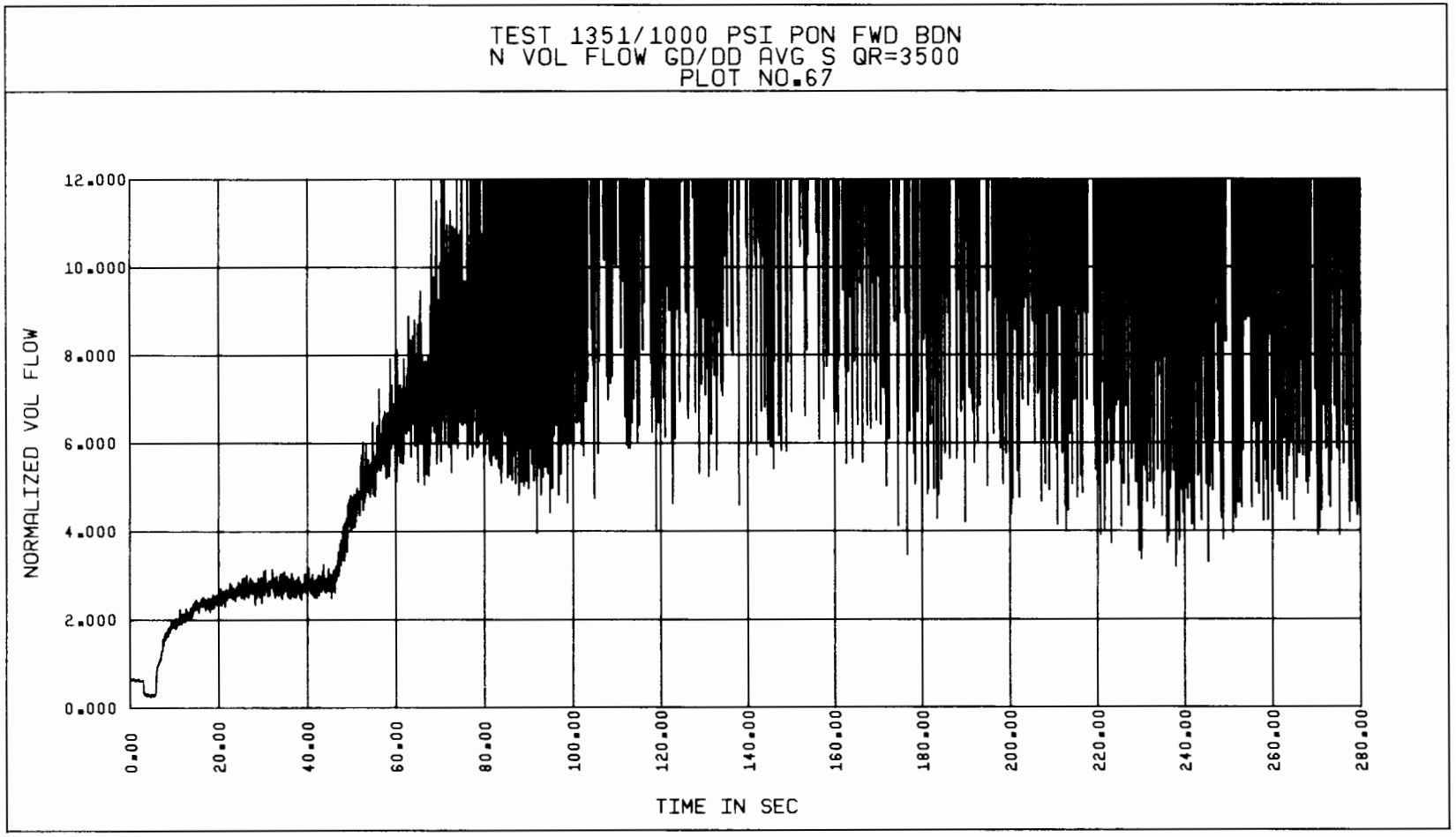

Figure 5-103. Test 1351, Normalized Suction Volumetric Flow Rate vs Time, Based on Gamma Densitometer and Average Drag Disc Data

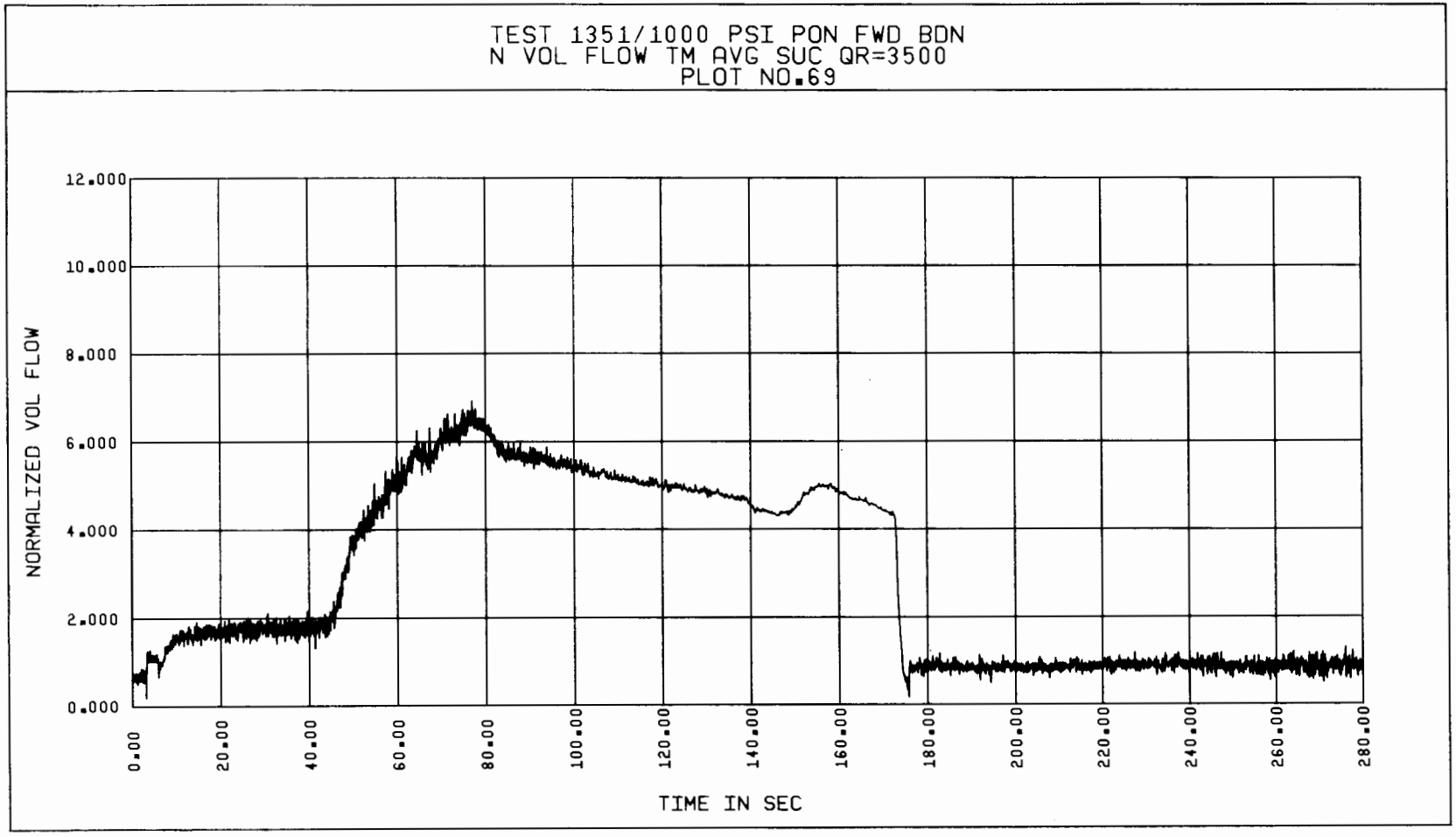

Figure 5-104. Test 1351, Normalized Suction Volumetric Flow Rate vs Time, Based on Average Turbine Meter Data

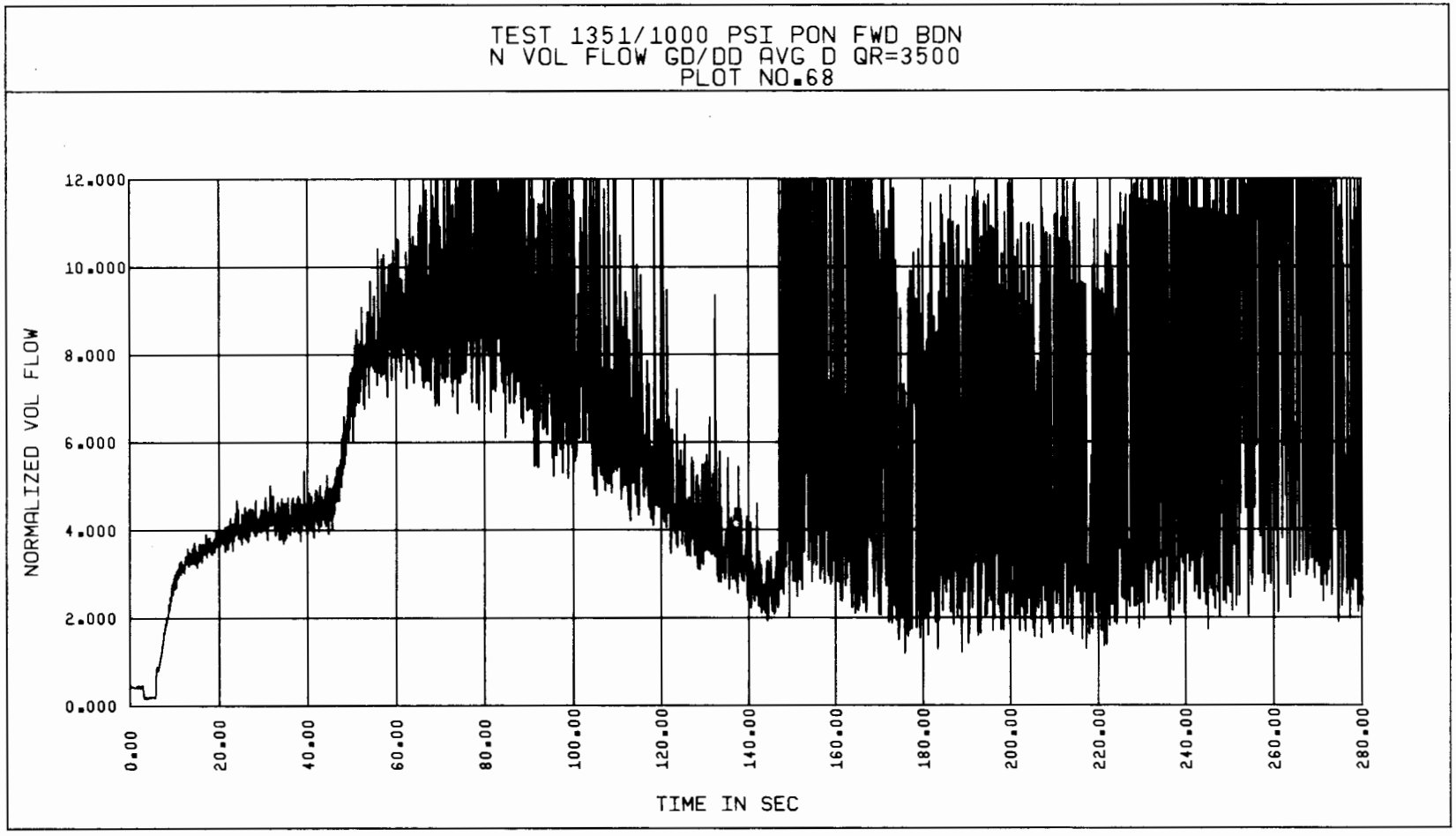

Figure 5-105. Test 1351, Normalized Discharge Volumetric Flow Rate vs Time, Based on Gamma Densitometer and Average Drag Disc Data

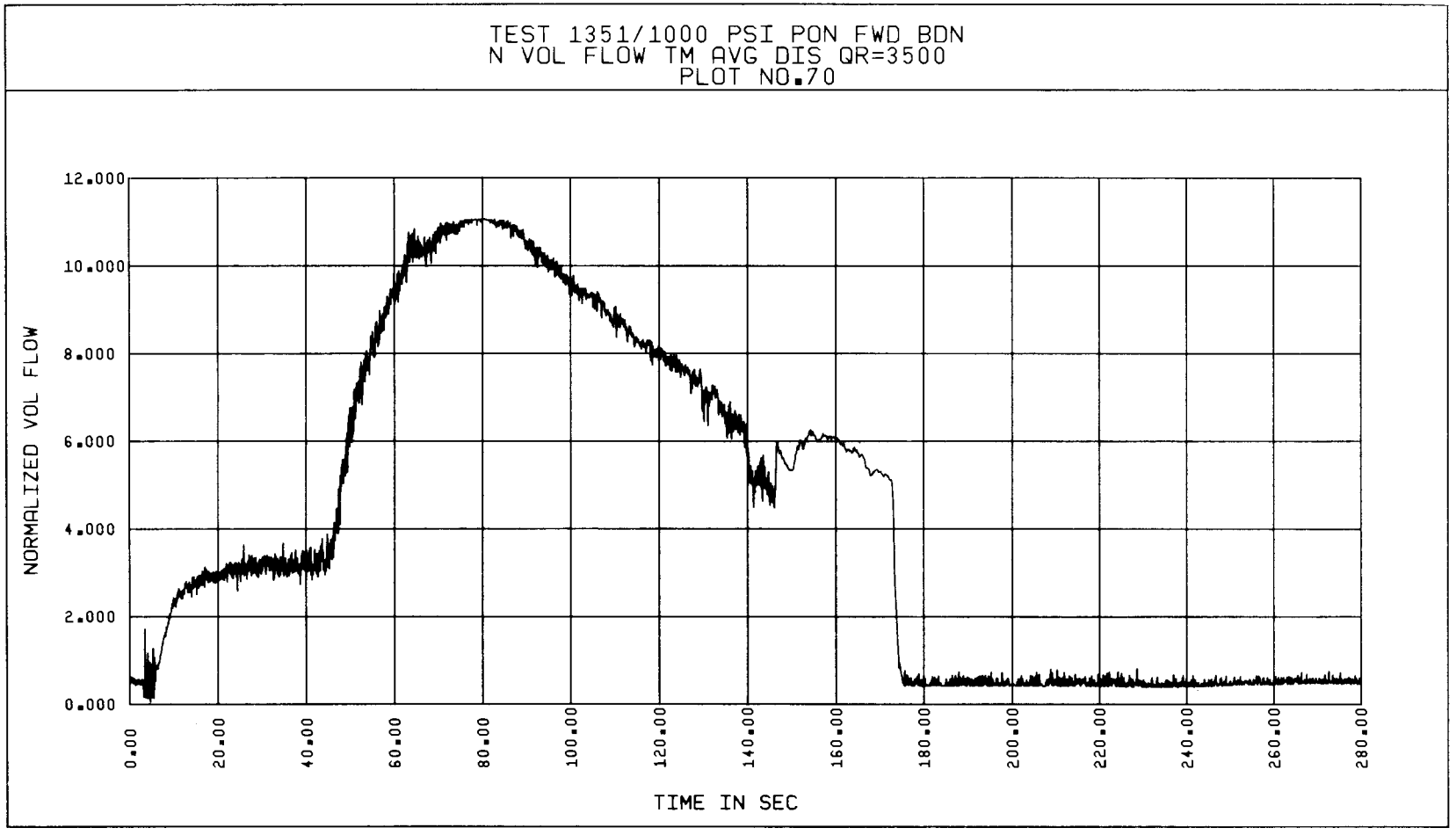

Figure 5-106. Test 1351, Normalized Discharge Volumetric Flow Rate vs Time, Based on Average Turbine Meter Data

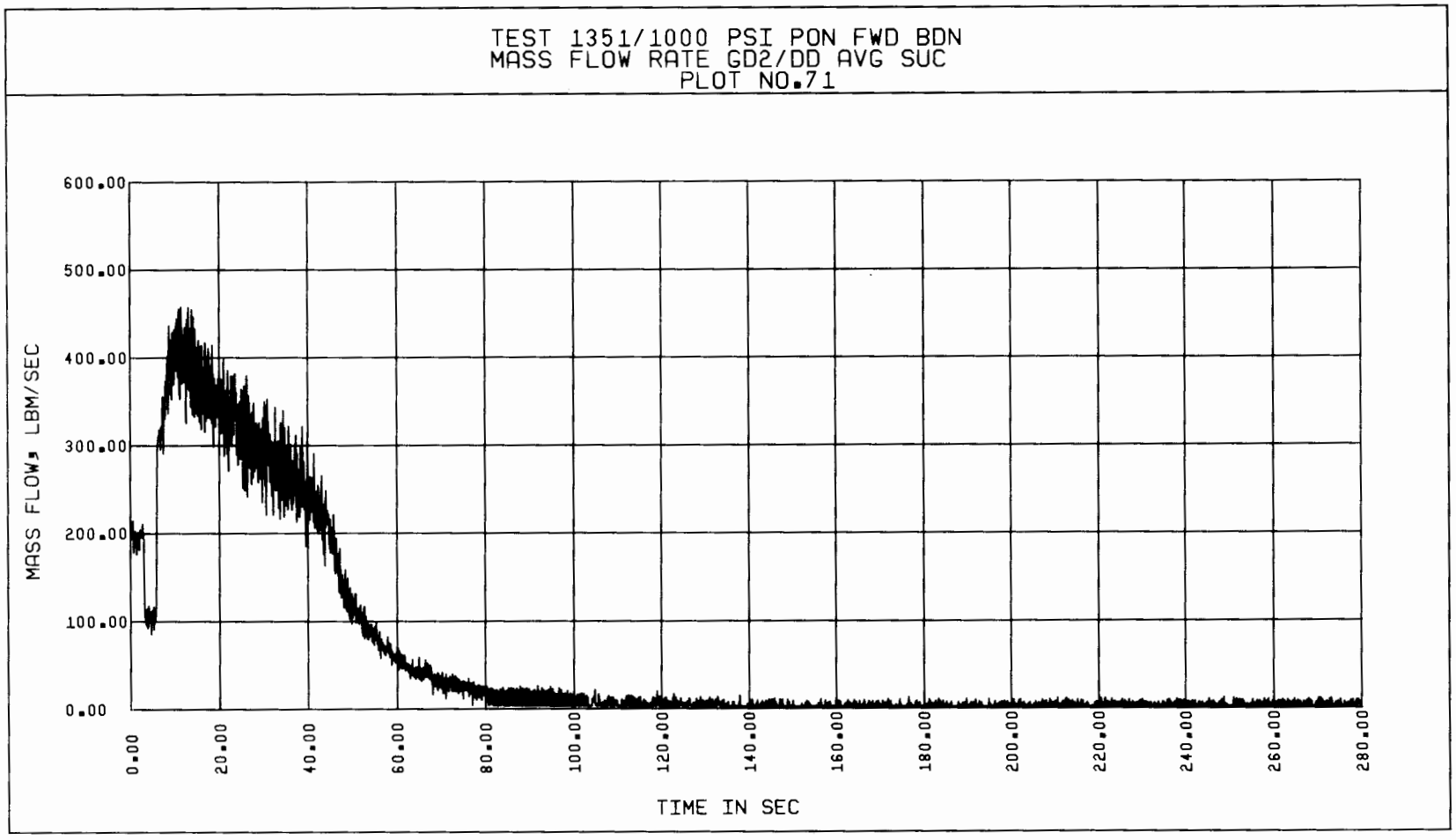

Figure 5-107. Test 1351, Suction Mass Flow Rate vs Time, Based on Gamma Densitometer and Average Drag Disc Data

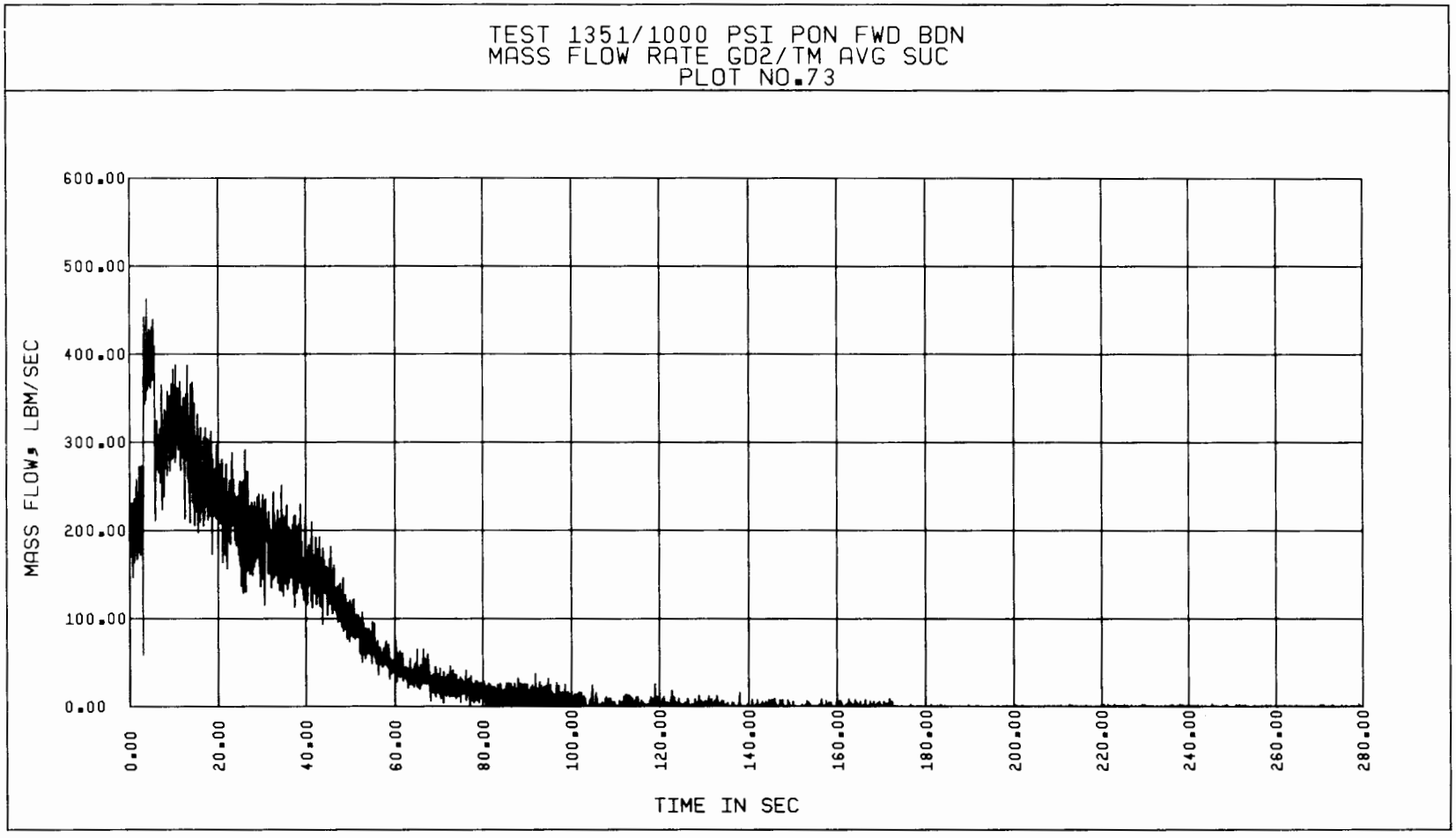

Figure 5-108. Test 1351, Suction Mass Flow Rate vs Time, Based on Gamma Densitometer and Average Turbine Meter Data

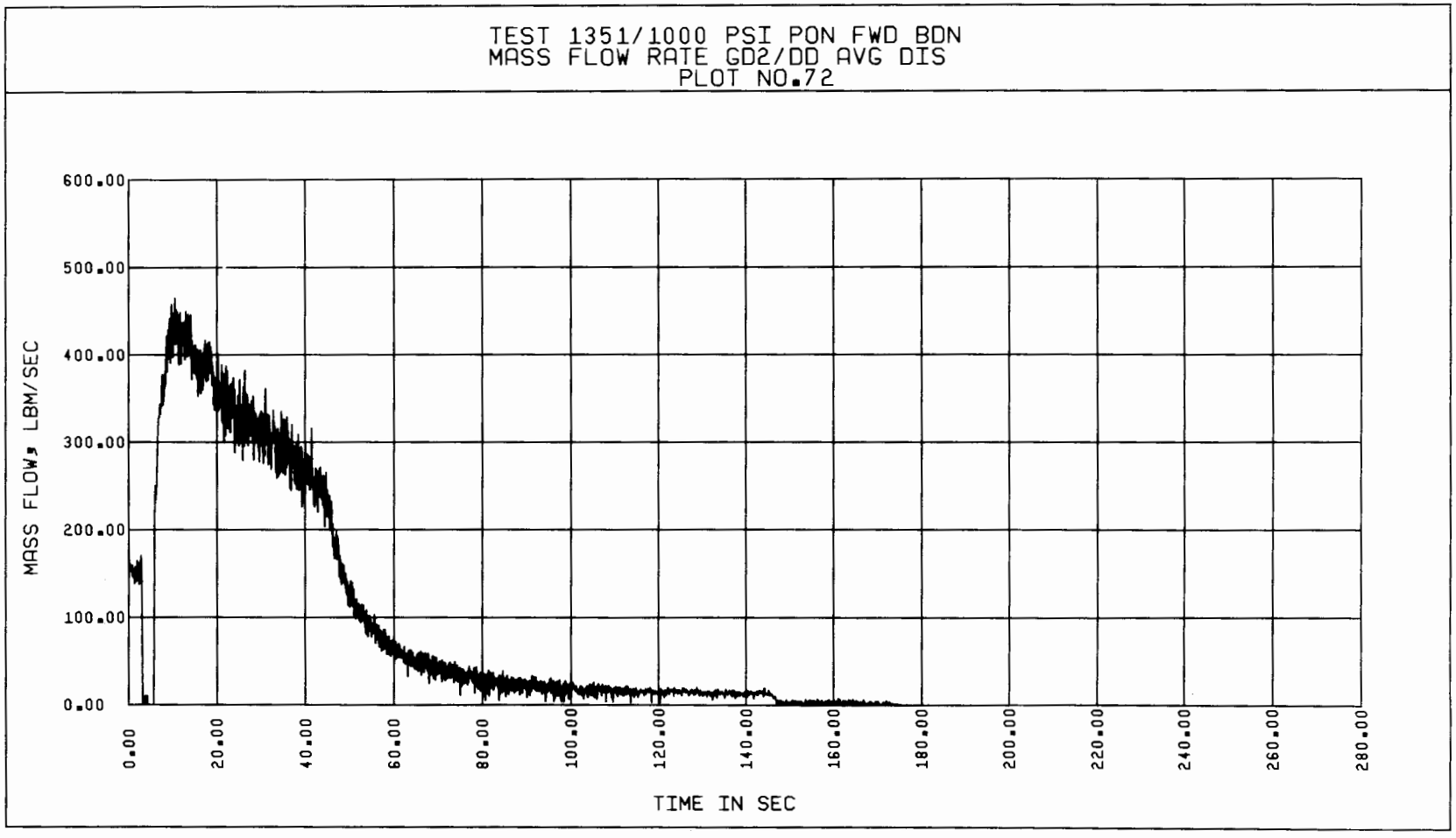

Figure 5-109. Test 1351, Discharge Mass Flow Rate vs Time, Based on Gamma Densitometer and Average Drag Disc Data

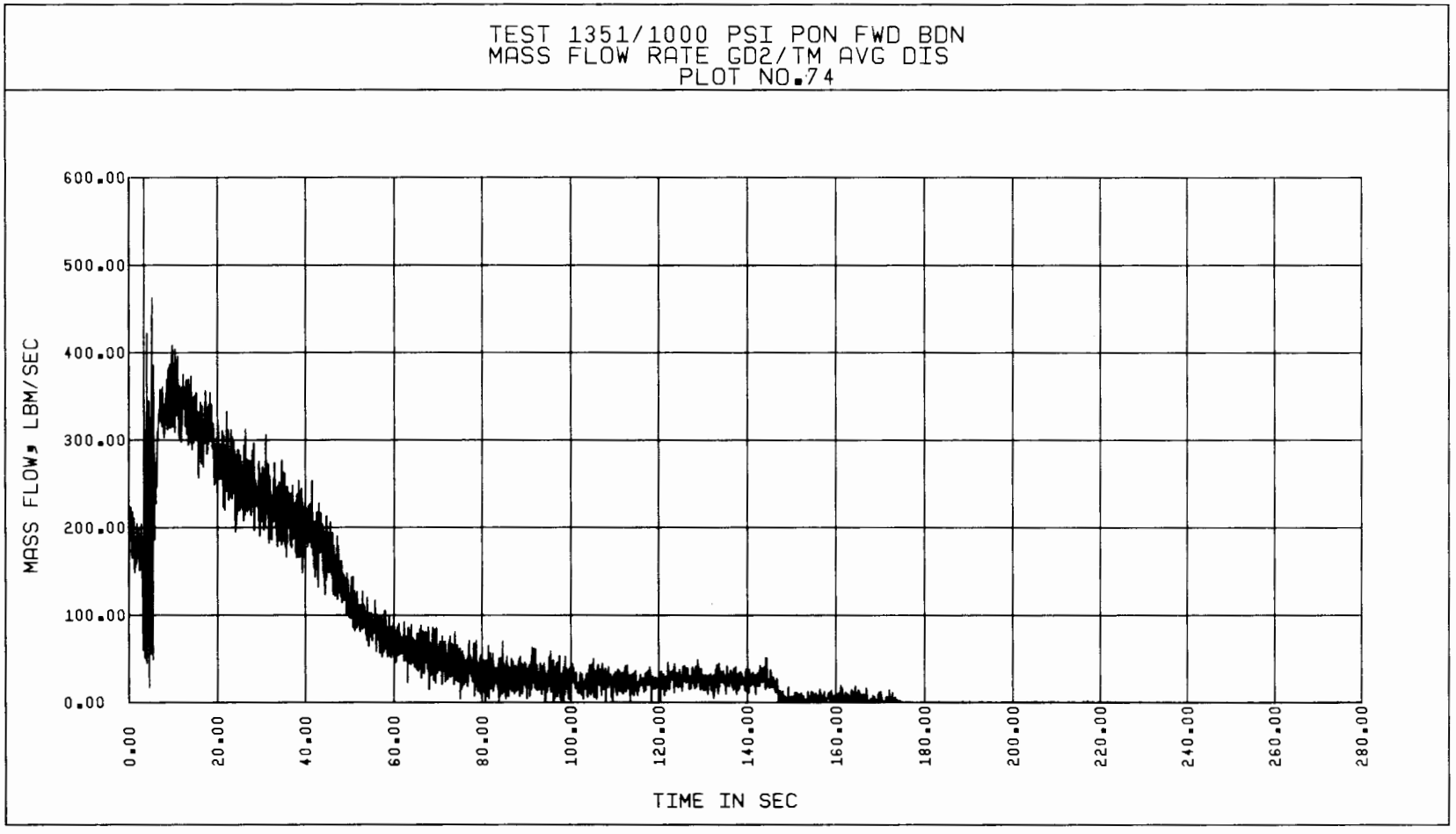

Figure 5-110. Test 1351, Discharge Mass Flow Rate vs Time, Based on Gamma Densitometer and Average Turbine Meter Data

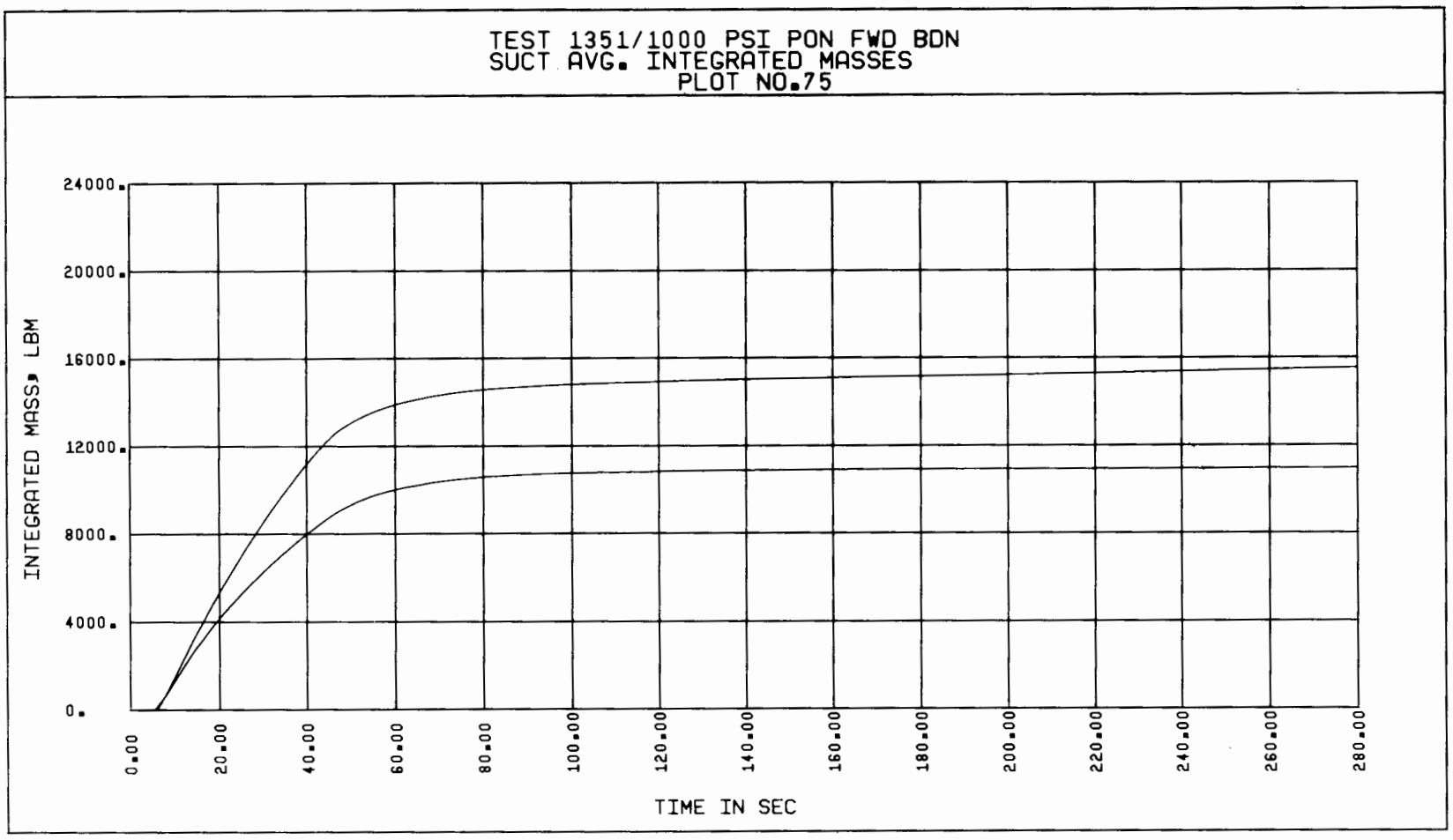

Figure 5-111. Test 1351, Average Suction Integrated Masses vs Time

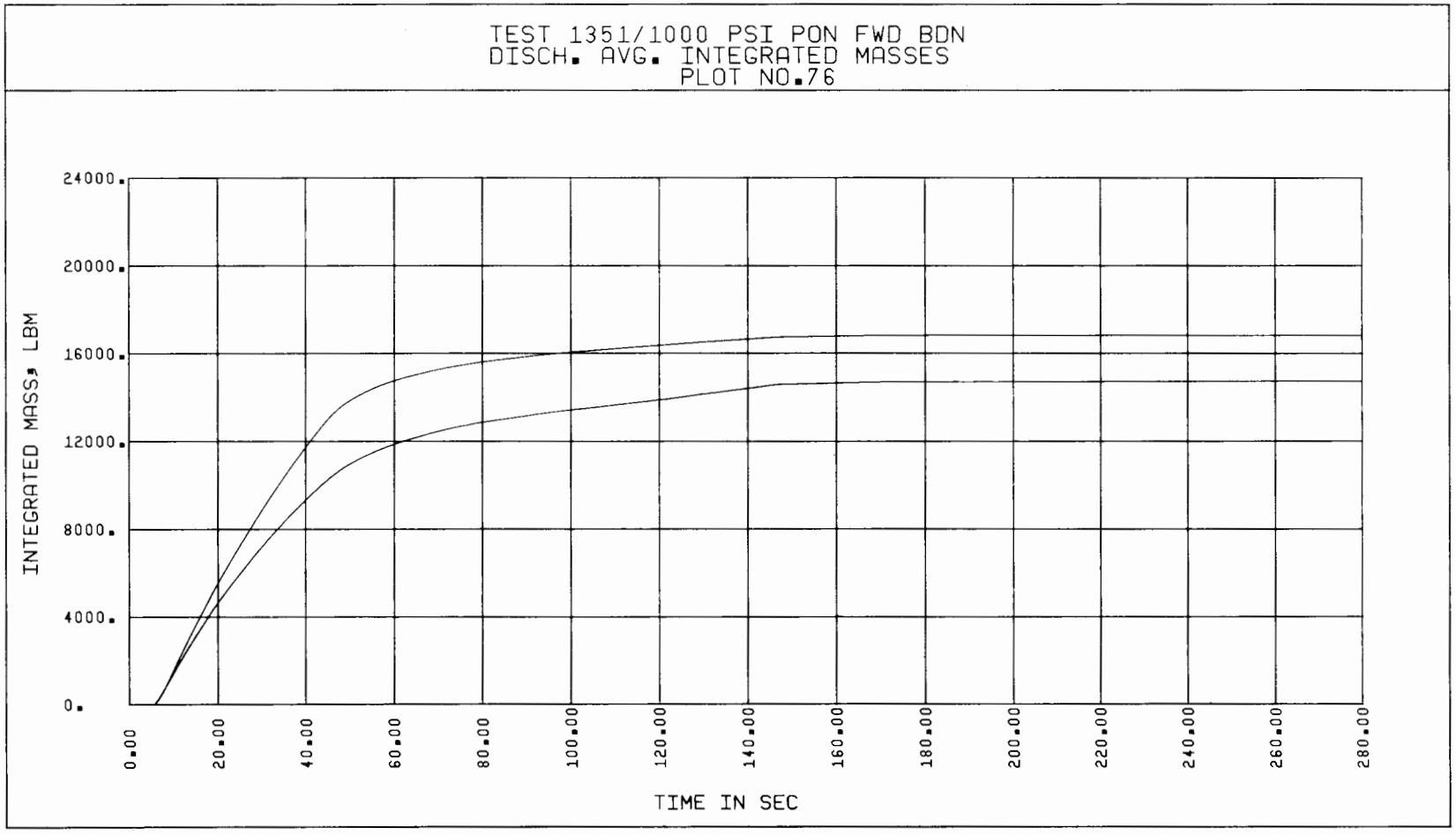

Figure 5-112. Test 1351, Average Discharge Integrated Masses vs Time

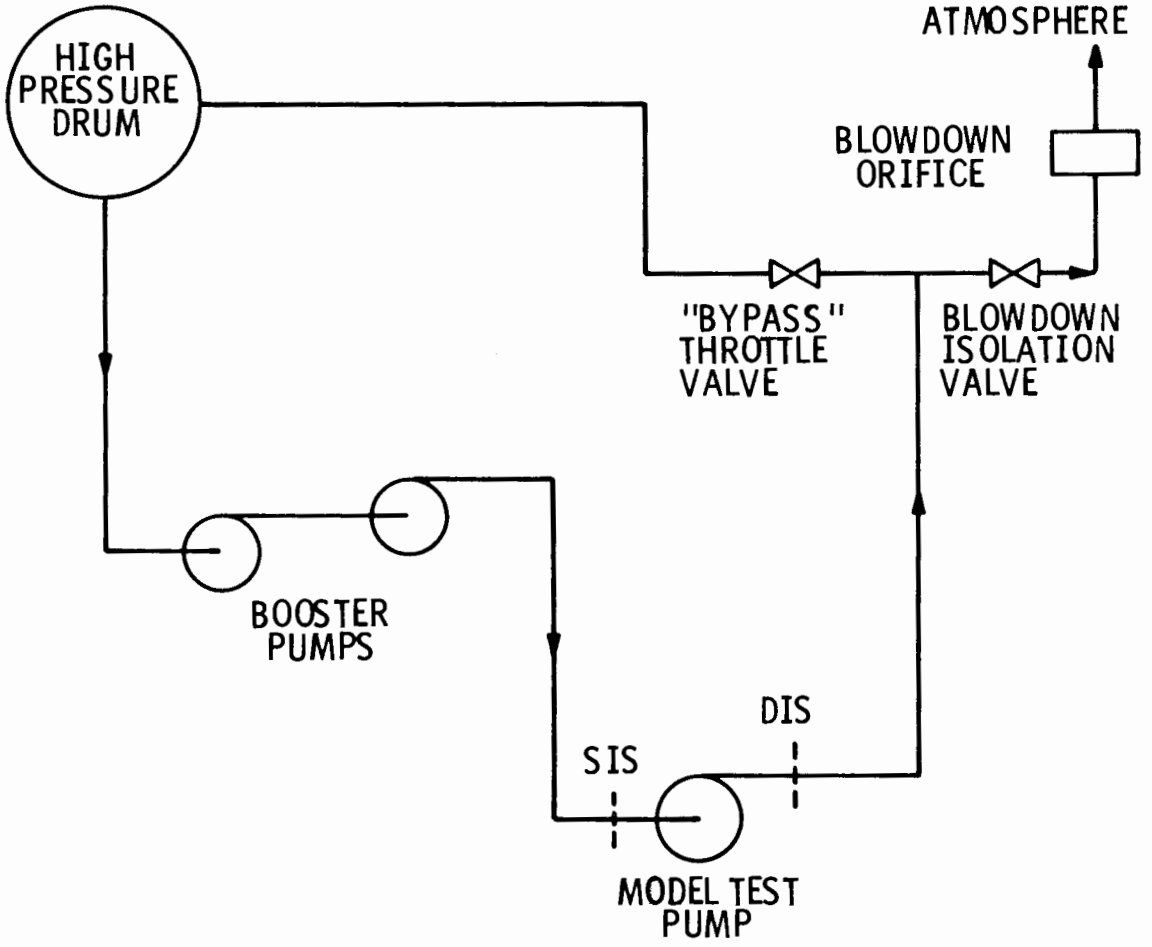

Figure 5-113. Idealized Schematic Diagram of Test System For Forward Flow Blowdown Tests

at the start of the blowdown and at 170 seconds into the blowdown. From these calculations (See Appendix A), the net mass flow through the SIS during the chosen time period considered turns out to be 13,800 lbm, and through the DIS during the same time period is calculated to be 14,240 lbm.

Examination of the averaged integrated masses of Figures 5-107 and 5-108 indicates that the SIS integrated mass at 180 seconds (plot time) is 15,133 lbm for the DD's and 10,933 lbm for the TM's, and the DIS integrated mass at the same time is 16,800 lbm for the DD's and 14,700 lbm for the TM's. These mass flow integral values are presented in Table 5-1 along with the computed values for the SIS and DIS. For the DD's at SIS, the error in the final integrated mass is less than 10 percent. For the TM's at DIS the error in the same parameter is similarly low. However for the other instruments at SIS and DIS, the errors are approximately 20 percent. Consequently, for the SIS, the average DD measurements are considered preferable to the average TM data. The averaged volumetric flow rate is derived from the average DD ρV^2 and GD ρ. However, due to fluctuations in the GD density, uncertainty in the GD-DD volumetric flow rate increases significantly as the density approaches steam values. As a result the GD-DD volumetric flow rate cannot be used after about 60 seconds into the blowdown. At that time the TM volumetric flow rate may have to be employed.

Test 1319 was a 100% break size, free-wheeling, forward flow blowdown test. Rupture of the diaphragms took place at about 5.7 seconds in the plots, and the blowdown was terminated at about 58.7 seconds due to the safety limit on the pump rotor speed. As seen from the speed and flow traces of Figures 5-114 and 5-115, the three distinct time periods -- initial surge, quasi-steady state time period, and the second surge -- discussed in Section 5.2 are also observable for this test. The blowdown was terminated during the second surge at the overspeed limit (2.3 x rated) by closing the blowdown isolation valve (HPSW-2). Subsequently the suction and discharge pressures slightly increased due to flow stagnation for a short period of time. Later on, as the fluid began to cool and condense, the pressures decreased slowly and the densities of the fluid at the SIS and DIS became larger. The seal injection leakage of cold water at the test pump was also responsible for increasing the densities at the measuring sections. The blowdown isolation valve was re-opened at about 246 seconds and fluid flowed out of the loop again. At the SIS, the

Table 5-1

Comparison of Mass Flow Integrals for Test 1351
at 175 Seconds

Data Used in Integral	Measurement Location	Mass Flow Integral (lbm)
Avg TM-GD	SIS	10,930
Avg DD-GD	SIS	15,130
Avg TM-GD	DIS	14,700
Avg DD-GD	DIS	16,800
Piping inventory	SIS	13,800
Piping inventory	DIS	14,240

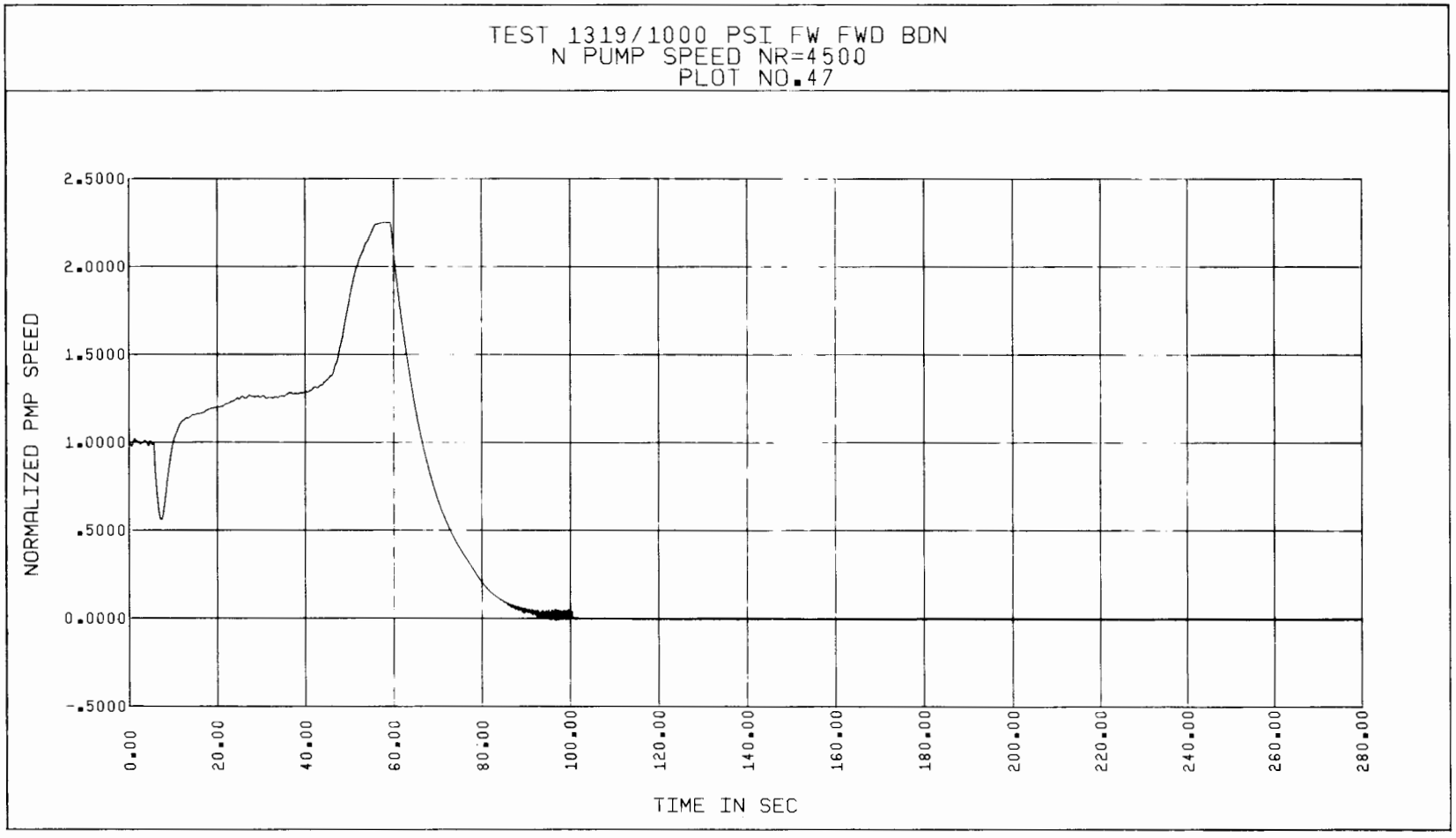

Figure 5-114. Test 1319, Normalized Pump Speed vs Time

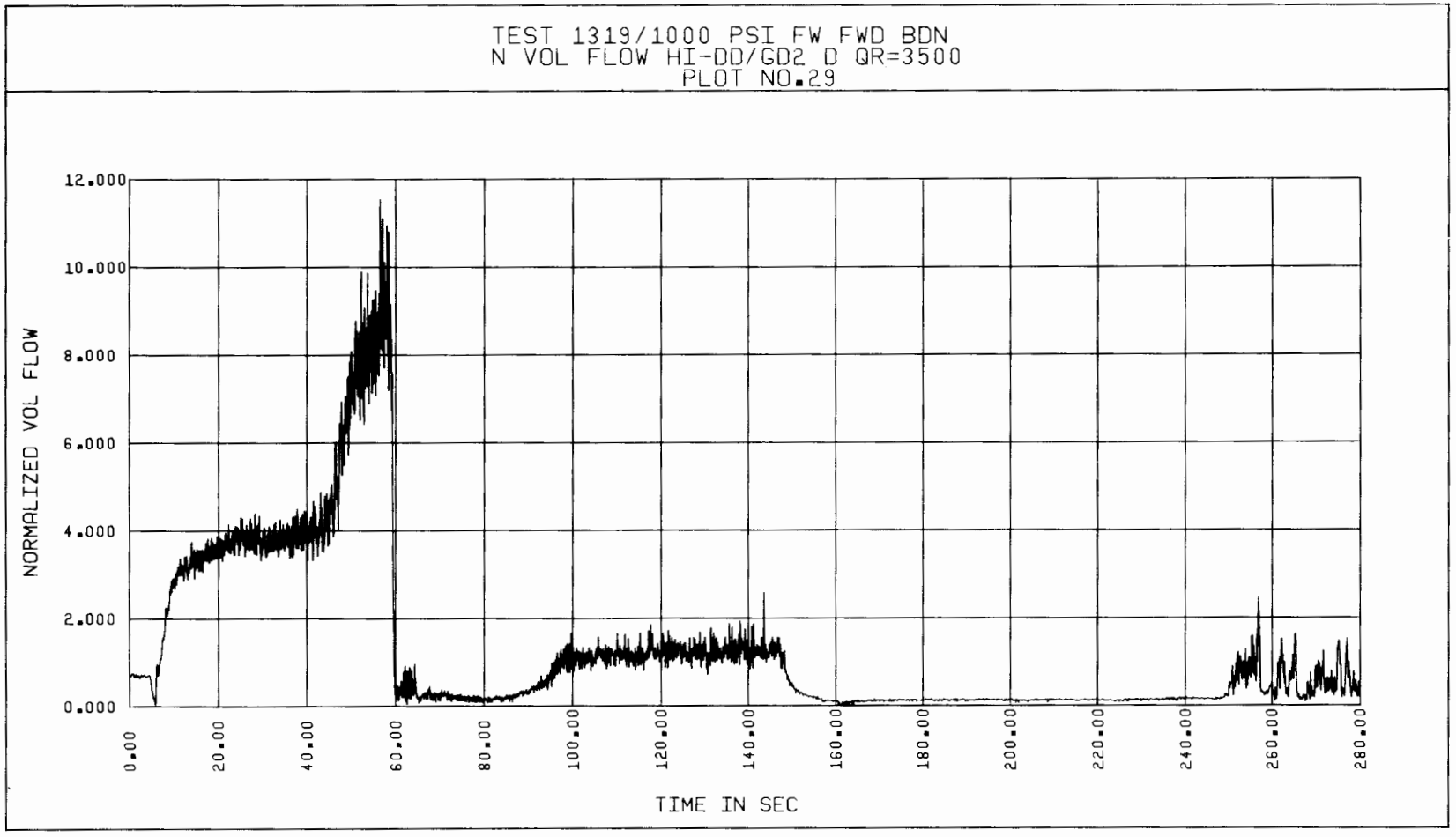

Figure 5-115. Test 1319, Normalized Discharge Volumetric Flow Rate vs Time, Based on Gamma Densitometer and High Drag Disc Data

density distribution was essentially uniform (see Figure 5-116 thru 5-118). At the DIS, the density distribution may also considered more uniform, if beam 3 measurement is disregarded (see Figure 5-119).

The volumetric flow rate, momentum flux, mass flow rate, and the integrated mass curves generated per step 1 for Test 1319 are presented in Figures 5-120 thru 5-141. The volumetric flow rates indicated by the SIS TM's are uniform up to about 45 seconds. Afterwards, the HI-TM shows larger volumetric flow rates than the LO-TM. Furthermore, the LO-TM exhibits an atypical behavior for this rate curve (a straight line shape instead of a concave shape exhibited by all other flow measuring instruments for the second surge). The SIS momentum fluxes as indicated in Figures 5-128 and 5-129 are seen to be quite different. The LO-DD shows significantly larger values for the momentum flux initially, and lower values finally (during the second surge) in comparison to the values indicated by the HI-DD. This may imply a non-uniform velocity field, if the density distribution is uniform. Both drag discs indicate non-zero momentum flux values (positive and negative) during the fluid stagnation time period after HPSW-2 is closed. This may be due to small flow rates induced by residual eddies or the density gradients at the measuring sections and/or instrument uncertainties.

In Figures 5-142 thru 5-151 the averaged flow parameter curves are shown. Application of the mass balance test of step 4 on the average mass flow rate curves generated for the DD-GD combination (see Figures 5-146 and 5-148) indicates that, the suction and discharge mass flow rates differ only by a small amount. Again, this difference is thought to be due to the seal injection leakage flow into the pump (see Figures 5-152 and 5-153). Comparison of the average mass flow rate curves generated for the TM-GD combination shows larger differences between the SIS and DIS curves (see Figures 5-147 and 5-149). These differences are seen to be larger than are explainable by the seal injection leakage flow. As before, these curves fail the mass balance test.

To perform the "mass flow integral test" of step 5, the time period available is between rupture time and approximately 53 seconds later (58.7 seconds plot time). The short duration of this time period is due to the fact that the blowdown was terminated at about 53 seconds after rupture. By this time, the fluid has not reached the 100% void fraction condition, and the fluid density

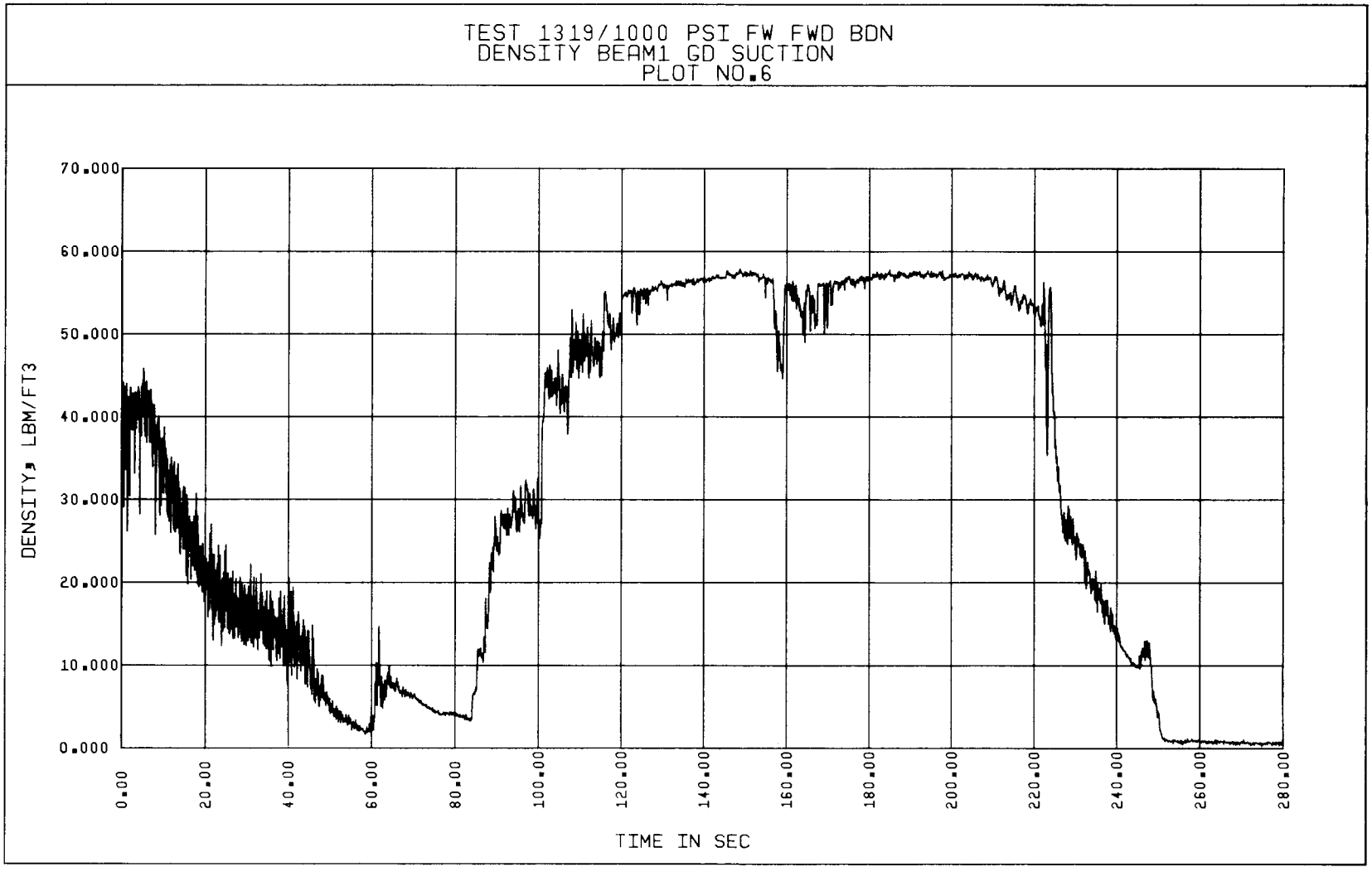

Figure 5-116. Test 1319, Suction Density vs Time, Based on Gamma Densitometer Beam 1 Data

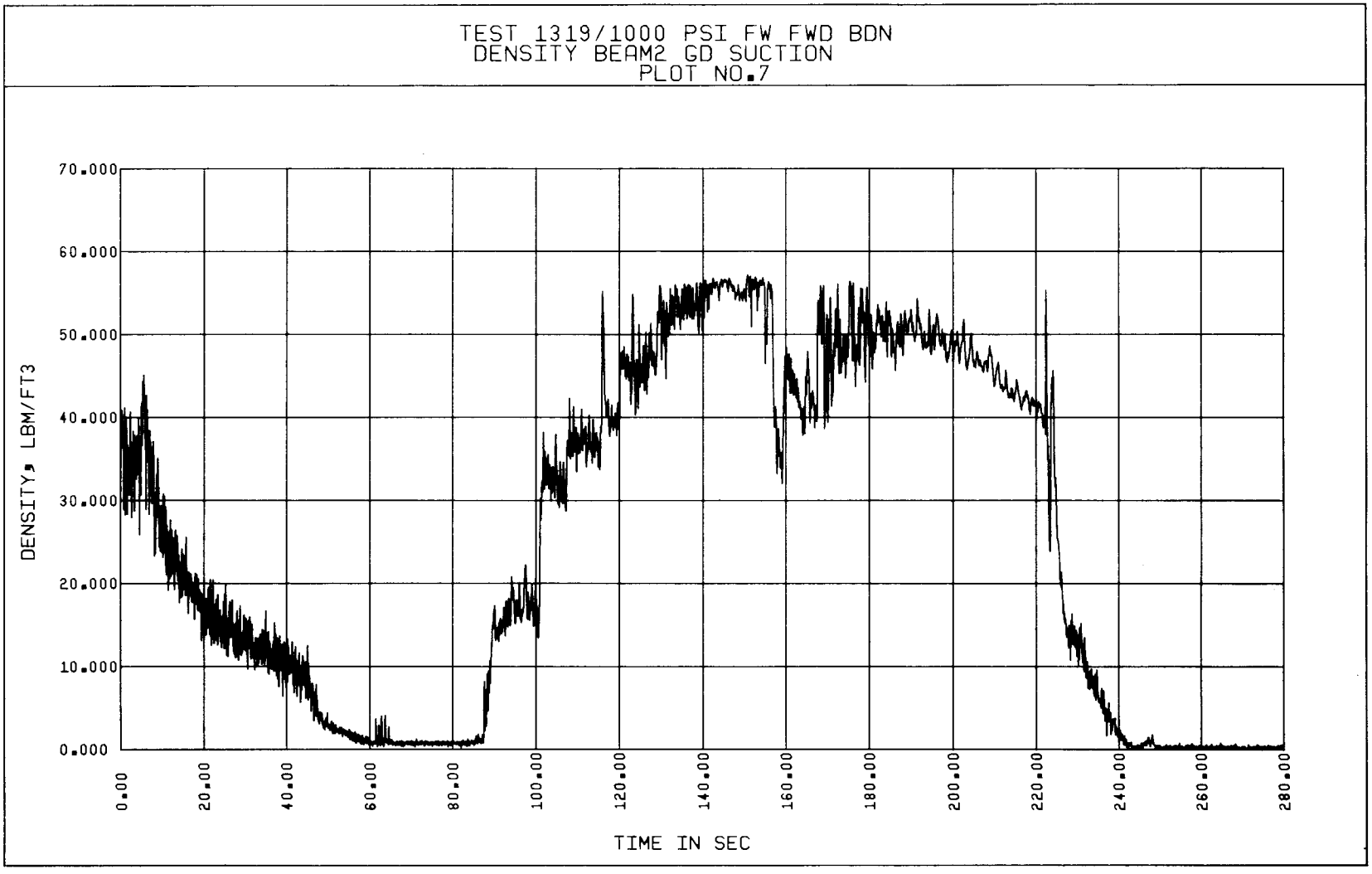

Figure 5-117. Test 1319, Suction Density vs Time, Based on Gamma Densitometer Beam 2 Data

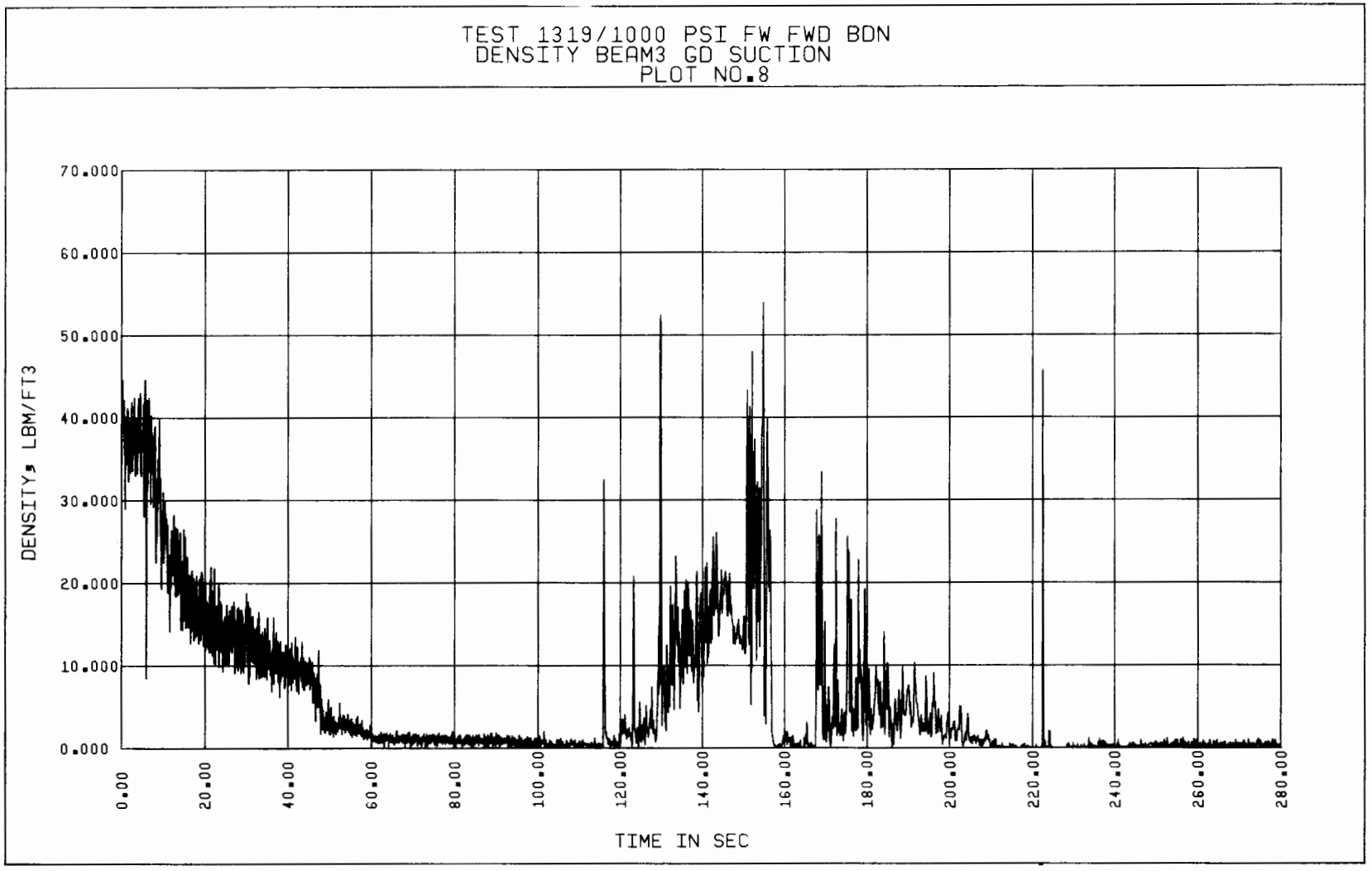

Figure 5-118. Test 1319, Suction Density vs Time, Based on Gamma Densitometer Beam 3 Data

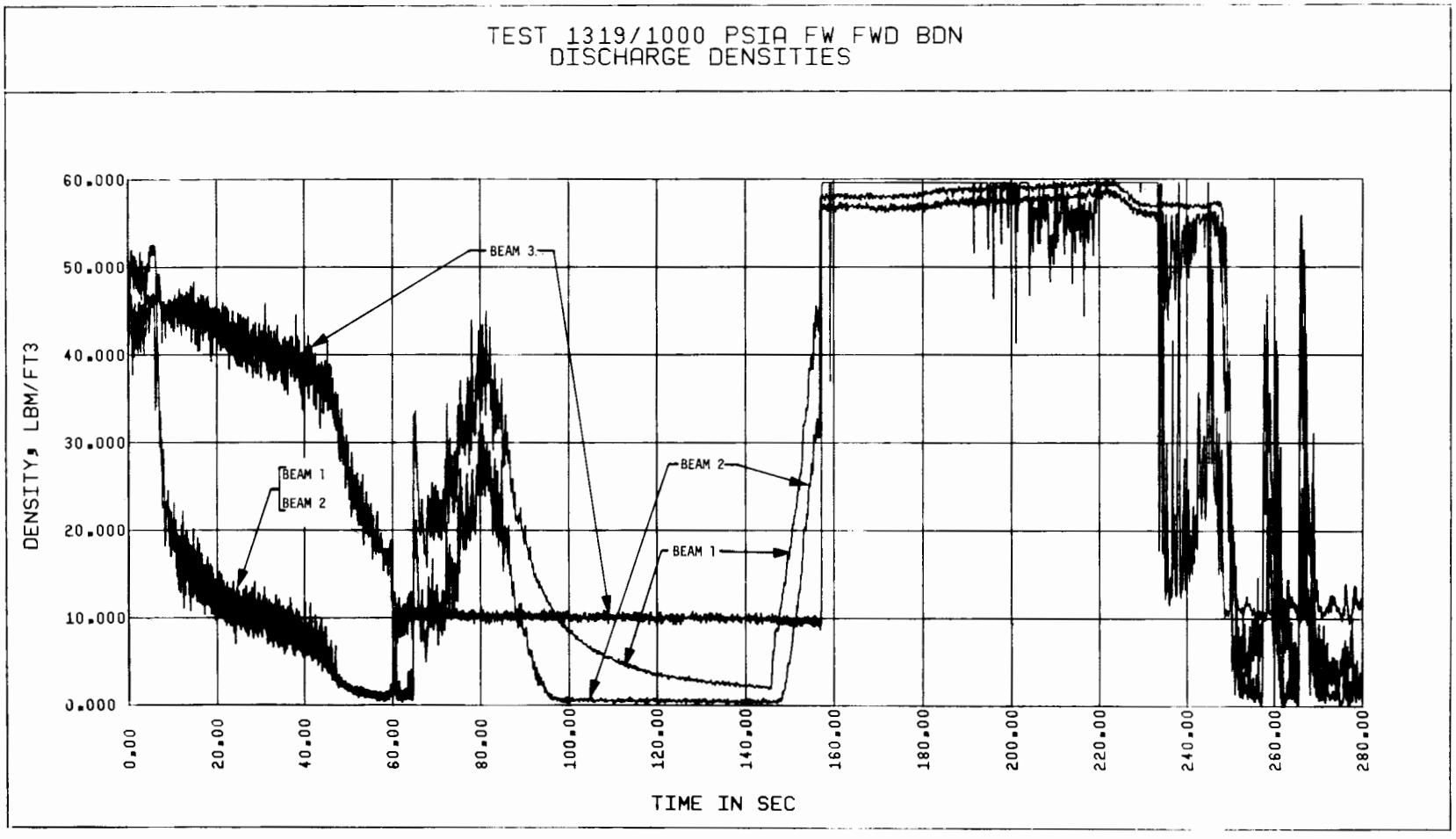

Figure 5-119. Test 1319, Discharge Densities vs Time

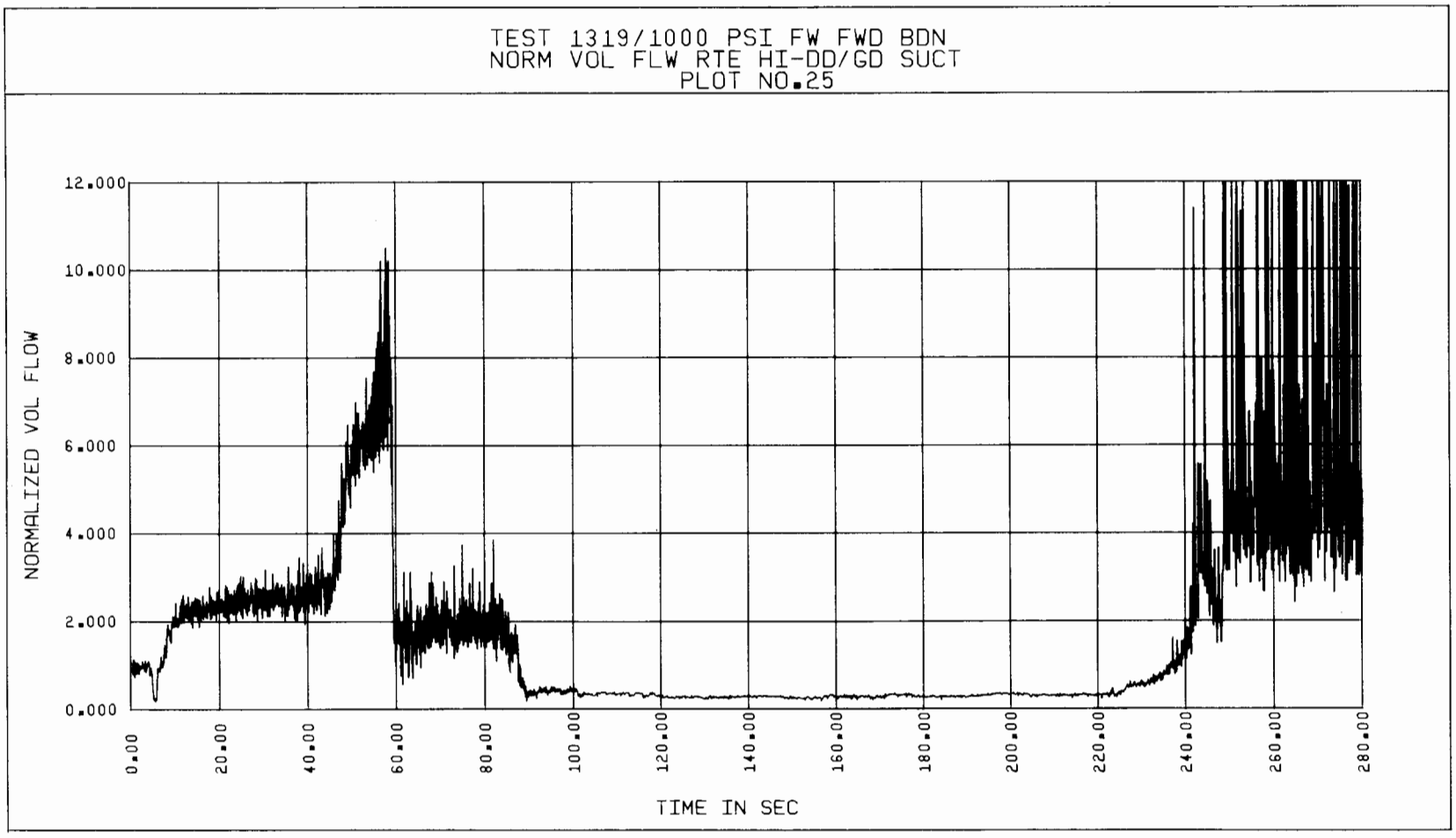

Figure 5-120. Test 1319, Normalized Suction Volumetric Flow Rate vs Time, Based on Gamma Densitometer and High Drag Disc Data

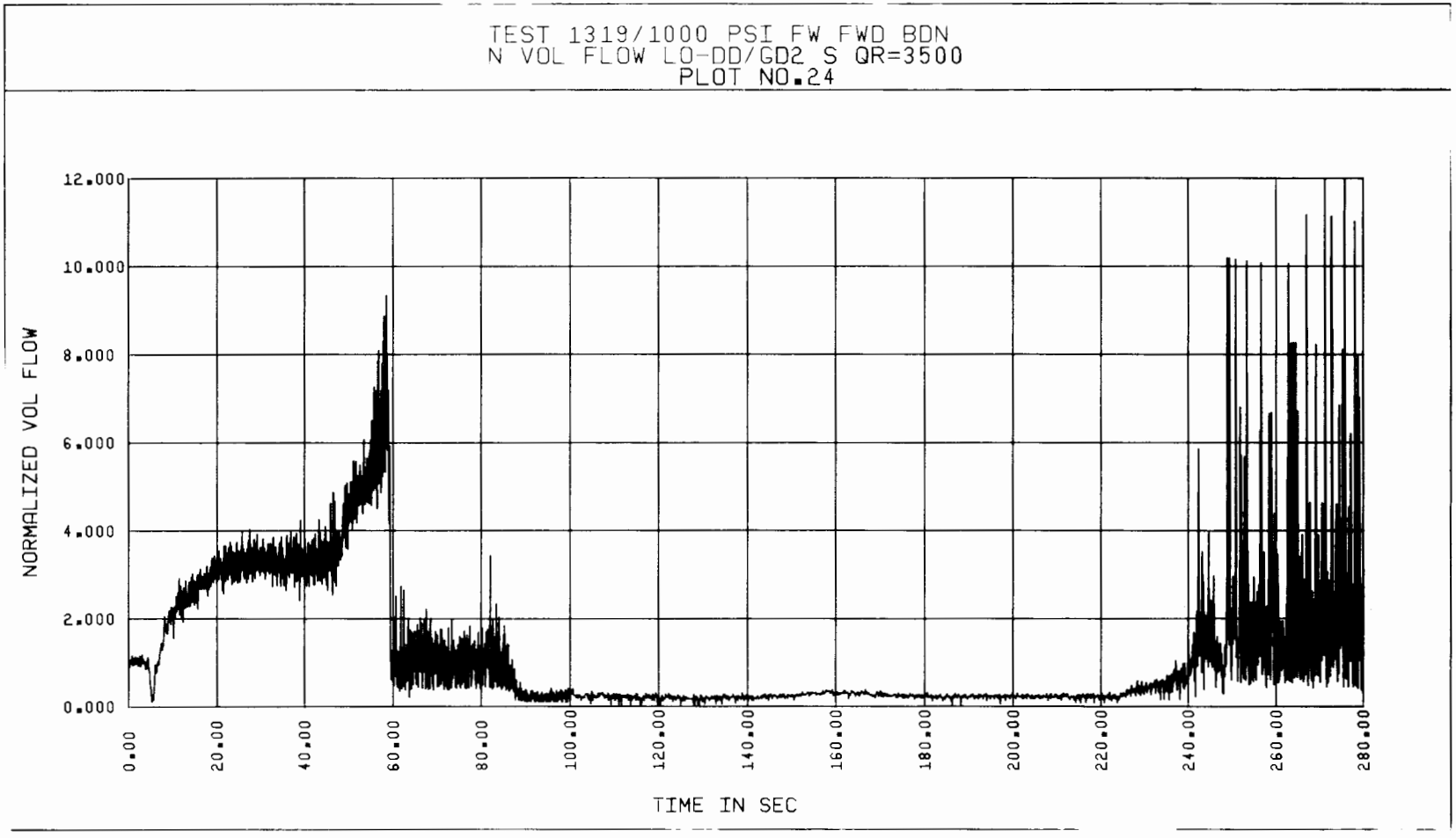

Figure 5-121. Test 1319, Normalized Suction Volumetric Flow Rate vs Time, Based on Gamma Densitometer and Low Drag Disc Data

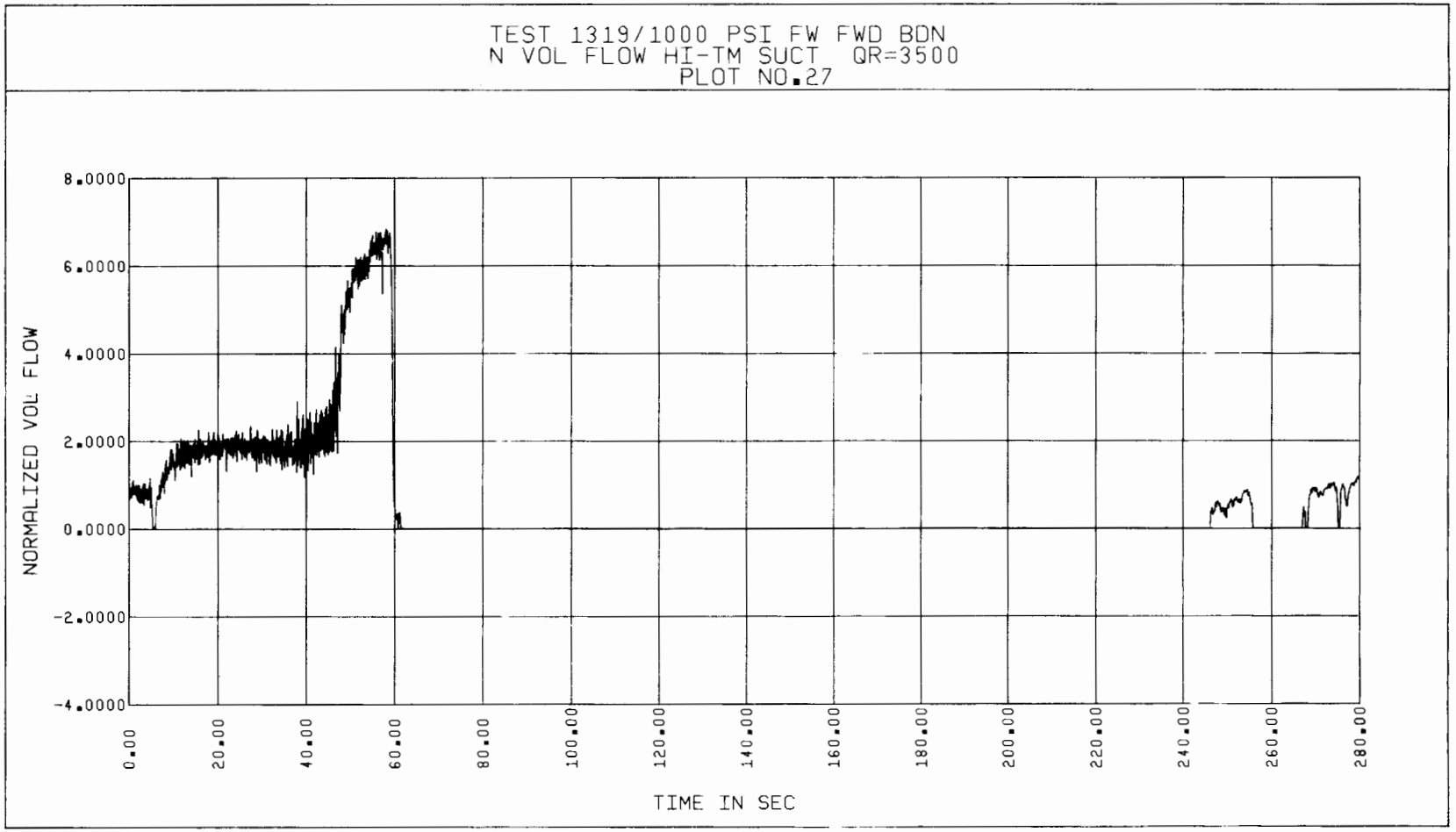

Figure 5-122. Test 1319, Normalized Suction Volumetric Flow Rate vs Time, Based on High Turbine Meter Data

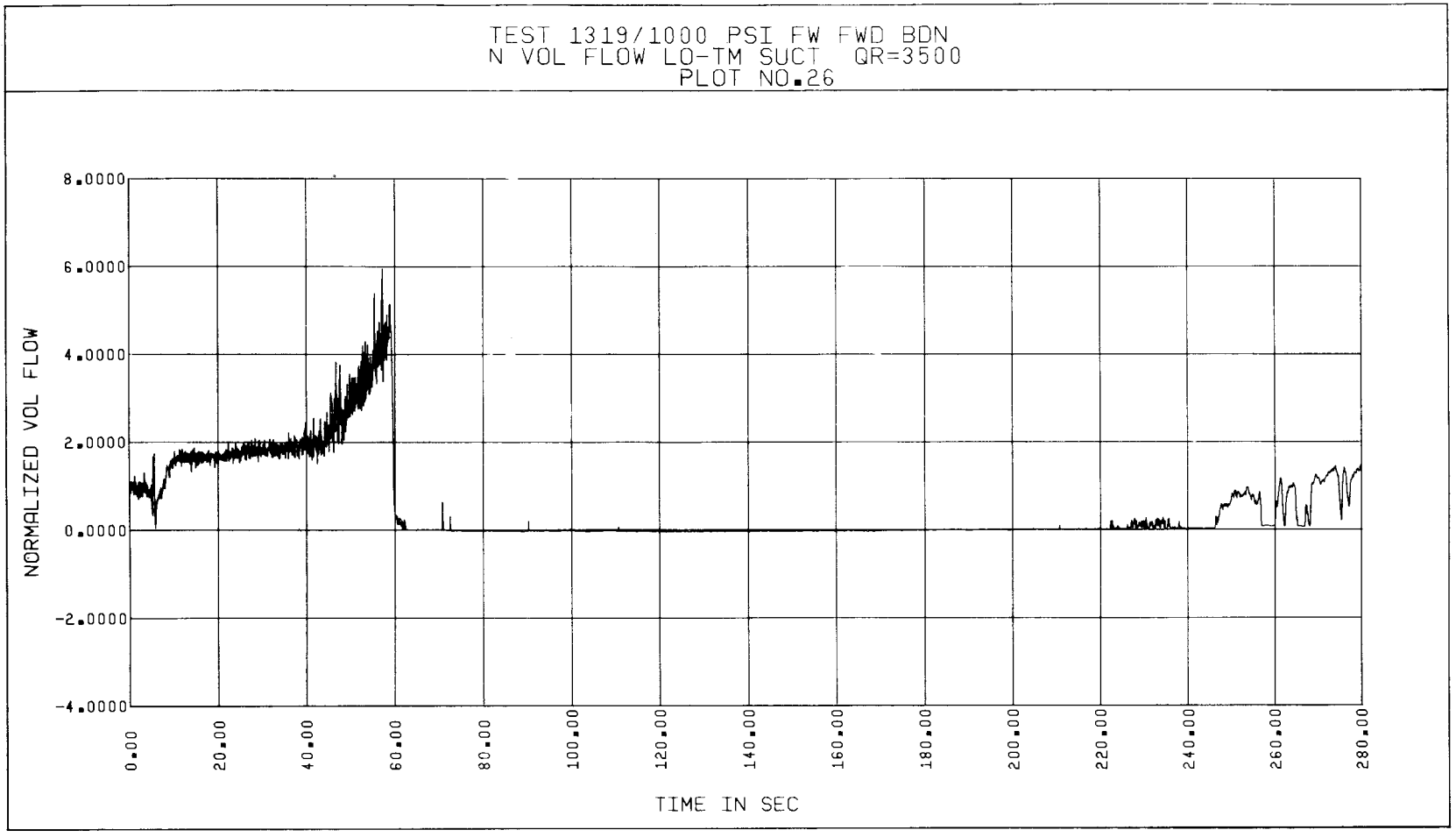

Figure 5-123. Test 1319, Normalized Suction Volumetric Flow Rate vs Time, Based on Low Turbine Meter Data

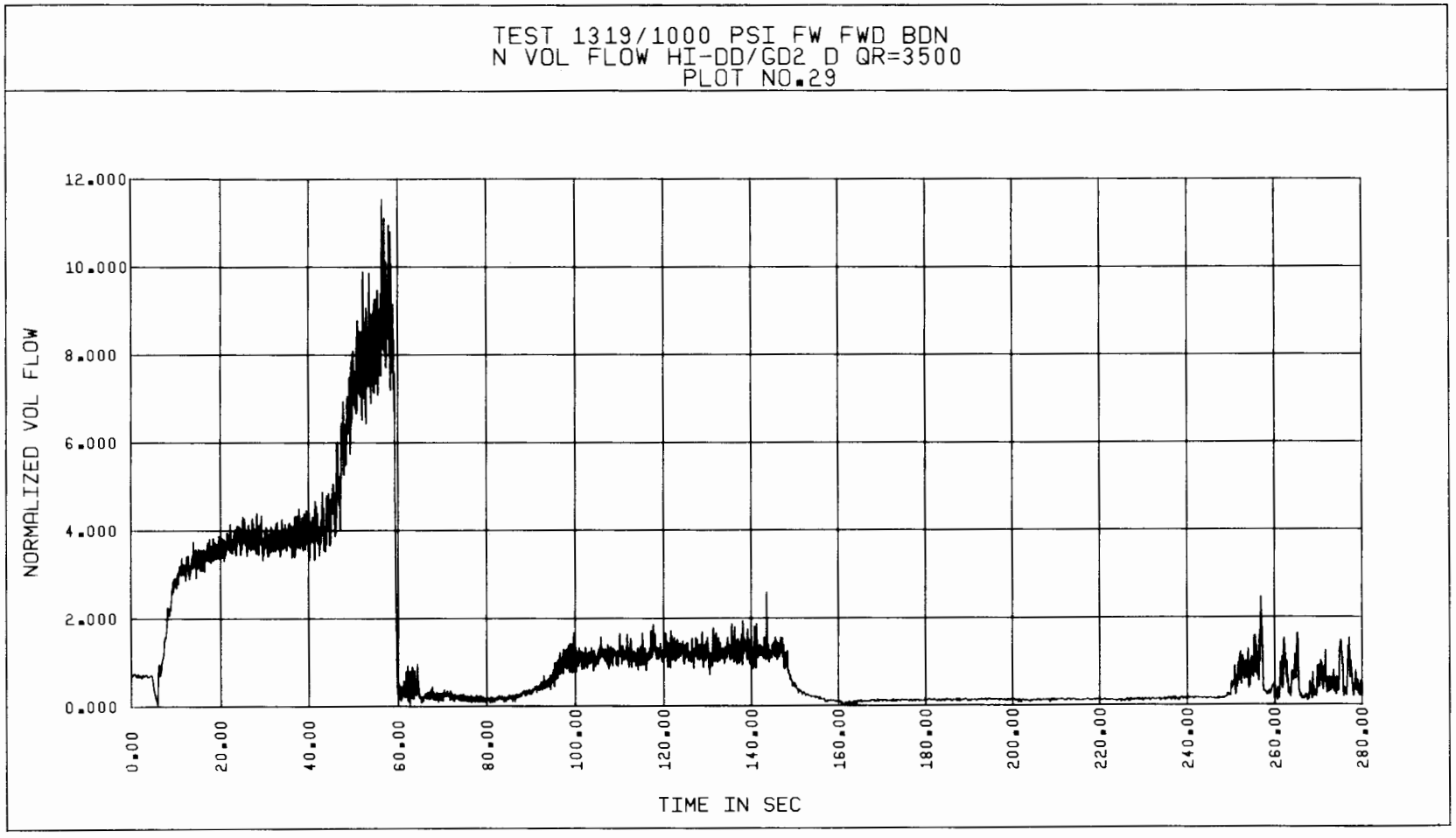

Figure 5-124. Test 1319, Normalized Discharge Volumetric Flow Rate vs Time, Based on Gamma Densitometer and High Drag Disc Data

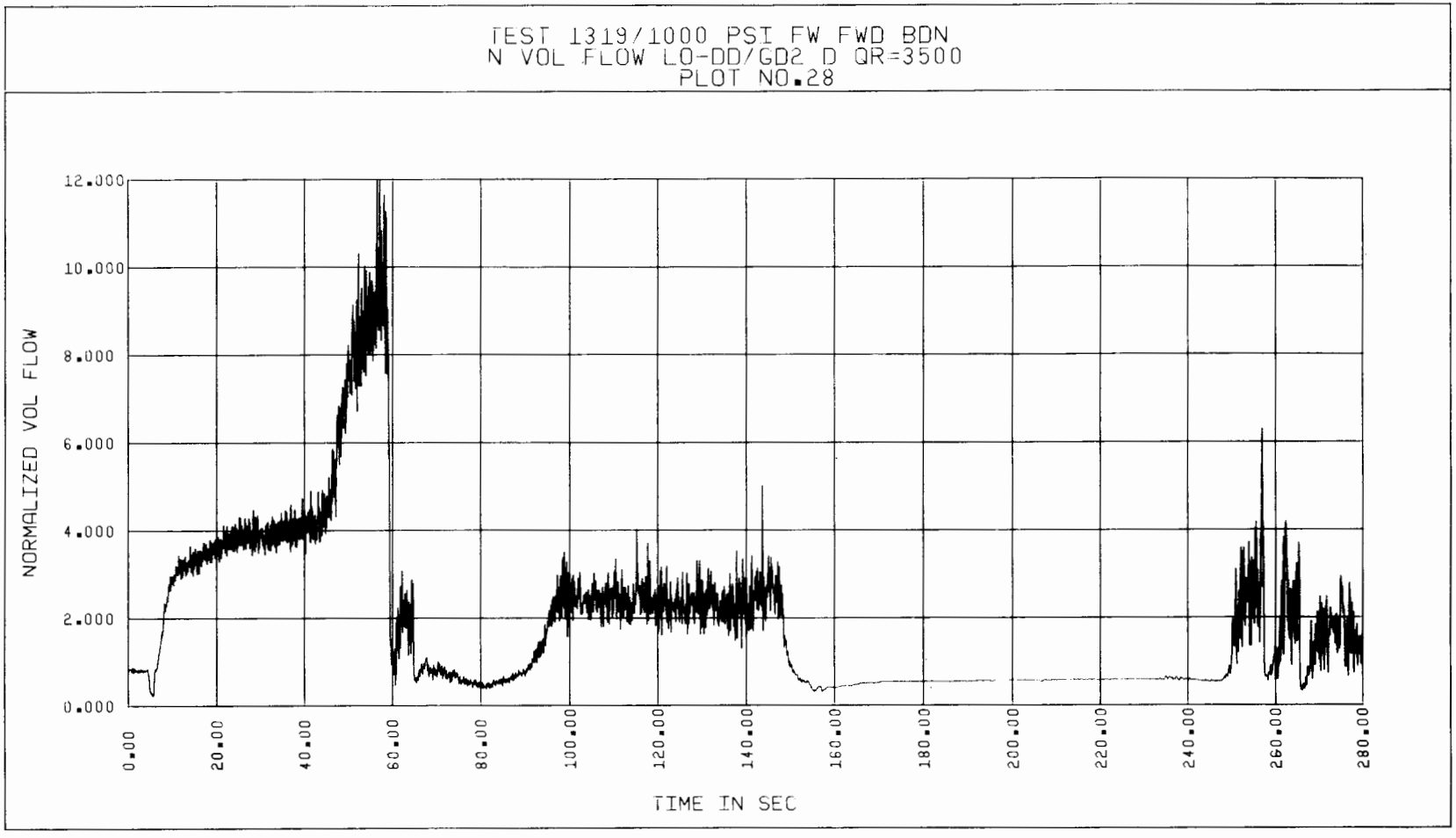

Figure 5-125. Test 1319, Normalized Discharge Volumetric Flow Rate vs Time, Based on Gamma Densitometer and Low Drag Disc Data

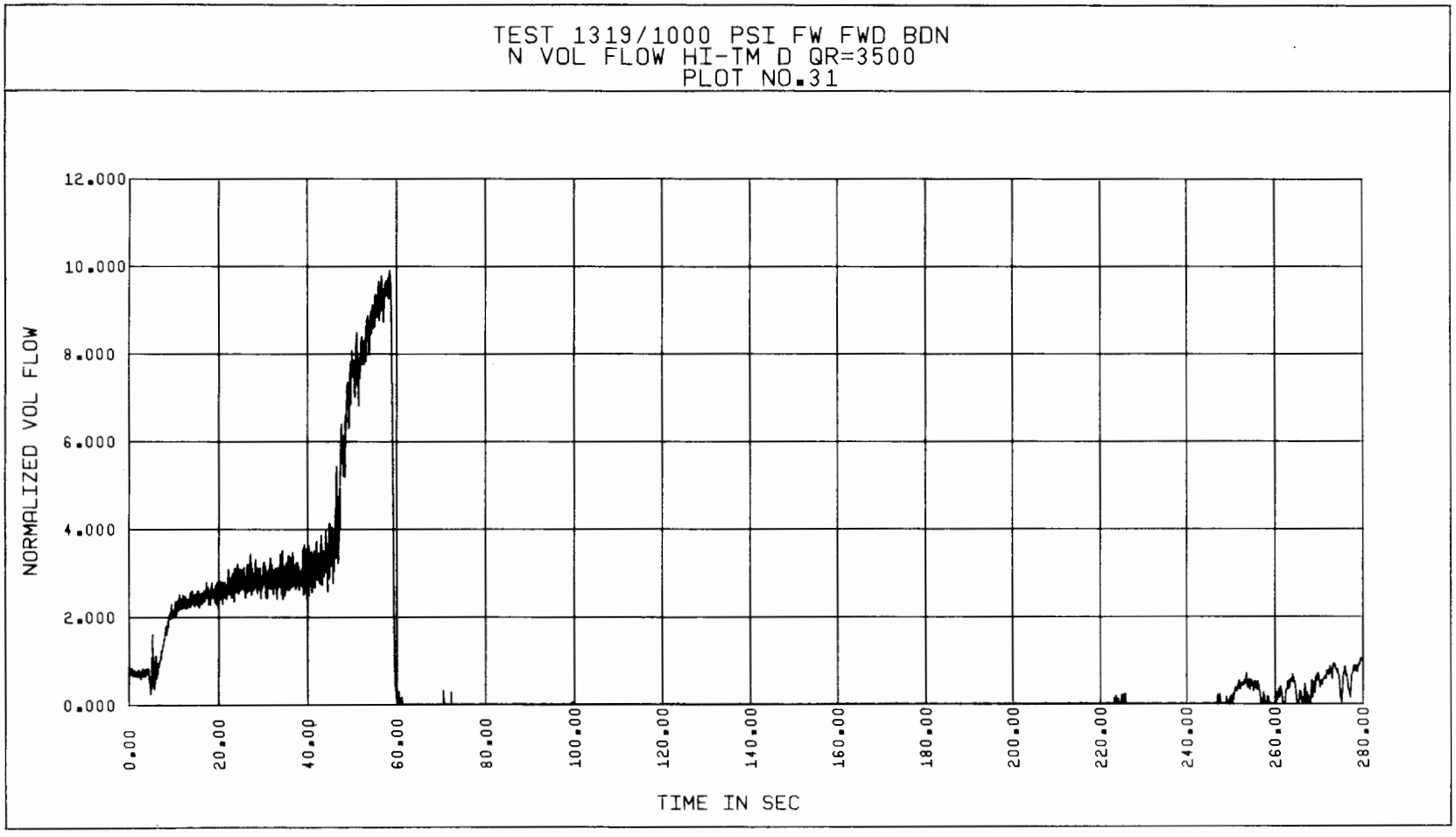

Figure 5-126. Test 1319, Normalized Discharge Volumetric Flow Rate vs Time, Based on High Turbine Meter Data

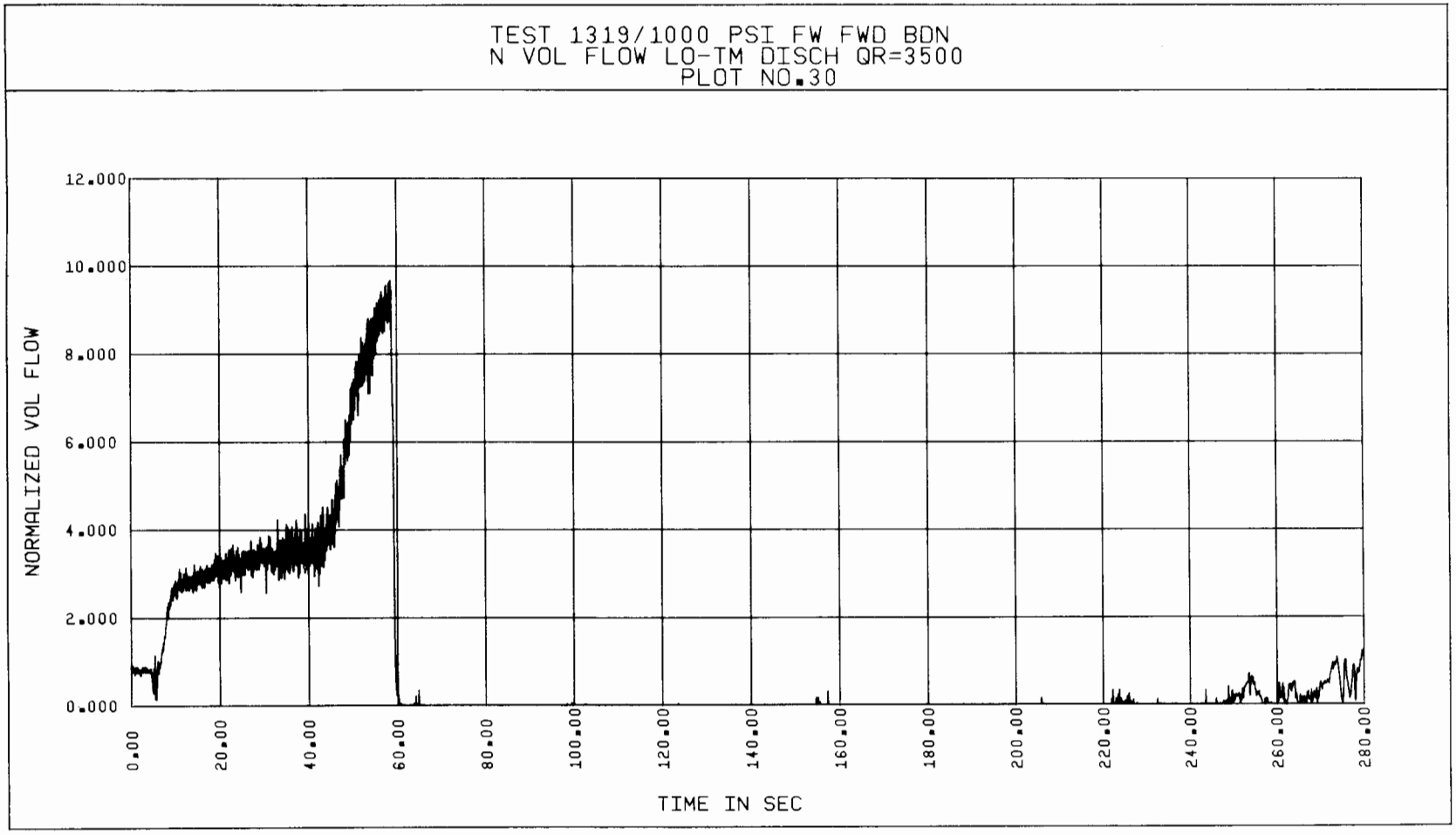

Figure 5-127. Test 1319, Normalized Discharge Volumetric Flow Rate vs Time, Based on Low Turbine Meter Data

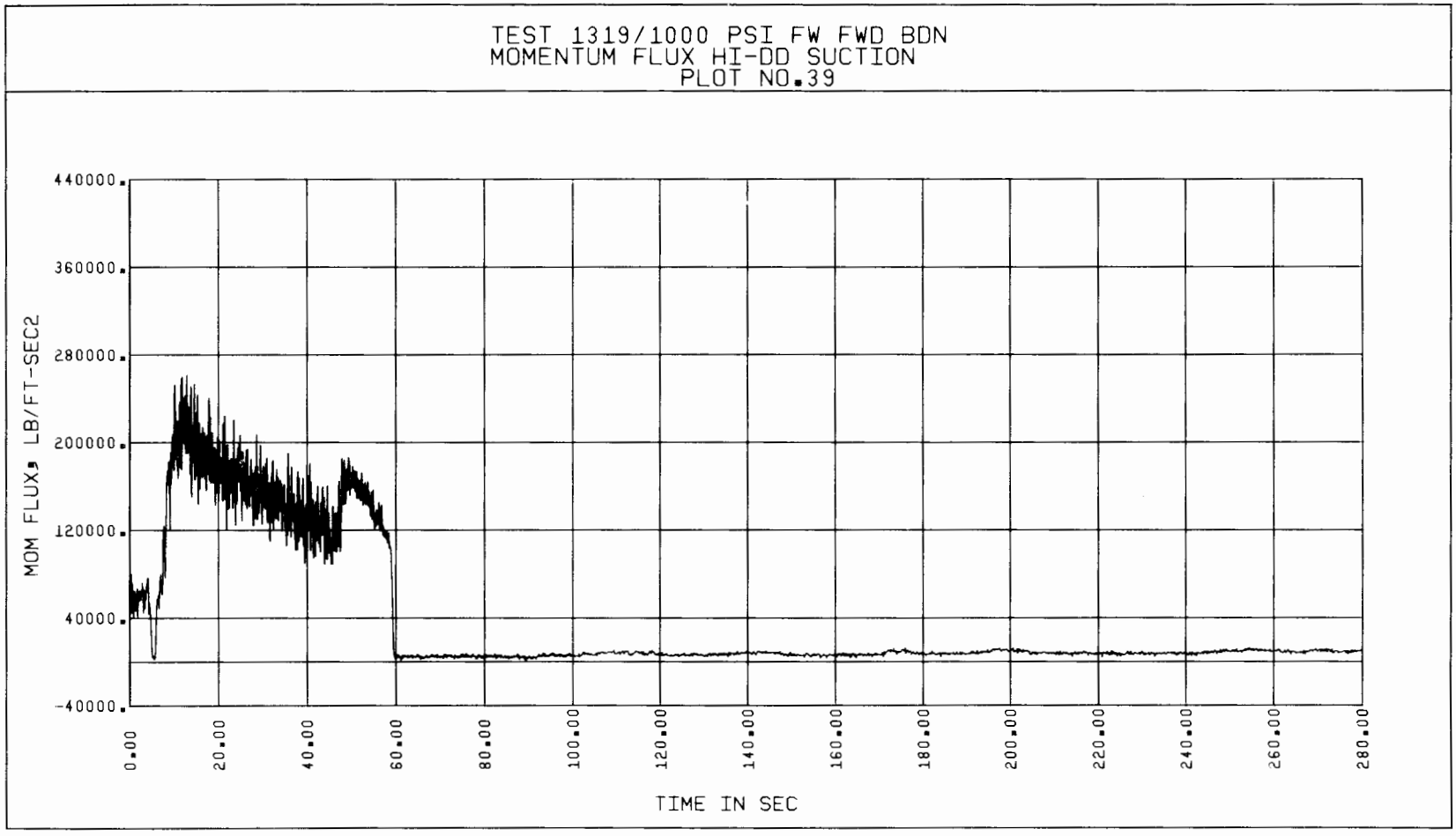

Figure 5-128. Test 1319, Suction Momentum Flux vs Time, Based on High Drag Disc Data

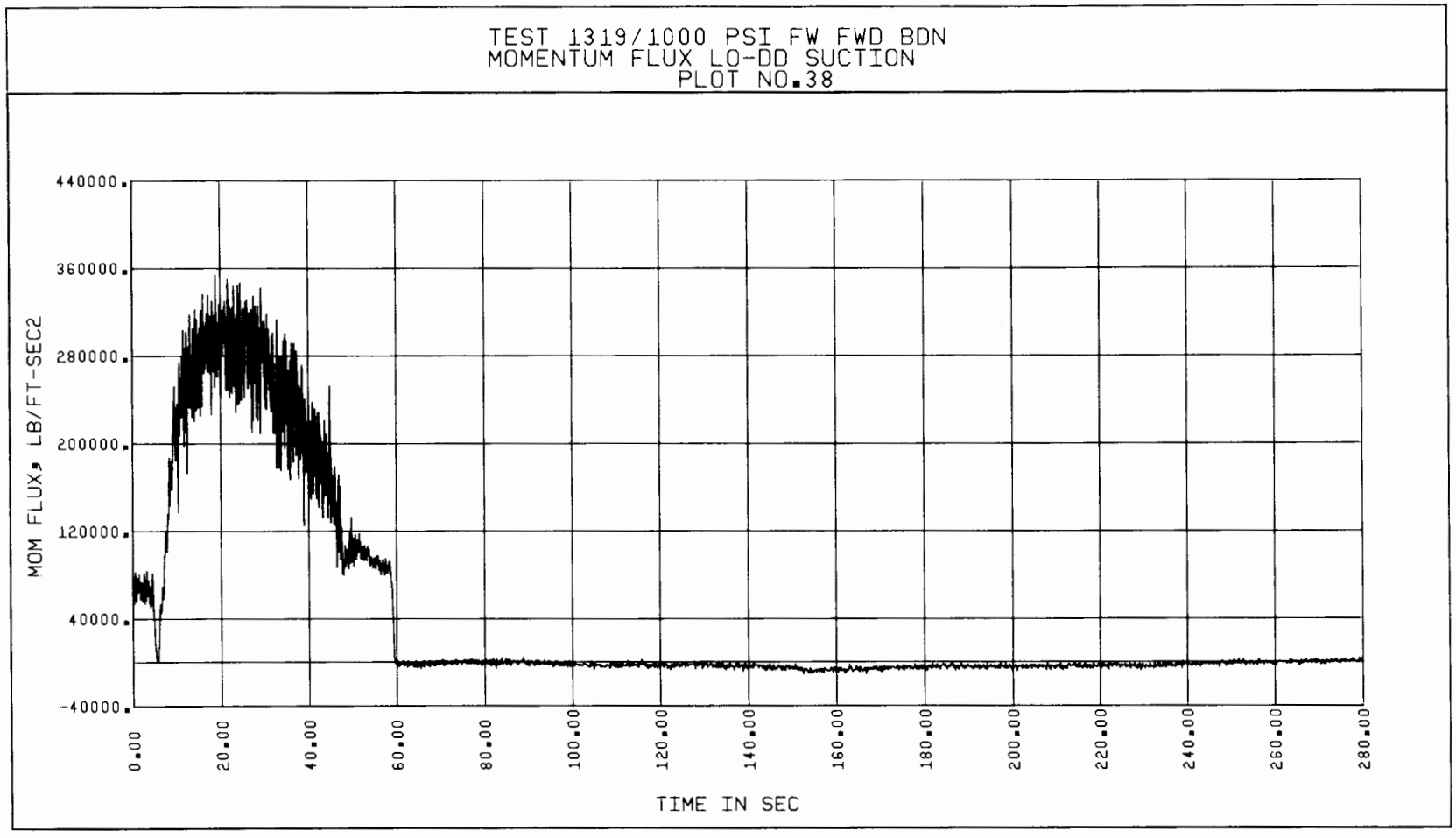

Figure 5-129. Test 1319, Suction Momentum Flux vs Time, Based on Low Drag Disc Data

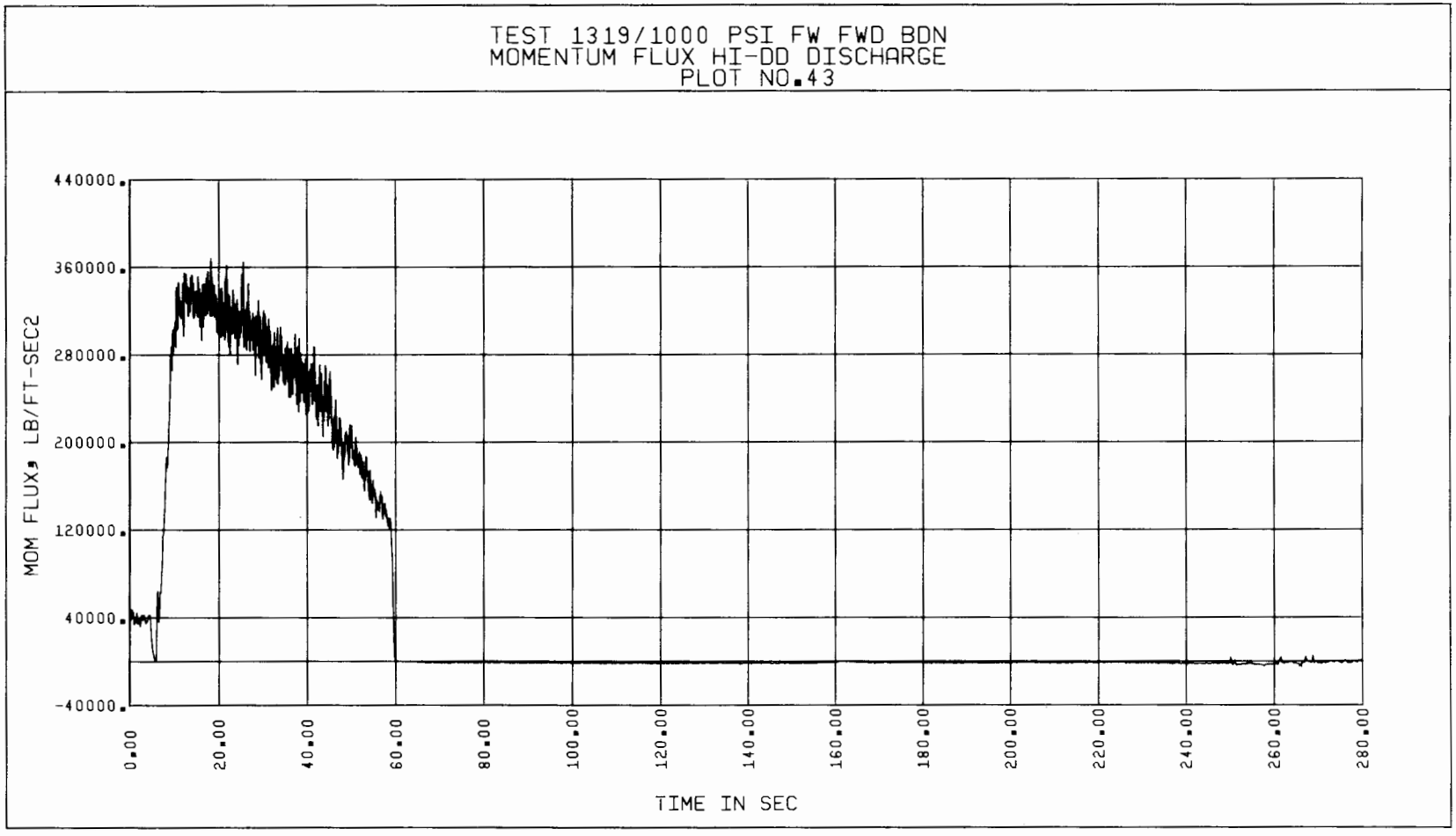

Figure 5-130. Test 1319, Discharge Momentum Flux vs Time, Based on High Drag Disc Data

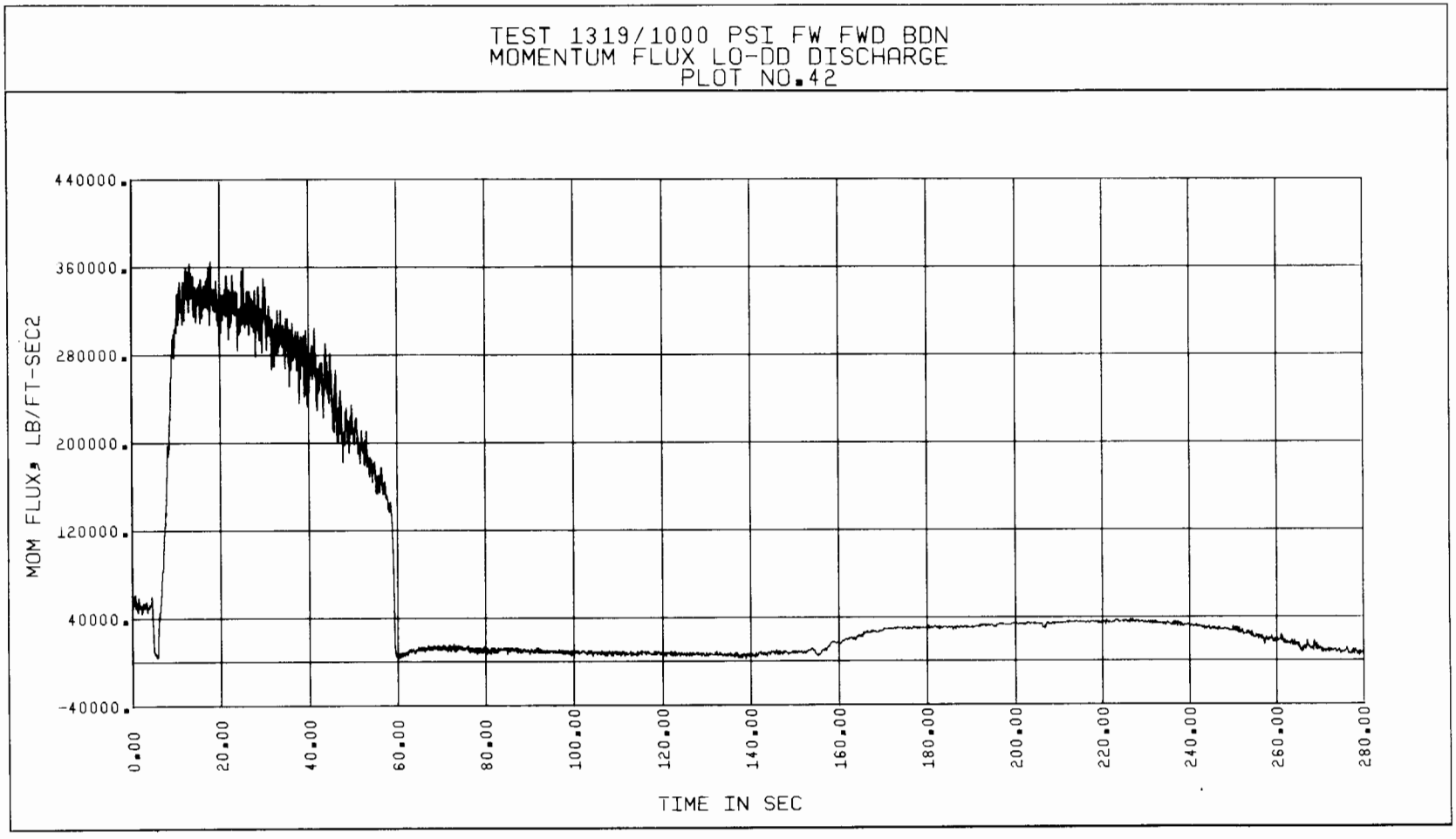

Figure 5-131. Test 1319, Discharge Momentum Flux vs Time, Based on Low Drag Disc Data

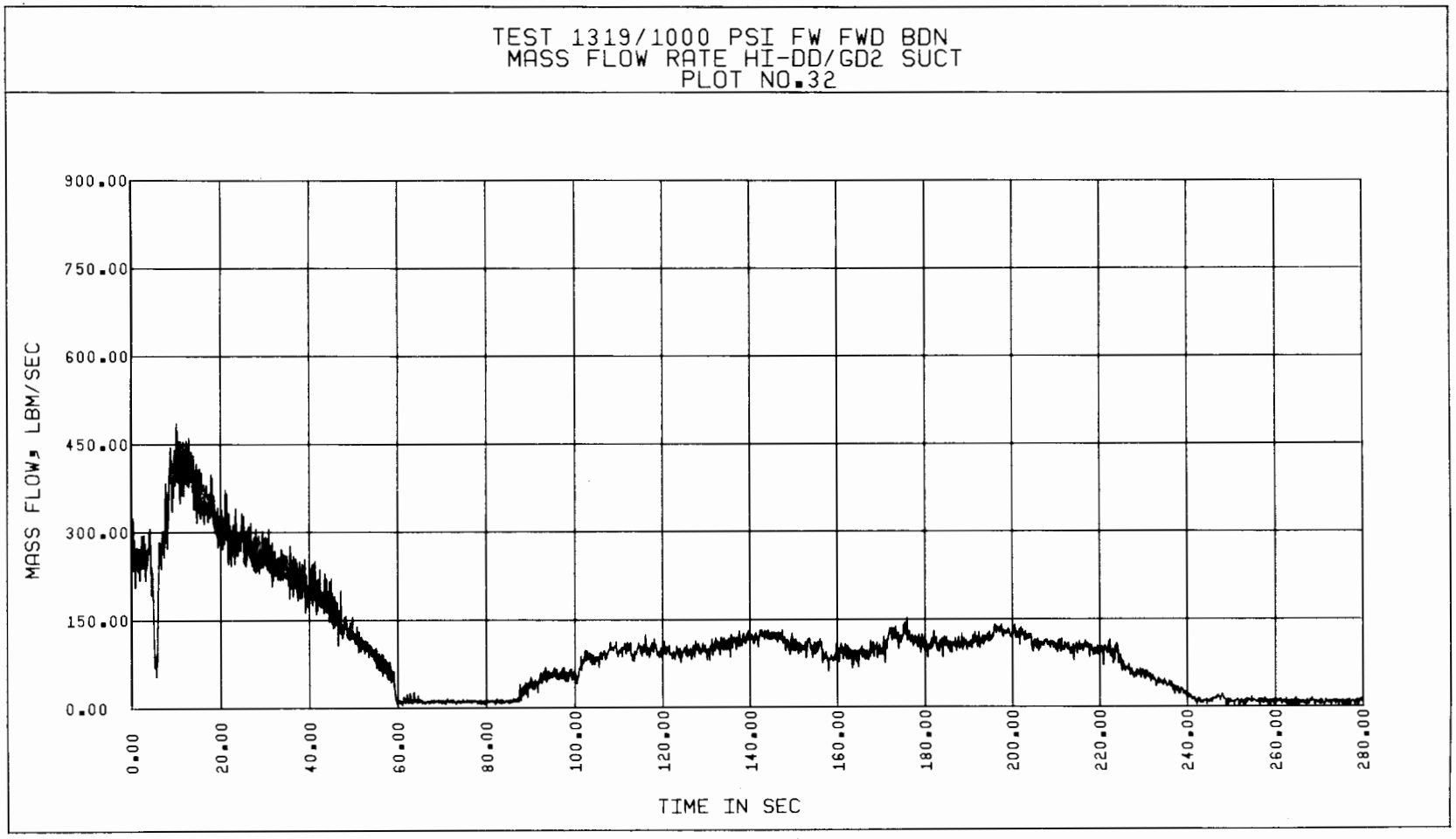

Figure 5-132. Test 1319, Suction Mass Flow Rate vs Time, Based on Gamma Densitometer and High Drag Disc Data

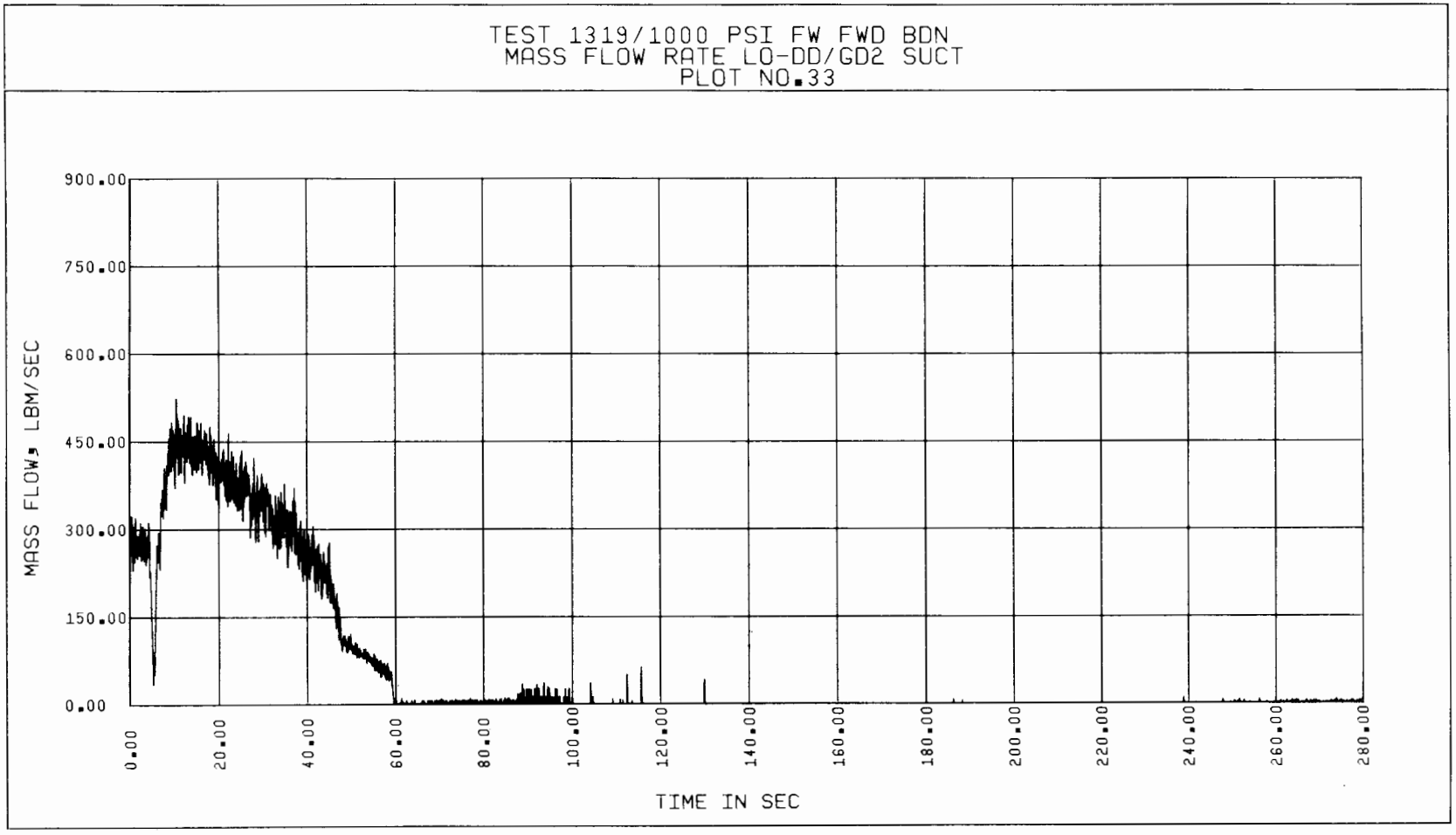

Figure 5-133. Test 1319, Suction Mass Flow Rate vs Time, Based on Gamma Densitometer and Low Drag Disc Data

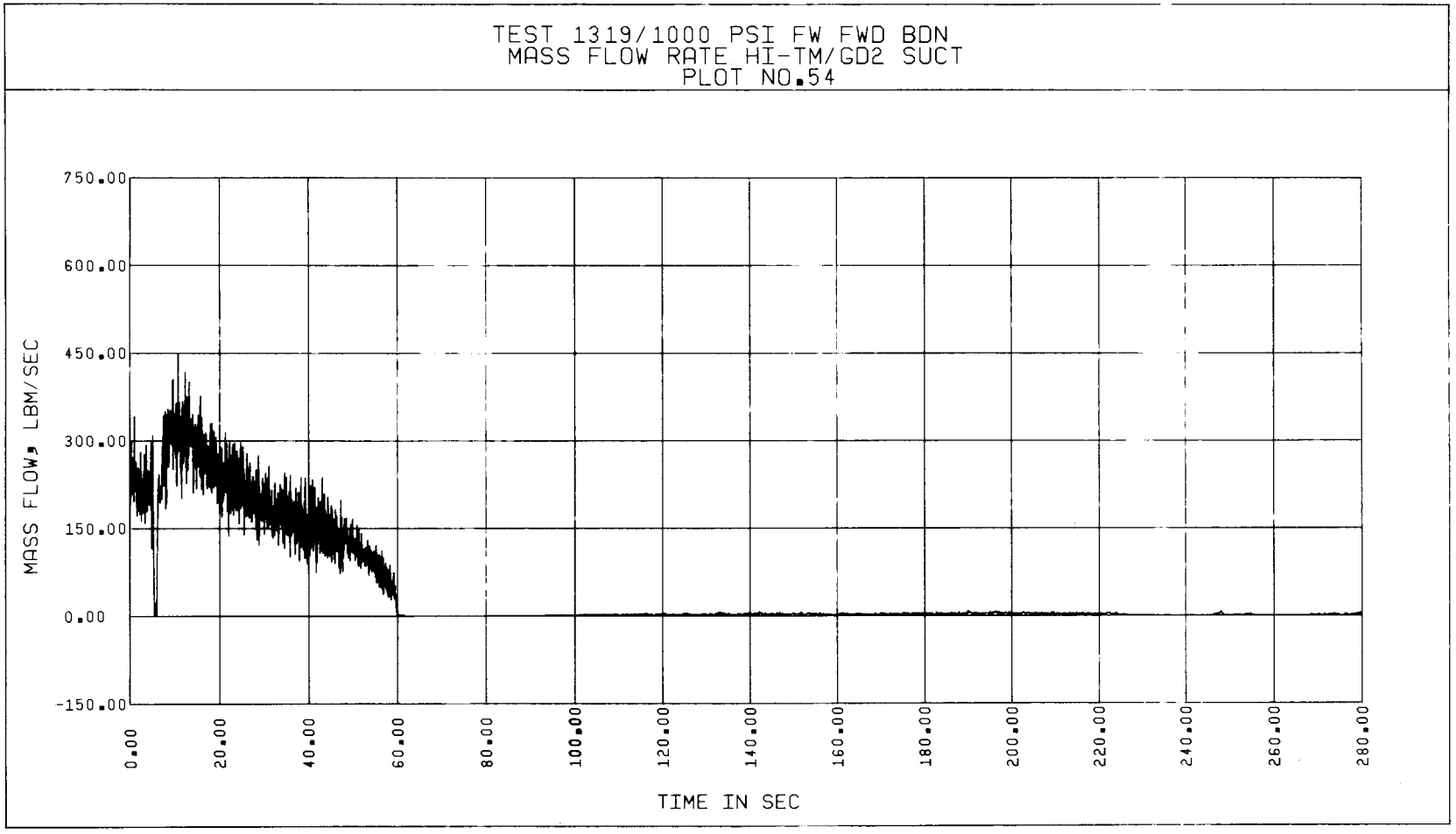

Figure 5-134. Test 1319, Suction Mass Flow Rate vs Time, Based on Gamma Densitometer and High Turbine Meter Data

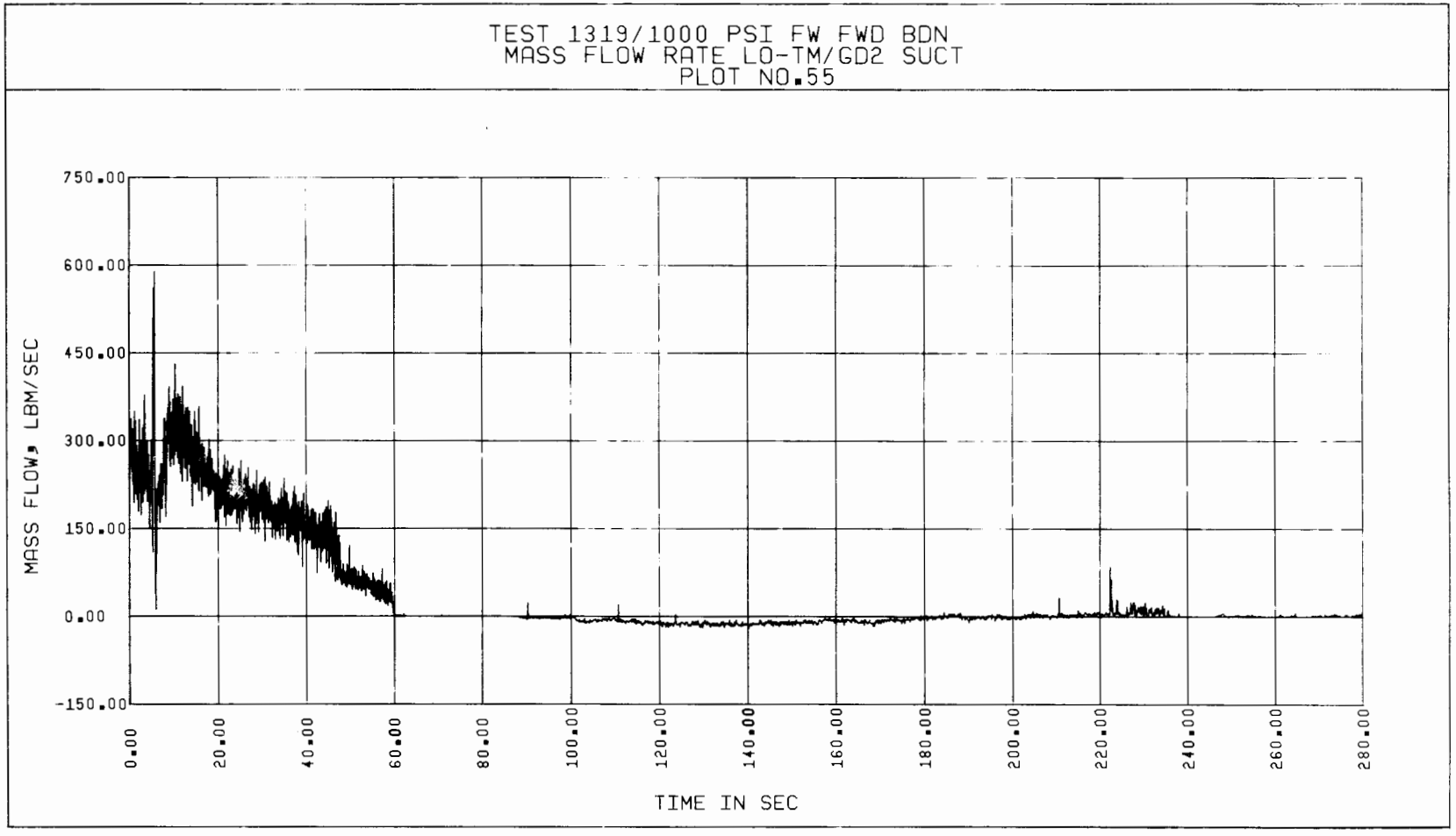

Figure 5-135. Test 1319, Suction Mass Flow Rate vs Time, Based on Gamma Densitometer and Low Turbine Meter Data

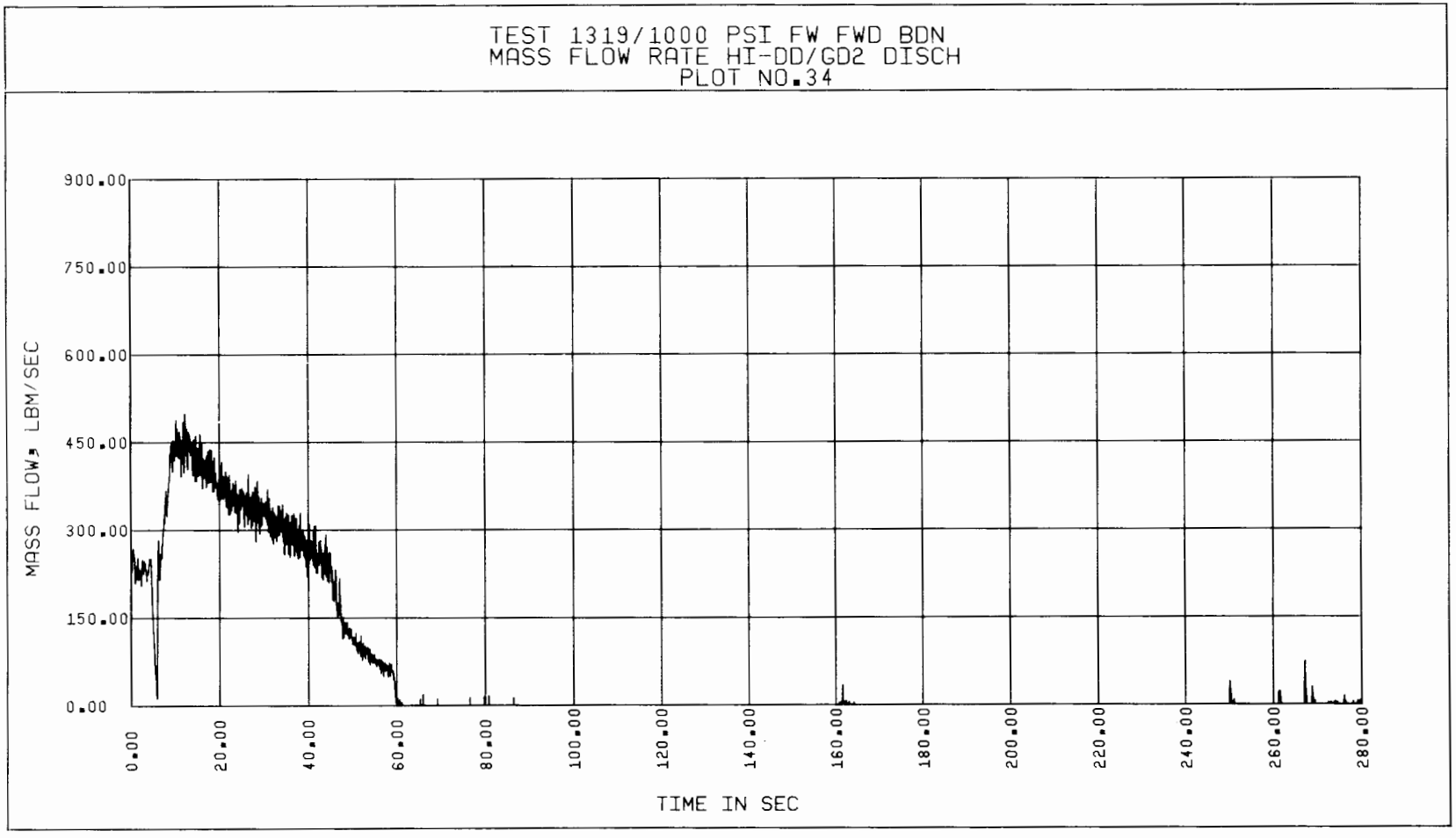

Figure 5-136. Test 1319, Discharge Mass Flow Rate vs Time, Based on Gamma Densitometer and High Drag Disc Data

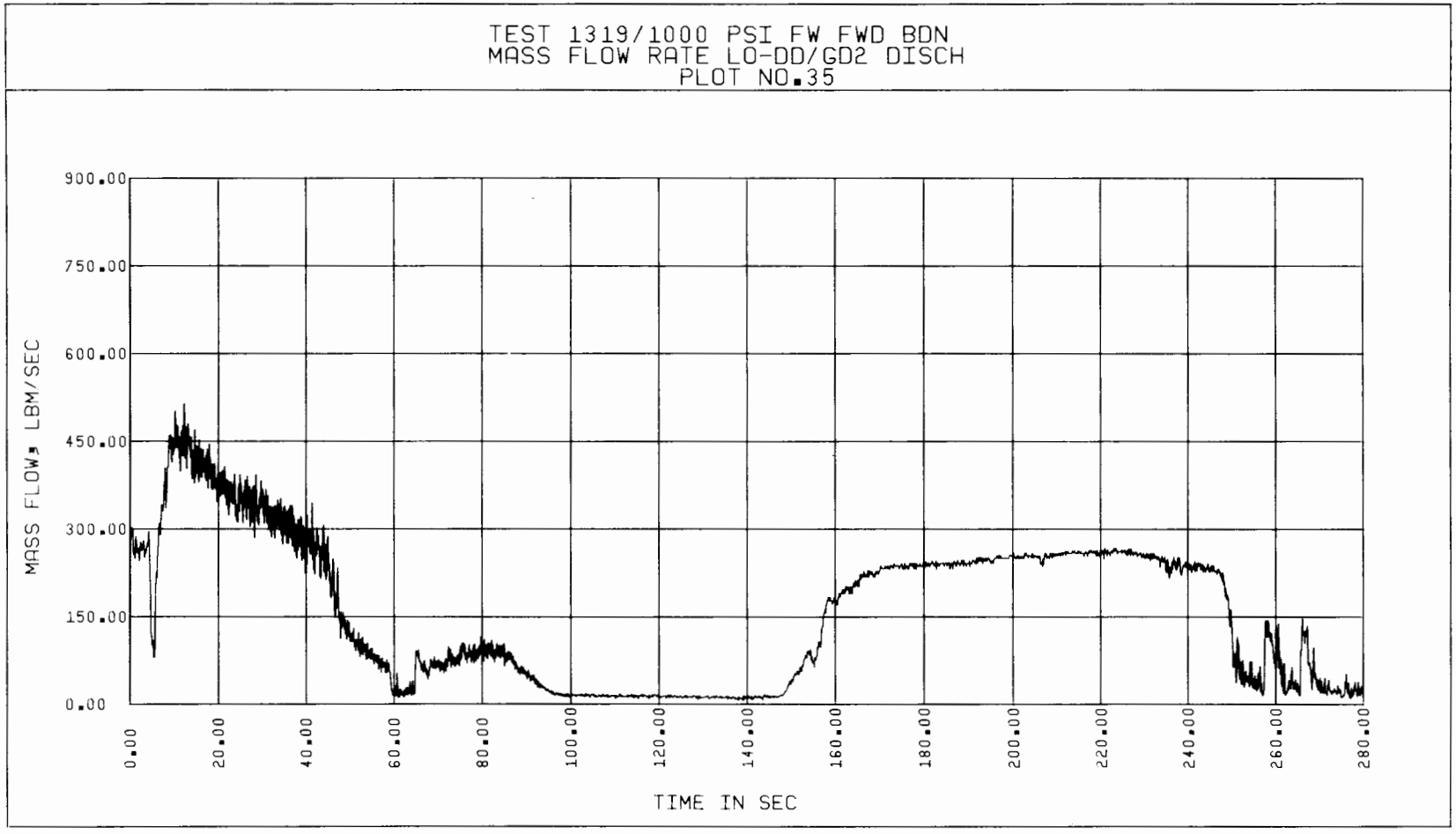

Figure 5-137. Test 1319, Discharge Mass Flow Rate vs Time, Based on Gamma Densitometer and Low Drag Disc Data

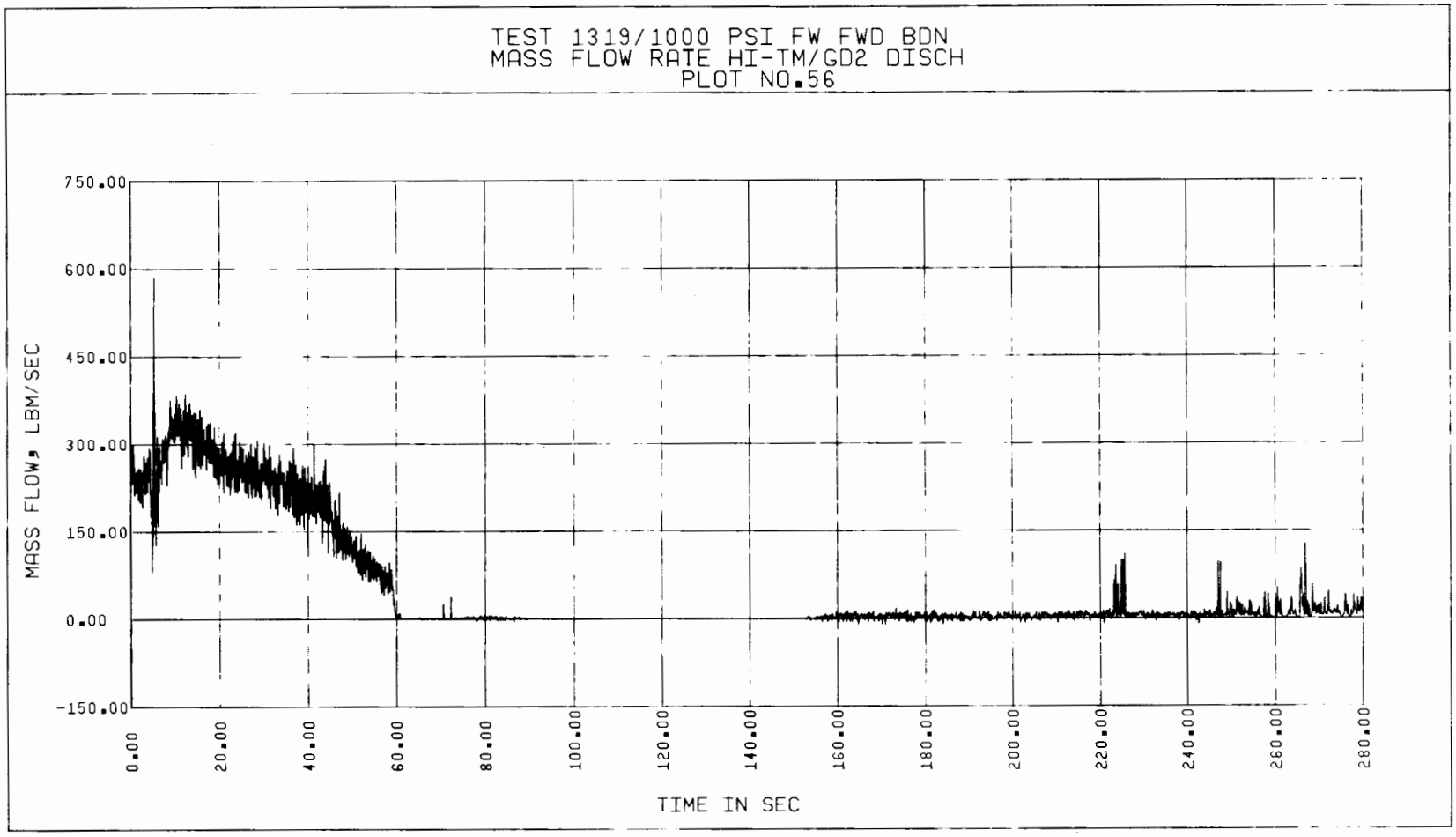

Figure 5-138. Test 1319, Discharge Mass Flow Rate vs Time, Based on Gamma Densitometer and High Turbine Meter Data

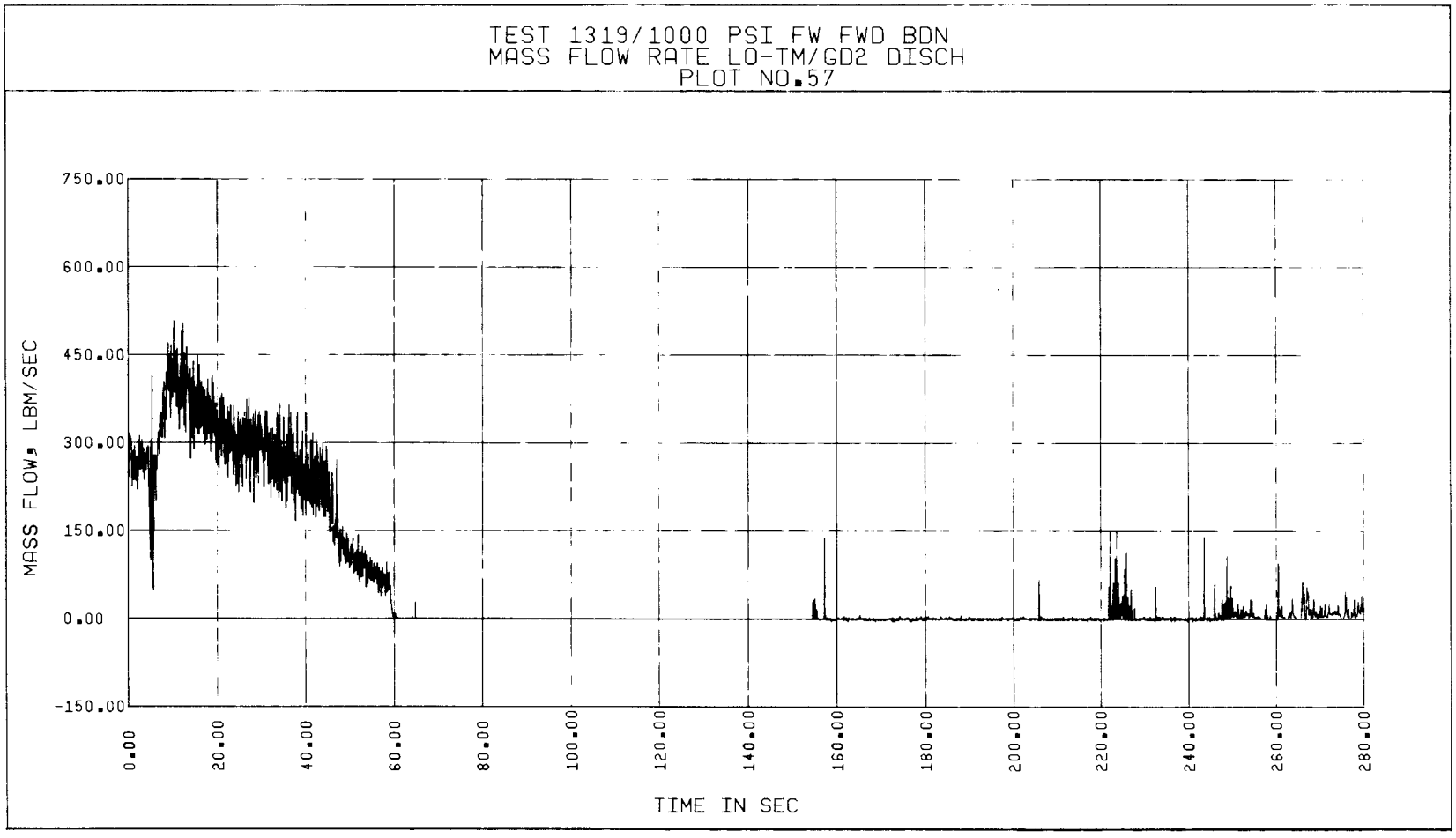

Figure 5-139. Test 1319, Discharge Mass Flow Rate vs Time, Based on Gamma Densitometer and Low Turbine Meter Data

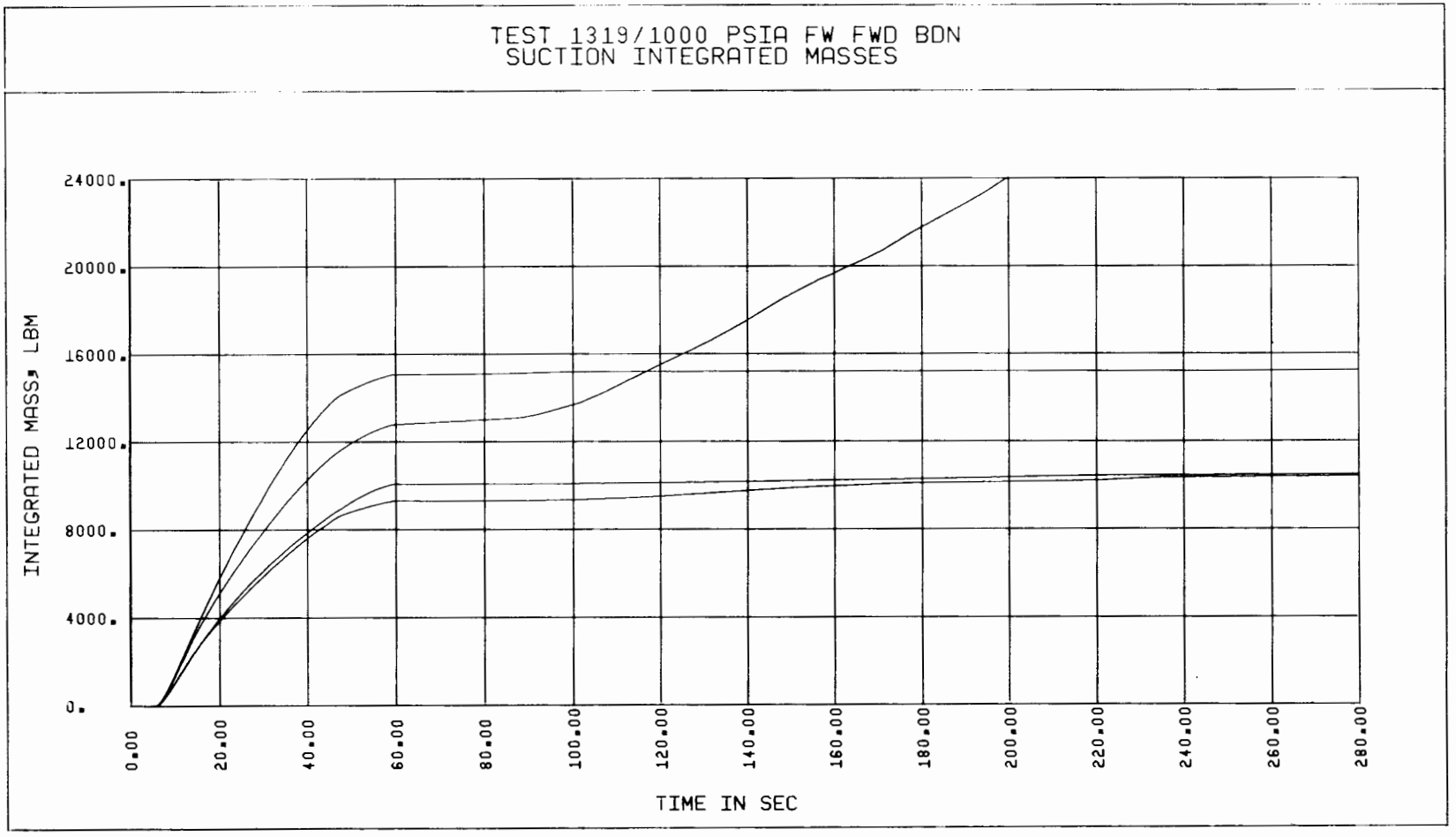

Figure 5-140. Test 1319, Suction Integrated Masses vs Time

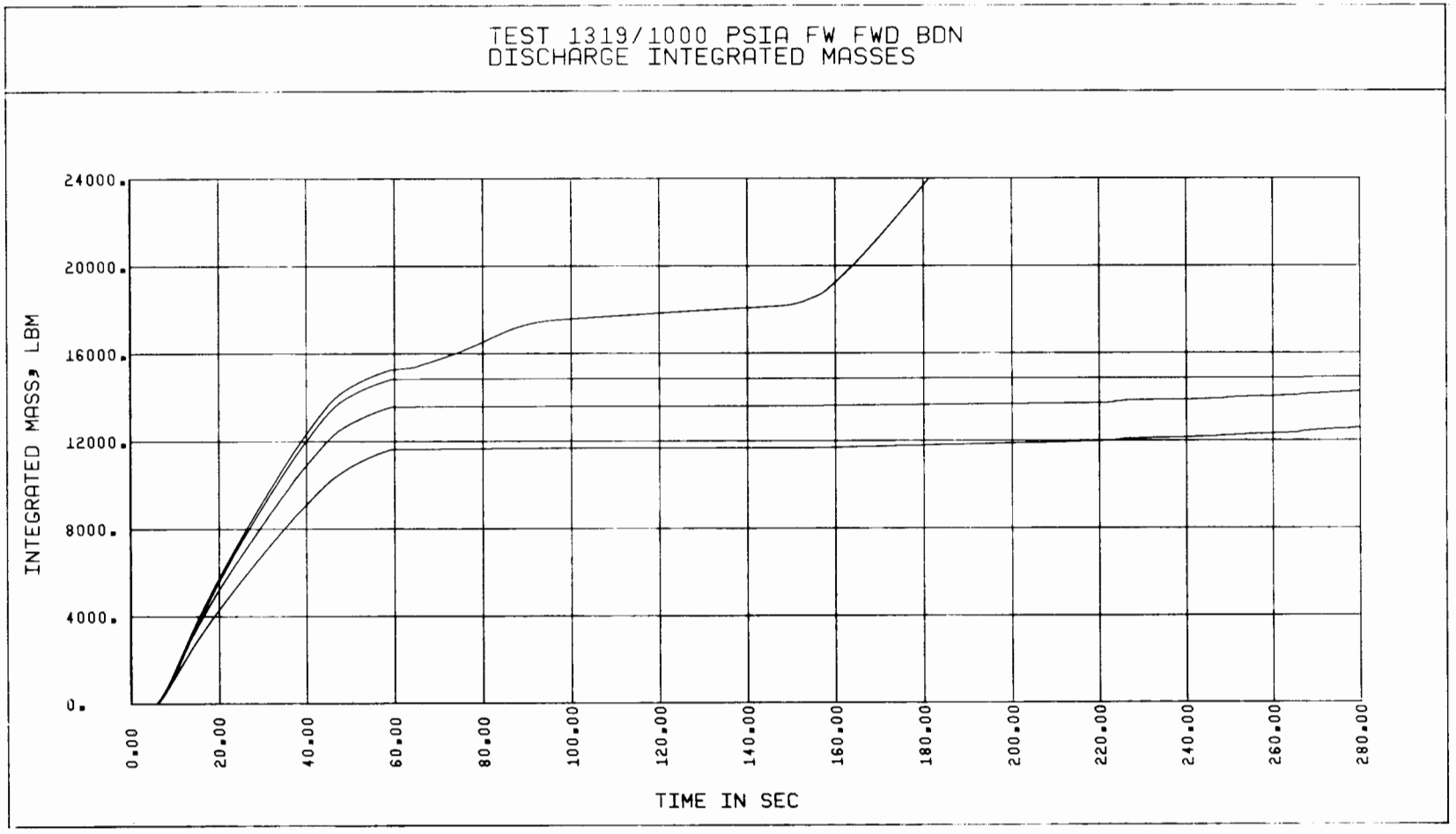

Figure 5-141. Test 1319, Discharge Integrated Masses vs Time

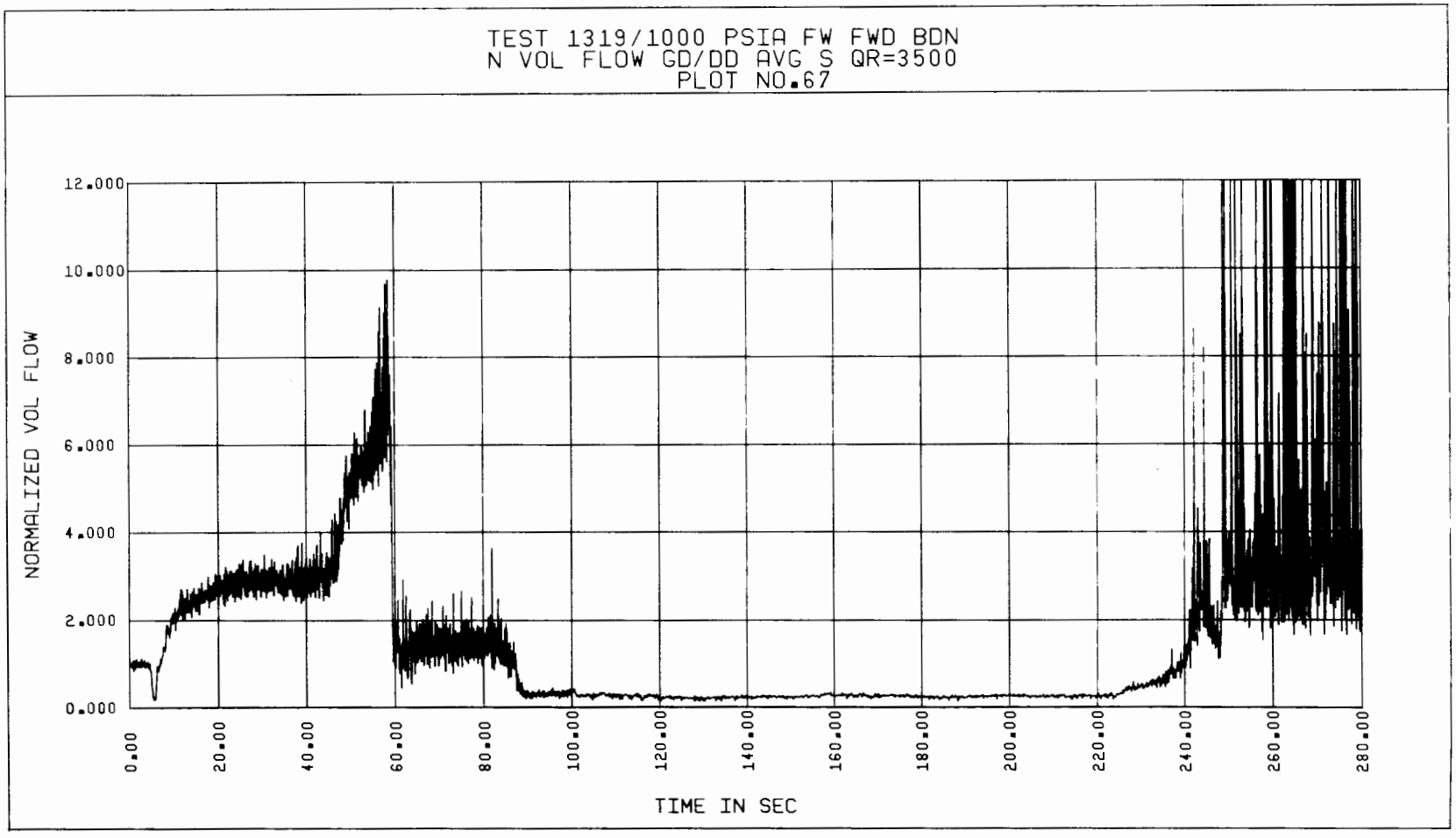

Figure 5-142. Test 1319, Normalized Suction Volumetric Flow Rate vs Time, Based on Gamma Densitometer and Average Drag Disc Data

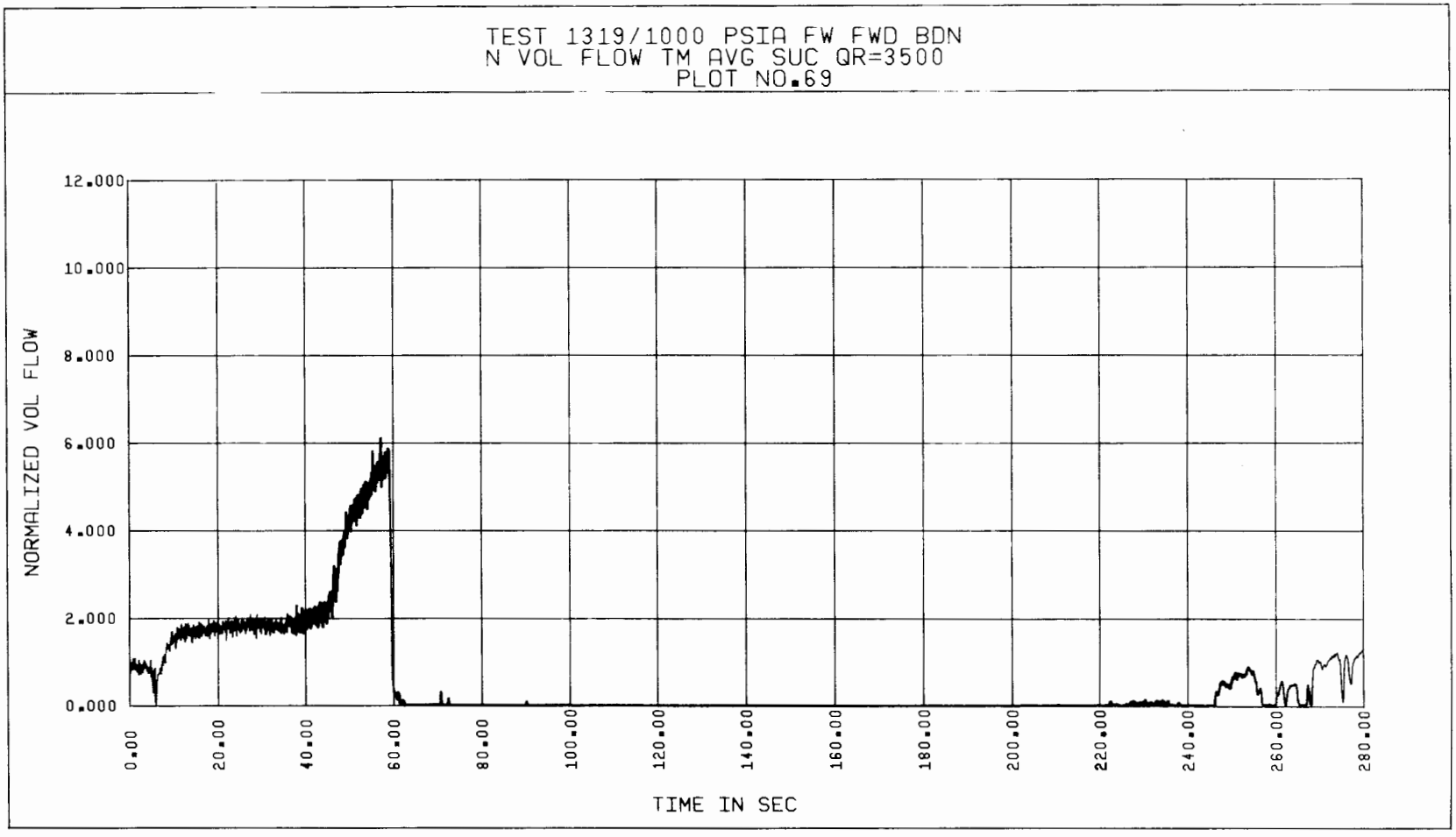

Figure 5-143. Test 1319, Normalized Suction Volumetric Flow Rate vs Time, Based on Average Turbine Meter Data

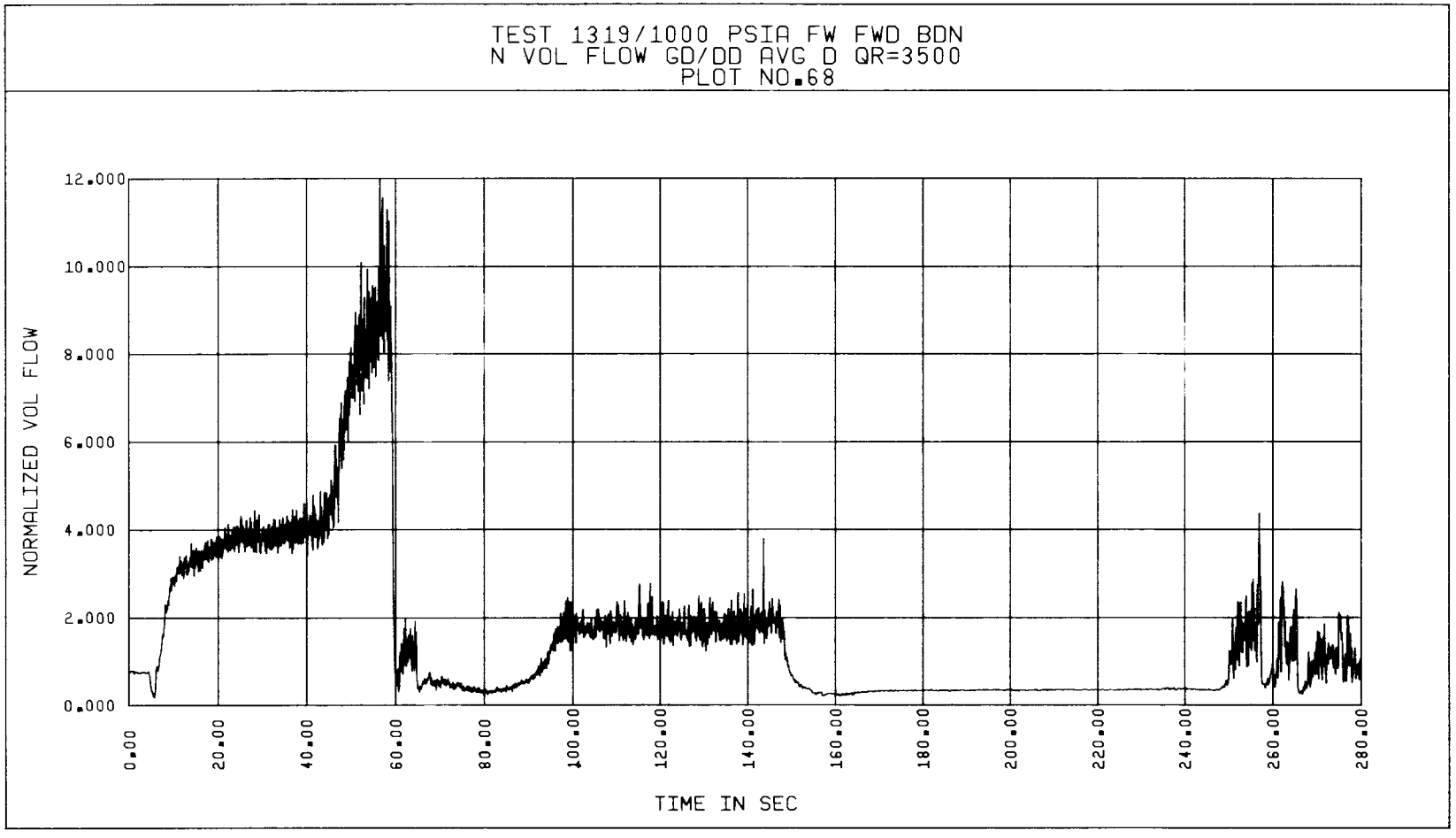

Figure 5-144. Test 1319, Normalized Discharge Volumetric Flow Rate vs Time, Based on Gamma Densitometer and Average Drag Disc Data

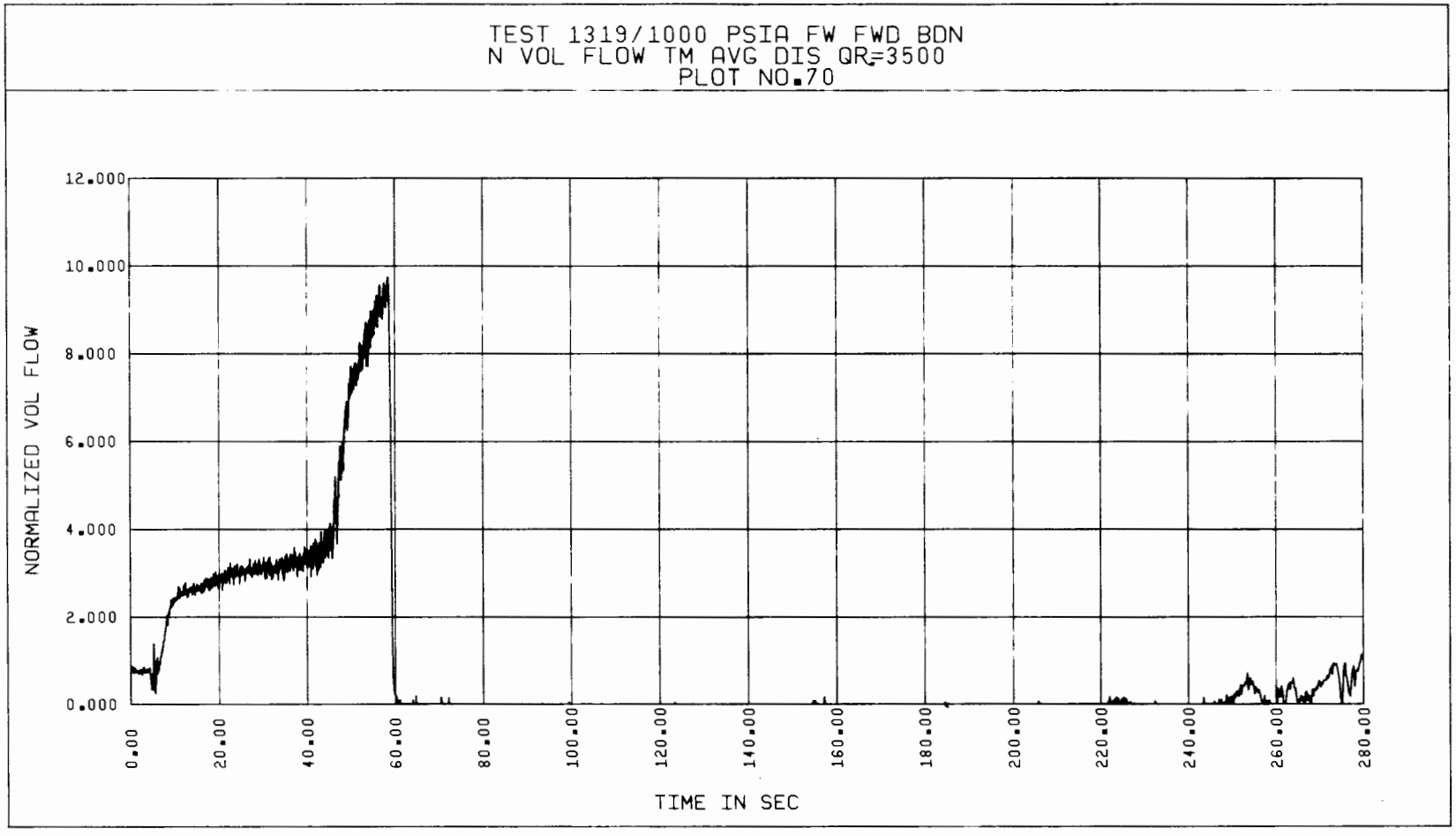

Figure 5-145. Test 1319, Normalized Discharge Volumetric Flow Rate vs Time, Based on Average Turbine Meter Data

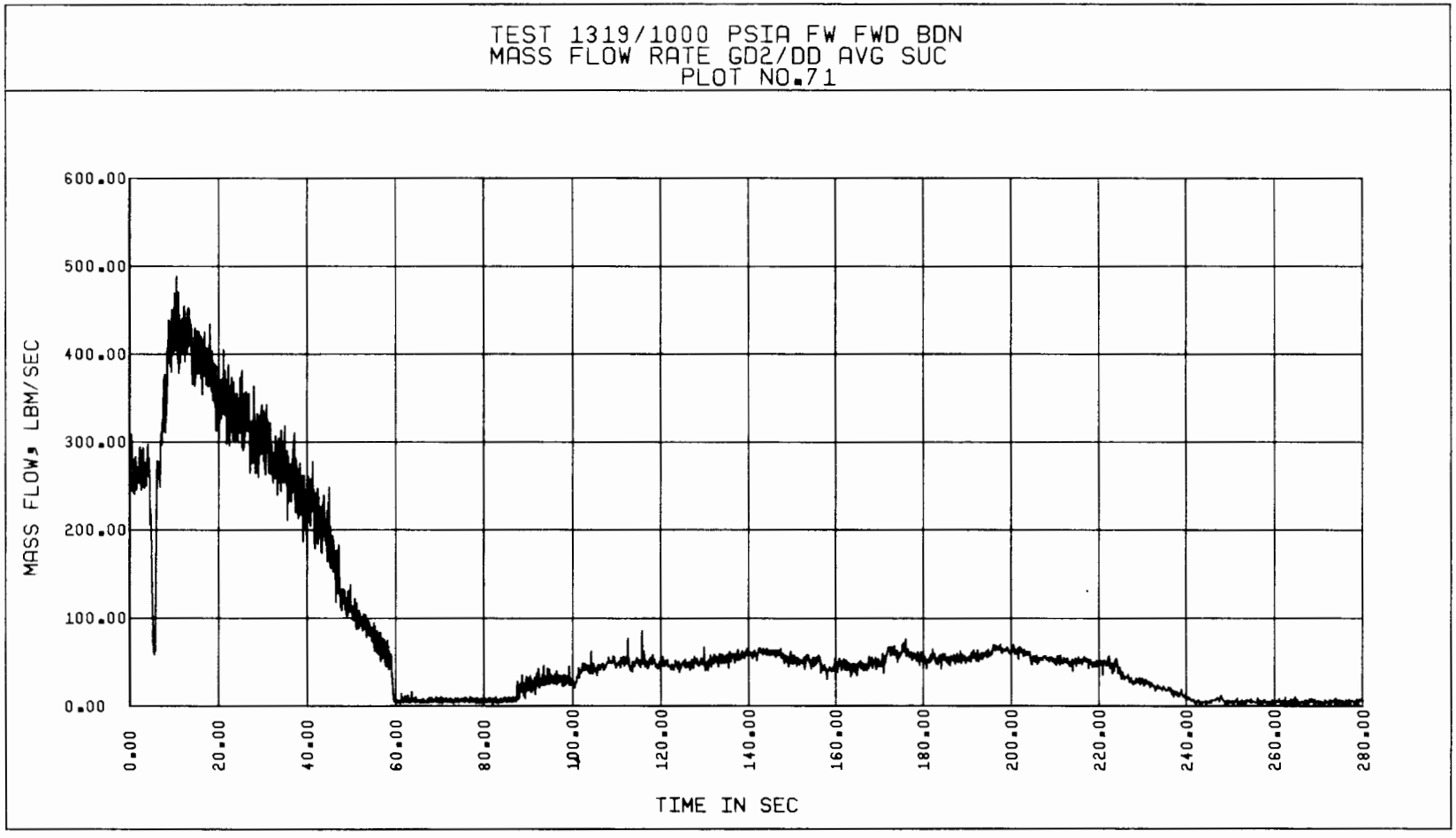

Figure 5-146. Test 1319, Suction Mass Flow Rate vs Time, Based on Gamma Densitometer and Average Drag Disc Data

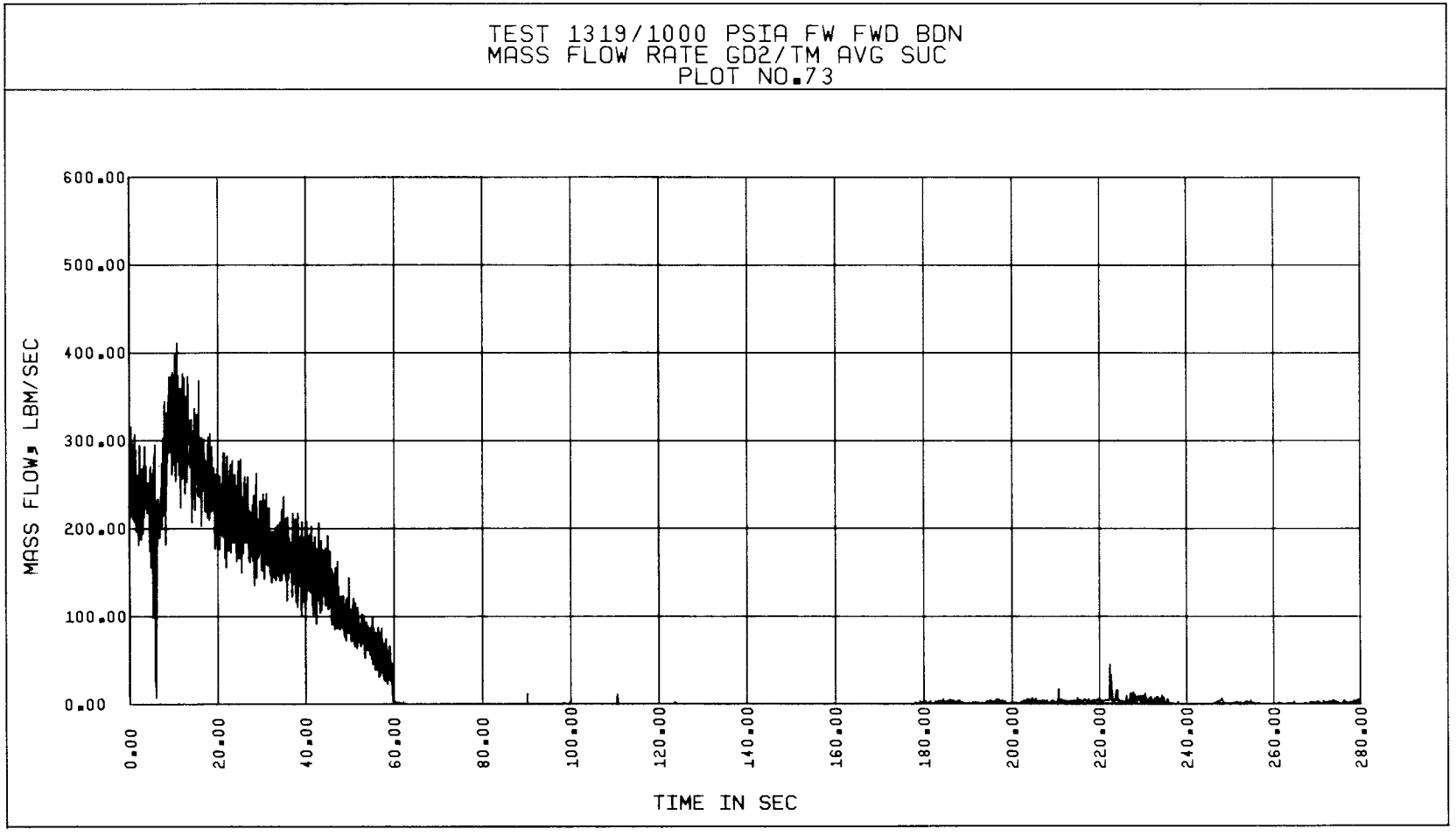

Figure 5-147. Test 1319, Suction Mass Flow Rate vs Time, Based on Gamma Densitometer and Average Turbine Meter Data

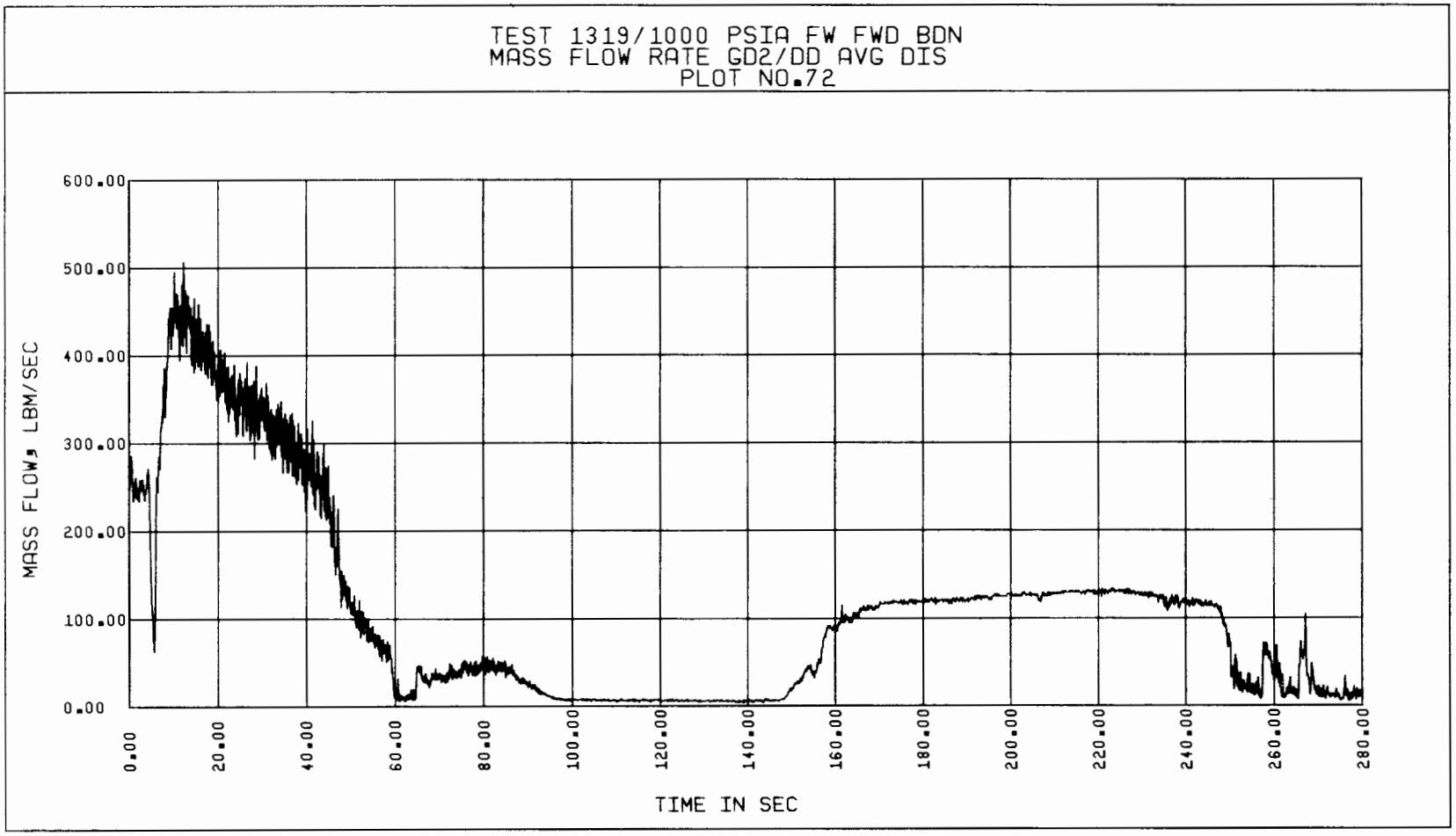

Figure 5-148. Test 1319, Discharge Mass Flow Rate vs Time, Based on Gamma Densitometer and Average Drag Disc Data

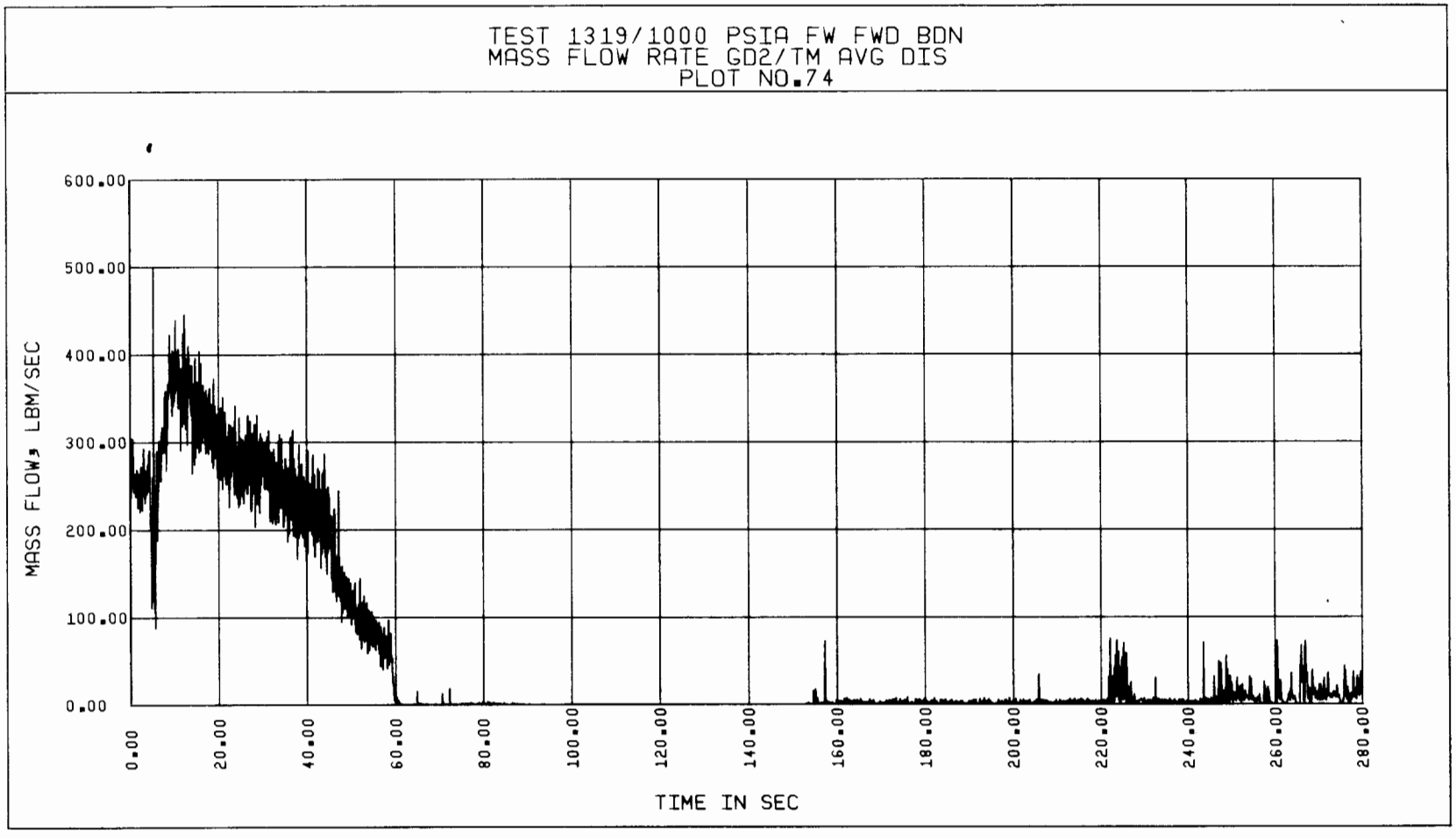

Figure 5-149. Test 1319, Discharge Mass Flow Rate vs Time, Based on Gamma Densitometer and Average Turbine Meter Data

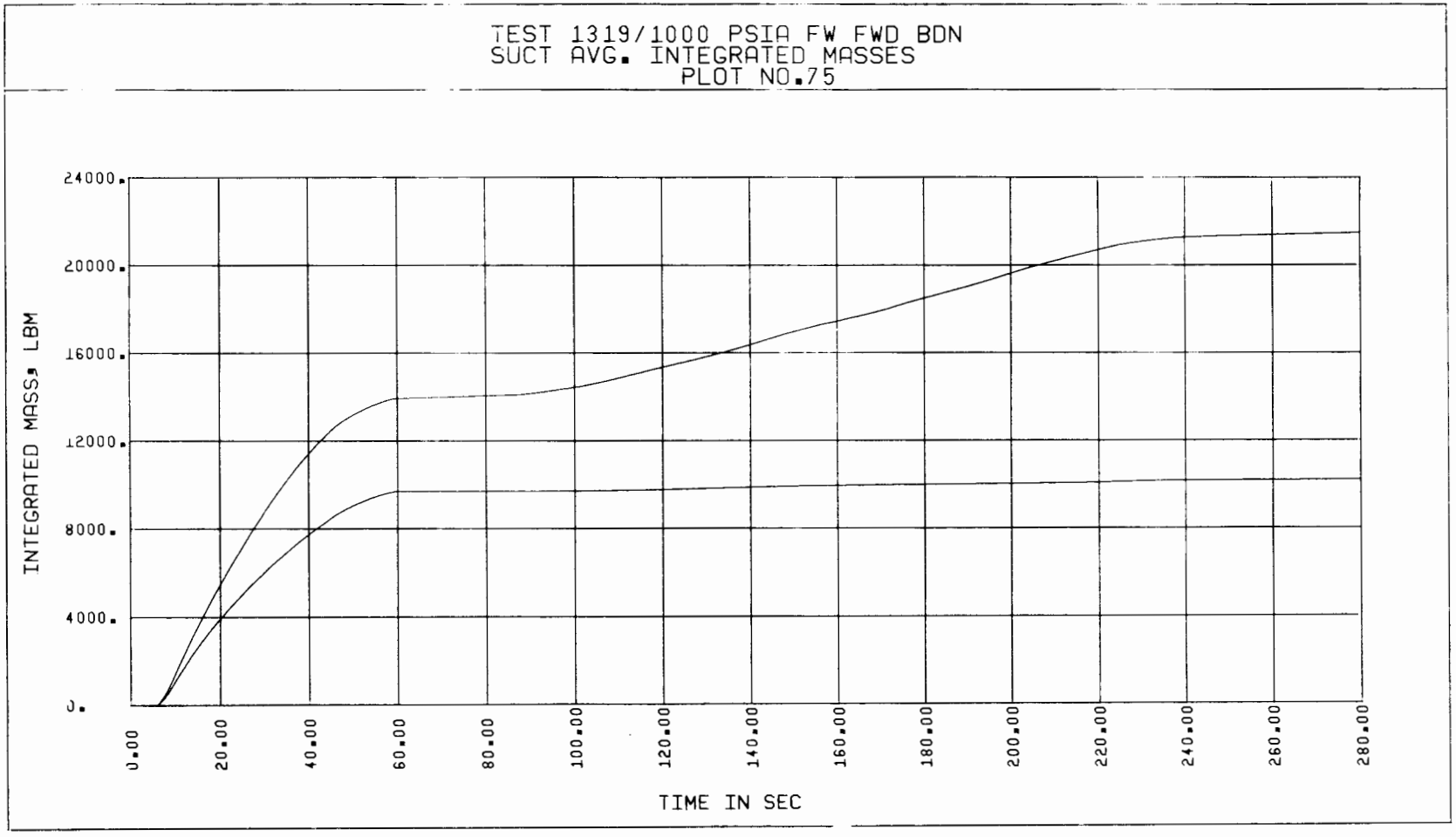

Figure 5-150. Test 1319, Average Suction Integrated Masses vs Time

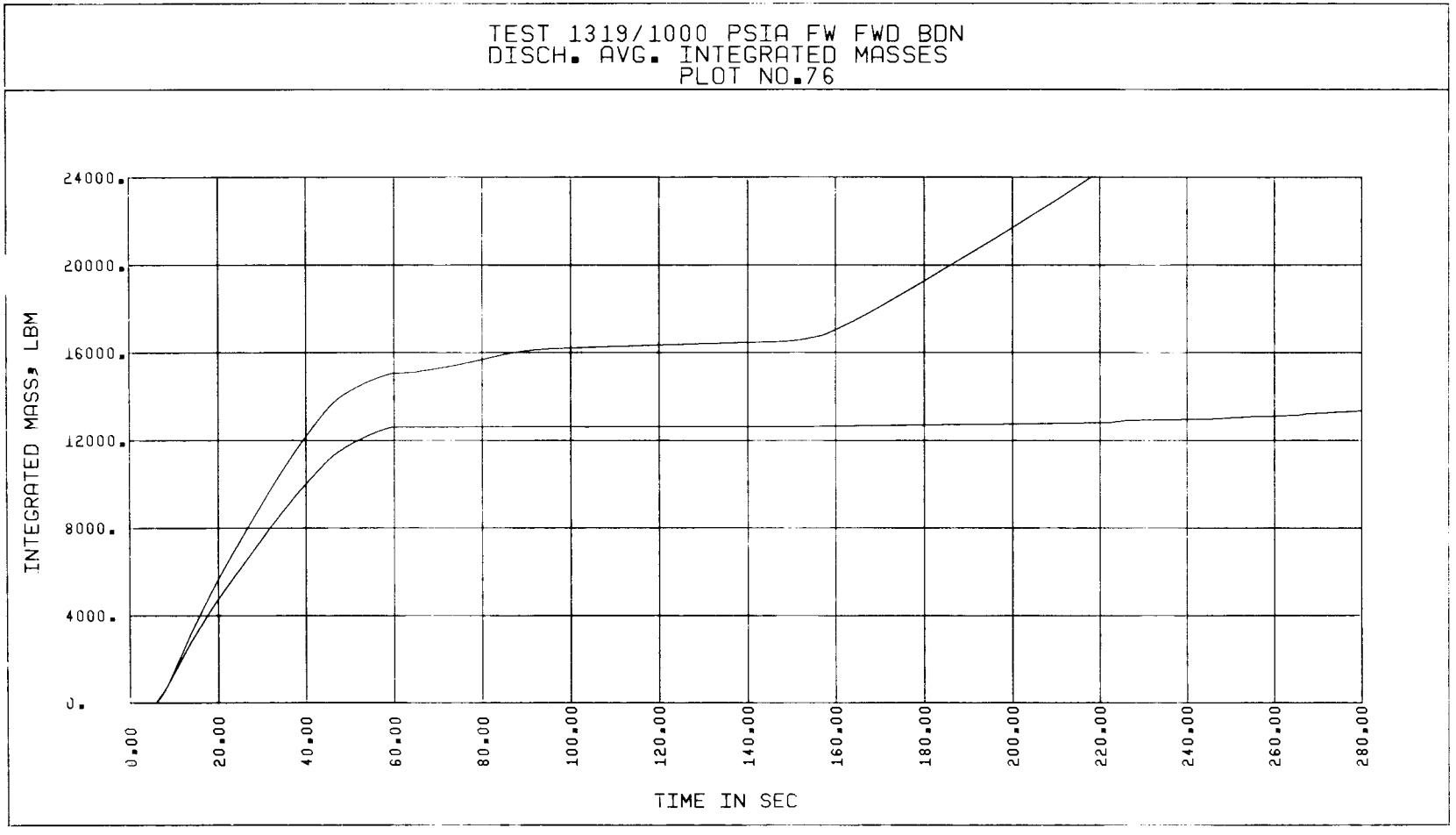

Figure 5-151. Test 1319, Average Discharge Integrated Masses vs Time

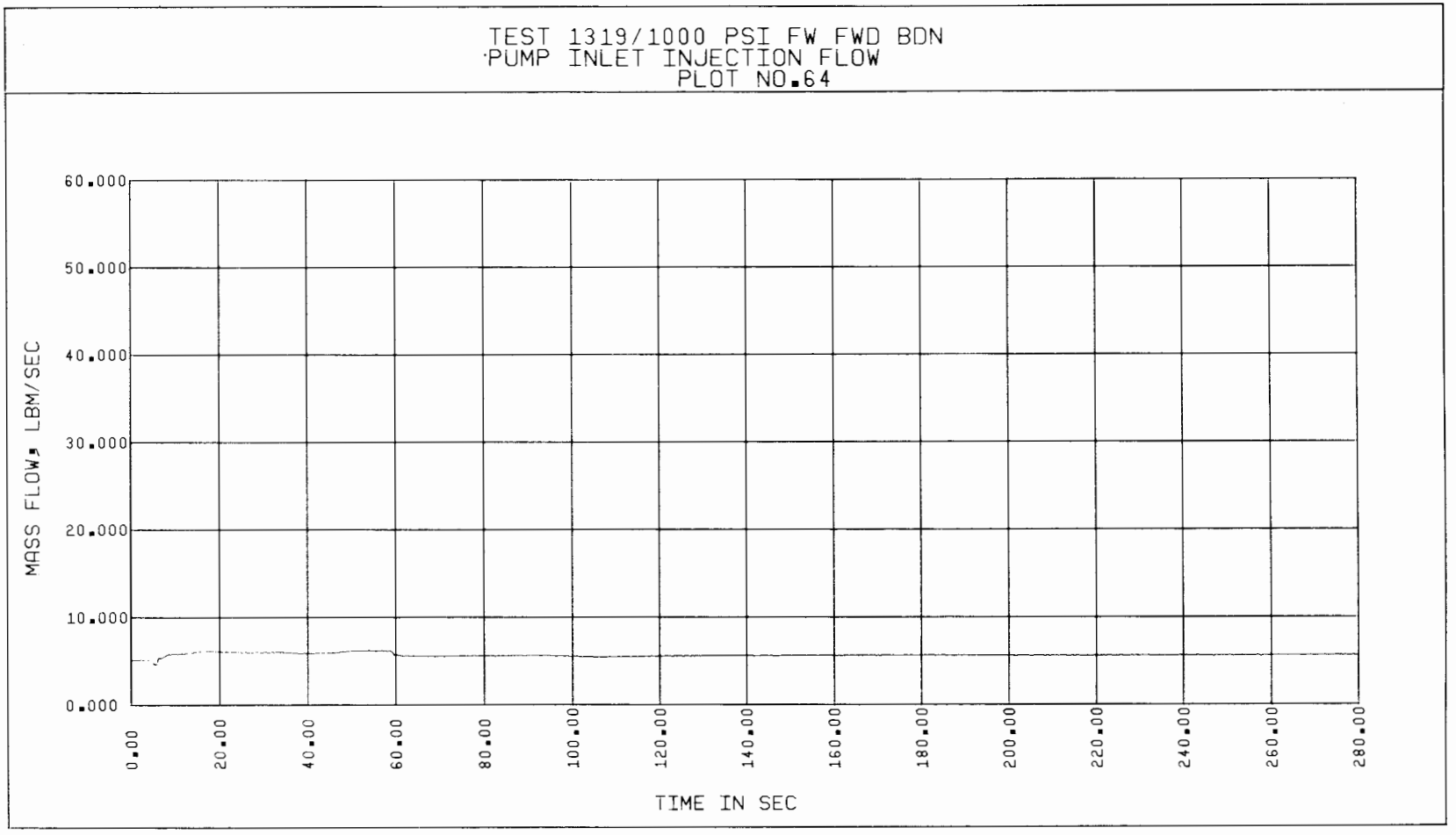

Figure 5-152. Test 1319, Pump Seal Injection Inlet Flow vs Time

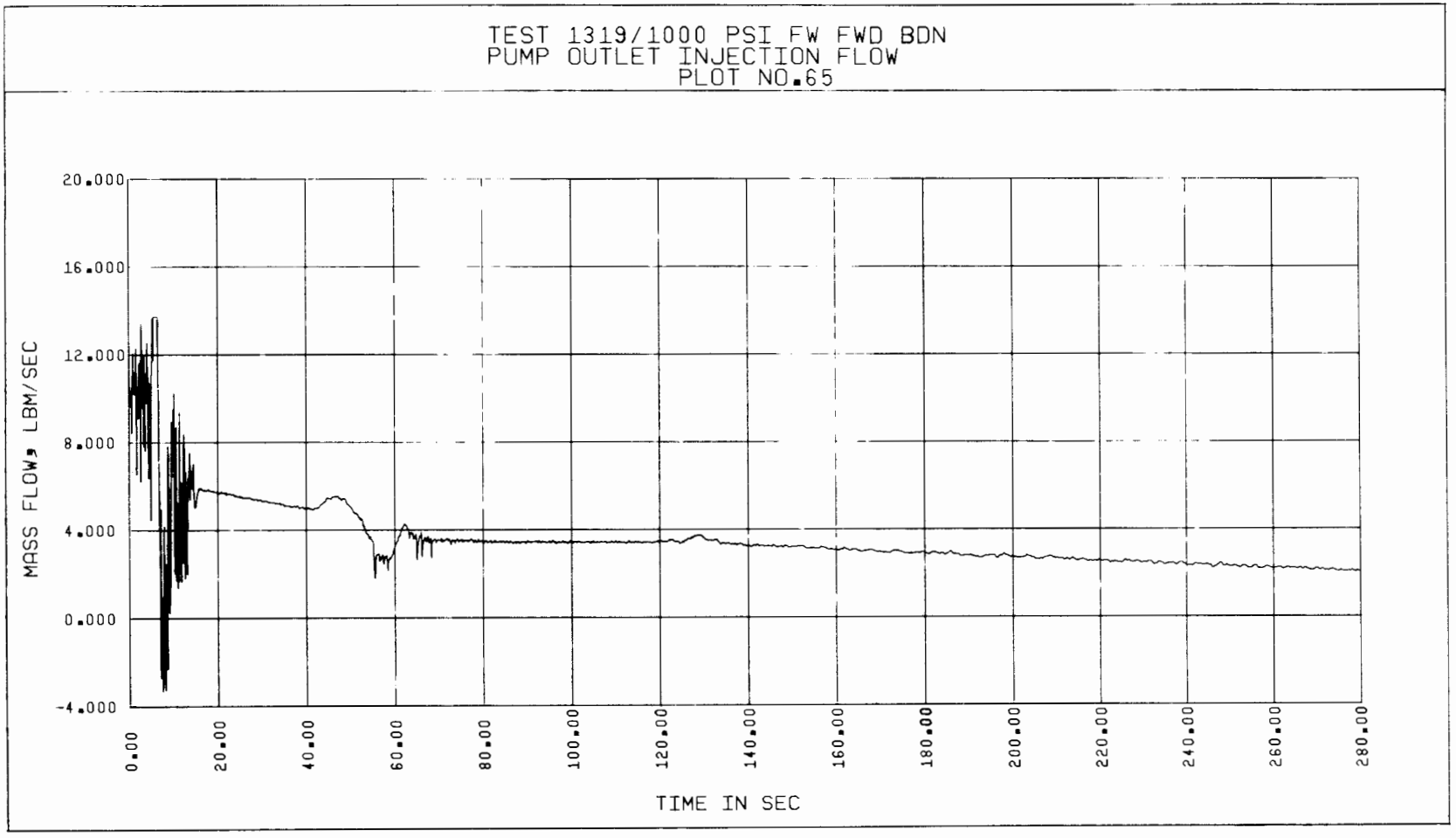

Figure 5-153. Test 1319, Pump Seal Injection Outlet Flow vs Time

may be relatively large enough to affect the accuracy in the calculation of the total mass that flowed out of the loop through the measuring sections during the blowdown. However, this quantity was calculated using the method employed for Test 1351 as described above (see Appendix A). The net mass flow through the SIS during the blowdown period turns out to be approximately 13,430 lbm, and through the DIS during the same time period it is determined to be about 13,620 lbm.

Examination of the averaged integrated masses of Figure 5-150 indicates that the SIS integrated mass at 58.7 seconds in 13,920 lbm for the DD's and 9,800 lbm for the TM's. The DIS integrated mass at the same time is 15,000 lbm for the DD's and 12,600 lbm for the TM's (see Figure 5-151). These values are tabulated in Table 5-2 for comparisons with the computed inventory values. For the DD's at SIS, the error in the final integrated mass is less than 5%. For the TM's and the DD's at DIS, the errors in the same parameter are similarly low. However for the TM's at SIS, the error is approximately 27 percent. Consequently, for the suction side the average volumetric flow rate calculated from the GD-DD measurements may be employed as the unique volumetric flow rate for this test also.

Table 5-2

Comparison of Mass Flow Integrals for Test 1319
at 58.7 Seconds

Data Used in Integral	Measurement Location	Mass Flow Integral (lbms)
Avg TM-GD	SIS	9,800
Avg DD-GD	SIS	13,920
Avg TM-GD	DIS	12,600
Avg DD-GD	DIS	15,000
Piping inventory	SIS	13,430
Piping inventory	DIS	13,620

Section 6

REFERENCES

1. W.G. Kennedy, M.C. Jacob, and J.R. Shuckerow, Two Phase Pump Performance Program Preliminary Test Plan. EPRI NP-128, September 1975.

2. "A FORTRAN-IV Digital Computer Program for Reactor Blowdown Analysis," Combustion Engineering, Inc., CENPD-133, August 1974 (Non-Proprietary).

3. Meyer, C.A. et al., Thermodynamic and Transport Properties of Steam, ASME, 1967.

4. Powell, R.L., et al., Thermocouple Reference Tables Based on the IPTS-68. National Bureau of Standards Monograph 125, March 1974.

5. "Power Test Codes, Flow Measurement Part 5 - Measurement of Quantity of Materials". New York: ASME, 1959. P. 56-58.

6. D.J. Olson, Single- and Two-Phase Performance Characteristics of the MOD-1 Semiscale Pump Under Steady-State and Transient Fluid Conditions. ANC, ANCR-1165, October 1974.

7. Interpreting Two-Phase Flow Measurements, Report prepared for USNRC, Reactor Safety Research, MPR-511, July 28, 1976.

8. Aya, I., A Model to Calculate Mass Flow Rate and Other Quantities of Two-Phase Flow in a Pipe with a Densitometer, a Drag Disk, and a Turbine Meter, Oak Ridge National Laboratory, ORNL-TM-4759, November 1975.

APPENDIX A

MASS FLOW INTEGRAL CALCULATION

As indicated in Section 5.5, the amount of mass that flowed through the measuring sections and out through the break during a particular time interval is calculated from the mass inventories at the beginning and end of this time interval. As an illustration, the amount of mass that discharged through the break during the first 170 seconds of blowdown Test 1351 is computed as follows:

Figure A-1 provides a schematic view of the test system with various piping sections individually identified. These sections are:

A: High Pressure (H.P.) Drum
B: Section from H.P. Drum to SIS
C: Section from SIS to DIS
D: Section from DIS to Bypass Throttle Valve
E: Section from Bypass Throttle Valve to Blowdown Orifice
F: Section from Bypass Valve to H.P. Drum inlet

From this figure it is seen that the fluid in Sections A, B and F can flow through the SIS and out through the break during the blowdown. The fluid from Section C in addition to that from the above sections can flow through the DIS during the transient. The initial (just prior to rupture) and final (at 170 seconds after rupture) fluid mass inventory and the mass of water entering the loop due to test pump seal injection leakage are employed in the derivation of the mass flow integrals for each of the measuring sections.

The initial mass in the high pressure drum (Section A) is calculated from the initial volume of water and steam in the drum and the saturation densities of the two phases. The volume of the phases are determined from the water level in the drum and the physical dimensions of the drum. The height of the water level with reference to the bottom of the drum was measured by means of a D.P. cell whose output was recorded by the Scanner Data Acquisition System. For Test 1351, this initial mass was calculated as,

$$M_{A,o} = 5204 \text{ lbm}$$

The initial mass of fluid in Section B is computed from the volume of piping between the high pressure drum and the SIS, and the average of the initial saturation densities at the high pressure drum and the SIS. For Test 1351, the initial inventory for Section B turns out to be

$$M_{B,O} = 6946 \text{ lbm}$$

The initial mass of fluid in Section F is calculated from the volume of piping between the bypass throttle valve and the high pressure drum, and the saturation density of water in the drum. This mass is determined as,

$$M_{F,O} = 1667 \text{ lbm}$$

The initial inventory in Section C is calculated from the volume of this section and the average of the suction and discharge saturation densities. The initial mass of fluid in this section is:

$$M_{C,O} = 143 \text{ lbm}$$

Thus the initial inventories of fluid that can flow through the measuring sections are:

$$IM_{SIS,O} = M_{A,O} + M_{B,O} + M_{F,O}$$

$$= 13817 \text{ lbm}$$

$$IM_{DIS,O} = M_{A,O} + M_{B,O} + M_{C,O} + M_{F,O}$$

$$= 13960 \text{ lbm}$$

The mass of fluid left in the above section at 170 seconds after rupture is calculated using a common average density as measured by the gamma densitometer at the SIS. This is only an approximation since, seal injection leakage flows at the booster pumps and test pump may produce differences in local densities. However, the effect of this assumption on the mass flow integral

for the time period under consideration is expected to be negligible due to the fact that almost all the fluid in the test system has changed into steam at about 170 seconds after rupture. The fluid density is relatively small (that for saturated steam) at this time.

Thus, the final mass inventories become:

$$IM_{SIS,170} = 14.93 \text{ lbm}$$

$$IM_{DIS,170} = 15.10 \text{ lbm}$$

The mass flow integral for the DIS will also include the contribution due to seal injection leakage into the pump cavity during the time period under consideration. This amount of mass is calculated from the curves of Figures 5-36 and 5-37 which show the seal injection inflow and outflow, respectively, for Test 1351. From these figures, the seal injection leakage mass flow integral into the pump cavity is calculated as:

$$IM_{SI} = 293 \text{ lbm}$$

Thus, the mass flow integral for the SIS becomes:

$$IM_{SIS} = IM_{SIS,0} - IM_{SIS,170}$$

$$= 13817 - 14.93 = 13802.07 \text{ lbm}$$

Similarly for the DIS, the mass flow integral becomes:

$$IM_{DIS} = IM_{DIS,0} + IM_{SI} - IM_{DIS,\ 170}$$

$$= 13960 + 293\text{-}15.1$$

$$= 14237.9 \text{ lbm}$$

Similar calculations as above are employed for Test 1319 to derive the mass flow integral values at the SIS and DIS.

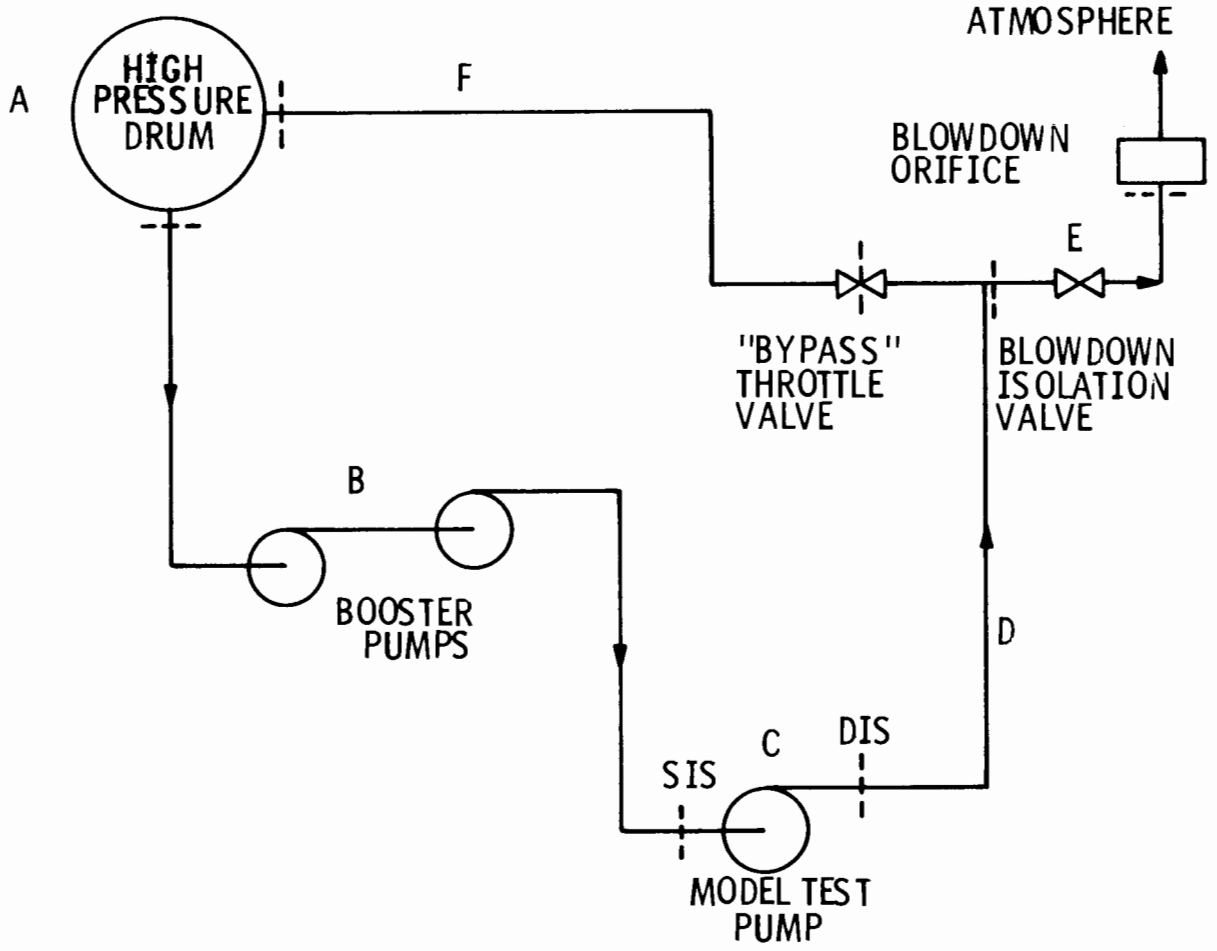

Figure A-1. Idealized schematic diagram of test system for forward flow blowdown tests.